

The role of Toll signaling in dorsoventral axis
formation in the milkweed bug *Oncopeltus*
fasciatus

Inaugural - Dissertation

zur

Erlangung des Doktorgrades

der Mathematisch-Naturwissenschaftlichen Fakultät

der Universität zu Köln

vorgelegt von

Yen-Ta Chen

aus Taiwan

Köln, den 2015

Berichterstatter/in: **Prof. Dr. Siegfried Roth**

Berichterstatter/in: **Prof. Dr. Günter Plickert**

Tag der letzten mündlichen Prüfung: 23.01.2015

Contents

Zusammenfassung (Abstract)	XII
1 Introduction	1
1.1 The conserved body plan	1
1.2 Conserved signaling for DV patterning	1
1.2.1 The emergence of Toll signaling in axis determination	2
1.3 Axial patterning in <i>Drosophila</i>	3
1.3.1 Symmetry breaking during <i>Drosophila</i> oogenesis	3
1.3.2 Determination of DV polarity during oogenesis	5
1.3.3 Communication between follicular epithelium and the embryo	5
1.3.4 Toll signaling pathway in <i>Drosophila</i>	7
1.3.5 Interaction between Dorsal and its inhibitor- Cactus	8
1.3.6 Nuclear Dorsal gradient and downstream target genes	9
1.4 DV patterning in the beetle <i>Tribolium</i>	11
1.5 Evolution of DV patterning mechanisms	11
1.5.1 Reasons to study DV patterning in the milkweed bug, <i>Oncopeltus fasciatus</i>	12
1.5.2 Objectives	13
2 Materials and Methods	15
2.1 Gene annotation and analysis	15
2.2 RNA extraction and cDNA synthesis	16
2.3 Molecular cloning of candidate genes	17
2.3.1 Degenerate PCR (deg-PCR) and RACE-PCR	17
2.4 Probe and double-stranded RNA (dsRNA) synthesis	19

2.5	Animal husbandry, embryo fixation, and ovary dissection	24
2.5.1	Husbandry of animals	24
2.5.2	Fixation of embryos	25
2.6	Ovary dissection	25
2.7	RNA interference and the analysis of knockdown phenotypes	25
2.7.1	Parental RNA interference (pRNAi)	25
2.7.2	The morphological analysis of knockdown phenotypes	26
2.7.3	Fuchsin staining	27
2.8	Knockdown efficiency validation	27
2.9	Quantification of gene expression level	27
2.10	<i>In situ</i> hybridization (ISH)	28
2.10.1	Two-color double ISH	29
2.10.2	Fluorescent ISH (FISH)	29
2.11	Antibody production and western blot	30
2.11.1	Molecular cloning	30
2.11.2	Protein induction	31
2.11.3	Protein purification	32
2.11.4	SDS-PAGE and Western blot	32
2.12	Whole-mount immuno-staining	33
2.13	Fluorescent dye staining	34
3	Results	37
3.1	Gene annotation in the transcriptome	37
3.1.1	Toll signaling components	37
3.1.2	Marker genes	39
3.2	Early expression patterns of marker genes	39
3.2.1	Anterior markers	40
3.2.2	Ventral markers	40
3.2.3	Dorsal marker	43
3.3	Genomic and transcriptomic analysis of Toll-like receptors	43
3.3.1	Conserved domain of Toll-like receptors	44
3.3.2	Phylogenetic analysis of the Toll family	45
3.3.3	Spatial distribution of <i>Toll-1</i> transcripts	48

3.4	NF κ B transcription factors in <i>Oncopeltus</i>	48
3.4.1	Conserved domain of the Rel/NF κ B family	48
3.4.2	Phylogenetic analysis of the Rel/NF κ B protein family	50
3.4.3	Expression pattern of <i>dorsal</i> transcripts	52
3.5	Disruption of Toll signaling severely impairs embryogenesis	52
3.6	Knockdown phenotypes and lifespan reduction after <i>Toll-1</i> knockdown . .	55
3.7	Validation of knockdown efficiency by the semi-quantitative PCR	55
3.7.1	Validation of <i>Toll-1</i> knockdown efficiency	56
3.7.2	Validation of <i>dll</i> knockdown efficiency	57
3.8	ISH staining of <i>Toll-1</i> and <i>dll</i> knockdown embryos during blastoderm stage	57
3.9	ISH staining of <i>Toll-1</i> knockdown embryos during germ band stage	59
3.10	Expression level of transcripts after <i>Toll-1</i> RNAi	61
3.11	ISH staining of <i>dll</i> knockdown embryos during germband stage	62
3.12	Phenotypic analysis of <i>dorsal2</i> knockdown by ISH staining	63
3.12.1	Early function of <i>dorsal2</i>	65
3.13	AP patterning in <i>Oncopeltus</i> is also dependent on Toll signaling	67
3.14	Interaction between Toll and BMP signaling	69
3.14.1	Double Knockdown of <i>Toll-1</i> and <i>dpp</i>	69
3.14.2	Validation of double knockdown efficiency	69
3.14.3	The contrary roles of Toll and BMP signaling	71
3.15	Twist has a conserved function in mesoderm formation	71
3.16	The distribution of Dorsal1 proteins	73
3.16.1	Dorsal1 is constantly expressed during development	73
3.16.2	Dorsal1 is ubiquitously expressed	73
3.16.3	Bioinformatic prediction of Dorsal binding sites	75
3.17	Signaling components downstream of the Toll receptors	78
3.17.1	Pelle or Tube? That is the question.	80
3.17.2	Phylogenetic analysis of Pelle, Tube, and Myd88	80
3.17.3	Tube or Tube-like kinase? case study in other insects	81
3.17.4	Knockdown of the adaptor and kinase proteins	83
3.18	Inhibitors of the NF κ B transcription factor (κ B)	84
3.18.1	The putative <i>cactus</i> genes in <i>Oncopeltus</i>	85

3.18.2	Expression pattern of putative <i>cactus</i> genes	85
3.18.3	Functional analysis of <i>cactus</i> (<i>cact</i>) genes	88
3.19	Maternal cues for axial determination in ovaries	90
3.19.1	Location of the oocyte nuclei	90
3.19.2	The ligand of the EGF receptor in <i>Oncopeltus</i>	91
3.19.3	The function of <i>pipe</i> in DV patterning	93
3.19.4	From the serine protease cascade to DV patterning	93
3.19.5	Expression of <i>TGFα</i> , <i>pipe</i> and <i>nudel</i> , <i>gd</i> , <i>snake</i> transcripts in ovarioles	96
3.19.6	Knockdown phenotypes of <i>nudel</i>	96
3.20	The ligands of Toll receptor: Spätzle	99
4	Discussion	103
4.1	Function of the Toll receptors	103
4.2	Knockdown of the Toll signaling pathway	104
4.2.1	Knockdown of <i>myd88</i> and the putative TIR-domain-containing adaptors	105
4.2.2	The functions of Spätzle ligands	105
4.2.3	Functions of Toll signaling upstream components	106
4.2.4	Short-germ development and the function of growth zone	107
4.2.5	Mesoderm formation and the possible function of <i>snail</i>	107
4.2.6	Phenotypes related to the function of NF κ B proteins	108
4.3	The Dorsal protein and the nuclear gradient	109
4.3.1	The <i>Oncopeltus</i> Dorsal1 and the relationship to <i>sog</i> expression	109
4.3.2	The interaction between Dorsal and its inhibitor Cactus	110
4.4	The DV patterning in <i>Oncopeltus</i> also contributes to AP patterning	111
4.4.1	Fate map shift	112
4.4.2	Dorsal might interact with the terminal system	112
4.4.3	AP patterning genes are also Dorsal target genes	113
4.5	Establishment of the DV axis in the milkweed bug	113
4.5.1	Interaction between BMP and Toll signaling	113
4.5.2	Evolutionary changes of the DV patterning system among insects	114
4.5.3	The emergence of Toll's role in DV axis formation	114
4.5.4	The regulation of <i>Toll</i> in insects	115

4.6	Summary of Toll's role in DV patterning of <i>Oncopeltus</i>	116
4.7	Future perspectives	116
4.7.1	Post-genomic era and the mechanism of DV patterning in the hemipterans	116
4.7.2	The novel imaging and transgenic techniques	118
4.7.3	The immune functions of Toll signaling in <i>Oncopeltus</i>	118
5	Supplementary data	143
5.1	Embryonic development in <i>Oncopeltus</i>	143
5.1.1	The difference of nuclear density along the dorsoventral (DV) axis	143
5.2	Detailed expression pattern of DV marker genes	144
5.2.1	Expression of columnar genes	146
5.2.2	The ISH difficulties in the milkweed bug	149
5.2.3	Late expression pattern of ventral markers	151
5.2.4	Expression pattern of the dorsal marker <i>SoxN</i>	153
5.2.5	Mesoderm formation and the expression of <i>snail</i>	153
5.3	Gene annotation in the <i>Oncopeltus</i> transcriptome	154
5.3.1	Identification of Toll or Toll-like receptors (TLRs)	156
5.4	Phosphorylation sites of Dorsal proteins	156
5.5	Phenotypes of the <i>cactus-2</i> knockdown	156
5.6	Experimental controls and the reference gene	160
5.6.1	The control for semi-quantitative PCR	160
5.6.2	The reference genes for qPCR normalization	162
5.6.3	The dsRNA targeting sites of <i>Toll-1</i>	162
5.7	Toll signaling together with Imd pathway are important for innate immunity among insects	163
5.7.1	Life span reduction of injected females after pRNAi	164
	Acknowledgement	166
	Erklärung	168
	Lebenslauf	169

List of Tables

2.2	Primers designed for RACE-PCR	17
2.1	Primers designed for deg-PCR	19
2.3	Gene Specific primers for probe synthesis	20
2.4	Gene Specific primers for dsRNA synthesis	22
2.5	The embryogenesis schedules of <i>Oncopeltus fasciatus</i>	24
2.6	Gene-specific primers designed for the validation of knockdown efficiency .	28
2.7	Gene Specific primers for qPCR	28
2.8	Specific primers of constructs used for protein induction	31
2.9	Recipes for the polyacrylamid gels	33
2.10	Antibody tested for immuno-staining in <i>Oncopeltus</i>	34
2.11	Fluorescent dyes tested in <i>Oncopeltus</i>	35
3.1	Annotation of Toll signaling components and marker genes	38
3.2	Toll-like receptors in transcriptome and genome annotation	45
3.3	Ratio of morphological phenotypes and lifespan reduction after <i>Toll-1</i> knock- down	56
3.4	Percentage of residual <i>sog</i> expression in <i>Toll-1</i> and <i>dll</i> knockdown embryos	59
3.5	Categorization of <i>twist</i> expression in <i>dll</i> knockdown embryos	63
3.6	Statistics of <i>dll2</i> knockdown phenotypes during blastoderm and germband stages	66
3.7	Statistics of anterior-shifted phenotypes with marker gene expression in <i>Toll-1</i> and <i>dll</i> knockdown embryos	68
3.8	Similarity of conserved domains compared with <i>Drosophila</i> Pelle and Tube	80
3.9	Statistics of <i>Myd88</i> , <i>Pelle</i> and <i>Tube-like kinase</i> Knockdown phenotypes . .	84
3.10	List of putative <i>cactus</i> genes in <i>Oncopeltus</i>	85

3.11	Genes required for DV patterning acting upstream of Toll signaling	91
5.1	Genes with more than one contigs in the <i>Oncopeltus</i> transcriptome	155
5.2	Percentage of knockdown phenotype produced by dsRNA-a and dsRNA-b .	163
5.3	Life span reduction after pRNAi	164

List of Figures

1.1	Conserved signaling for DV patterning and immunity in metazoans	3
1.2	The ovariole and the position of oocyte nucleus during <i>Drosophila</i> oogenesis	4
1.3	Proteolytic cascade and the activation of Toll signaling	6
1.4	Scheme of Toll signaling pathway	8
1.5	Fatemap and domains of gene expression along the embryonic DV axis . .	10
2.1	Adult injection	26
2.2	handmade mesh-bottom baskets placed in plates ready for ISH	30
3.1	Expression pattern of <i>msh</i> in <i>Oncopeltus</i> embryos	40
3.2	Expression pattern of <i>sog</i> in <i>Oncopeltus</i> embryos	41
3.3	Expression pattern of <i>twist</i> in <i>Oncopeltus</i> embryos	42
3.4	Expression pattern of <i>sim</i> in <i>Oncopeltus</i> embryos	42
3.5	Expression pattern of <i>SoxN</i> in <i>Oncopeltus</i> embryos	44
3.6	The conserved domains of putative Toll-like receptors	46
3.7	Phylogenetic analysis of the Toll family	47
3.8	Spatial distribution of <i>Toll-1</i> transcripts during <i>Oncopeltus</i> embryogenesis	49
3.9	Conserved domain of Rel/NF κ B proteins	50
3.10	Phylogenetic analysis of the Rel/NF κ B family	51
3.11	Expression pattern of <i>dl1</i> and <i>dl2</i> transcripts	53
3.12	Disruption of Toll signaling severely impairs embryogenesis	54
3.13	Validation of knockdown efficiency by the semi-quantitative PCR	56
3.14	ISH staining of <i>Toll-1</i> and <i>dl1</i> knockdown embryos during blastoderm stage	58
3.15	<i>Toll-1</i> knockdown phenotypes during germ band stage	60
3.16	Gene expression is down-regulated in <i>Toll-1</i> knockdown embryos	61

3.17	Expression of <i>twist</i> in <i>dl1</i> knockdown embryos during germband stage . . .	62
3.18	Expression of <i>SoxN</i> and <i>engrailed</i> in <i>dl1</i> knockdown embryos during germband stage	64
3.19	Expression of <i>twist</i> and <i>sim</i> in <i>dl2</i> knockdown embryos during germband stage	65
3.20	Nuclear staining of <i>dl2</i> knockdown embryos during blastoderm stages . . .	66
3.21	Anterior-shifted phenotypes after <i>Toll-1</i> and <i>dl1</i> knockdown	67
3.22	Expression of <i>sog</i> and <i>twist</i> in <i>dpp</i> knockdown and double knockdown embryos	70
3.23	Validation of <i>Toll-1</i> and <i>dpp</i> knockdown efficiency by the semi-quantitative PCR	70
3.24	The expression levels of <i>sog</i> and <i>twist</i> after <i>Toll-1</i> and <i>dpp</i> knockdown . .	72
3.25	Fuchsin staining of <i>twist</i> knockdown during germband stages	73
3.26	ISH staining of <i>twist</i> knockdown embryos during blastoderm stage	74
3.27	OfDorsal1 antibody specifically detects endogenous proteins	75
3.28	Whole-mount immunostaining of Dorsal1 in blastoderm embryos	76
3.29	Prediction of all Dorsal binding sites in <i>Oncopeltus sog</i>	77
3.30	Prediction of high-affinity Dorsal binding sites on <i>Oncopeltus sog</i>	79
3.31	Phylogenetic analysis of Pelle, Tube, and Myd88	81
3.32	Comparison of Tube or Tube-like kinase in different insect species	82
3.33	Knockdown phenotypes of <i>myd88</i> , <i>pelle</i> and <i>tube-like kinase</i>	83
3.34	Alignments of ankyrin repeats (Ank) between <i>Drosophila Cactus</i> and putative Cactus in <i>Oncopeltus</i>	86
3.35	Expression pattern of <i>cactus-1, 2, 4</i> in <i>Oncopeltus</i> embryos	87
3.36	Expression pattern of <i>cactus-3</i>	88
3.37	Expression pattern of <i>sog</i> in <i>cactus</i> knockdown embryos	89
3.38	Location of the oocyte nucleus	92
3.39	Knockdown phenotypes of <i>pipe</i> in <i>Oncopeltus</i>	94
3.40	Phylogenetic analysis of serine protease families	95
3.41	Expression of <i>TGFα</i> , <i>pipe</i> and <i>nudel</i> , <i>gd</i> , <i>snake</i> transcripts in ovarioles . .	97
3.42	Knockdown phenotypes of <i>nudel</i> in <i>Oncopeltus</i>	98
3.43	Expression pattern of the two <i>spätzle</i> transcripts	99

3.44 Fuchsin staining of <i>spz1</i> and <i>spz2</i> knockdown embryos during germband stages	100
4.1 Phylogeny of recently sequenced hemiptera insects	117
5.1 Fluorescent staining of nuclei and membranes in <i>Oncopeltus</i> blastoderm embryos	144
5.2 The difference of nuclear density between dorsal and the ventral sides . . .	145
5.3 The early expression of the <i>msh</i> stripe is on the dorsal side with a higher nuclear density	146
5.4 Expression pattern of <i>msh</i> in <i>Oncopeltus</i> germband embryos	147
5.5 Expression pattern of <i>ind</i> in <i>Oncopeltus</i> embryos	148
5.6 Alignment of <i>ind</i> protein sequences	149
5.7 Double ISH of <i>vnd</i> and <i>msh</i> expression in <i>Oncopeltus</i> embryos	150
5.8 The fluorescent signals of <i>sog</i> expression in <i>Oncopeltus</i> embryos	151
5.9 Expression pattern of <i>sog</i> in <i>Oncopeltus</i> germband embryos	152
5.10 Expression pattern of <i>twist</i> in <i>Oncopeltus</i> germband embryos	152
5.11 Expression pattern of <i>SoxN</i> in <i>Oncopeltus</i> germband embryos	153
5.12 Expression pattern of <i>snail</i> and <i>klumpfuss</i> in <i>Oncopeltus</i> embryos	154
5.13 Phylogenetic analysis of the Toll family	157
5.14 Phylogenetic analysis of the Toll family	158
5.15 The critical phosphorylation site for nuclear import is conserved in all insect Dorsal proteins	159
5.16 Morphological phenotype of <i>cactus2-RNAi</i> embryos	160
5.17 The gene <i>actin</i> served as a perfect control for RT-PCR	161
5.18 The dsRNA targeting sites of <i>Toll-1</i>	163

Zusammenfassung

Die Etablierung der dorsoventralen (DV) Achse des *Drosophila* Embryos hängt von dem Toll/Dorsal Signalweg ab. Der Transkriptionsfaktor Dorsal wirkt stromabwärts von Toll und bildet einen Kerngradienten, der die verschiedenen Zelltypen entlang der DV Achse festlegt. Die Rolle von Toll in der DV Achsenbildung wurde bereits in zwei anderen holometabolen Insekten, dem Käfer *Tribolium* und der Wespe *Nasonia*, studiert. Es liegen aber bisher noch keine entsprechenden Studien für hemimetabole Insekten vor. In dieser Arbeit wurde die Funktion der Komponenten des Toll-Signalwegs und einiger stromabwärts wirkender Faktoren in einem Vertreter der hemimetabolen Insekten, der Baumwollwanze *Oncopeltus fasciatus*, untersucht. Die Komponenten des Toll-Signalwegs, einschließlich der Spätzle-Liganden, der Toll Rezeptoren, des Adaptorproteins Myd88, der Serin/Threoninproteinkinasen Pelle und Tube-like kinase und der Dorsal Transkriptionsfaktoren wurden im Transkriptom von *Oncopeltus* identifiziert und ihre Funktion wurde mit Hilfe der parentalen RNAi-Technik ausgeschaltet. In den pRNAi-Embryonen werden die ventral exprimierten Gene *twist* und *short gastrulation (sog)* sowie das lateral exprimierte Gen *single minded* nicht aktiviert, was darauf hindeutet, dass eine Dorsalisierung vorliegt. Für einige Gene wurde außerdem eine anteriore Verschiebung der Expressionsdomänen beobachtet, die eine zusätzliche Funktion von Toll bei der anteriorposterioren Musterbildung nahelegen. Überraschender Weise sind zentrale Komponent, die stromabwärts von Toll wirken und für die Aktivierung des Toll Liganden Spätzle benötigt werden, zwischen *Drosophila* und *Oncopeltus* konserviert. In *Oncopeltus* werden die Serinprotease Nudel und die Sulfotransferase Pipe wie in *Drosophila* im Follikelepithel, das die Oozyte einhüllt, exprimiert und ihr Funktionsverlust führt zu dorsalisierten Embryonen. Somit scheinen die Mechanismen, die für die Weitergabe der DV Polarität der Eikammer an den Embryo verantwortlich sind, evolutionär sehr alt zu sein. Sie waren bereits vor der Aufzweigung von Wanzen und holometabolen Insekten vor 350 Millionen Jahren vorhan-

den. In einer früheren Studie wurde gezeigt, dass der BMP-Signalweg in *Oncopeltus* zur Bildung der gesamten DV Achse beiträgt. Um den relativen Beitrag der BMP- und Toll-Signalwege bei der DV Musterbildung zu untersuchen, wurden beide Signalwege gleichzeitig ausgeschaltet. Gleichzeitiger Verlust des BMP-Liganden *dpp* und von *Toll1* führt zu einer Expansion der Expression von *sog* und *twist* entlang des gesamten Eiumfangs. Dieser Phänotyp ist identisch zu dem BMP-Verlustphänotyp. Der BMP-Signalweg ist also epistatisch zu dem Toll-Signalweg. Diese Beobachtung, zusammen mit weiteren Befunden, deuten daraufhin, dass der BMP-Signalweg in *Oncopeltus* von größerer Bedeutung für die DV Musterbildung ist als der Toll-Signalweg. Da außerhalb der Insekten bisher keine Tiergruppe gefunden wurde, bei der Toll eine Funktion für die Achsenbildung erfüllt, repräsentiert der reduziert Einfluss von Toll auf die DV Musterbildung in *Oncopeltus* verglichen mit holometabolen Insekten vermutlich eine evolutionär ursprüngliche Situation.

Abstract

The establishment of dorsoventral (DV) axis in the *Drosophila* embryo relies on the Toll/Dorsal signaling pathway. The transcription factor Dorsal acts downstream of *Toll* forming a nuclear gradient that determines different cell fates along the DV axis. The formation of the DV axis has been studied in two other holometabolous insects, the beetle *Tribolium* and the wasp *Nasonia*. However, the role of Toll signaling has not been addressed in the more basally branching hemimetabolous insects. Here, the functions of Toll signaling components have been studied in a representative of the hemimetabola, the milkweed bug *Oncopeltus fasciatus*. All components of the Toll signaling pathway were identified from the *Oncopeltus* transcriptome, including the Spätzle ligands, Toll receptors, Myd88 adaptors, Pelle and Tube-like protein kinases, and the Dorsal transcription factors. Knockdown of these components by parental RNAi (pRNAi) leads to a loss of expression of the ventral marker genes *twist*, *short gastrulation (sog)* and the lateral marker gene *sim*, indicating a dorsalization of the embryos. Anterior-shifted expression of several marker genes in *Toll-1* and *dorsal-1* RNAi embryos indicates that Toll signaling also modulates the AP patterning system. Surprisingly, even some genes required upstream of Toll to activate the Toll ligand Spätzle are conserved between *Drosophila* and *Oncopeltus*. Thus, in *Oncopeltus* transcripts of the serine protease Nudel and the sulfotransferase Pipe are expressed in the follicle cells surrounding the oocyte like in flies and knockdown of their function results in dorsalized embryos. This indicates that the mechanisms responsible for transmitting the DV polarity of the egg chamber to the embryo are evolutionarily conserved within insects predating the split between bugs and the holometabola 350 million years ago. Previous work has shown that in addition to Toll signaling BMP signaling also plays a crucial role for patterning the entire DV axis in *Oncopeltus*. To investigate the relationship between Toll and BMP signaling, double knockdown experiments were performed. Simultaneous loss-of-function of *dpp* and *Toll-1*,

which encode the BMP ligand and Toll receptor, leads to an expansion of *twist* and *sog* expression around entire embryonic circumference like in the *dpp* single knockdown, indicating that BMP is epistatic to Toll. Thus, BMP signaling seems to be more important than Toll signaling for establishing the cell fates along the DV axis in *Oncopeltus*. As a DV function of Toll signaling has not been observed outside of insects, the diminished function of Toll signaling in *Oncopeltus* (compared to holometabolous insects) is likely to represent an ancestral aspect of DV axis formation in insects.

Chapter 1

Introduction

1.1 The conserved body plan

During the developmental processes, it is necessary to define the main body axes and to form patterns in an embryo. For bilaterally symmetric animals, there are two major orthogonal axes of symmetry: the anterior-posterior (AP) axis, from mouth to anus; and the dorsal-ventral (DV) axis, which is perpendicular to the AP axis. No matter what the strategy for an animal to achieve axial determination during embryogenesis is, some positional information of signaling seems to be conserved during evolution. For example, Wnt signaling and Hox cluster play conserved roles for AP patterning in most bilaterian animals (Petersen and Reddien, 2009). When referring to DV patterning, BMP signaling is conserved among bilaterians (De Robertis and Sasai, 1996).

1.2 Conserved signaling for DV patterning

Embryonic studies in the frog *Xenopus* and the fly *Drosophila* reveal the conserved patterning signals from the bone morphogenetic protein (BMP) in the non-neurogenic region of the embryos, while the antagonists of BMP are deposited on the other side determining the neural fate (Hawley et al., 1995; Ray et al., 1991). The nomenclature of BMP signaling molecules is different in the frog and the fly. The gene coding for the ligand *BMP2/4* in vertebrates is homologous to *decapentaplegic (dpp)* in *Drosophila* and the gene encoding the BMP antagonist *chordin* is homologous to *short gastrulation (sog)* in *Drosophila*.

In *Drosophila*, *dpp* null mutant embryos are ventralized, indicating that the gene is required for DV patterning (Irish and Gelbart, 1987). In *Xenopus*, Chordin was originally found as a novel dorsalizing factor (Sasai et al., 1994), which can bind to BMP proteins and transport them to the non-neuronal side as an antagonist and to regulate neural induction (Sasai et al., 1995). Sog and Chordin are functionally conserved for dorsal-ventral patterning in insects and vertebrates, antagonizing Dpp and BMP ligands (Holley et al., 1995). Injection of *chordin* RNA promotes ventral development in *Drosophila*, and injection of *sog* RNA promotes dorsal development in *Xenopus*, indicating a common plan for dorsoventral (DV) patterning in bilaterians (De Robertis and Sasai, 1996).

1.2.1 The emergence of Toll signaling in axis determination

Bilateria are a major group of organisms including a myriad of animal phyla. BMP signaling plays a central role to pattern the DV axis in vertebrates, basal chordates (Yu et al., 2007) and other metazoans (summarized in Figure 1.1). However, not all bilaterally symmetric animals utilize BMP signaling for DV axis formation. For example, a series of asymmetric cell divisions are more crucial to establish the body axes in the nematode *C. elegans* (Sulston et al., 1983; Gönczy and Rose, 2005).

Besides BMP signaling, *Toll* and other dorsal group genes were first identified to be important during embryogenesis to establish the DV axis in the fly *Drosophila* (Anderson et al., 1985b). It was found that manipulation of a single gene leads to an extreme variety of phenotypes. While overexpression of *Toll* causes a ventralized embryo, depletion of *Toll* causes a dorsalized embryo (Anderson et al., 1985b). It is an evolutionary novelty to recruit Toll signaling for DV axis formation because the Toll signaling pathway plays an ancestral role in pathogen recognition and immune defense (Takeda and Akira, 2005). The discovery of Toll or Toll-like receptors (TLRs) in cnidarians (Miller et al., 2007) and a *Porifera* sponge (Wiens et al., 2007) suggests the origin of TLRs in the eumetazoan ancestor as part of the innate immune defense system.

Therefore, the novelty of recruiting Toll signaling for DV patterning might have arisen within the insect lineage. Before studying DV patterning in a basally branching insect, it is important to review fundamental findings in the well-studied fruit fly *Drosophila melanogaster*, which has been used as a model to study the generation of dorsal-ventral (DV) polarity for a long time.

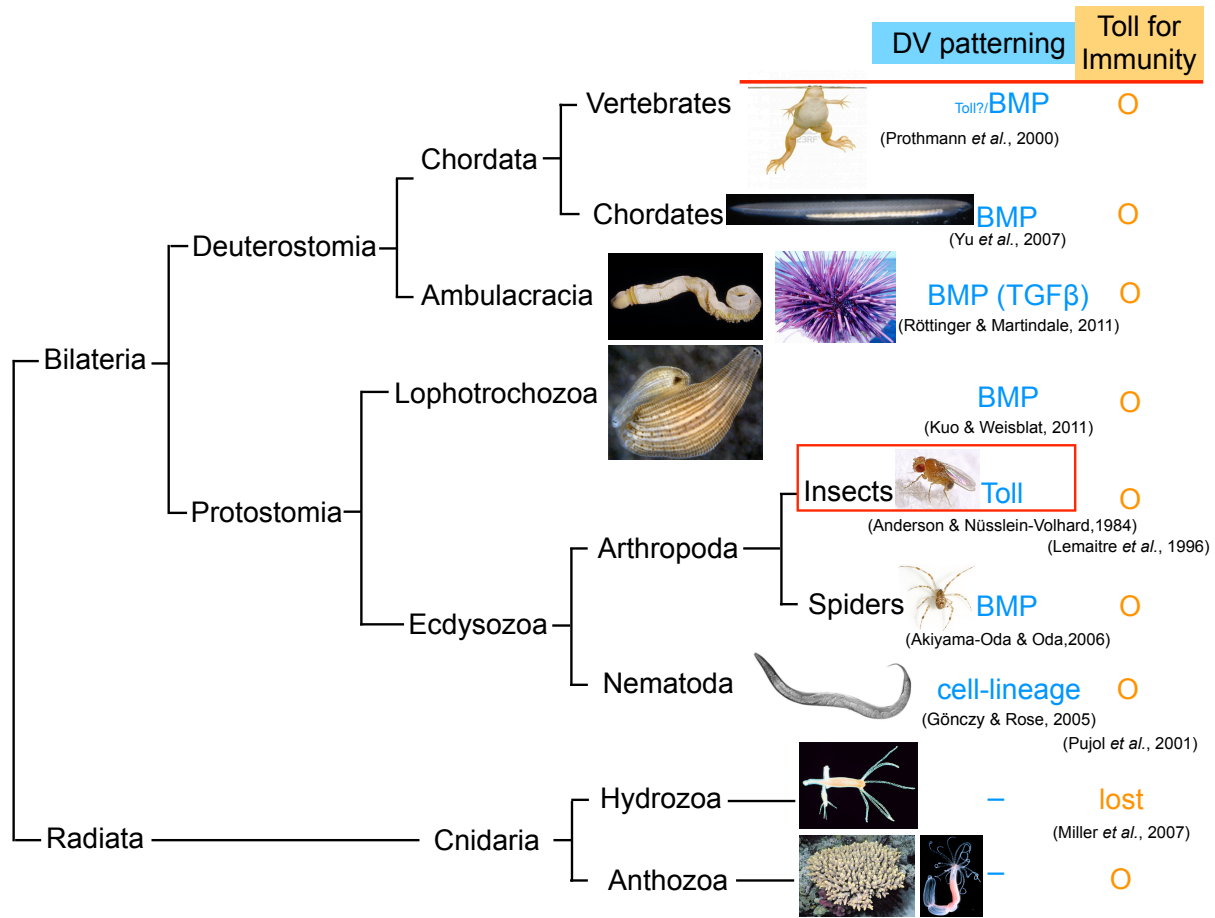


Figure 1.1. Conserved signaling for DV patterning and immunity in metazoans

BMP signaling plays a major role in DV patterning among metazoans, although a contradicting study in *Xenopus* implies that a Toll receptor binding protein is required for axis formation (Prothmann *et al.*, 2000). In the fly *Drosophila*, Toll signaling is more dominant than BMP signaling for DV patterning (Anderson *et al.*, 1985b). Although Toll is important for development and pathogen recognition in nematodes (Pujol *et al.*, 2001), axis formation in *C. elegans* depends more on the differentiation of cell-lineages. Toll signaling has a conserved function for innate immunity in all Cnidarians and bilaterians, though there is an independent loss of Toll and the nuclear factor NFκB in hydra (Miller *et al.*, 2007).

1.3 Axial patterning in *Drosophila*

1.3.1 Symmetry breaking during *Drosophila* oogenesis

The polytrophic, meroistic ovaries of *Drosophila* are made up of clusters of ovarioles. Each ovariole is a bag-like structure with gradually maturing egg chambers connected to each other along the long axis. The anterior tip of the ovariole is the germarium, producing

primordial germ cells and somatic stem cells. In each egg chamber, only one of 16 germ cells will become oocyte. The rest of them will become nurse cells (Roth and Lynch, 2009, review).

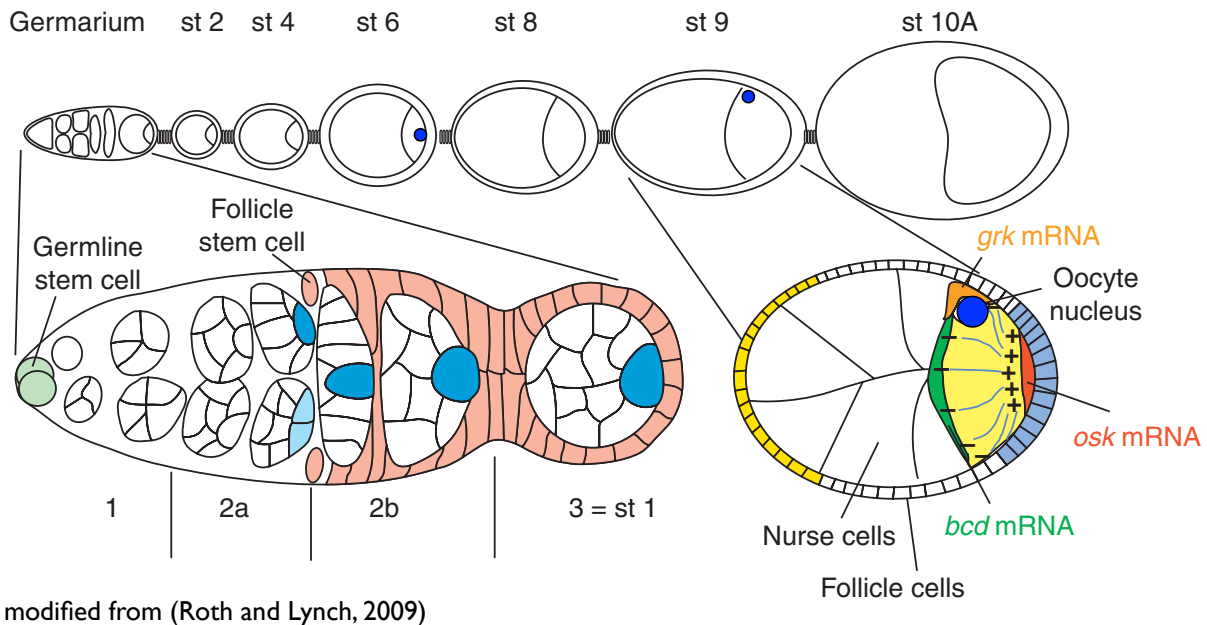


Figure 1.2. The ovariole and the position of oocyte nucleus during *Drosophila* oogenesis

Drawing of one *Drosophila* ovariole with the germarium at the left tip. The developing egg chambers are divided to 14 stages. Stage 1-6 are early stages, and stage 7-10 are mid stages. During stage 6 of oogenesis, the oocyte nucleus is localized at the posterior pole. During stage 9, the oocyte nucleus moves to the anterior position, the future dorsal side of the egg chamber. A magnification of a stage 9 egg chamber depicts the mRNA localization of three axis determinants: *bicoid* (*bcd*), *gurken* (*grk*), *oskar* (*osk*), the organization of cytoskeletons, and the position of oocyte nucleus. The dorsal-ventral (DV) polarity is established by asymmetrically localized Gurken around the oocyte nucleus (Neuman-Silberberg and Schüpbach, 1993), activating EGF signaling. The figure is modified from (Roth and Lynch, 2009, review).

During stage 6 of oogenesis, the oocyte nucleus is localized at the posterior pole. The mRNA of *gurken* encodes a transforming growth factor ($TGF\alpha$) which is the ligand for the epidermal growth factor receptor (EGFR) (Neuman-Silberberg and Schüpbach, 1993). After translation, Gurken protein is then secreted from the oocyte and activates the receptor on the adjacent follicle cells (Queenan et al., 1999). This triggers a back signaling from the posterior follicle cells and results in the re-organization of microtubules inside the oocyte (Theurkauf et al., 1992). The growing microtubules push the oocyte nucleus to the anterior side neighboring the nurse cells and the follicular epithelium, which

is a symmetry-breaking event (Zhao et al., 2012). If the oocyte nucleus does not move to the anterior position, the DV polarity is disrupted (Micklem et al., 1997). Although the types of meristic ovaries differ among different species, the movement of the oocyte nucleus is a symmetry-breaking event in insects (Lynch et al., 2010).

1.3.2 Determination of DV polarity during oogenesis

During oogenesis, the dorsal-ventral (DV) polarity is established by asymmetrically localized Gurken around the oocyte nucleus (Neuman-Silberberg and Schüpbach, 1993), activating EGF signaling. The *Drosophila* EGF receptor is Torpedo, which is distributed in the follicular epithelium surrounding the oocyte (Roth and Schüpbach, 1994). However, only the follicle cells neighboring the oocyte nucleus receive the second round of signaling from Gurken protein and exclusively activate the EGF signaling pathway. Activated EGF signaling represses *pipe*, and restrict its expression to a ventral domain (Sen et al., 1998). EGF signaling via TGF α ligands has an evolutionary conserved role in encapsulation of oocytes and in establishing the DV axis in the ovaries of the wasp *Nasonia vitripennis*, the beetle *Tribolium castaneum*, and the cricket *Gryllus bimaculatus* (Lynch et al., 2010). Ectopic activation of the Torpedo protein/EGF receptor in *Drosophila* follicle cells dorsalizes both the follicular epithelium and the embryo (Queenan et al., 1997).

1.3.3 Communication between follicular epithelium and the embryo

The communication between follicular epithelium and the embryo is important to integrate follicular and embryonic polarity. However, how is the communication achieved since the follicular epithelium has vanished before the egg is completely formed?

When EGF signaling is activated, the expression of *pipe* is restricted to the ventral follicular epithelium (Sen et al., 1998). *pipe* encodes an enzyme similar to the glycosaminoglycan-modifying enzyme heparan sulfate 2-O-sulfotransferase. Some vitelline membrane-like (VML) components are sulfated by Pipe and being secreted and incorporated to the vitelline membrane (Zhang et al., 2009), conveying the positional information from the egg chamber to the embryo.

Although Nudel is not the direct target of Pipe, it is required for embryonic pattern-

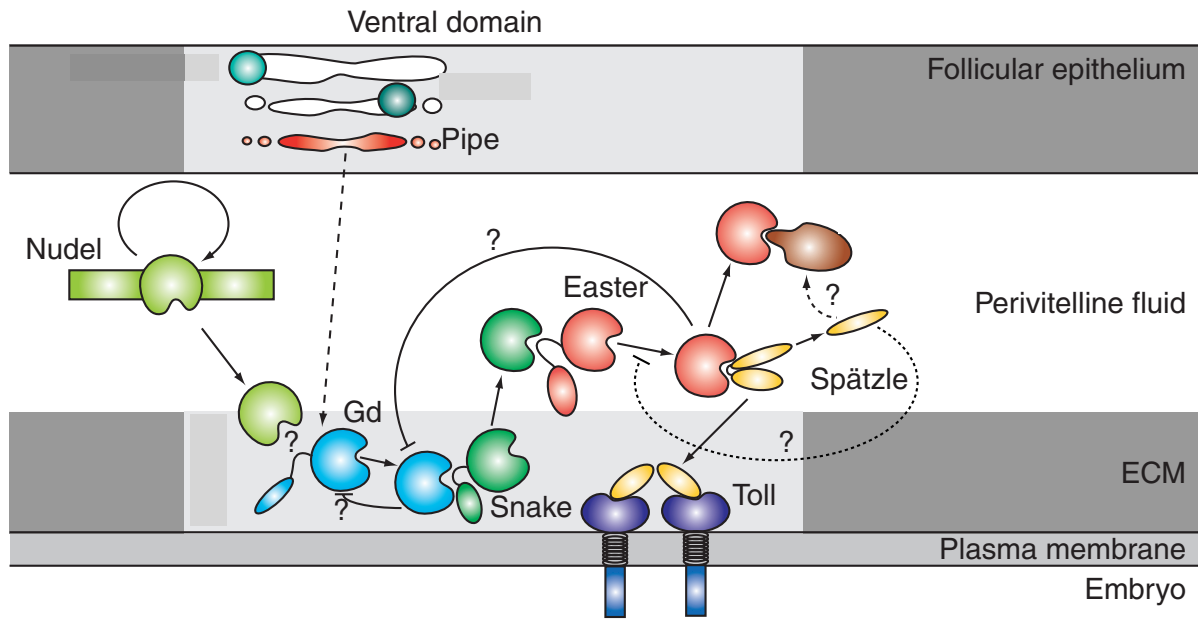


Figure 1.3. Proteolytic cascade and the activation of Toll signaling

When EGF signaling restricts *pipe* expression to the ventral follicular cells, the positional information is transferred to the vitelline membrane. This leads to a cascade of protease activation occurring in the perivitelline space, between the vitelline membrane and the oocyte membrane. The cascade of protease activation includes Nudel, Gd, Snake, and Easter resulting in the processed Spätzle. Once the Spätzle ligand is cleaved, the dimers bind to the Toll receptor, and the signaling is initiated. The figure is modified from (Moussian and Roth, 2005, review).

ing and eggshell biogenesis (LeMosy and Hashimoto, 2000) and the glycosaminoglycans (GAGs) attached on Nudel protein might need Pipe-mediated sulfation, which is important for DV patterning (Turcotte and Hashimoto, 2002). Once the eggshell biogenesis is disrupted in *nudel* mutants, the perivitelline environment might be affected and influences the activity of a downstream protease cascade (Hong and Hashimoto, 1996). The positional signal is transferred through sequentially activated serine proteases located in the fluid-filled perivitelline space between the embryonic membrane and the eggshell. The proteolytic process transform the inactive zymogen (or proenzyme) to a cleavage active form. The proteolytic cascade includes Gd (Gastrulation defective), Snake, and Easter to be activated sequentially (LeMosy et al., 2001). Besides sequential activation of the cascade, there are also some autoproteolytic and feedback mechanisms reported in the protease cascade (Dissing et al., 2001). In addition, GD also interacts with Pipe-sulfated molecules that are embedded in the ventral vitelline membrane, further facilitating the

cleavage of Easter by Snake (Cho et al., 2012).

Finally, activated Easter cleaves the Toll ligand Spätzle, generating two fragments. Functional C-terminal fragments of Spätzle dimerize through disulfide-bonds and bind to the Toll receptor (DeLotto and DeLotto, 1998), activating the Toll signaling pathway. Transplantation of the perivitelline fluid can restore the defect of some DV mutants and injection of serine protease inhibitors results in dorsalized phenotypes (Stein et al., 1991). Taken together, the proteolytic processes occurring in the perivitelline fluid are important for the DV patterning. A model for the upstream activation of Toll signaling is shown in Figure 1.3.

1.3.4 Toll signaling pathway in *Drosophila*

A scheme of the Toll signaling pathway in *Drosophila* is shown in Figure 1.4. Once the Spätzle dimers bind to the extracellular leucine-rich repeats (LRR) of the Toll receptor, Toll is activated and undergoes a conformational change (Gangloff et al., 2008). Toll signaling is mediated by the adaptor proteins Krapfen/dMyd88 (Myd88) and Tube. The activated Toll receptors recruit Myd88 adaptor proteins to the intracellular Toll/interleukin-1 receptor (TIR) domain (Horng and Medzhitov, 2001). Myd88 recruits another adaptor Tube through the death domain (DD) to achieve protein-protein interaction (Xiao et al., 1999), while the Myd88/Tube complex recruits a serine/threonine protein kinase Pelle. Pelle is activated by Tube to transduce the Toll signaling (Galindo et al., 1995) and the Pelle kinase can be further activated by autophosphorylation during Toll signaling (Shen and Manley, 2002). It is proved that Cactus, the I κ B (inhibitor of NK κ B) family member (Geisler et al., 1992), is the direct target of Pelle kinase in *Drosophila* (Daigneault et al., 2013). Phosphorylation of Cactus protein leads to Cactus degradation and releases the transcription factor-Dorsal to the cytoplasm (Bergmann et al., 1996). However, it is still under debate whether Dorsal protein is directly phosphorylated by Pelle or other kinase proteins (Edwards et al., 1997). Phosphorylation of Dorsal is important for the stability and nuclear transportation (Whalen and Steward, 1993; Drier et al., 1999). When Dorsal protein is released from the Cactus retention, it is translocated into the nucleus forming a nuclear gradient (Roth et al., 1989). Once the ventral signaling is totally disrupted, Dorsal remains in the cytoplasm (Roth et al., 1989).

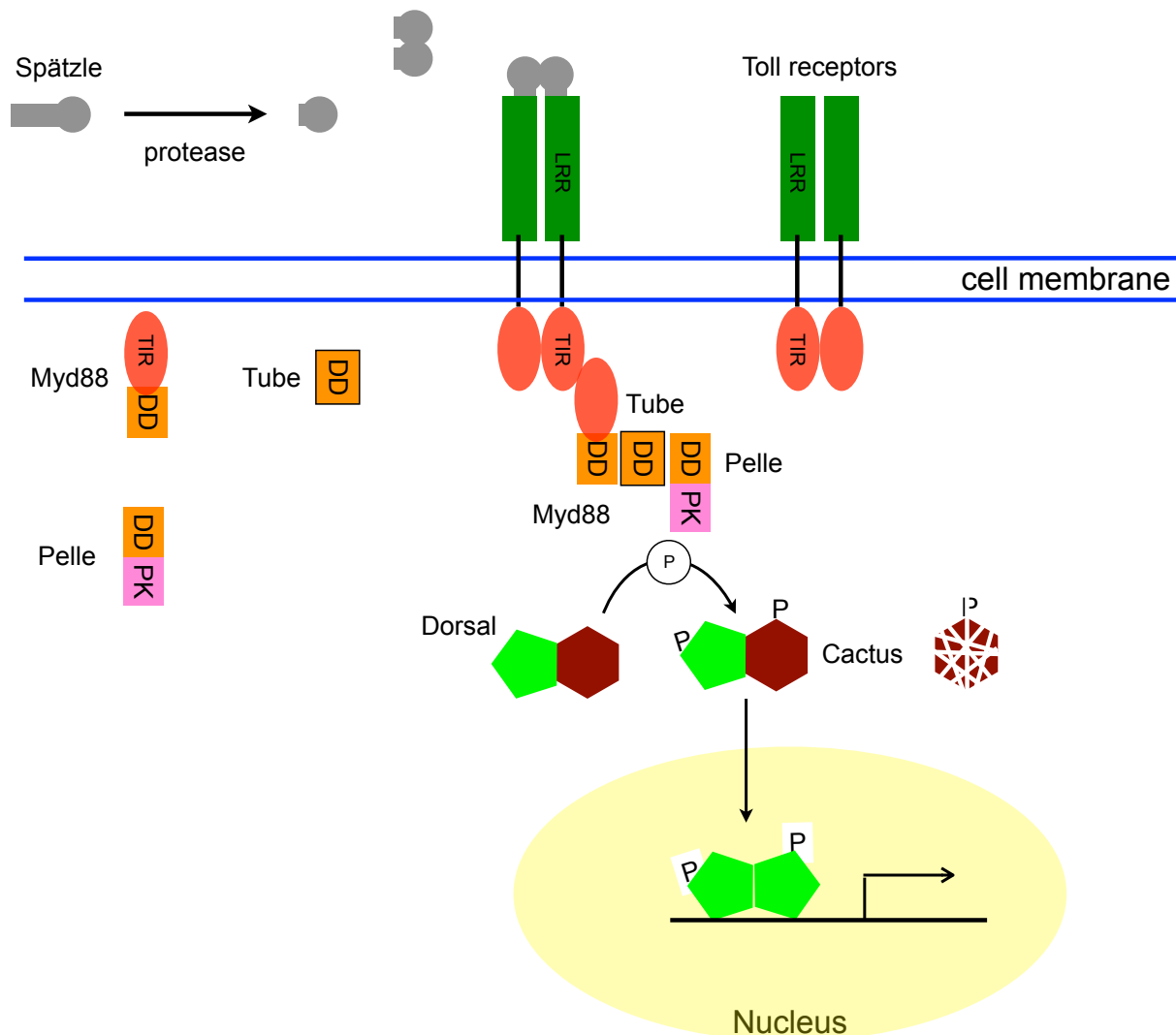


Figure 1.4. Scheme of Toll signaling pathway

Key components of the Toll signaling pathway are illustrated in this scheme. When the ligand Spätzle is cleaved through protease processing, functional C-terminal fragments of Spätzle dimerize and bind to the extracellular leucine-rich repeats (LRR) of the Toll receptor (Weber et al., 2003). Activated Toll receptors recruit Myd88 adaptor proteins to the intracellular Toll/interleukin-1 receptor (TIR) domain (Horng and Medzhitov, 2001). Myd88 recruits another adaptor Tube through the death domain (DD) and the Myd88/Tube complex interacts with a protein kinase Pelle (Xiao et al., 1999). Pelle kinase phosphorylates Cactus and leads to the degradation of Cactus, releasing Dorsal protein. Phosphorylated and dimerized Dorsal proteins are transported to the nucleus and act as transcription factors. The Toll signaling pathway in *Drosophila* is reviewed in (Valanne et al., 2011).

1.3.5 Interaction between Dorsal and its inhibitor- Cactus

With the activation of Toll signaling, Cactus is phosphorylated and degraded. The consequence of Cactus degradation is the release of Dorsal. The degradation of free Cactus

can occur through a signal-independent manner mediated through the carboxyl-terminal PEST domain, whereas signal-dependent degradation requires ankyrin repeats (ANK) (Belvin et al., 1995). The degradation of Cactus is highly reactive to the signal on the ventral side, albeit the existence of Dorsal protein stabilizes Cactus (Bergmann et al., 1996). In the *dorsal* null mutant and when the ventral signaling is blocked, Cactus cannot be detected (Belvin et al., 1995; Drier et al., 2000).

Although the dissociation of the cytoplasmic Dorsal–Cactus complex correlates with the degradation of Cactus, low level of Dorsal nuclear import can be achieved via a signal-dependent phosphorylation (Drier et al., 2000). The phosphorylation of Dorsal is important for the nuclear import (Drier et al., 2000). In the *cactus* null mutant, embryos are still polarized with a shallow gradient of nuclear Dorsal distribution (Bergmann et al., 1996). Nuclear import of Dorsal is not only dependent on Cactus degradation, but also depends on the ventral signal.

1.3.6 Nuclear Dorsal gradient and downstream target genes

Dorsal protein forms a nuclear gradient along the DV axis in the *Drosophila* blastoderm embryo, with the highest level at the ventral side while the protein remains in the cytoplasm at the dorsal side (Roth et al., 1989). However, how is the Dorsal gradient maintained in the embryo after every mitotic division? With the help of live imaging techniques using a Dorsal-GFP fusion protein, it was found that the level of nuclear Dorsal is dynamically balanced between import and export (DeLotto et al., 2007). This constant shuttling between cytoplasm and nucleus explains the dynamic maintenance of the Dorsal gradient (DeLotto et al., 2007). The nuclear Dorsal gradient specifies different cell fates along the DV axis in a concentration-dependent manner (reviewed in Stathopoulos and Levine, 2004), which is shown in Figure 1.5. At least three regions are differentiated by the Dorsal gradient, as shown in Figure 1.5. On the most ventral side is the mesodermal fate. The neurogenic ectoderm is on the lateral side and the dorsal ectoderm is determined on the dorsal side (Reeves and Stathopoulos, 2009).

As a transcription factor, Dorsal binds to the cis-regulatory regions cooperating with other transcription factors and regulating the expression of downstream target genes (Zeitlinger et al., 2007). More than 50 genes are regulated by Dorsal as downstream targets constructing a complicated gene regulatory network (Levine and Davidson, 2005).

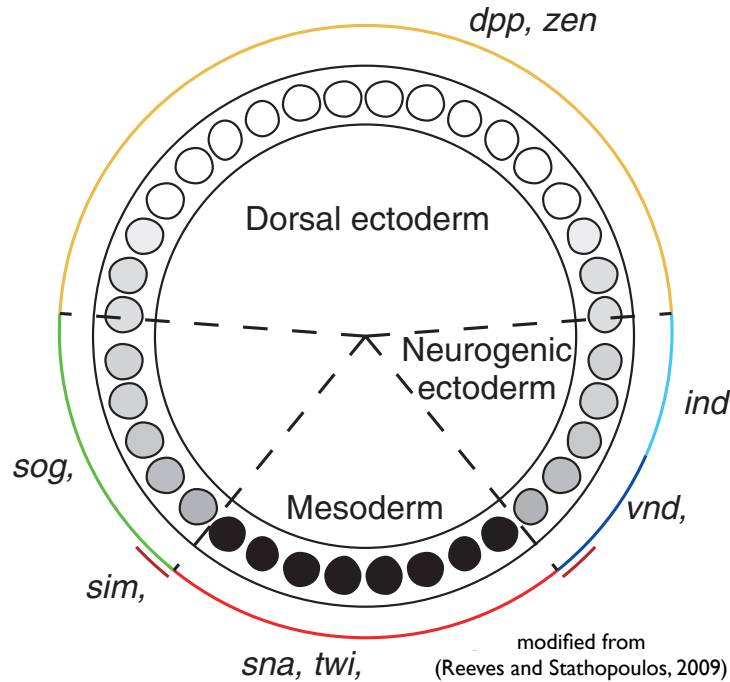


Figure 1.5. Fatemap and domains of gene expression along the embryonic DV axis

Diagram of a cross-section through an early *Drosophila* embryo.

Filled black circles represent high levels of nuclear Dorsal protein, shaded grey and empty circles represent intermediate and low levels, respectively. From ventral to dorsal side of the embryo, there are three main regions: mesoderm, neurogenic ectoderm, and dorsal ectoderm, separated by dashed lines. Downstream target genes of Dorsal are expressed in subdivided domains. The orange line indicates the expression domain of *dpp* and *zen* on the dorsal side. The green line indicates the expression domain of *short gastrulation* (*sog*) in the neurogenic ectoderm, including the expression of *ind*, *vnd* and *sim* in a more defined region. The red line indicates the mesodermal fate with the expression of *snail* and *twist* in the most ventral side (modified from [Reeves and Stathopoulos, 2009](#)).

According to the expression domain of *dorsal* target genes, Dorsal-dependent enhancers can be categorized into three groups (Type I, II, III) ([Stathopoulos and Levine, 2004](#)). Type I enhancers contain low-affinity Dorsal binding sites, or binding sites for Twist, which is a helix-loop-helix (bHLH) transcription factor cooperating with Dorsal in the mesoderm ([Stathopoulos and Levine, 2002](#)). Type II enhancers mediate the activation of gene expression by intermediate levels of nuclear Dorsal inside of the neurogenic ectoderm. Type III enhancers respond to the lowest level of nuclear Dorsal with high-affinity Dorsal binding sites located on the cis-regulatory elements of *decapentaplegic* (*dpp*) and *zerknüllt* (*zen*). These genes are expressed in dorsal regions of the embryo and repressed

by low level of nuclear Dorsal. The number and affinity of Dorsal binding sites combined with inputs from other transcription factors constitute the distinct regulatory code (Hong et al., 2008). The transcriptional outcome then drives the diverse expression patterns along the DV axis.

1.4 DV patterning in the beetle *Tribolium*

Beetles and flies have diverged about 250 million years ago (mya). In contrast to other holometabolous insects, the red flour beetle *Tribolium* has retained more ancestral traits for embryogenesis (Grimaldi and Engel, 2005), exhibiting a short-germ development. While only the head and thorax are specified early before gastrulation, the abdominal segments emerge from a posterior growth zone after gastrulation (Sommer and Tautz, 1993; Brown et al., 1994). Studies in *Tribolium castaneum* show that DV patterning genes are highly conserved, but utilized in a different way (Lynch and Roth, 2011). The Dorsal protein gradient is initiated uniformly and progressively restricted to a narrow ventral stripe (Chen et al., 2000). The Dorsal gradient is transient and dynamic reflecting negative feedback controls with downstream target genes (Chen et al., 2000; Nunes da Fonseca et al., 2008). The dynamic change of nuclear Dorsal could be attributed to multiple levels of self-regulatory circuits, which govern the DV axis formation in *Tribolium* (Nunes da Fonseca et al., 2008). Besides the Toll pathway, BMP signaling is also essential for DV patterning in *Tribolium*. The BMP inhibitor Sog is expressed on the ventral side and transports BMP ligands toward the dorsal side of the embryo establishing peak levels of BMP signaling (van der Zee et al., 2006). Furthermore, Sog is also required for the head formation and the entire neurogenic ectoderm in *Tribolium* (van der Zee et al., 2006). BMP signaling is still active even in the absence of Toll signaling and shows residual DV patterning along the AP axis in germband embryos (Nunes da Fonseca et al., 2008).

1.5 Evolution of DV patterning mechanisms

Comparative phylogenetic studies indicate that Toll signaling was recruited for DV patterning during the evolution of insects (Lynch and Roth, 2011). When considering other arthropods, DV patterning has been studied in spider embryos. The depletion experi-

ments suggest that *dpp* is required for symmetry transformation and *sog* is required for ventral patterning (Akiyama-Oda and Oda, 2006). According to the preliminary data, DV patterning in spiders does not rely on Toll signaling (personal communication with Dr. M. Pechmann). During the divergence between spiders and insects, is there a gradual change from BMP to Toll signaling governing the DV axis determination? Within insects, mechanisms of DV patterning have never been studied in more basally branching insects. Therefore, a hemimetabolous bug retaining ancestral traits might be a good candidate to address this question.

1.5.1 Reasons to study DV patterning in the milkweed bug, *Oncopeltus fasciatus*

The milkweed bug, *Oncopeltus fasciatus*, is an insect belonging to the order Hemiptera. It has been used as a research animal (Feir, 1974) and can be easily maintained in the laboratory. Furthermore, embryonic development of *Oncopeltus fasciatus* has been described in detail (Butt, 1949). The development of the milkweed bug represents a more ancestral type of short germ development with abdominal segments established from a posterior growth zone (Liu and Kaufman, 2005b). Moreover, it exhibits the presence of two extraembryonic tissues- serosa and amnion (Dorn, 1976). In contrast, *Drosophila* embryos show a derived mode of long germ segmentation with all segments determined simultaneously at the syncytial blastoderm stage (Hartenstein and Campos-Ortega, 1985). Furthermore, *Drosophila* has an extremely reduced extraembryonic development with only one extraembryonic tissue called amnioserosa (Frank and Rushlow, 1996).

Functional analysis via embryonic or parental RNAi injection with double-stranded RNA (dsRNA) is established in *Oncopeltus* (Hughes and Kaufman, 2000; Angelini and Kaufman, 2004). Recently, the maternal and early embryonic transcriptome of *Oncopeltus* has become available (Ewen-Campen et al., 2011), and the whole genome sequencing is finished and under ongoing annotation. These advantages allow us to study gene functions in the milkweed bug.

1.5.2 Objectives

The main focus of this study is to investigate the role of Toll signaling for DV axis formation in the milkweed bug *Oncopeltus fasciatus*. The purpose of this investigation is to understand the transition from BMP- to Toll- dominated DV patterning mechanism during the evolution of insects.

Chapter 2

Materials and Methods

2.1 Gene annotation and analysis

The sequence data from the *Oncopeltus* transcriptome (Ewen-Campen et al., 2011) was obtained in *fna* or *fasta* format. To conduct a local blast (basic local alignment search tool), blast databases were established using NCBI blast+ toolkit (*ncbi-blast-2.2.28+.dmg*)¹ or the BioEdit software (with PC only). Amino acid sequences of orthologs from *Drosophila melanogaster* and *Tribolium castaneum* were used to blast against the *Oncopeltus* transcriptome using the tBlastN algorithm.² Due to the assembly of the transcriptome, long transcripts were assembled into small sequence contigs. If the sequence contigs shared the identical best-hit when blasted against NCBI database using the blastX or tblastX algorithm, the sequence of the best-hit could be used as the connecting template. Specific primers of the sequence contigs could be designed to confirm the connection and the existence of the transcript by molecular cloning, which is further described in section 2.3.

DNA sequences of annotated genes were blasted against NCBI database³ using the blastX or tblastX algorithm to find a homolog in another organism. Further analysis of annotated genes were conducted using the following links:

¹The *makeblastdb* command line was typed into the terminal-based environment, for example:
`makeblastdb -in Of.fna -dbtype nucl -out Of.fna -logfile Of.logfile`
`makeblastdb -in OfORF.fna -dbtype prot -out OfORF.fna -logfile Of.logfile`

²The *tblastn* command line was typed into the terminal-based environment, for example:
`tblastn -query newseq.fna -db Of.fna -out filename.blast`

³<http://blast.ncbi.nlm.nih.gov/Blast.cgi>

Contigs were translated to corresponding peptide sequences predicted on EMBOSS (http://www.ebi.ac.uk/Tools/st/emboss_sixpack/) with 6-frame translations. Open reading frames were predicted by ORF Finder (<http://www.ncbi.nlm.nih.gov/projects/gorf/>). Translation of annotated genes were compare with orthologs from *Drosophila*, *Tribolium* and other insect species. Multiple sequence alignment was achieved by ClustalW2 (<http://www.ebi.ac.uk/Tools/msa/clustalw2/>). Conserved domains within a protein were predicted by Pfam (<http://pfam.sanger.ac.uk/>) or by NCBI conserved domain search (<http://www.ncbi.nlm.nih.gov/Structure/cdd/wrpsb.cgi>). The transmembrane domain can be predicted by TMHMM Server v. 2.0 (<http://www.cbs.dtu.dk/services/TMHMM/>). PEST motifs as potential proteolytic cleavage sites were predicted online (<http://emboss.bioinformatics.nl/cgi-bin/emboss/epestfind>). Location of signal peptide cleavage sites in amino acid sequences were predicted by (<http://www.cbs.dtu.dk/services/SignalP/>). Phylogenetic and molecular evolutionary analyses were then conducted using MEGA version 5 and 6 (Tamura et al., 2011, 2013). Sequences of the hover fly were predicted from the Sequence Read Archive (SRA) of NCBI database. Sequences from the jewel wasp *Nasonia vitripennis* (*Nv*) were kindly provided by T. Buchta. The transcriptome of the bean beetle *Callosobruchus maculatus* was kindly provided by J. Lynch.

2.2 RNA extraction and cDNA synthesis

Total RNA from a single batch of staged embryos or knockdown embryos were homogenized with Micro-pestles (Eppendorf) and extracted by TRIzol reagent (Life Technologies). RNA samples were digested with Turbo DNase (Ambion) treatment (2U/ μ l) at 37 °C for 10 minutes, followed by phenol/chloroform extraction, and precipitated in 100% ethanol. The concentration of RNA samples were measured by NanoDrop 2000c Spectrophotometer (Thermo Scientific). About 2.5 μ g of RNA was used to synthesize cDNA by SuperScript[®] VILO cDNA Synthesis Kit (Invitrogen) according to manufacturer's

protocol. For Rapid Amplification of cDNA Ends (RACE) PCR, cDNA was synthesized by SMARTer RACE cDNA Amplification Kit (Clontech).

2.3 Molecular cloning of candidate genes

Specific primers of the sequence contigs were designed by Primer3Plus

(<http://www.bioinformatics.nl/cgi-bin/primer3plus/primer3plus.cgi>).

Final concentration of forward and reverse primers were 1 μ M in a PCR reaction. A normal PCR reaction (Mullis et al., 1987) was performed using the Expand High Fidelity PCR System (Roche) following the manufacturer’s protocol. Annotated genes were cloned by PCR or cloned into TOPO TA cloning vector (Invitrogen) and the DNA sequencing was performed by the GATC Biotech company. After DNA sequencing, sequences were assembled by CAP3 programs (<http://doua.prabi.fr/software/cap3>).

2.3.1 Degenerate PCR (deg-PCR) and RACE-PCR

If there was no hit after the local blast against the transcriptome, degenerate PCRs were performed and followed by 5’ or 3’ RACE to extend the sequence information. The SMARTerTMRACE cDNA Amplification Kit (Clontech) was used for RACE. Degenerate PCR primers were designed by Block Maker and CODEHOP parameters to set the degeneracy (http://blocks.fhcrc.org/blocks/blockmkr/make_blocks.html).

Degree of degeneracy was set to less than 128. Primers designed for deg-PCR are listed in Table 2.1.

RACE-PCR primers were designed by Primer3Plus (<http://www.bioinformatics.nl/cgi-bin/primer3plus/primer3plus.cgi>).

The criteria for RACE primer design was described in the SMARTerTMmanual. RACE PCR programs were performed according to manufacturer’s protocol (Clontech) with Expand High Fidelity PCR Polymerase (Roche). RACE PCR primers are listed in Table 2.2.

Table 2.2. Primers designed for RACE-PCR

Name	F or R	Primers (5’-3’)
------	--------	-----------------

<i>twist</i>	R	CATCCTCCAGACGCTGAAGGCGTAG
<i>SoxN</i>	R	AGACCGGCGTCCAGCAAGTAGTCTC
<i>dorsal-2</i>	R	GATTGGCAAAGGTGGCAGTCATGGT
<i>msh</i>	F	GAGGCGGAGATCGAGAAGCTGAAGA
<i>vnd</i>	R	AGACCTTTCTCCTGTTGCGCCCTCT
<i>ind</i>	F	CCAACATGTACCTCTCCAGGCTGCG
	R	GGTCCCAAGTCCACCATGCCCTG
<i>myd88</i>	F	TCTTGAAAGTCCTGCAAACAAA
<i>cactus-1</i>	F	CACTGACACGGAAGAGGAAGATGAAG
	R	CGGTGCTACTGCAATTTGTAGCGGTGTA
<i>pipe</i>	F	TCCCTAGGTTCTTCAGAGGTGCCCA
	R	AGATCCTGTGGAGAGGGTGATCTCTTGG
<i>spätzle-2</i>	R	CACATGGCACAACACCAGTCTCAT
<i>snail</i>	R	CAAGTGCAAGCTCTGCGGCAAGG
<i>imd</i>	F	GTAAACATAGTTGGAAGGAATTAGCA
	R	ATATAGGCTGACAGTCGTTTAGCAG

Table 2.1. Primers designed for deg-PCR

Genes	Primers (5'-3')	Product size (bp)
<i>sim</i>	CCGCCATCACCTCCCAGytngayaargc GTCAGGAACCGGTAGTACTTGgtngtnacytg	546
<i>msh</i>	AAGTGCAACCTGCGGaarcayaarmc GCGGCCATCTTCAGCTTYTCNADYTC	237
<i>vnd</i>	TGTTTCAGCAAGGCCCAGacntwygaryt GTCTCTCACCAGCACGGGNACNGCNAC	273
<i>ind</i>	ATGTCCCGGTCCttyytnrtnga GCTTCACCCGCCGGttytgraacca	508

Symbols:

A+C+T+g=N, A+g=R, C+T=Y, A+C=M, T+g=K, C+g=S, A+T=W, A+T+C=H, T+C+g=B,
A+T+g=D, A+C+g=V

2.4 Probe and double-stranded RNA (dsRNA) synthesis

Specific primers used for cloning were designed by Primer3Plus ⁴, with linkers (Forward Linker 5'-ggccgcgg; Reverse Linker 5'-cccggggc) attached to the 5' end. Self-complementarity of primers with linkers was checked with the OligoCalc program ⁵. All gene-specific primers for probe synthesis are listed in Table 2.3. The cDNA extracted from embryos or ovaries was used as the template for PCR amplification. The PCR amplification were performed with *ReadyMix*TM Taq PCR Reaction Mix (Sigma) following the manufacturer's standard PCR protocol. Products from the first PCR were used as templates for the second PCR with the annealing temperature at 58°C. To make the template for a labeled antisense probe, a gene-specific forward primer together with the T7 3' universal primer (agggatcctaatacgaactcactatagggcccgggc) were used. To make the template for a control sense probe, a the gene-specific reverse primer together with the T7 5' universal primer (gagaattctaatacgaactcactatagggccgcgg) were used. Probes were synthesized by T7 RNA polymerase (Roche) mixed with DIG (digoxigenin) RNA Labeling Mix (Roche) and Protector RNase Inhibitor (Roche) and incubated at 37°C for four hours. Products were precipitated by 100% ethanol, washed with 70% ethanol, and resuspended

⁴Primer3Plus (<http://www.bioinformatics.nl/cgi-bin/primer3plus/primer3plus.cgi>)

⁵OligoCalc (<http://www.basic.northwestern.edu/biotools/oligocalc.html>)

in probe solution (50% formamide, 2X SSC).

Table 2.3. Gene Specific primers for probe synthesis

Probes		Primers (5'-3')	Product size (bp)
<i>sog</i>	F	GTTTGGCAAGTCGTTTCGTA	1182
	R	TTCTACCAGCCTTGGTGAGG	
<i>twist</i>	F	TCGGAGCTTTGCCGAGAC	706
	R	GGAATAGTAACATTTCTGGCTTGG	
<i>sim</i>	F	CCTCCATCATCAGACTGACC	648
	R	GCGAGAAGTGTATGATGAGAATATC	
<i>soxN</i>	F	CAGCACCTCATCATCAGC	839
	R	AGGTTGGCACTGGGATCA	
<i>msh</i>	F	ACCTGCGGAAGCACAAGC	1032
	R	TCTGATTTGCTATAATAATGAACTGC	
<i>vnd</i>	F	AGCAGTGGTACAACGCACAG	751
	R	CGTCTTGTACCTGTGGTTCTGA	
<i>ind</i>	F	GGGCAAGCAGTGGTATCAA	1039
	R	TACTTACATCTAATCACAGCACGTC	
<i>otd</i>	F	GGCCCTCGCTGTGAACAT	958
	R	TGGTTTCATTTGCGATGGT	
<i>Toll-1</i>	F	CAGTTCACACTCACATTGAATTACT	1162
	R	GGATATGTGACTGTCAAGCAAA	
<i>dorsal-1</i>	F	CCCTCCTTACAGACCTCATCC	1394
	R	AGAGAGAGATGAGAAGGATGTcG	
<i>dorsal-2</i>	F	GCAAGCCTCGTAAAGCTATCA	1297

	R	GGGCGTGCTGTAGTAGTTGTC	
<i>cactus-1</i>	F	AGGACTTGACTCCCACATCG	1365
	R	TGCACTATATACAAATATGAGACCACA	
<i>cactus-2</i>	F	GTGCGTCGTAACGTCaTAGC	1098
	R	CCGACAGACTGGACGA _g GTA	
<i>cactus-3</i>	F	TTCAATTATCaTATATGTTGGTTTCCA	1262
	R	CATTGTGACAGTAACCGGTGTG	
<i>cactus-4</i>	F	AGTG _g CTTCGAaTCTTGGTG	1387
	R	TCT _g CTCTCATTCTTCATTG	
<i>TGFα</i>	F	AGTGGCAGATCCGGTACG	1026
	R	AGGGCTATATAGAACAATAAGGGTTG	
<i>pipe</i>	F	CTGCCTTCAGATCGGTGAGT	1136
	R	TAACGGGTGGTTTGAAGGAG	
<i>nudel</i>	F	TGATGaaCGATGTGGCacT	944
	R	ACTGCATTTGATTGGAAT _g G	
<i>gd</i>	F	CaACTTCCAgGGCaAgGtaA	1432
	R	CCTTAAATGCCAGGCCAGT	
<i>snake</i>	F	CCCAATTCATTATTGTTCTGTG	1687
	R	TCCATAACCTGAAGTACAAATCC	
<i>spätzle-1</i>	F1	GACTGCAGAAGCTCCCTGTC	1150
	R1	CTGGGCAGAGAAGAATTTGG	
	F2	GGCGTACATATTTAGGCTTTGC	1376
	R2	GAGTGGTGTGTGTGGGTTTG	
<i>spätzle-2</i>	F	CCCTACGTGCACTTCAACA	775
	R	TTATTTACATGAAGATCACAAACATGA	

<i>snail</i>	F	TCGTCAAGGATGAGGATAACA	924
	R	CTGCAATTCCGACAGGAGTA	
<i>klumpfuss</i>	F	CAGGATTCTCCTCTCGACTTG	1118
	R	GGAAATGATTGTTTAACAGTGCTTAG	

Sequence of *engrailed* was obtained from NCBI database with the accession number AY460340.1, which was published in [Liu and Kaufman \(2004\)](#). The probe design of *orthodenticle (otd)* was obtained from the RACE-PCR data, which extended the partial sequence of *otd* kindly provided from Dr. J. Lynch).

Specific primers for dsRNA synthesis are listed in Tabel 2.4. Both of the T7 5' and 3' universal primers were used in the second PCR reaction to make the dsRNA. The dsRNA was synthesized by MEGAscript RNAi Kit (Ambion) according to manufacturer's protocol. If dsRNA products were longer than 800 bp, they were incubated at 75°C for 5 min, and left on the bench to cool to room temperature. After synthesis, products of the probes and dsRNAs were run on an agarose gel by electrophoresis. To avoid off-target effects via pRNAi, dsRNA sequences were verified by a web-based estimation (<http://dsCheck.RNAi.jp/>).

Table 2.4. Gene Specific primers for dsRNA synthesis

dsRNA		Primers (5'-3')	Product size (bp)
<i>Toll-1</i>	F1	AGATATGGCTATACTCTCACCGATT	479
	R1	GAGGGAGAGCATAGCGGAGT	
	F2	ATTCCCATTCCGGCTAGAAGG	387
	R2	GGATTGCTAACATCGCACTTG	
<i>myd88</i>	F	TCTTGAAAGTCCTGCAAACAAA	572
	R	TTGAAAGGAGAGAAGCAGTTG	
<i>pelle</i>	F	CCATATCAGGAACGAAAGACA	490
	R	TGAGTCTCAGGTTTCATCTCCAA	

<i>tube-like kinase</i>	F	GCAGCTTATCTTTTCGGATTCA	554
	R	CaGGCATTaTATGGaCTTGCAG	
<i>dorsal-1</i>	F	CAGACAATGTGACAAAGCCATA	557
	R	TGAGAAGATCAAGTGTGGCTTT	
<i>dorsal-2</i>	F	CAACGATACAGATTGTTGGATATAA	744
	R	TTCATTCCCTTGTCGATCTGG	
<i>twist*</i>	F	TCGGAGCTTTGCCGAGAC	706
	R	GGAATAGTAACATTTCTGGCTTGG	
<i>pipe</i>	F	GGGACCACATACAGCGAGTT	640
	R	TAACGGGTGGTTTGAAGGAG	
<i>nudel</i>	F	TGATGaaCGATGTGGCacT	533
	R	TTGCAGCGAGATCTTCTTGA	
<i>cactus-1*</i>	F	AGGACTTGACTCCCACATCG	1365
	R	TGCACTATATACAAATATGAGACCACA	
<i>cactus-2*</i>	F	GTGCGTCGTAACGTCaTAGC	1098
	R	CCGACAGACTGGACGA _g GTA	
<i>cactus-3*</i>	F	TTCAATTATCaTATATGTTGGTTTCCA	1262
	R	CATTGTGACAGTAACCGGTGTG	
<i>cactus-4*</i>	F	AGTG _g CTTCGAaTCTTGGTG	1387
	R	TCT _g CTCTCATTCCCTTCATTG	
<i>spätzle-1</i>	F	GGCGGAGCACCTACATTAAA	408
	R	TCATTCAATTTATTTGTTGATGAAA	
<i>spätzle-2*</i>	F	CCCTACGTGCACTTCAACA	775
	R	TTATTTACATGAAGATCACAAACATGA	

<i>relish</i>	F	CCTGGACATTATTGAGCAACCT	717
	R	TTGCTTCCCACATTCTCTTT	

The primers for dsRNA (marked with *) are identical to the specific primer for probe synthesis (Table 2.3). The dsRNA of *dpp* was kindly provided by L. Sachs (Sachs, 2014).

2.5 Animal husbandry, embryo fixation, and ovary dissection

2.5.1 Husbandry of animals

The large milkweed bugs *Oncopeltus fasciatus* were cultured in an incubator (Rubarth Apparate GmbH) at 25°C, supplied with water and de-hulled sunflower seeds. Detailed husbandry conditions for *Oncopeltus* were described in Liu, Paul and Kaufman, Thomas C. (2009). Embryology of the milkweed bug has been well studied (Butt, 1949). The developing processes of *Oncopeltus* cultured at 22°C were described in Capco and Jeffery (1977). There is no major difference to the embryogenesis schedules if the bugs were cultured at 22 or 25°C, so the developmental stages can be calculated approximately. Once the bugs mated, adult females will lay eggs on the cotton. Embryos of different stages were collected according to the time table (Table 2.5).

Table 2.5. The embryogenesis schedules of *Oncopeltus fasciatus*

Approximate time (hr after egg lay, AEL)	Developmental stages	Characteristic event
0-16	Nuclear division	energids migrate to the periplasm
18-24	Early blastoderm	syncytial blastoderm without obvious yolk nuclei
26-32	Mid blastoderm	cellularized blastoderm with yolk nuclei
32-36	Late blastoderm	the invagination site appears on the posterior side
38-40	Invagination	embryo starts to invaginate into the egg lateral condensation of nuclei
40-48	Germband elongation	germband extended from the posterior to the anterior
54-92	Gastrulation	
92-220	Organogenesis	
220	Hatching	nymph

The developmental events are summarized from (Capco and Jeffery, 1977).

2.5.2 Fixation of embryos

Eggs were collected into the Screw-Capped Microcentrifuge Tubes (SARSTEDT), and filled with distilled water (ddH₂O). Eggs were boiled for 3 minutes in water and kept on ice for 5 minutes. After adding heptane and methanol with gently shaking, eggs will be cracked. Embryos were fixed for 1 hour in 4% formaldehyde in PBT (phosphate buffered saline with 0.1% Tween-20), as previously described ([Liu and Kaufman, 2004](#)). Fixed embryos were stored in methanol at -20°C.

For some antibody stainings, the usage of methanol should be avoided. Instead, the eggs were boiled, briefly fixed and the eggshell was removed manually by fine forceps in PBS (phosphate buffered saline) solution. The dissected embryos were fixed again for 1 hour in 4% formaldehyde in PBT. After fixation, there was one extra step to increase the permeability by adding iced acetone for 1 minute. Embryos were washed several times in PBT and the freshly fixed embryos were prepared for the immuno-staining.

2.6 Ovary dissection

Female bugs were anesthized by CO₂. Ovarioles were carefully dissected out from the abdomen using fine forceps. The sheath surrounding the ovarioles were carefully removed on double-sided tape immersed in PBS. Dissected ovarioles were washed in PBT and then fixed in 4% formaldehyde for one hour, followed by several PBT washing and stored in methanol at -20°C. Ovarioles were mounted on glass slides with 2 spacers, which were made from the coverslips. Samples were analyzed under the ApoTome.2 microscope (Zeiss).

2.7 RNA interference and the analysis of knockdown phenotypes

2.7.1 Parental RNA interference (pRNAi)

Gene-specific dsRNA for pRNAi were injected into virgin females ([Angelini and Kaufman, 2004](#)). The procedures of pRNAi injection was described previously ([Liu and Kaufman,](#)

2004). The dsRNA was diluted in injection buffer (0.1 mM NaPO₄, 5 mM KCl, pH=6.8) (Hughes and Kaufman, 2000) and loaded in the Hamilton syringe (Hamilton). About 5 μ l was injected into the the abdomen of virgin females. The injection position was between 4th and 5th segment boundaries (sternites) in the abdomen (Figure 2.1). It is suggested not to inject close to the ventral midline to avoid damaging the nervous system. After each injection, the syringe was cleaned with 3% H₂O₂, 1% Tween-20 in PBS, and rinsed by injection buffer before the next injection. Females injected with only the injection buffer were used as the mock-treated control. Injected females were cultured individually and crossed with two males on the next day after injection.



Figure 2.1. Adult injection

The needle was inserted into the abdomen of female *Oncopeltus*.

2.7.2 The morphological analysis of knockdown phenotypes

Eggs laid by the injected females were collected and kept at 25°C for further development. After 7 days of development, knockdown embryos were analyzed using the stereo microscope Stemi 2000 (Zeiss). Percentage of knockdown phenotypes was also calculated. Pictures of the knockdown phenotypes were taken under the microscope- SteREO Lumar V12 (Zeiss). Knockdown embryos from the collection of 7-21 days post-injection were fixed and stored in methanol at -20°C for fuchsin staining or *in situ* hybridization (ISH). After ISH, late germband stage embryos were immersed in 80% glycerol in PBS, dissected out carefully, and mounted on slides. Pictures were taken using the SteREO Lumar V12 microscope (Zeiss).

2.7.3 Fuchsin staining

The alcoholic fuchsin staining was modified from (Barbara Wigand, 1998), which was used in *Tribolium* embryos. Fixed embryos (described in section 2.5.2) were transferred to glass vials and washed in 70% ethanol for 20 minutes. Once the ethanol was removed, 2 N HCl was added and the embryos were incubated at 60°C for 10 minutes, followed by ddH₂O washing for 5 minutes and 70% ethanol 2 times for 5 minutes. After washing, the embryos were incubated in fuchsin staining solution (100 mg Pararosanilin in 4 ml distilled water and 16 ml absolute ethanol) for 30 min. Excessive color was washed out with 95% ethanol several times. At last, the embryos were dehydrated by 100% ethanol and sequentially immersed in Solution C (100% ethanol : solution D= 1:1) and solution D (also called BBBA, Benzyl benzoate : Benzyl alcohol= 4:1). Stained embryos were stored at 4°C, protected from light.

2.8 Knockdown efficiency validation

The efficiency of RNAi is variable depending on the studied genes. It is feasible to test the knockdown efficiency by a semi-quantitative PCR (Marone et al., 2001) to assess the expression levels of multiple transcripts. The PCR amplification were performed with ReadyMix™ Taq PCR Reaction Mix (Sigma) with the elongation time about 30 seconds, 30 thermal cycles, and annealing temperature at 60°C. The cDNA of knockdown embryos was synthesized by the protocol described in section 2.2 and 50 ng of cDNA was used as the template for the PCR reaction. Gene-specific primers for the semi-quantitative PCR were designed by Primer3Plus and listed in Table 2.6. PCR products were examined on a 0.5% agarose DNA gel electrophoresis in 0.5X TAE buffer. SmartLadder MW-1700-10 (Eurogentec) was used as the DNA size marker.

2.9 Quantification of gene expression level

A quantitative polymerase chain reaction (qPCR), also called real-time PCR, was performed to measure the expression level of target genes by 7500 Fast Real-Time PCR system (Applied Biosystems). Specific primers were designed by GenScript (<https://www.genscript.com/>).

Table 2.6. Gene-specific primers designed for the validation of knockdown efficiency

Genes	Primers (5'-3')	Product size (bp)	
<i>actin</i>	F	AGTTGCTGCACTCGTTGTTG	133
	R	TCCCATACCGACCATCACTC	
<i>Toll-1</i>	F	CAGCAATGCCTACGAACTCA	148
	R	GCCACTGACCAATGACAGTTT	
<i>dorsal-1</i>	F	GCTTGCAGTGAGACAAGAGC	296
	R	ACAATTGCCCAGGTGTGTTA	
<i>dpp</i>	F	GCTGAAATCCGAGACAGTGA	143
	R	CCTTTGCCGAGTCTAGCAGT	

The amplicon of *actin* transcripts served as the control.

([//www.genscript.com/ssl-bin/app/primer](http://www.genscript.com/ssl-bin/app/primer)). The PCR amplicon size was ranging from 75 to 150 bp. All of the qPCR primers were listed in Table 2.7.

Table 2.7. Gene Specific primers for qPCR

Genes	Primers (5'-3')	Amplicon size (bp)	
<i>18S ribosomal</i>	F1	GATGACTACCGGCGAGATTT	100
	R1	CCCAGAACATCTAAGGGCAT	
<i>twist</i>	F1	TCGGACAAGCTCTCCAAGATAC	147
	R1	GTAGGCGCACTCTGACATCC	
<i>sog</i>	F1	TGTCTGGTTGAGCCACATTCCACT	78
	R1	TTGCCATGTCCGCAGTCTATCAGT	
<i>Toll-1</i>	F1	CAGCAATGCCTACGAACTCA	148
	R1	GCCACTGACCAATGACAGTTT	
<i>dpp</i>	F1	GCTGAAATCCGAGACAGTGA	143
	R1	CCTTTGCCGAGTCTAGCAGT	

The *18S ribosomal* served as the reference gene.

2.10 *In situ* hybridization (ISH)

Detection of gene expression was performed by ISH with digoxigenin (DIG)-labeled probes. The protocol used here was mainly described by (Liu and Kaufman, 2004), with slight

modifications. The antibody blocking solution was made from 2% Blocking reagent (Invitrogen), 1% Bovine Serum Albumin (BSA, Sigma), and 10% normal goat serum (NGS) in PBT (with 1% Tween-20). The NBT/BCIP Stock Solution (Roche) was diluted in fresh prepared alkaline phosphatase (AP) buffer (0.1M Tris-HCl, 50mM MgCl₂, 100mM NaCl, pH=9.5). Levamisole (Sigma) was added to the AP buffer (final concentration is 1mM) to reduce the background alkaline phosphatase activity. Coloration was developed by keeping in dark at room temperature for 4 hours to few days.

During whole-mount ISH, a method of solution exchange using handmade mesh-bottom baskets was applied to facilitate the handling (Yu and Holland, 2009). The mesh basket was made from the 1.5 ml eppendorf tube and the nylon mesh (pore size is 20 μ m) was attached to the bottom on a heating plate. The mesh baskets were placed into a 24-well plate as shown in Figure 2.2. A triple mesh-basket was made from 0.6 ml microcentrifuge tubes. The triple mesh-baskets were placed into a 12-well plate as shown in Figure 2.2. An advantage to do ISH in the triple mesh-baskets was that three different batches of eggs (or ovarioles) can be tested under the same condition.

2.10.1 Two-color double ISH

To perform two-color double ISH, two different probes were labeled with Fluorescein and DIG RNA Labeling Mix (Roche), respectively. The anti-Fluorescein-AP and anti-DIG-AP antibodies were used sequentially for the detection. Detection of the two-color ISH was performed by HNPP and NBT/BCIP, respectively. When the first-color staining is completed, embryos were incubated in 0.1M Glycine-HCl, pH=2.2 with 0.1% Tween20 for 10 minutes to inactive the first AP antibody, followed by washing, blocking, and the second anti-DIG-AP antibody incubation. The other procedures are identical to the single color *in situ*.

2.10.2 Fluorescent ISH (FISH)

To perform fluorescent ISH, DIG-labeled probes and anti-DIG antibodies (Roche) conjugated with alkaline phosphatase (AP) or horseradish peroxidase (HRP) were used. Before anti-DIG-HRP antibody incubation, *Oncopeltus* embryos were treated with 0.3% hydrogen peroxide (H₂O₂) to block endogenous peroxidase, followed by several PBT washing.



(a) mesh baskets in 24-well plate

(b) triple mesh-baskets in 12-well plate

Figure 2.2. handmade mesh-bottom baskets placed in plates ready for ISH

Detection was developed by HNPP Fluorescent Detection Set (Roche) or Tyramide Signal Amplification (TSA) Kits- Alexa Fluor 488 (Invitrogen) together with the TSA plus DNP system (PerkinElmer) to amplify the signal.

2.11 Antibody production and western blot

2.11.1 Molecular cloning

Partial sequence of *dorsal-1* (*dl1*) and *dorsal-2* (*dl2*) was cloned by Expand High Fidelity PCR Polymerase (Roche). The fragment of *dl1* encoding the Rel-homology domain (RHD) was cloned into pRSET A vector (Invitrogen) using XhoI and HindIII restriction enzyme cutting sites. Specific primers for cloning were listed in Table 2.8. Plasmid DNA of these constructs was transformed into BL21(DE3)pLysS competent cells (supplied by the pRSET A, B, and C kit; Cat. no . V351-20).

The fragment of *dl2* encoding the Rel-homology domain (RHD) was cloned into pENTRTM/SD/D-TOPO[®] (Invitrogen) and then ligated to Gateway pET-62-DEST (Novagen) vector by Gateway LR ClonaseTMII enzyme mix. Plasmid DNA of construct was transformed into Rosetta competent cells (Merck Millipore). Specific primers for cloning were listed in Table 2.8. Values of pI were listed in the last column of Table 2.8. Theoretical pI was calculated by the ProtParam tool (<http://web.expasy.org/protparam/>).

Table 2.8. Specific primers of constructs used for protein induction

Constructs	F or R	Primers (5'-3')	Predicted size (aa)	Theoretical pI
Dl1-RHD	F	CTCGAGAGGTtCAGACATGGTtGTGAGG	284	9.57
	R	AAGCTTCCAGTGCTATGCCTCAACC		
Dl2-RHD	F	CACCATGACTGCCACCTTTGC	383	6.25
	R	AAGCCTCGTAAAGCTATCAGTGTTGT		

Dl1-RHD was constructed in the pRSET A vector and Dl2-RHD was constructed in the Gateway pET-62-DEST vector.

2.11.2 Protein induction

The competent cell BL21(DE3)pLysS was specifically designed for expression of genes regulated by the T7 promoter. Transformation was made by a heat-shock at 42 °C water bath for 45 seconds and incubated on ice for 5 minutes. Then, 1 ml SOC medium (Sigma) was added to incubate at 37 °C for one hour. After centrifuge in 10,000 g, only 20-50 μ l medium mixed with the pelle was spread on the LB plate containing 50 μ g/ml Ampicillin. On the next day, a single recombinant clone was picked and incubated in 5 ml of LB medium containing 50 μ g/ml Ampicillin at 37 °C overnight. On the next day, the cultured 5 ml medium was poured into pre-warmed 50 ml LB medium containing 50 μ g/ml Ampicillin. The culture was incubated at 37 °C with vigorous shaking until the OD₆₀₀ value was 0.4-0.6. 1 ml of the culture was collected as the non-induction group. After centrifugation, the pellet was mixed with 5X loading buffer (0.3M Tris, pH=6.8, 0.2M DTT, 4% SDS, 40% glycerol, 0.5M β -mercaptoethanol and 1% Bromophenol) and stored at -20 °C. The isopropyl β -D-1-thiogalactopyranoside (IPTG) was added to a final concentration of 1 mM and the culture was incubated at 37 °C with vigorous shaking for 4 to 6 hours. After IPTG induction, 1 ml aliquots of cells were collected every hour as induction groups, followed by a centrifugation and the pellet was resuspended in 5X loading buffer and stored at -20 °C. The final culture was harvested at 37 °C for the optimal time (about 4 to 6 hours). About 10-20 μ l of each samples were loaded to the appropriate SDS-PAGE gel after boiling for 5 minutes, and the electrophoresis was performed.

2.11.3 Protein purification

After induction, more than 50 ml of bacteria cells were collected and centrifuged. Lysis buffer with pH value different from pI (listed in Table 2.8) was used to avoid the formation of inclusion-body (insoluble proteins). The RIPA Buffer (150mM NaCl, 1% NP-40, 0.5% sodium deoxycholate, 0.1% SDS, 50mM Tris, pH=8.0) was used here as the lysis buffer. Induced Fusion protein labeled with poly-histidine (6xHis) tag was purified by the ProBondTM purification system (Invitrogen, Cat. no. R801-01), following manufacturer's instructions. Purified proteins were lyophilized in 20 μ l aliquots and sent to the commercial company (Eurogentec) as antigens to produce a polyclonal antibody in rabbits. Further immuno-affinity purification of sera was performed by Eurogentec.

2.11.4 SDS-PAGE and Western blot

Polyacrylamide gels with 12% lower gel and 3% upper gel were made inside of the glass plate sandwiches (Bio-Rad). The chemicals of the lower gel were mixed and loaded to the glass plate sandwiches as soon as possible. The lower gel was covered by 1ml ddH₂O for more than 10 minutes for the polymerization. The recipes to make the polyacrylamid gels were listed in Table 2.9.

The chemicals of the upper gel were mixed and loaded on top of the lower gel. The comb was added on top. After polymerization for 10 minutes, the gel with glass plates were combined with the running module in the Mini-PROTEAN[®] Tetra Cell (Bio-RAD) chamber, which was filled with 1X running buffer. The 5X running buffer was made by adding 30 gram Tris base, 10 gram SDS (Sodium dodecyl sulfate), and 144 gram glycine mixed in 2 liter ddH₂O. The SDS-PAGE was performed at 200 volt (150mA) for two hours. The SeeBlue[®] Plus2 Pre-stained Standard (Invitrogen) was used as the molecular weight marker. Signals on the SDS-PAGE gel were transferred to the Protran Nitrocellulose Membrane (Whatman) in Wet/Tank Blotting Systems (Bio-RAD), which was filled with transfer buffer. The transfer buffer was made by adding 29 gram Tris base, 14.6 gram Glycine, 1.875 gram SDS, and 1 liter methanol mixed in 5 liter ddH₂O. The transfer was performed at 100 volt (150mA) for one hour. Western blot was performed following the immunoblotting protocol from the handbook of anti-HisG antibody (Invitrogen, cat No. R941-25). Diluted (1:1000) anti-HisG antibody conjugated with HRP (Invitrogen) was

Table 2.9. Recipes for the polyacrylamid gels

Chemicals and Volumes					
12% lower gel:					
30% AA	2 ml	-> 60% mix:			
60% mix	3 ml				
40% APS	10 μ l				
TEMED	10 μ l				
		Lower Tris	200 ml	-> Lower Tris:	
		Glycerol	60 ML		
		H ₂ O	120 ml		
				Tris base	18.2 g
				10%SDS	4 ml
				add HCl to pH 8.8	
				add H ₂ O to 100 ml	
3% upper gel:					
30% AA	0.2 ml	-> 90% mix:			
90% mix	1.5 ml				
40% APS	5 μ l				
TEMED	5 μ l				
		Upper Tris	31 ml	-> Upper Tris:	
		H ₂ O	80 ml		
				Tris base	6.1 g
				10%SDS	3 ml
				add HCl to pH 6.7	
				add H ₂ O to 100 ml	

AA= Rotiphorese[®] Gel 30 (37,5:1) (ROTH)
 APS= Ammoniumpersulfate in H₂O

used to detect induced fusion protein, which is labeled by 6xHis tag. Western Blocking Reagent (Roche) was used as the blocking solution (1:10 diluted in PBT). Pierce ECL Western Blotting Substrate (Thermo) was used to detect the signals with films (Kodak) in the cassette, following the manufacturer's protocol.

2.12 Whole-mount immuno-staining

BMP signaling activity was detected by the antibody phospho-Smad1/5 (Cell Signaling 41D10), with 1:30 dilution in the blocking solution. The phospho-Smad (pMad) is the readout of the BMP signaling. Details of immunohistochemistry were all described previously (Patel et al., 1989), except that we introduced the TSA plus DNP system (PerkinElmer) to amplify the signal before DAB detection (or DAB with 0.05% nickel ammonium sulfate). All of the antibody used are listed in Table 2.10.

Table 2.10. Antibody tested for immuno-staining in *Oncopeltus*

Antibody	Host species	Working Conc.	References
Primary antibody			
Phospho-Smad1/5	Rabbit	1:30	Cell Signaling 41D10
Dorsal1 (Dl1)	Rabbit	1:10	Self-produced
Dorsal2 (Dl2)	Rabbit	1:100	Self-produced
Engrailed (en) 4D9 monoclonal	Mouse	1:100	(Patel et al., 1989)
Nuclear pore complex	Mouse	1:2000	Sigma N8786 (Lynch et al., 2010)
MAP Kinase (dpErk)	Mouse	1:1000	Sigma M8159 (Lynch et al., 2010)
Secondary antibody			
Anti-Rabbit-HRP	Sheep	1:1000	Promega
Anti-mouse-HRP	Sheep	1:1000	Jackson Immunological
Anti-DNP-HRP monoclonal	Rat	1:100	PerkinElmer

Note: The secondary antibody conjugated with Alexa Fluor[®] (Life technologies) was not working in *Oncopeltus*. The TSA amplification or TSA plus DNP system (PerkinElmer) is needed for fluorescent staining in *Oncopeltus*.

2.13 Fluorescent dye staining

Some fluorescent dyes were available to use in *Oncopeltus* by simple staining procedures to visualize the nucleus or cell margins after ISH and immuno-staining. All of the fluorescent dyes tested in *Oncopeltus* are listed in [Table 5.1](#).

Table 2.11. Fluorescent dyes tested in *Oncopeltus*

Staining Target	Name	Working Conc.	Filter	Cat. No or Reference
Nucleic Acid	SytoxGreen	1:1000	FITC	Molecular Probes
	Hoechst33258*	1:1000	DAPI	Invitrogen
	Hoechst33342	1:1000	DAPI	Invitrogen
	Propidium Iodide	1:500	Cy3	Invitrogen
Plasma membrane	FM1-43FX	1:100	Cy3	Molecular Probes
	WGA (Wheat Germ Agglutinin)	1:100	FITC	Invitrogen
F-actin	Fluorescent phallotoxins:	1:40		Invitrogen
	Alexa Fluor [®] 488 phalloidin		FITC	A12379
	Alexa Fluor [®] 546 phalloidin		Cy3	A22283
	Alexa Fluor [®] 568 phalloidin		Cy3	A12380

* The Hoechst33258 was found to be more efficient than Hoechst33342 in the milkweed bug.

Chapter 3

Results

3.1 Gene annotation in the transcriptome

With the accessibility of the *Oncopeltus* transcriptome ([Ewen-Campen et al., 2011](#)), it is possible to do local BLASTs against the transcriptome to search for candidate genes.

3.1.1 Toll signaling components

The components of the Toll signaling pathway seem to be conserved, and can be found in the *Oncopeltus* transcriptome (listed in Table [3.1](#)). There are 11 transcripts coding for Toll or Toll-like receptors. Among these transcripts, only one is homologous to *Drosophila Toll-1*, which was shown to be responsible for DV patterning ([Anderson et al., 1985b](#)). Further characterization and phylogenetic analysis of Toll family members is discussed in the section [3.3](#). A gene encoding the adaptor of the Toll receptor, *myeloid differentiation primary response gene 88 (myd88)*, is also present in the transcriptome. Furthermore, there are two genes encoding serine/threonine protein kinases. One is suggested to be *pelle* and the other is *tube-like kinase*. Moreover, two NF κ B transcription factors were found in the transcriptome. In this thesis, they are given the names *dorsal1* and *dorsal2* because both of them are homologous to *Drosophila dorsal*. Further characterization and phylogenetic analysis of NF κ B family-related members is discussed in the section [3.9](#). In addition, four genes encoding the inhibitor of NF κ B (I κ B) were found, which are homologous to *Drosophila cactus*.

With the protein BLAST (BlastX) against the NCBI database, these candidates were confirmed to be the orthologs with the best matching sequences in other insect species (listed in Table 3.1). Expression of these transcripts was confirmed by PCR amplification with specific primers, followed by sub-cloning and DNA sequencing. RACE-PCRs were performed for *Toll-1*, *myd88*, *cactus-1*, and *dorsal2* to extend the 5'-end sequence.

Table 3.1. Annotation of Toll signaling components and marker genes

Category	Gene	Transcripts	Protein family	Best Hit *
Toll pathway				
	<i>Toll</i>	isotig03359†	Toll-like receptor	<i>Phc Toll</i>
	<i>myd88</i>	contig06363†	adaptor of Toll receptor	<i>Phc Myd88</i>
	<i>pelle</i>	isotig15858	protein kinase	<i>Ap pelle-like</i>
	<i>tube-like kinase</i>	isotig05547	adaptor of Toll receptor	<i>Phc protein kinase</i>
	<i>dorsal1</i>	isotig01051	NF κ B transcription factor	<i>Cb dorsal</i>
	<i>dorsal2</i>	isotig04590†	NF κ B transcription factor	<i>Rp dorsal 1A</i>
	<i>cactus</i>	cap3_contig12011	inhibitor of NF κ B	<i>Phc IκB</i>
Marker genes				
Segmentation	<i>engrailed</i> (<i>invected</i>)	AY460340.1	homeobox family	<i>Of engrailed</i>
Anterior	<i>msh</i>	ABB81837.1. †	homeobox family	<i>Ap msh</i>
Anterior	<i>otd</i>	ND †	homeobox family	<i>Of otd</i>
Ectoderm	<i>sim</i>	ND †	transcription factor	<i>Phc sim</i>
Ventral	<i>sog</i>	GAP9EXG07H2FSD GEQE5QV02IPW3J	Chordin family	<i>Ap sog</i>
Dorsal	<i>SoxN</i>	isotig18590 †	transcription factor	<i>Tc Sox-3</i>
Mesoderm, ventral	<i>twist</i>	ND †	bHLH transcription factor	<i>Phc twist</i>

* Best Hits with accession number were significant alignments obtained from NCBI using the blastX algorithm.

ND: Genes were not found in the transcriptome, but obtained by deg-PCR.

† Sequence information was further extended by RACE-PCR.

Abbreviation of insect species are listed here: *Phc*= *Pediculus humanus corporis*, *Ap*= *Acyrtosiphon pisum* (pea aphid), *Cb* = *Cerapachys biroi* (clonal raider ant), *Rp*= *Rhodnius prolixus*, *Of*= *Oncopeltus fasciatus*.

3.1.2 Marker genes

According to previous studies in *Drosophila*, *Tribolium*, and *Oncopeltus*, genes with specific expression patterns during embryonic development can be used as markers to investigate the embryogenesis and knockdown phenotypes. The candidates of marker genes were identified and annotated in the *Oncopeltus* transcriptome (listed in Table 3.1). These marker genes were cloned by PCR and confirmed to be expressed in specific regions of *Oncopeltus* embryos by ISH. The expression patterns of these marker genes are described in details in the following sections.

3.2 Early expression patterns of marker genes

In the milkweed bug, the segment polarity gene *engrailed* (*en*) is expressed in six stripes from head to thorax on the blastoderm surface (Liu and Kaufman, 2004). In later stages, it is expressed in a band of epidermal cells located anteriorly to the abdominal segment border of *Oncopeltus* germband embryos (Campbell and Caveney, 1989). According to the analysis of intron/exon structures during the genome annotation, the partial sequence of *Oncopeltus engrailed* (*en*) with the NCBI accession number AY460340.1 is claimed to be *invected*, and there is another transcript for *en* (personal communication from Dr. B. Vreede). In *Drosophila*, *en* and *invected* are closely related in sequence and pattern of expression (Coleman et al., 1987).

The marker genes and the blastodermal fate map for head development has been described by Birkan et al. (2011) in the milkweed bug. However, more marker genes are needed to study DV patterning in *Oncopeltus*, especially the genes expressed differentially on one side of the embryonic circumference during early blastoderm stages. Here, genes known to be markers along the DV axis in *Drosophila* were identified in *Oncopeltus* (Table 3.1) and the only genes with specific expression patterns in blastoderm embryos were selected as early ISH makers to identify the DV polarity such as *muscle segment homeobox* (*msh*), *single-minded* (*sim*), *short gastrulation* (*sog*), *SoxNeuro* (*SoxN*) and *twist* (*twi*). The other marker genes and detailed expression pattern during embryogenesis are shown in the supplementary data.

3.2.1 Anterior markers

In this thesis, *orthodenticle* (*otd*) and *muscle segment homeobox* (*msh*) were selected as anterior markers based on their expression patterns in blastoderm embryos. The original sequence of *otd* was obtained from Dr. J. Lynch, and the sequence was extended by RACE-PCR in this study. During blastoderm stages, *otd* is expressed anteriorly; During germband stages, *otd* is expressed in the head lobes and in a medial stripe along the trunk. The expression pattern of *otd* has been described by Birkan et al. (2011).

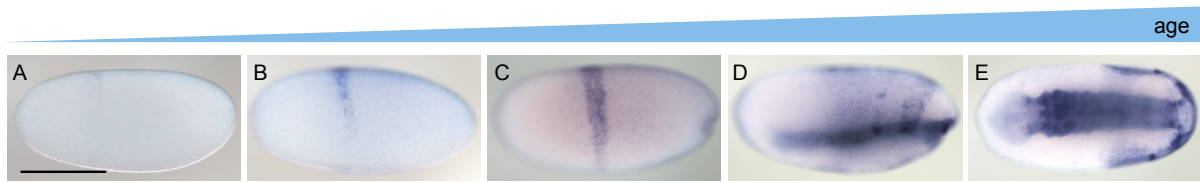


Figure 3.1. Expression pattern of *msh* in *Oncopeltus* embryos

The expression pattern of *msh* transcripts in blastoderm embryos (A-C), and after gastrulation (D, E). During blastoderm stages, *msh* is expressed in a fine stripe along the DV axis, marking the presumptive head anlage. After gastrulation, *msh* is expressed extensively on the lateral side and extended in each segments. Scale bar size corresponds to 500 μ m. Lateral view of embryos is shown in A-D; ventral view of the embryo is shown in E.

The expression pattern of *msh* is shown in Figure 3.1. In the early blastoderm embryo, *msh* starts to be expressed in a fine stripe along the DV axis, which is supposed to be part of the head anlage. Before gastrulation, the stripe extends to the ventral side (Figure 3.1C). After gastrulation, *msh* is expressed extensively on the lateral side. Similarly, early expression pattern of *msh* in the head anlage was reported in the wasp *Nasonia vitripennis* (Buchta et al., 2013).

3.2.2 Ventral markers

short gastrulation (sog)

Transcripts of the BMP/Dpp inhibitor *sog* is expressed ventrally in the beetle *Tribolium* (van der Zee et al., 2006). The expression pattern of *sog* transcripts in *Oncopeltus* blastoderm embryos is similar to the one in *Tribolium*. During the blastoderm stages, *sog* is expressed mainly on the ventral side of the embryo (Figure 3.2). The ubiquitous expres-

sion of *sog* in the beginning of syncytial blastoderm stages might be provided maternally or due the early zygotic expression (Figure 3.2A).

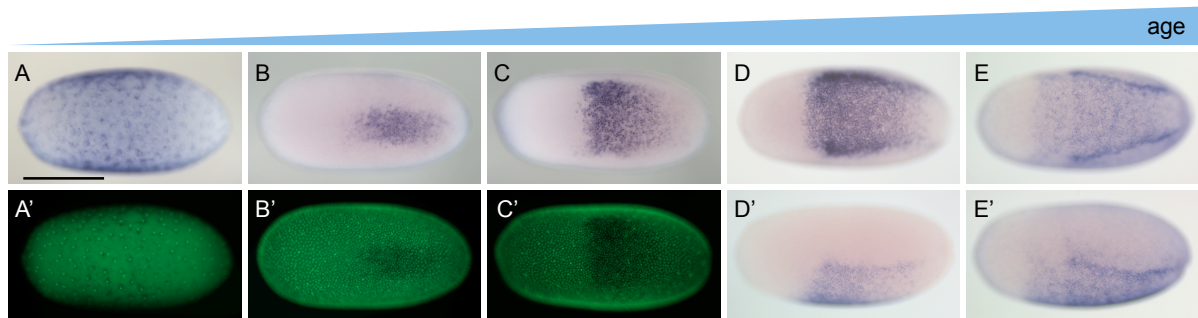


Figure 3.2. Expression pattern of *sog* in *Oncopeltus* embryos

The expression pattern of *sog* transcripts in blastoderm embryos (A-E). During the blastoderm stages, *sog* is expressed mainly on the ventral side of the embryo. In later stages close to gastrulation, *sog* is expressed more strongly in lateral stripes than on the ventral side (E, E'). Scale bar size corresponds to 500 μ m. Upper row of embryos is identical to the lower row. Ventral view of embryos is shown in A-E; lateral view of the embryo is shown in D' and E'. SytoxGreen staining of embryos is shown in A'-C', representing gradual blastoderm stages.

twist (twi)

The original sequence of *twist (twi)* was cloned by A. Drechsler, and the sequence was extended by RACE-PCR in this study. Twist is an important transcription factor required for mesoderm formation in *Drosophila* (Leptin and Grunewald, 1990; Thisse et al., 1988). Studies in *Tribolium* indicate that *twist* plays a conserved role for mesoderm formation and specification (Sommer, R. J. and Tautz, D., 1994; Handel et al., 2005). The expression pattern of *twist* transcripts in *Oncopeltus* embryos is similar to the staining in *Tribolium*. During blastoderm stages, *twist* is expressed in the ventral domain, but not in the anterior region (Figure 3.3). The *sog* expression is slightly broader than the *twist* expression domain on the ventral side of the embryo. In this thesis, *sog* and *twist* were selected as the ventral markers expressed in blastoderm embryos.

single-minded (sim)

The gene *single-minded (sim)* encodes a bHLH (basic helix-loop-helix) protein acting as a transcription factor, which is important for ventral midline development in *Drosophila*

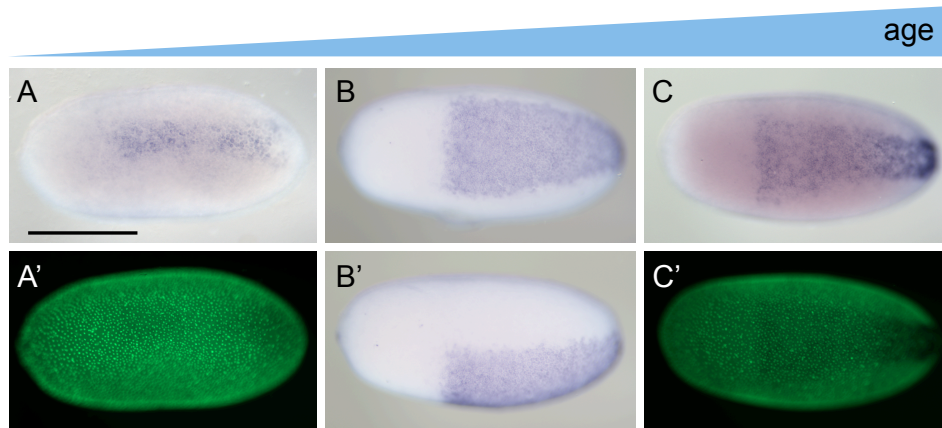


Figure 3.3. Expression pattern of *twist* in *Oncopeltus* embryos

The expression pattern of *twist* transcripts in blastoderm embryos (A-E) before gastrulation. During blastoderm stages, *twist* is expressed in the ventral domain. Expression pattern of *twist* in later stages after gastrulation is shown in supplementary data. Scale bar size corresponds to 500 μm . Upper row of embryos is identical to the lower row. Ventral view of embryos is shown in Figure A-C; lateral view of the embryo is shown in Figure B'. SytoxGreen staining of embryos are shown in A' and C', representing gradual blastoderm stages.

(Nambu et al., 1991). In the late blastoderm stage of the *Oncopeltus* embryo, *sim* is expressed in narrow lateral stripes flanking the mesoderm and in an anterior ventral stripe perpendicular to the AP axis (Figure 3.4). In this thesis, *sim* was selected as the lateral marker.

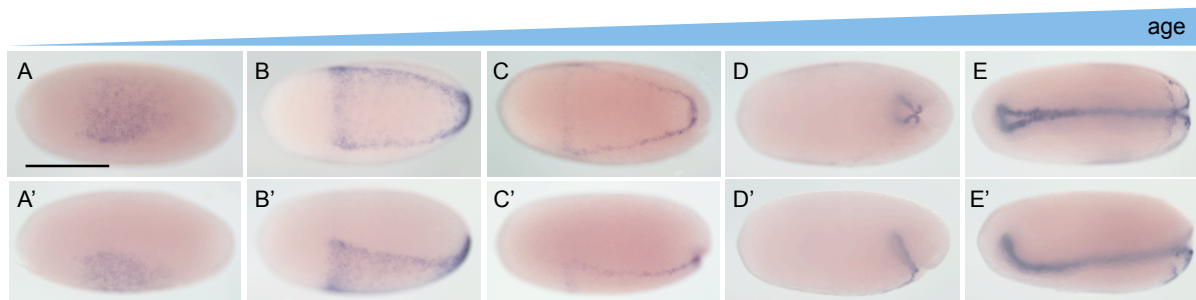


Figure 3.4. Expression pattern of *sim* in *Oncopeltus* embryos

The expression pattern of *sim* transcripts in blastoderm embryos (A-C), and after gastrulation (D, E). In the early blastoderm stage, *sim* starts to be expressed asymmetrically on one side of the embryo. During blastoderm stages, *sim* is expressed in narrow lateral stripes flanking the mesoderm. After gastrulation, it expressed in the ventral midline. Scale bar size corresponds to 500 μm . Upper row of embryos is identical to the lower row. Ventral view of embryos is shown in A-E; lateral view of the embryo is shown in A'-E'.

3.2.3 Dorsal marker

SoxNeuro (SoxN)

As one of the earliest transcription factors to be expressed in the pan-neuroectodermal region of *Drosophila* embryos, *SoxNeuro (SoxN)* is essential for the formation of the neural progenitor cells in central nervous system (CNS) development (Buescher et al., 2002). In *Drosophila* blastoderm embryo, the expression of *SoxN* is in a cephalic domain and neuroectoderm (Crémazy et al., 2000). In contrast to *Drosophila*, *SoxN* is expressed asymmetrically on the dorsal side of *Oncopeltus* early blastoderm embryos (Figure 3.5A, B). In later blastoderm stages before gastrulation, the expression is expanded to the ventral side, but still stronger on the dorsal side. During gastrulation, *SoxN* is expressed in the head region and in each segment as stripes invaginated into the embryo.

3.3 Genomic and transcriptomic analysis of Toll-like receptors

Since the *Oncopeltus* genomic sequence has been released on the i5K websites and the gene annotation starts in 2014, it is possible to search for all members of Toll-like receptors. All of the *Toll-like* candidates found from the genome annotation are listed in the Table 3.2 and compared with the transcripts found from the transcriptome with different GeneIDs indicated.

From the genome annotation, six putative Toll or Toll-like receptors (TLRs) were found in *Oncopeltus* (Table 3.2). According to the blastX results, they are homologous to different Toll subfamilies. In the *Oncopeltus* genome, two additional Toll-like genes were found with 342 and 622 amino acids (aa) in length. These two additional Toll-like genes (OFAS006184 and OFAS008757) are shorter than the other Toll-like receptors. According to the blastX results, OFAS006184 is homologous to *Tribolium Toll-13* and OFAS008757 is homologous to *Toll-13* of the brown planthopper (Bao et al., 2013). Unexpectedly, the transcript GAP9EXG07H56OG from the transcriptome can not be found in the genome.

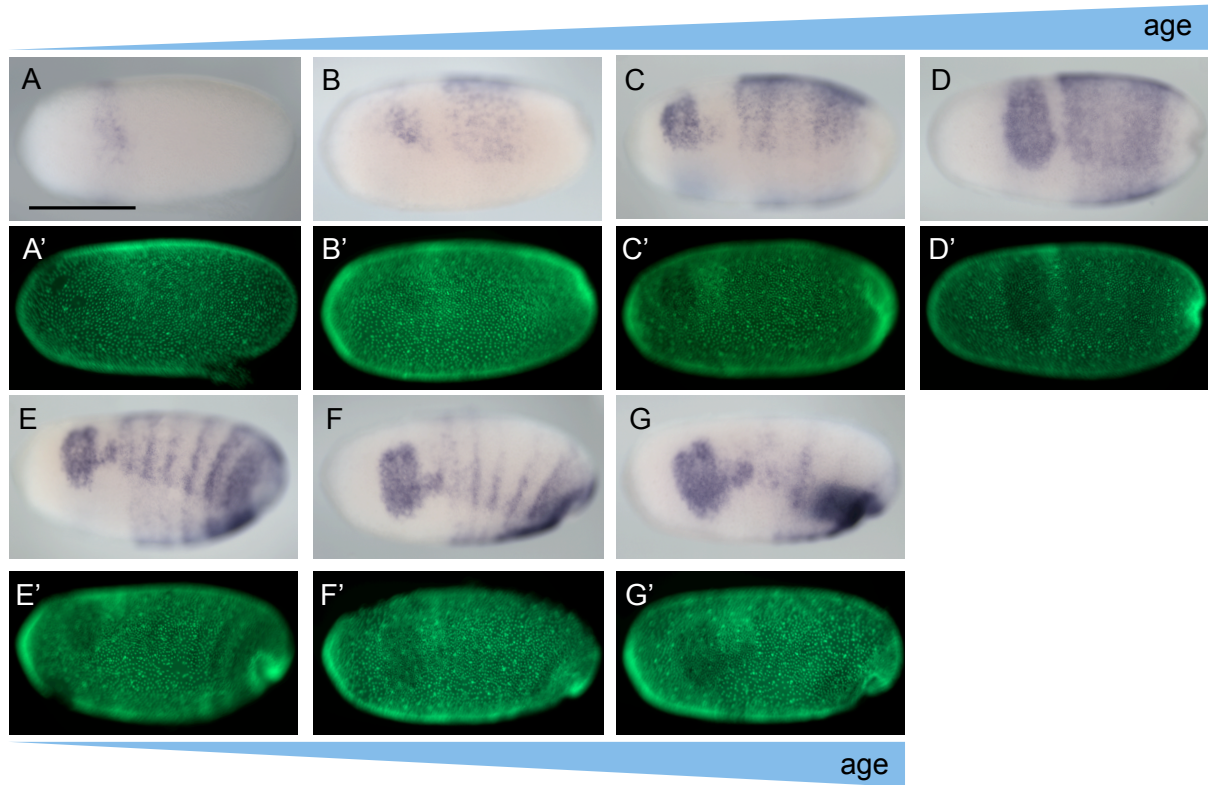


Figure 3.5. Expression pattern of *SoxN* in *Oncopeltus* embryos

The expression pattern of *SoxN* transcripts in blastoderm embryos (Figure A-D), and after gastrulation (Figure E-G). In the early blastoderm stage, *SoxN* starts to be expressed asymmetrically on one side of the embryo. After gastrulation, its expression is flanking the ventral midline. Scale bar size corresponds to 500 μm . Upper row of embryos are identical to the lower row (A to A'...) with the SytoxGreen staining to show the nuclei. Lateral view of the embryo is shown in Figure A-G.

3.3.1 Conserved domain of Toll-like receptors

Conserved domains of putative TLRs were analyzed (Figure 3.6). They contain the extra-cellular leucine-rich repeats (LRR) on the N-terminus, a transmembrane domain (TM), and an intracellular Toll/interleukin-1 receptor (TIR) domain on the C-terminus. The conserved domains of LRR, TM, and TIR characterize the identity of a Toll-like receptor, although *Tribolium Toll-9* does not have a TIR domain (Zou et al., 2007). The identification for *Toll-13* is more controversial because the protein sequence of OFAS006184 is homologous to *Tribolium Toll-13*, but the LRR domain on the N-terminus is absent. In contrast, the protein sequence of OFAS008757 is homologous to Toll-13 of the brown planthopper, but both of them lack the (TIR) domain on the C-terminus. Conserved

Table 3.2. Toll-like receptors in transcriptome and genome annotation

Name	GeneID in		Best Hit
	Transcriptome	Genome Annotation	
<i>Toll putative</i>	isotig03359	OFAS011521	<i>Phc Toll</i>
<i>Toll-6 putative</i>	GEQE5QV02GW91E +Contig24056	OFAS002038	<i>Nl Toll-6</i>
<i>Toll-7 putative</i>	FQTBZRY01BD13M +isotig11499	OFAS002798	<i>Nl Toll-7</i>
<i>Toll-8 putative</i>	GEQE5QV01D10V5 +isotig20558	OFAS005704	<i>Nl Toll-8</i>
<i>Toll-9 putative</i>	GAP9EXG07H56OG	ND*	<i>Dmi CG5528</i>
<i>Toll-10 putative</i>	GESJTKM01BPGV1 +FQTBZRY02I7PQ6 +isotig09603	OFAS009055	<i>Nl Toll-10</i>
<i>Toll-13 putative</i>	ND*	OFAS006184	<i>Tc Toll-13</i>
<i>Toll-13 putative</i>	ND*	OFAS008757	<i>Nl Toll-13</i>

* ND = Not Detected

Abbreviation of insect species: *Phc*=*Pediculus humanus corporis*, *Nl*= *Nilaparvata lugens* (brown planthopper), *Dmi* =*Drosophila miranda*, *Tc* =*Tribolium castaneum*

domains and the structure of TLRs are illustrated in Figure 3.6.

3.3.2 Phylogenetic analysis of the Toll family

Protein sequences of the Toll or Toll-like receptors from different insect species were compared to conduct a phylogenetic analysis. Toll receptors of the fly *Drosophila melanogaster* (*Dm*) were obtained from the Flybase and NCBI databases. Members of the immune-related Toll receptors were annotated in the mosquito *Anopheles gambiae* (*Ag*) (Christophides et al., 2002; Luna et al., 2002). Toll and Toll-like receptors have been identified for pathogen recognition in the honey bee *Apis mellifera* (*Am*) (Evans et al., 2006). Members of the Toll receptors were annotated in the red flour beetle *Tribolium castaneum* (*Tc*) (Zou et al., 2007) and in the brown planthopper *Nilaparvata lugens* (*Nl*) (Bao et al., 2013). Only the Toll receptors encoding the LRR, TM, and TIR were aligned together to conduct a phylogenetic tree.

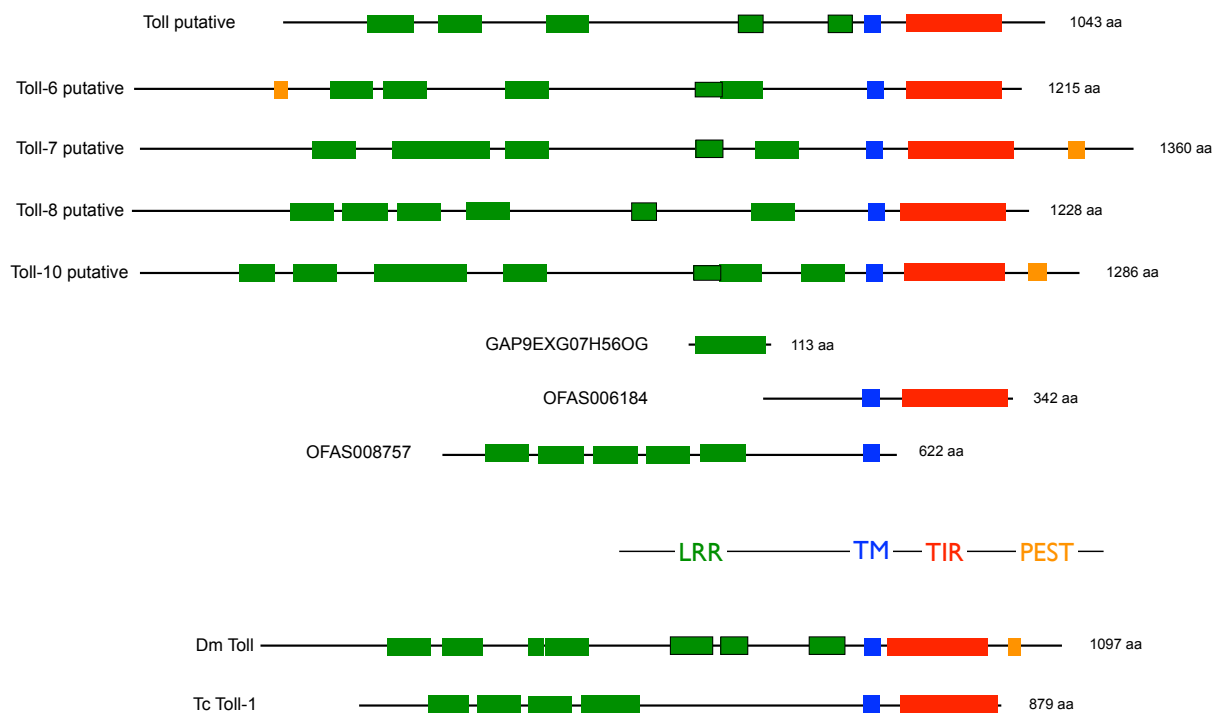


Figure 3.6. The conserved domains of putative Toll-like receptors

All Toll proteins contain the leucine-rich repeats (LRR) on the N-terminal end, and an intracellular Toll/interleukin-1 receptor (TIR) domain on the C-terminus. In between, there is a transmembrane domain (TM). Conserved domains of *Drosophila* Toll (NP_524518) and *Tribolium* Toll-1 (XP_008190422.1) have been studied (Maxton-Küchenmeister et al., 1999) and severed for comparison. PEST domains were predicted in putative *Oncopeltus* Toll-6, Toll-7 and Toll-10. In Toll-7 and Toll-10, the PEST domains are located in the most C-terminal end as shown for *Drosophila* Toll1. However, the N-terminal LRR domain of OFAS006184, and the C-terminal TIR domain of OFAS008757 are absent.

In the phylogenetic tree (Figure 3.7), only one *Oncopeltus* Toll is in the same clade with *Drosophila* Toll and *Tribolium* Toll1, which are known to be involved in DV patterning. This single transcript isotig03359 found in the transcriptome is named *Toll-1* in the following paragraphs. The lineage-specific duplications of *Drosophila* Toll-3, Toll-4, *Anopheles* Toll-1, Toll-5, and *Tribolium* Toll 1-4 (described in Christophides et al., 2002; Luna et al., 2002; Evans et al., 2006; Zou et al., 2007) are confirmed in the Toll-1 clade. The Toll-1 clade is a sister group to the other Toll-like receptors.

The remaining Toll-like receptors are clustered into three subgroups, which are Toll-6/8, Toll-7/18w, Toll-10, respectively. In addition, Toll-6 and Toll-8 are closely related sister clades. Toll homologs of *Oncopeltus* are closest related to Toll homologs of the brown planthopper *Nilaparvata lugens* (Nl) in each clade. Toll-9 and Toll-13 are clustered

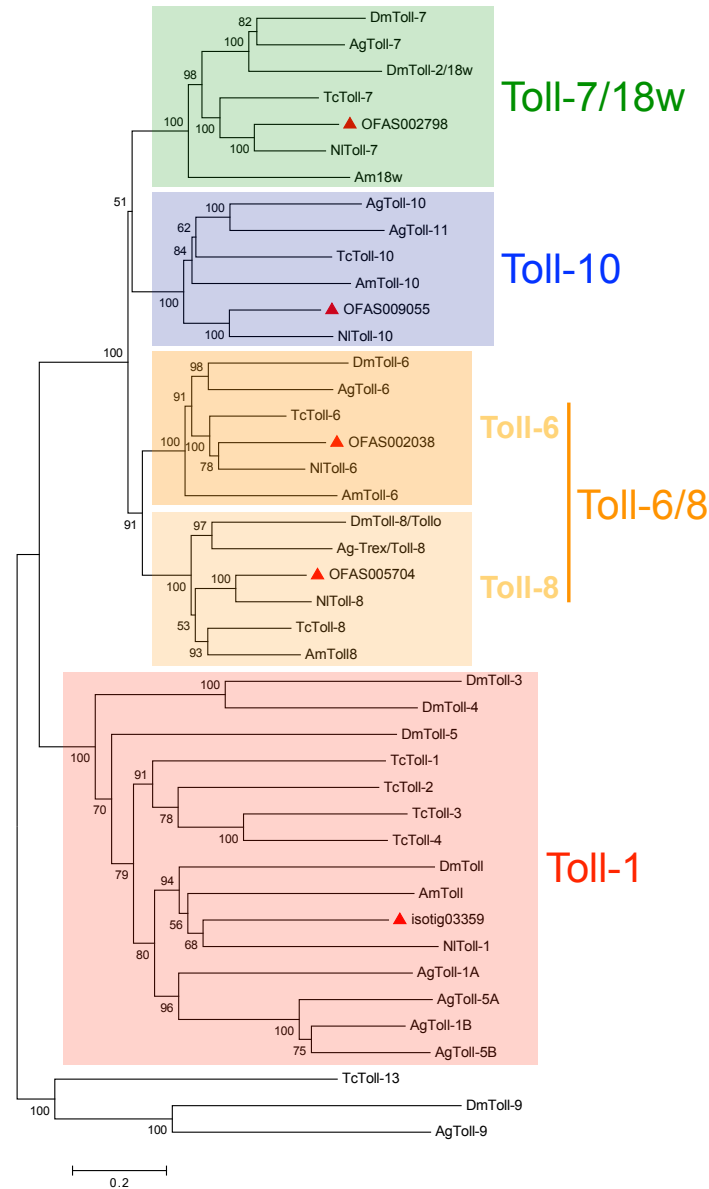


Figure 3.7. Phylogenetic analysis of the Toll family

Toll-2 in *Drosophila* is also known as 18wheeler(18w). There is also a *18w* identified in the honey bee *Apis mellifera* (*Am*). Toll-8 in the mosquito *Anopheles gambiae* (*Ag*) is also known as Trex. Toll-8 in *Drosophila* is also known as Tollo. The phylogenetic tree was constructed using the Neighbor-Joining method. The percentage of replicate trees in which the associated taxa clustered together in the bootstrap test (1000 replicates) are shown next to the branches. The tree is drawn to scale, with branch lengths in the same units as those of the evolutionary distances used to infer the phylogenetic tree. The evolutionary distances were computed using the Poisson correction method. Only one *Oncopeltus Toll* is branched in the same clade with *Drosophila Toll* and *Tribolium Toll1*, which are known to be involved in DV patterning. The other Toll-like receptors are clustered into three subgroups, which are Toll-6/8, Toll-7/18w, Toll-10, respectively.

together as a sister group to the other Toll receptors. The phylogenetic analysis of Toll-9 and Toll-13 is discussed in the Supplementary data.

3.3.3 Spatial distribution of *Toll-1* transcripts

The expression pattern of *Toll-1* transcripts during embryonic development is exhibited by single color ISH or fluorescent ISH (FISH) (Figure 3.8). The *Toll-1* gene is expressed very early in blastoderm stage and becomes gradually expressed more intensively on one side of the embryos with increasing age. FISH shows the expression pattern and the nuclear staining more clearly. Nuclear density is used to distinguish dorsal and ventral regions of the blastoderm embryo (described in the supplementary data). According to the calculation of nuclear density and marker genes staining, the nuclei are more condensed on the dorsal side. Therefore, the expression of *Toll-1* is on the presumptive ventral side. In the late blastoderm stage, *Toll-1* is expressed strongly in the invagination site. *Toll-1* is expressed ubiquitously during germband extension stages.

The asymmetric distribution of *Toll* transcripts was published in *Tribolium*, but not in the mothfly *Clogmia albipunctata* or the fly *Drosophila* (Maxton-Küchenmeister et al., 1999). In *Drosophila*, *Toll* transcripts are inherited maternally and distributed ubiquitously in early embryos (Gerttula et al., 1988). In contrast to *Drosophila*, the asymmetric distribution of *Toll-1* transcripts is similar to the expression pattern in *Tribolium*.

3.4 NF κ B transcription factors in *Oncopeltus*

There are two putative *dorsal* genes (isotig01051 and isotig04590) in the *Oncopeltus* transcriptome (Table 3.1). Both of them are homologous to *Drosophila dorsal*. Additionally, a putative *relish* gene (isotig02403) was found during the search for *dorsal* genes.

3.4.1 Conserved domain of the Rel/NF κ B family

To understand whether the NF κ B proteins are distinct from the Relish (Rel) proteins, conserved domains of the NF κ B and Rel proteins from *Drosophila*, *Tribolium* and *Oncopeltus* were analyzed (Figure 3.9). All of the NF κ B and Relish proteins share a conserved Rel-homology domain (RHD) and a immunoglobulin-plexin-transcription (IPT) domain.

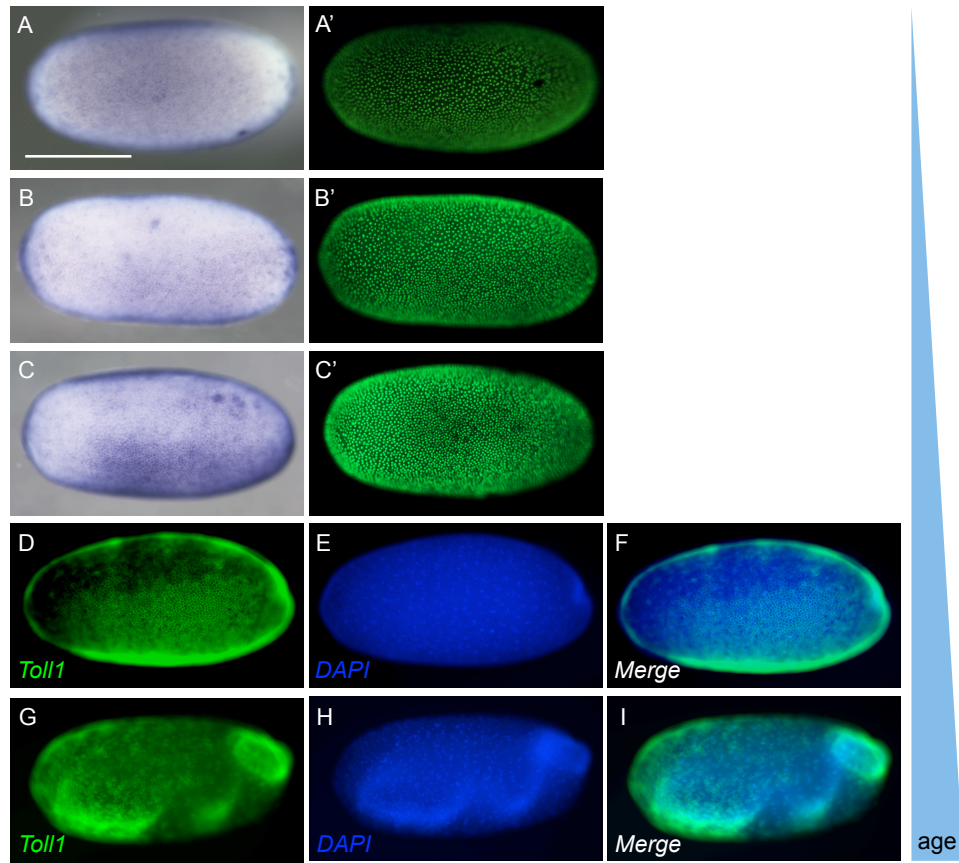


Figure 3.8. Spatial distribution of *Toll-1* transcripts during *Oncopeltus* embryogenesis

Embryos shown in the left column (A-C) are identical to the embryos in the right column, with nuclear staining by SytoxGreen (A'-C'). According to the developmental stages, embryos are arranged from top to bottom (A-C, D, G). Embryos are at the blastoderm stage (A-C). The late blastoderm embryo is shown in D-F, with green color labeling *Toll-1* transcripts (D), nuclear staining by DAPI (E) and merged channels (F). The expression of *Toll-1* is on the presumptive ventral side. The germband embryo is shown in G-I, with green color labeling *Toll-1* transcripts (G), nuclear staining by DAPI (H) and merged channels (I). During germband extension stage, *Toll-1* is expressed ubiquitously. Lateral view is shown in all embryos. Scale bar (A) size corresponds to 500 μm .

However, only Relish proteins share conserved ankyrin repeats (ANK) on the C-terminus. The conserved ANK domain of Relish proteins is characteristic and can be used to distinguish Relish from the other NF κ B proteins.

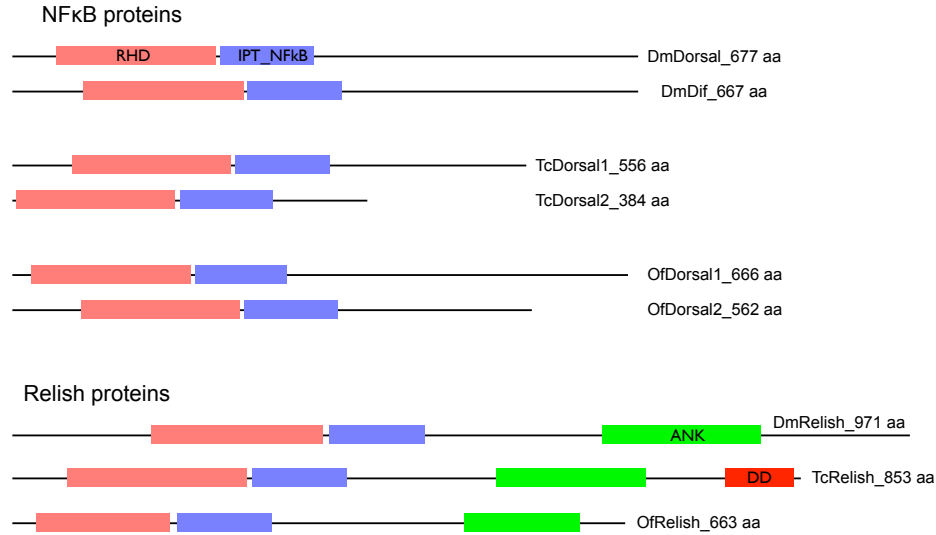


Figure 3.9. Conserved domain of Rel/NF κ B proteins

The conserved domains are drawn to scale. The length of the lines corresponds to the number of amino acids. NF κ B and Relish proteins of *Drosophila*, *Tribolium* and *Oncopeltus* are compared. The number of amino acids is indicated on the right side. The abbreviations of conserved domains are listed below: rel-homology domain (RHD), immunoglobulin-plexin-transcription (IPT) domain, ankyrin repeats (ANK), death domain (DD). All of the Rel/NF κ B proteins share a conserved RHD and an IPT domain. However, only Relish proteins share conserved ankyrin repeats (ANK) on the C-terminus, which is characteristic and can be used to distinguish Relish from the other NF κ B proteins.

3.4.2 Phylogenetic analysis of the Rel/NF κ B protein family

Within the Dorsal-related NF κ B family, there are two candidates in *Oncopeltus*. To clarify the phylogenetic relationship of these Dorsals, protein sequences from different insect species were compared to conduct a phylogenetic analysis (Figure 3.10). The Dorsal-related NF κ B proteins of the fly *Drosophila melanogaster* (*Dm*), the red flour beetle *Tribolium castaneum* (*Tc*), the honey bee *Apis mellifera* (*Am*), and the body louse *Pediculus humanus humanus* were obtained from the Flybase and NCBI databases. Additionally, there is one early expressed *dorsal1A* characterized in the kissing bug *Rhodnius prolixus* (Ursic-Bedoya et al., 2009), which is included for comparison.

The Relish proteins of *Drosophila* and *Tribolium* were obtained from the Flybase,

Beetlebase, and NCBI databases. Sequences from the jewel wasp *Nasonia vitripennis* (*Nv*) were kindly provided by T. Buchta. Additionally, there is one *relish* annotated in the stinkbug *Riptortus pedestris* (Futahashi et al., 2013), which is included for comparison. The immune-related *dorsal* is annotated in the pea aphid *Acyrtosiphon pisum* (*Ap*) (Gerardo et al., 2010), but the *relish* is lost independently in the pea aphid.

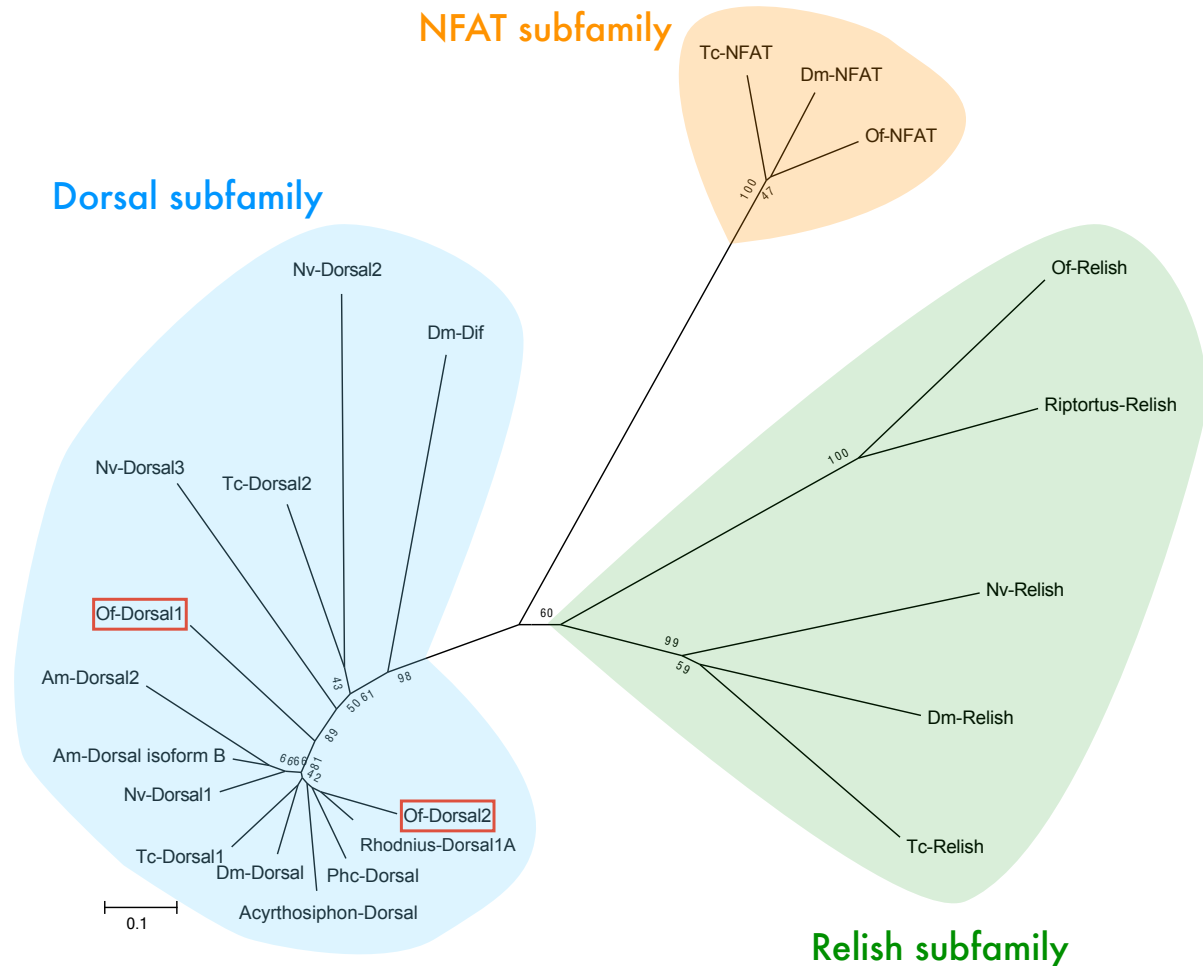


Figure 3.10. Phylogenetic analysis of the Rel/NFκB family

Phylogenetic analysis of the Rel/NFκB family based on the shared RHD domain. The phylogenetic tree was constructed using the Neighbor-Joining method. The percentage of replicate trees in which the associated taxa clustered together in the bootstrap test (1000 replicates) are shown next to the branches. The tree is drawn to scale, with branch lengths in the same units as those of the evolutionary distances used to infer the phylogenetic tree. The evolutionary distances were computed using the Poisson correction method. The Relish and Dorsal-related NFκB proteins of all studied insects are clustered as separate subfamilies. NFAT proteins served as an outgroup of the Relish and Dorsal subfamily. Within the Dorsal subfamily, *Oncopeltus* Dorsal1 is related to other Dorsals as a sister branch.

During the genome annotation, another transcription factor encoding the RHD was

found in *Oncopeltus*. It belongs to the nuclear factor of activated T-cells (NFAT) family, which is important for immune response (Rao et al., 1997). NFAT of *Drosophila*, *Tribolium*, and *Oncopeltus* served as an outgroup in the phylogenetic analysis. The phylogenetic analysis shows that Relish proteins of all studied insects are clustered as a subfamily. Within the Relish subfamily, *Oncopeltus* Relish is closely related to the Relish of the stinkbug *Riptortus*. The Dorsal-related NF κ B proteins of all studied insects are clustered as a subfamily, which is called the Dorsal subfamily. Within the Dorsal subfamily, *Oncopeltus* Dorsal2 is closely related to the Dorsal of the kissing bug *Rhodnius* and *Oncopeltus* Dorsal1 is related to other Dorsals as a sister branch.

3.4.3 Expression pattern of *dorsal* transcripts

ISH was used to detect the spatial distribution of *dorsal* transcripts in *Oncopeltus*. Transcripts of *dorsal1* (*dl1*) can be detected during oogenesis in the tropharium and oocytes (Figure 3.11A). In contrast, transcripts of *dorsal2* (*dl2*) are expressed in the tropharium, but not in the late developing oocytes (Figure 3.11B). There is no significant expression of *dl2* transcripts in early blastoderm embryos (Figure 3.11D). Before gastrulation, *dl1* and *dl2* are intensively expressed around the invagination site. Transcripts of *dl1* are also expressed in the posterior half of the blastoderm embryo. In contrast, transcripts of *dl2* are expressed in the anterior part of the late blastoderm embryo. Due to the strong expression of *dl1* in the oocytes and early blastoderm embryos, it is more likely to play an early role in DV patterning (Figure 3.11A, C).

3.5 Disruption of Toll signaling severely impairs embryogenesis

To study the loss-of-gene function, parental RNAi (pRNAi) is used in *Oncopeltus* (Angelini and Kaufman, 2004). The technique was used here to understand the function of Toll pathway components. However, total amount of dsRNA has to be adjusted for each gene to obtain the knockdown phenotype. From the literature, the amount of dsRNA used for pRNAi is ranging from 4 to 10 μ g (Angelini and Kaufman, 2004; Liu and Kaufman, 2004, 2005a; Panfilio et al., 2006; Liu and Patel, 2010; Ben-David and Chipman, 2010;

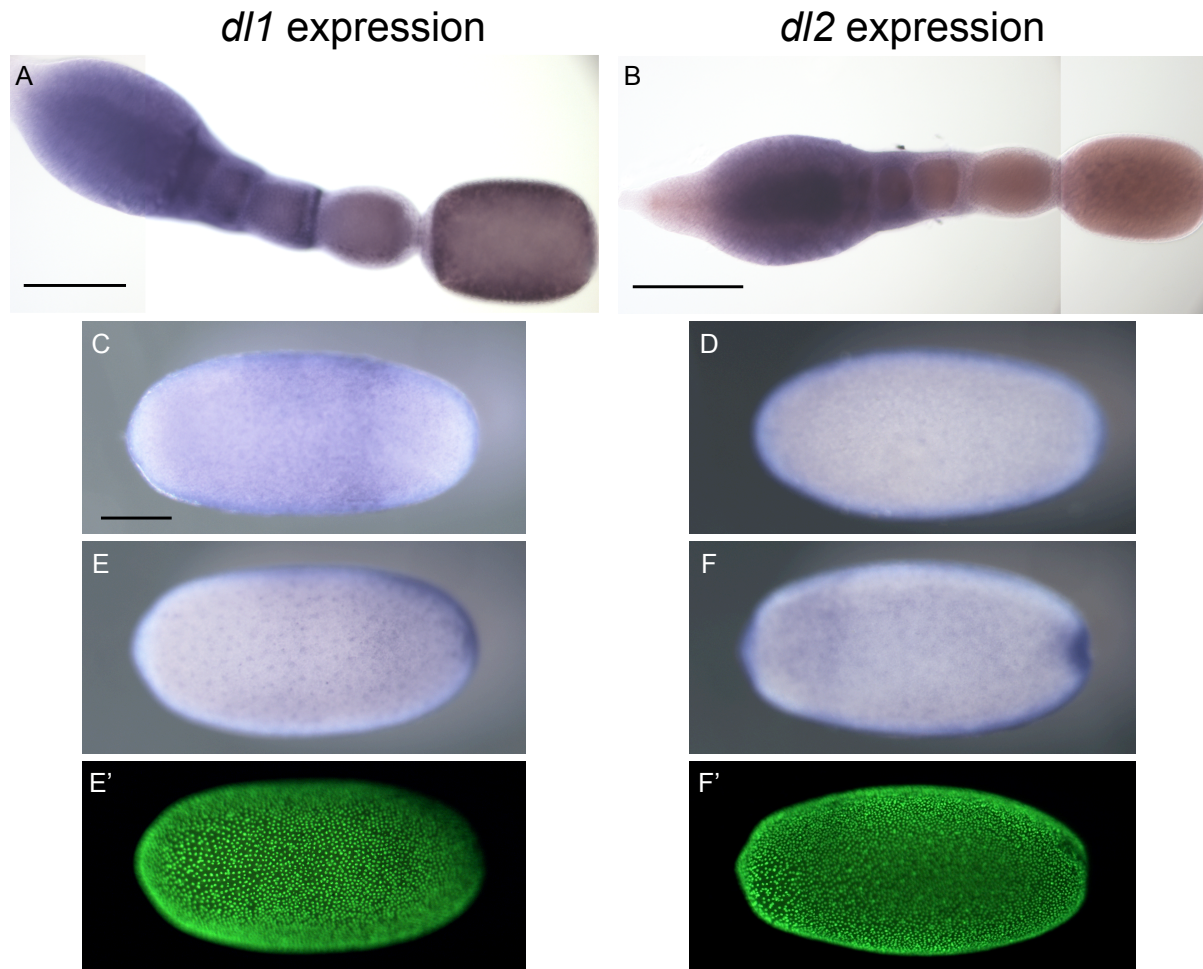


Figure 3.11. Expression pattern of *dl1* and *dl2* transcripts

The expression pattern of *dl1* and *dl2* transcripts in ovarioles (A, B). *dl1* is expressed in the tropharium and oocytes. In contrast, *dorsal2* (*dl2*) is expressed in the tropharium, but not in the late developing oocytes. Scale bar size corresponds to 500 μm (A, B). The expression pattern of *dl1* and *dl2* transcripts in blastoderm embryos (Figure C-F). *dl1* is expressed in the early blastoderm embryo, but *dl2* is not. E' and F' are identical embryos from E and F with nuclear staining by SytoxGreen. Scale bar size corresponds to 250 μm (C-F'). Before gastrulation, *dl1* and *dl2* are intensively expressed around the invagination site. While *dl1* is expressed more posteriorly, *dl2* is expressed in the anterior part of the late blastoderm embryo.

Ewen-Campen et al., 2013). It was decided to inject dsRNA at a lower amount (4 μ g per female) as a starting point.

The morphology of 5-day-old embryos is shown in Figure 3.12A. They keep developing and hatch after seven days. However, disruption of Toll signaling severely impairs embryogenesis. Eggs laid by the injected females stop to develop during the embryogenesis, and show significant morphological defects. The phenotypic analysis of Toll signaling knockdown embryos is shown in Figure 3.12.

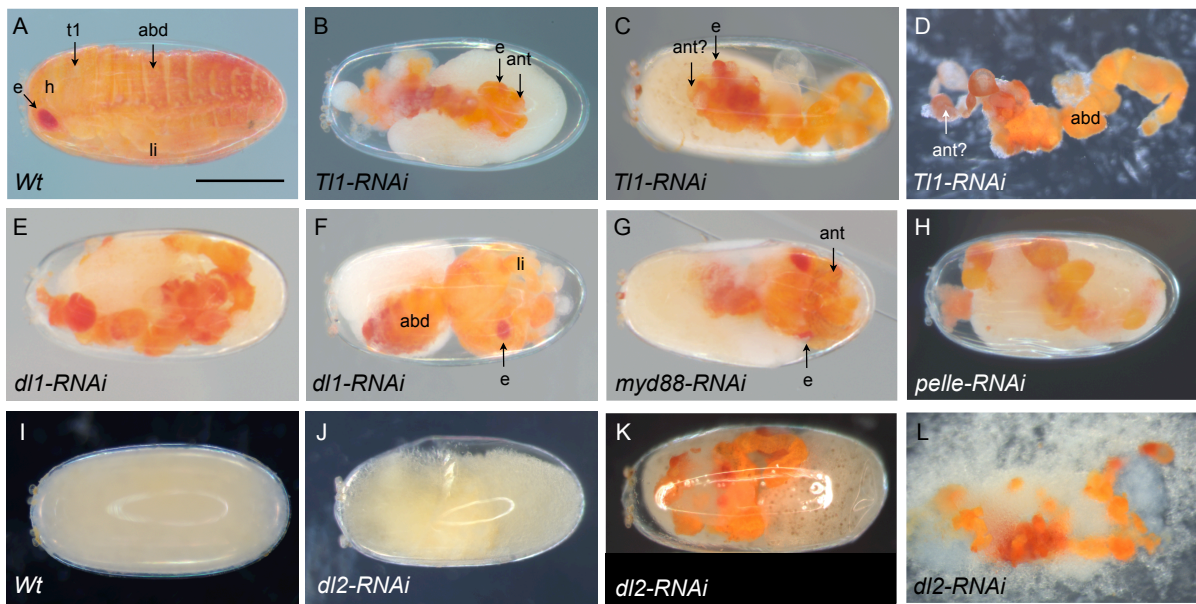


Figure 3.12. Disruption of Toll signaling severely impairs embryogenesis

After knockdown of Toll signaling components, tissues can be barely recognized in comparison to wildtype morphology. Especially, the limbs are absent from the ventral side in knockdown embryos. This indicates that disruption of Toll signaling severely impairs embryogenesis and the DV polarity might be disturbed. The structures are indicated in figure A, B, C, D, F, G with the following abbreviations (e: eye, h: head, T1: thorax1, abd: abdomen, li: limb, ant: antenna). The anterior pole of the egg is always to the left, indicated by the micropyles near the anterior side of the egg (Dorn, 1976; Chapman et al., 2013). The embryos shown in D and L are dissected out of the eggshell. Scale bar (A) size corresponds to 500 μ m.

After *Toll-1* knockdown, embryos usually form a twisted tube-like shape and lack appendages. Furthermore, only the antenna can be recognized (Figure 3.12B, C, D). The twisted tube-like shape is similar to the typical dorsalized phenotype reported in *Drosophila* (Anderson et al., 1985b). Morphological phenotypic analysis of *dl1* knockdown embryos is shown in Figure 3.12E and F. After *dl1* RNAi, embryos with severe defects

resemble the *Toll-1* knockdown phenotype, which is shown in Figure 3.12E. The mild phenotype of *dll* knockdown is shown in Figure 3.12F. Although the head-thorax part with red eyes and some appendages remains, the embryos fail to develop. Knockdowns of the other Toll signaling components lead to impaired developing embryos, which are similar to *Toll-1* knockdown phenotypes (Figure 3.12G, H, K, L). A detailed analysis of RNAi phenotypes is described in the following sections.

3.6 Knockdown phenotypes and lifespan reduction after *Toll-1* knockdown

According to the morphological phenotypic analysis, knockdown of *Toll-1* impairs embryogenesis severely and shows a high percentage of phenotypes. More than 90% of knockdown embryos develop into a twisted tube-like shape without appendages forming (shown in Figure 3.12B, C, D). The knockdown efficiency of *Toll-1* seems to be dosage-insensitive. Different amounts of *Toll-1* dsRNA (two or four μ g per female) were tested for pRNAi, and both conditions produce a high penetrance of knockdown phenotypes in embryos (Table 3.3).

Compared to mock-treated controls who can survive 20 days in average, females injected with *Toll-1* dsRNA could be more vulnerable and their lifespan is reduced to 14 days in average (Table 3.3). This could indicate that knockdown of *Toll-1* expression reduces lifespan of injected females. However, there is no significant difference between the injection groups and mock-treated control through the logrank test (Bland and Altman, 2004). Lifespan reduction of injected females using other dsRNAs and the function of Toll signaling in immune response is described in the Supplementary data.

3.7 Validation of knockdown efficiency by the semi-quantitative PCR

The efficiency of a knockdown was estimated by the semi-quantitative PCR to validate the expression level of the transcripts.

Table 3.3. Ratio of morphological phenotypes and lifespan reduction after *Toll-1* knockdown

Group	dsRNA Amount (μ g)	Surviving days of injected females			knockdown phenotypes in embryos	Embryos
		Average	Standard deviation	♀n=	(%)	n=
Mock-treated control	-	20.4	7.38	28	0%	576
<i>Tl1-RNAi</i>	4	13.9	8.43	10	93.3%	262
<i>Tl1-RNAi</i>	2	14.1	6.22	17	92.4%	588

Identical *Toll-1* dsRNA with different amount was used for pRNAi. In each group, more than ten individual females were injected. Percentage of knockdown phenotypes were calculated from the morphological phenotypic analysis after five-seven days of embryogenesis.

3.7.1 Validation of *Toll-1* knockdown efficiency

The validation by the semi-quantitative PCR shows that the expression level of *Toll-1* transcripts is significantly lower after RNAi compared to the mock-treated control (shown in Figure 3.13a). The absence of *Toll-1* transcripts on the gel is an evidence that the knockdown of *Toll-1* is efficient. In addition, other supporting data of sufficient knockdown comes from the results of qPCR (section 3.10).

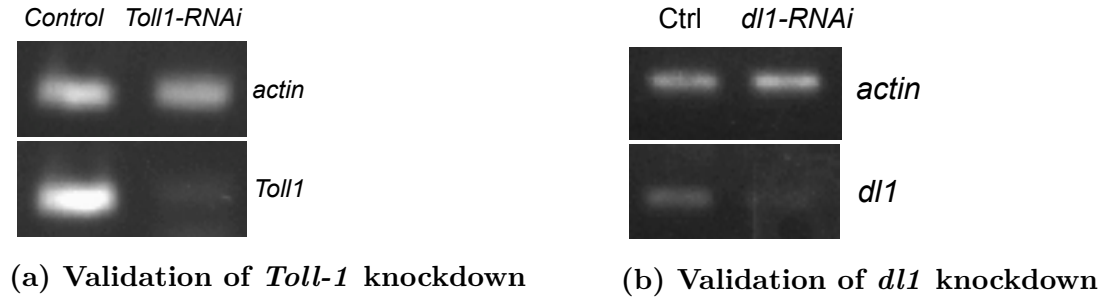


Figure 3.13. Validation of knockdown efficiency by the semi-quantitative PCR

(a) The *Toll-1* expression is highly down-regulated after pRNAi. cDNA was synthesized from the RNA of early blastoderm embryos (0-17 AEL) and served as the template for the semi-quantitative PCR.

(b) The *dl1* expression is highly down-regulated after pRNAi. cDNA was synthesized from the RNA extraction of germ band embryos (40-48 AEL) and served as the template for the semi-quantitative PCR. Expression of the gene *actin* served as the internal control.

3.7.2 Validation of *dll* knockdown efficiency

The expression of *dll* transcripts is totally abolished or highly down-regulated after RNAi (Figure 3.13b), which was confirmed by the semi-quantitative PCR. This is an evidence that knockdown of *dll* is efficient via pRNAi.

3.8 ISH staining of *Toll-1* and *dll* knockdown embryos during blastoderm stage

In order to describe the developmental defects resulting from gene knockdown, marker genes differentially expressed along the DV axis were used to perform ISH staining in *Toll-1* and *dll* knockdown embryos. After knockdown of *Toll-1* in *Oncopeltus*, the expression of *twist*, *sog* and *sim* is eliminated (Figure 3.14). Similarly, the expression of *twist* and *sim* is eliminated after *dll* knockdown (Figure 3.14). Abolished expression of the ventral marker *twist*, *sog* and *sim* indicates that knockdown embryos might lose the whole ventral fate or that even the lateral fate is disrupted.

Absence of *dll* expression in *dll* knockdown embryos validates the knockdown efficiency. However, in the absence of Toll signaling, the expression of *sog* is not lost completely. Minimal amounts of *sog* expression can be detected by ISH. Statistic data of remnant *sog* expression in *Toll-1* and *dll* knockdown embryos during blastoderm stages is listed in Table 3.4.

Expression patterns of *sog* in *Toll-1* knockdown embryos were categorized into three groups- with remnant (37%), ubiquitous (34%) or no expression (28%). Expression of *sog* is still detectable in all *dll* knockdown embryos. Hence, the expression patterns are categorized into two groups- with asymmetric (47%) or ubiquitous (53%) expression of *sog*. Asymmetric expression of *sog* on the ventral side indicates that there might be some DV polarity cues left in *dll* knockdown embryos. From the aspect of residual *sog* expression, *dll-RNAi* shows a weaker knockdown phenotype than *Toll1-RNAi*.

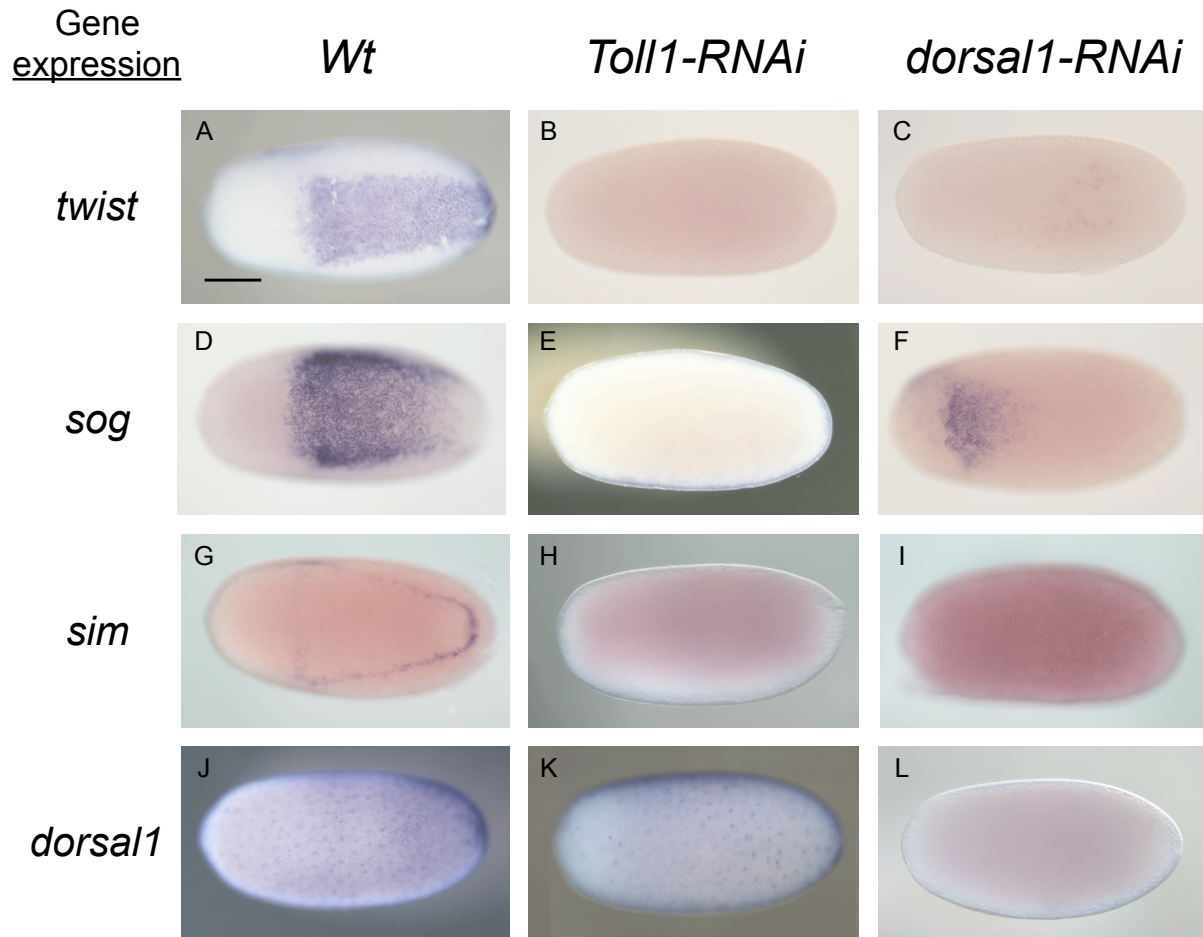


Figure 3.14. ISH staining of *Toll-1* and *dl1* knockdown embryos during blastoderm stage

In *Toll-1* and *dl1* knockdown embryos, the expression of *twist*, *sog* and *sim* is reduced. Blastoderm embryos are shown from the ventral view (A, D, F, G), while in the others the DV polarity can not be determined. Expression in wildtype embryos (A, D, G, J) is compared with the *Toll-1* knockdown embryos (B, E, H, K) and *dl1* knockdown embryos (C, F, I, L). The scale bar size (A) correspond to 250 μm .

Table 3.4. Percentage of residual *sog* expression in *Toll-1* and *dl1* knockdown embryos

<i>Toll1-RNAi</i>	Knockdown phenotype			Embryos n=67
	residual expression 37%	no expression 34%	ubiquitous expression 28%	

<i>dll1-RNAi</i>	Knockdown phenotype		Embryos n=32
	asymmetric expression with DV polarity (+) 47%	ubiquitous expression without DV polarity (-) 53%	

Expression patterns of *sog* in *Toll-1* knockdown embryos from six independent ISH experiments were analyzed and categorized into remnant, ubiquitous or no expression.

Expression patterns of *sog* in *dl1* knockdown embryos from four independent ISH experiments were analyzed and categorized into asymmetric or ubiquitous expression.

Total number of ISH embryos was counted and listed in the last column (n=).

3.9 ISH staining of *Toll-1* knockdown embryos during germ band stage

Absence of *Toll-1* results in the loss of DV polarity and the knockdown phenotype is not recovered during late stages of development. The expression of *twist* and *sim* is lost in *Toll1-RNAi* embryos during germ band stage (Figure 3.15). The germband embryos with *Toll-1* knockdown form a tube-like shape lacking DV polarity. Residual expression of *sim* can exclusively be detected in the most posterior end of germ band embryo (Figure 3.15D). The most posterior end of germ band embryo is called proctodeum (Butt, 1949) and the expression suggests that posterior patterning in the terminal end is not affected by *Toll-1* disruption.

Although the *Toll1-RNAi* embryos form a tube-like shape lacking DV polarity, the segmentation of the germband embryos is not affected, which is shown by the staining of *msh* and the segment polarity marker *en* (Figure 3.15F, H). Knockdown embryos lacking DV polarity possess an active growth zone and undisturbed segment polarity along the AP axis. This proves that the germ band extension and segmentation are independent of Toll signaling.

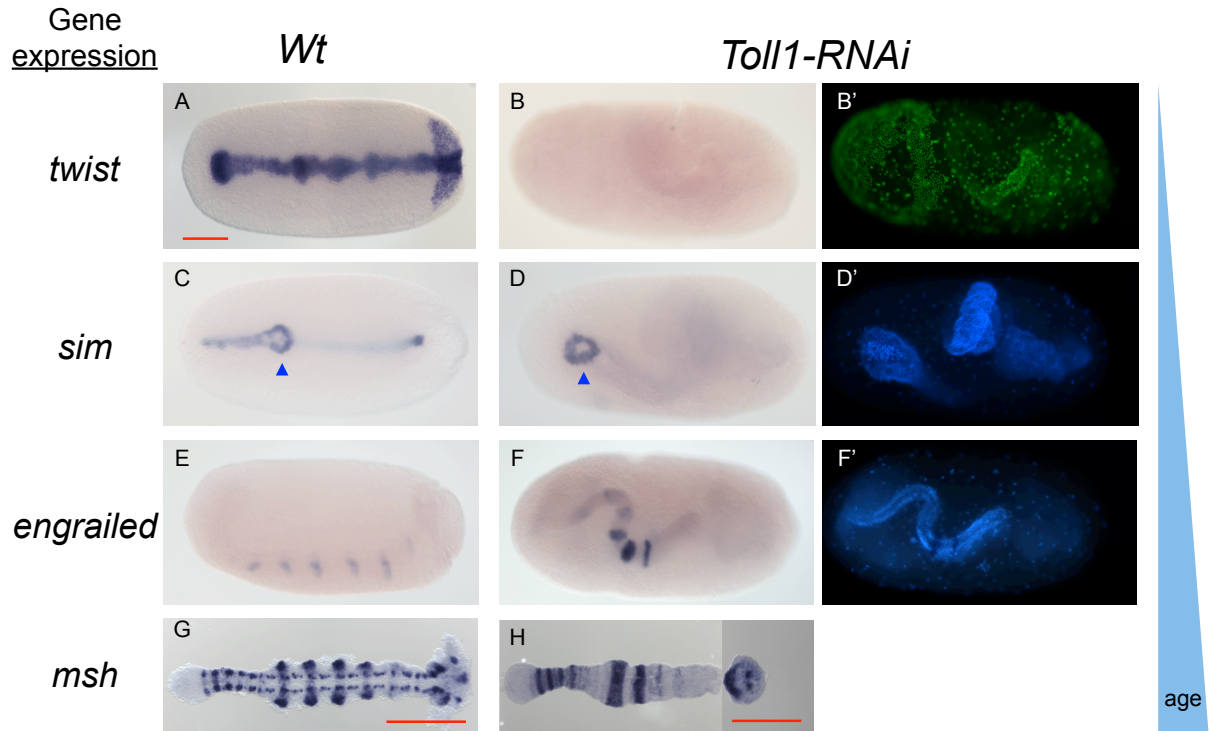


Figure 3.15. *Toll-1* knockdown phenotypes during germ band stage

The expression of *twist* and *sim* is eliminated in *Toll1-RNAi* embryos during germ band stage. Knockdown of *Toll-1* leads to the periodic expression in the germ band embryos, which is shown by the segment polarity marker *en* and the staining of *msh*. Anterior pole of the egg is to the left. Embryo anterior is to the right. Ventral view of the embryo is shown in A; dorsal view of the embryo is shown in C; lateral view of the embryo is shown in E. In *Toll-1* knockdown embryos (B, D, F), the orientation can not be determined due to the absence of DV polarity. Embryos shown in B', D', F' are identical to B, D, F showing nuclear staining by SytoxGreen and Hoechst33258. The arrowheads indicate the proctodeum of the germ band embryo. Scale bar size corresponds to 200 μm in A-F', while the scale bar size corresponds to 500 μm in G and H. The embryos shown in G and H are dissected out of the egg.

3.10 Expression level of transcripts after *Toll-1* RNAi

The gene expression level of *Toll-1* knockdown embryos was estimated by qPCR. After knockdown, the expression of *sog*, *twist* and *Toll-1* is down-regulated as shown in Figure 3.16.

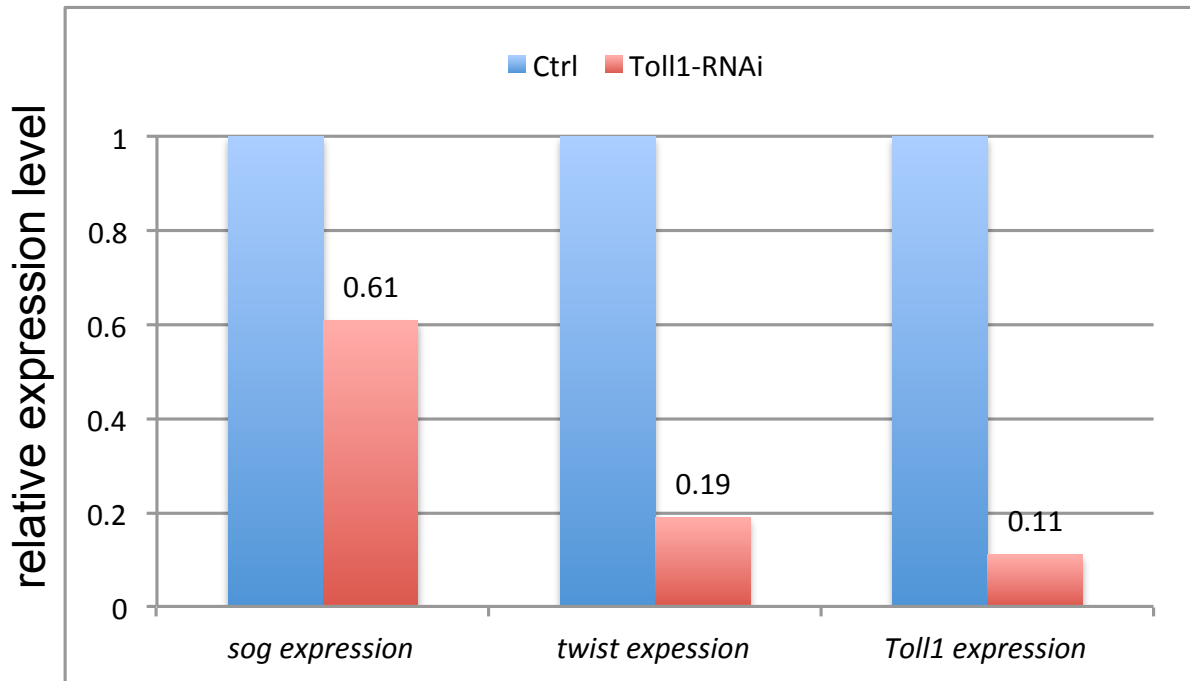


Figure 3.16. Gene expression is down-regulated in *Toll-1* knockdown embryos

The expression levels of *sog*, *twist* and *Toll-1* are estimated in blastoderm embryos (26-29 hours after egg lay). The gene expression level of mock-treated embryos served as control and set to 1.0. After *Toll-1* knockdown, the expression of *sog*, *twist* and *Toll-1* are down-regulated. Gene expression levels were normalized using 18S ribosomal RNA gene as reference gene.

Compared to the control group, the expression level of *Toll-1* is down-regulated about ten-fold (0.11) in *Toll-1* knockdown embryos. This proves that *Toll1-RNAi* is efficient to breakdown the transcripts. The expression levels of *twist* and *sog* are also down-regulated in *Toll-1* knockdown embryos. Expression of *twist* is about five-fold lower (0.19) and *sog* expression is about 30% lower (0.61) than the expression in the control group.

Down-regulation of *twist* expression indicates that *twist* is activated by Toll signaling. In contrast, down-regulation of *sog* is not significant after *Toll-1* knockdown. Minimal amounts of *sog* expression are still detectable in some of the *Toll-1* knockdown embryos

(about 37% listed in Table 3.4). This indicates that *sog* expression is not totally dependent on Toll signaling. In fact, the *sog* transcripts are expressed ubiquitously in early blastoderm embryos (Figure 3.2). Taken together, transcripts of *sog* might be provided maternally or there is an early zygotic expression.

3.11 ISH staining of *dll* knockdown embryos during germband stage

Expression of *twist* in *dll* knockdown embryos during germband stage is shown in Figure 3.17. All expression patterns of *twist* are represented in a schematic drawing shown below the individual ISH images. In wildtype embryos, *twist* is expressed in the presumptive mesodermal domain during gastrulation. In *dll* knockdown, there are varied expression patterns of *twist* in germband embryos. In some embryos, the *twist* expression is absent or reduced (Figure 3.17).

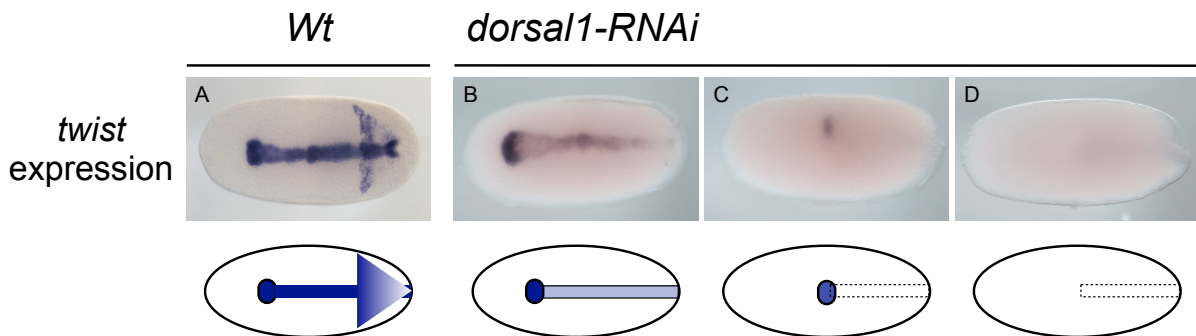


Figure 3.17. Expression of *twist* in *dll* knockdown embryos during germband stage

In *dll* knockdown germband embryos, there are varied expression patterns of *twist*. Expression is either reduced or totally abolished (B-D). Staining pattern of *twist* expression are illustrated under the individual ISH images. The darker or lighter color indicate the degree of *twist* expression. Embryos are at the germband extension stage after gastrulation.

The DV defect after *dll* knockdown is weaker compared to *Toll-1 RNAi*. In contrast to *Toll-1* knockdown embryos, *twist* expression can be detected prevailing after *dll-RNAi* (71%). The *twist* expression in *dll* knockdown embryos can be categorized into three staining patterns (Figure 3.17 B, C, D), named class I, II, III respectively in Table 3.5. In class I, *twist* expression is slightly attenuated along the ventral side of the germband

embryo. In class II, *twist* expression can be detected in the proctodeum exclusively. In class III, there is no *twist* expression after *dll1-RNAi*. This is identical to *Toll1-RNAi* although the ratio is low (10%). The *twist* expression in *dll1* knockdown embryos is further categorized in Table 3.5. The weaker DV phenotype after *dll1-RNAi* is not due to the insufficient knockdown, which is validated by the semi-quantitative PCR (Figure 3.13).

Table 3.5. Categorization of *twist* expression in *dll1* knockdown embryos

<i>dll1</i> knockdown phenotypes			
In Figure 3.17	B	C	D
<i>twist</i> expression pattern	ventral germband	proctodeum	no expression
Classification	I	II	III
Percentage	71%	19%	10%
			n=42

Patterns of *twist* expression were analyzed from three independent ISH stainings.
Embryos counted: n=42

The *dll1* knockdown phenotypes were also analyzed by other marker genes such as *SoxN* and *engrailed* (Figure 3.18). In the beginning of gastrulation, lateral stripes of *SoxN* expression become more straight and perpendicular to the AP axis, because of the dorsalization after *dll1* knockdown (Figure 3.18). The expression of *engrailed* during germband stage is located anterior to the segment border in the abdomen (Campbell and Caveney, 1989). The segmental stripes remain in the *dll1* knockdown condition, but the embryos are lacking DV polarity and form a tube-like shape. A nuclear staining shows clearly the tube-like germband embryo (Figure 3.18 D’).

Another difference between *Toll-1* and *dll1* knockdown is that *sog* expression is strongly reduced and restricted to a more anterior position in *dorsal1-RNAi* embryos. This is not observed in *Toll-1* knockdown (Figure 3.14). More anterior-shifted phenotypes after *Toll-1* and *dll1* knockdown are shown in the section 3.13 by using the other markers.

3.12 Phenotypic analysis of *dorsal2* knockdown by ISH staining

Using the same amount of dsRNA (4 μ g per female) as in previous experiments, females injected with *dl2* dsRNA laid empty eggs exclusively (100%). These eggs stop to develop

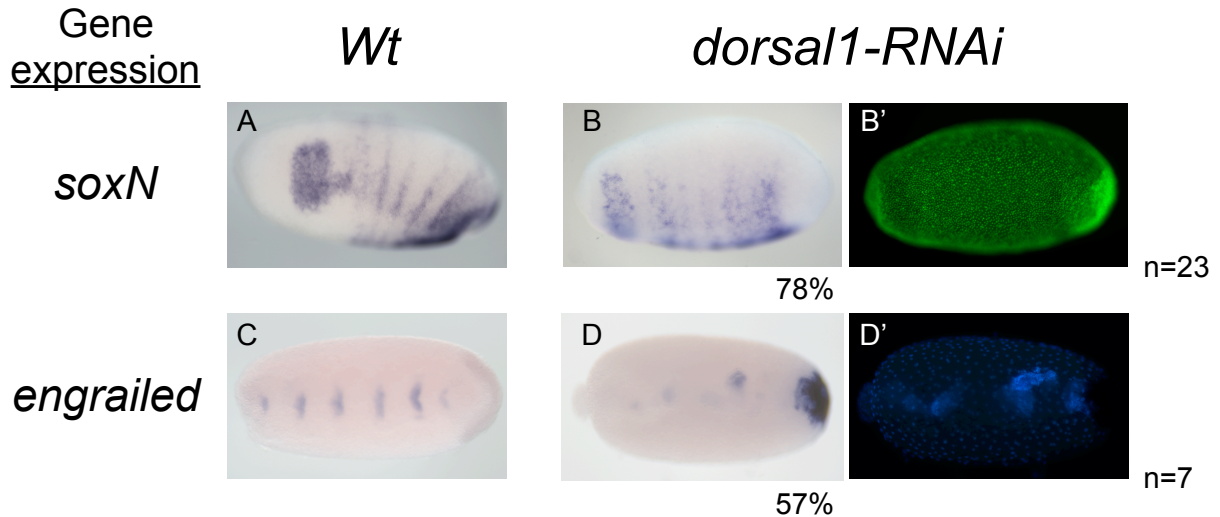


Figure 3.18. Expression of *SoxN* and *engrailed* in *dl1* knockdown embryos during germband stage

In the beginning of gastrulation, lateral stripes of *SoxN* expression become more straight because of the dorsalization after *dl1-RNAi* (B). Lateral view of embryos is shown in A and B; Ventral view of embryos is shown in C. Embryos shown in B' and D' are identical to B and D, with nuclear staining by SytoxGreen and Hoechst33258. During germband extension, the segmental stripes of *engrailed* expression remain in *dl1-RNAi* embryos, but the embryo forms a tube-like shape. The orientation of the knockdown embryo (D) can not be determined due to the absence of DV polarity. Percentage of knockdown embryos with the same expression pattern are indicated below the figure.

as shown in Figure 3.12 J. Probably, the eggs are unfertilized and enriched with yolk. There are some knockdown phenotypes appearing after lowering the amount of dsRNA (0.1 μ g per female). Morphological analysis of *dl2* knockdown embryos shows that they resemble the *Toll-1* knockdown phenotype (Figure 3.12 K and L). ISH staining of *dl2* knockdown embryos during germband stages shows weaker DV phenotypes compared to *Toll-1* and *dl1* RNAi.

In the beginning of gastrulation, expression of the mesoderm marker *twist* and the neuroectodermal marker *sim* can only be detected in the proctodeum of *dl2* knockdown embryos (Figure 3.19 B and D). During germband extension, the *dl2* knockdown phenotype is not recovered. The expression of *sim* is not visible in the ventral midline, but only in the most posterior proctodeum (Figure 3.19 F). This supports that *dl2* is needed for proper DV patterning similar as *dl1*. The knockdown phenotypes suggest a redundant function between *dl1* and *dl2*. Perhaps the transcription factors- Dorsal1 and Dorsal2

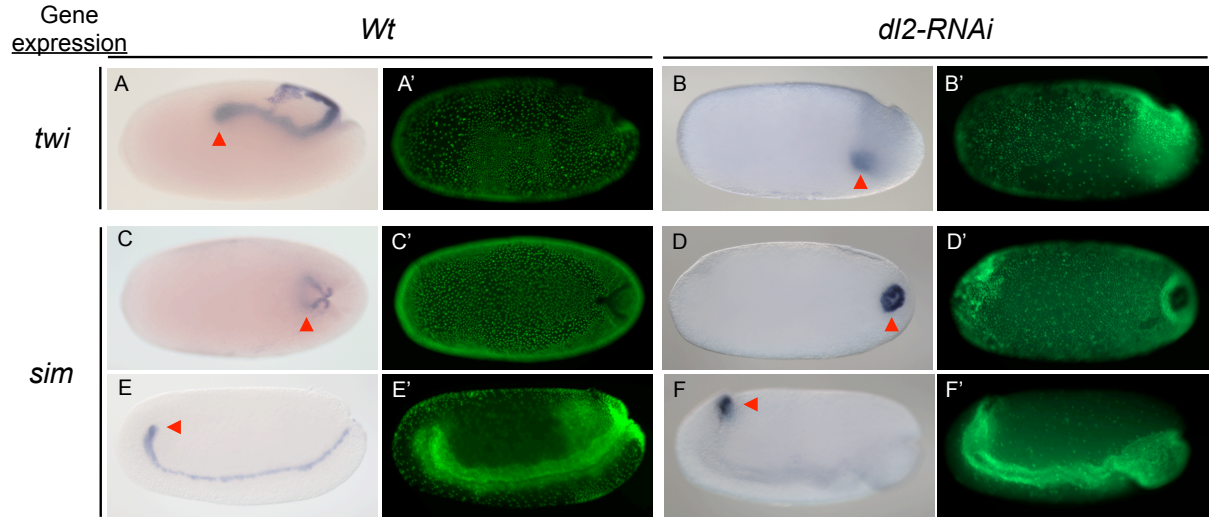


Figure 3.19. Expression of *twist* and *sim* in *dl2* knockdown embryos during germband stage

In the beginning of gastrulation, expression of *twist* and *sim* is detected in the proctodeum of *dl2* knockdown embryos (B and D). The arrowheads indicate the most posterior part (proctodeum) of the germband embryo. During germband extension, the *dl2* knockdown phenotype is not recovered. The expression of *sim* is only detected in the proctodeum (F). Embryos shown in A-F are identical to A'-F', with nuclear staining by SytoxGreen.

cooperate together as heterodimers for proper DV patterning.

3.12.1 Early function of *dorsal2*

The elimination of *twist* and *sim* expression in *dl2* knockdown embryos during gastrulation and germband extension stages are shown in Figure 3.19 and the percentage of those DV patterning defects is given in Table 3.6. However, an additional phenotype of the *dl2* knockdown is observed abundantly at blastoderm stage (about 89%, N=64). In contrast to wildtype, the nuclei are distributed unequally in the blastoderm embryo after *dl2* knockdown. Percentages of the *dl2* knockdown phenotype with unequal nuclear distribution are given in Table 3.6.

The nuclear staining shows clearly the unequal distribution in early blastoderm embryos (Figure 3.20). This could indicate that the nuclei are degrading in *dl2* knockdown embryos, which results in patches of empty spaces in the blastoderm embryo (Figure 3.20B).

The phenotype of unequally distributed nuclei indicates an early function of *dorsal2*.

Table 3.6. Statistics of *dl2* knockdown phenotypes during blastoderm and germband stages

Knockdown phenotypes	Blastoderm stages	Germband stages
	Percentage	Percentage
Wt-like	11 %	12 %
unequal nuclear distribution	89 %	48 %
DV patterning defect	-	40 %
Total embryos	n=64	n=25

Knockdown embryos were analyzed from more than three independent injections.

- The DV patterning defect after *dl2-RNAi* can not be categorized during blastoderm stages because of the unequal nuclear distribution disrupting the marker gene expression. The DV patterning defect is the late knockdown phenotype of *dl2-RNAi*, but not resulting from the unequal nuclear distribution. The structure of the extended germband is normal as in wildtype and the gastrulation is not affected, which is shown in Figure 3.19.

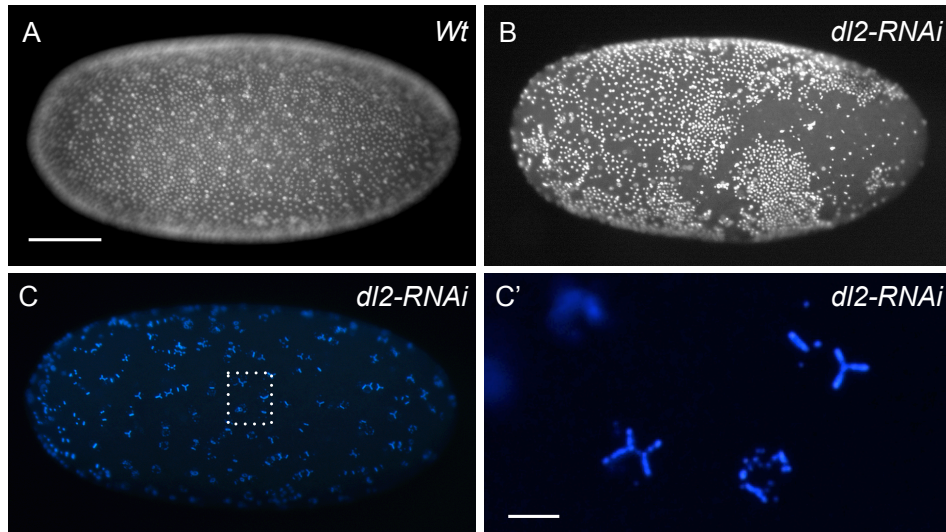


Figure 3.20. Nuclear staining of *dl2* knockdown embryos during blastoderm stages

Embryos shown in A and B are at the blastoderm stage. After *dl2* knockdown, there are patches of empty spaces in the blastoderm embryo. The embryo shown in C is at early blastoderm stage with nuclear staining by Hoechst33258. C' is the magnification from the dotted area in C. The staining shows that the nuclei are degrading. The scale bar size (A-C) corresponds to 200 μm , while the scale bar size (C') corresponds to 25 μm .

Together with the life span reduction after *dl2-RNAi* (shown in the supplementary data), the gene- *dl2* might be involved in innate immunity and DV patterning simultaneously.

3.13 AP patterning in *Oncopeltus* is also dependent on Toll signaling

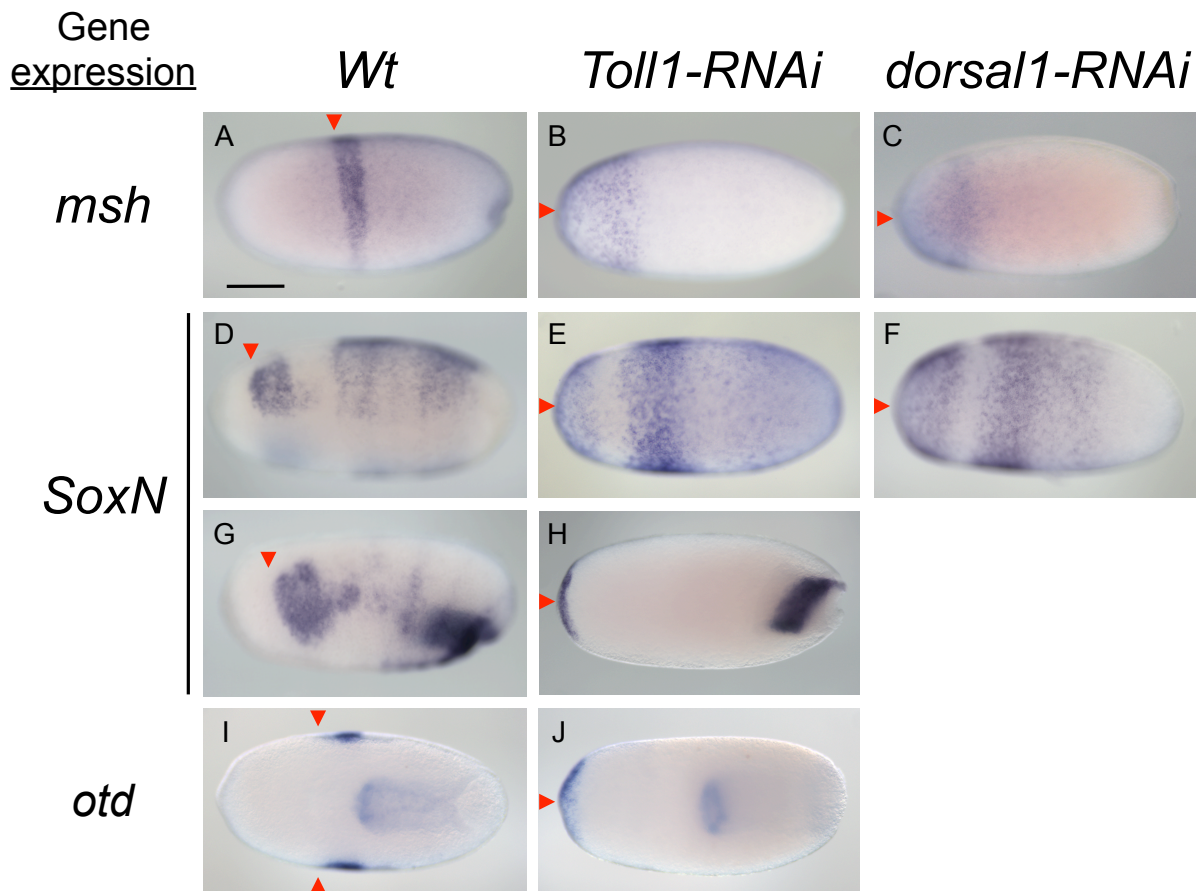


Figure 3.21. Anterior-shifted phenotypes after *Toll-1* and *dl1* knockdown

Embryos are at the blastoderm stage (A-F), or at the beginning of gastrulation (G-J). During blastoderm stages, the expression of *msh*, *SoxN* and *otd* shifts anteriorly after *Toll-1* and *dl1* knockdown (B, E, H, J and C, F). After *Toll-1* and *dl1* knockdown, the stripes of *msh* and *SoxN* expression show no differences along the DV axis. Red arrowheads mark the anterior border of expression. At the beginning of gastrulation, the expression of *SoxN* and *otd* remains in the anterior pole of the embryo and in the extended germband. Furthermore, the expression vanishes from the lateral stripes or the presumptive head region after *Toll-1* knockdown (H and J). The scale bar size corresponds to 250 μ m.

Interestingly, an unexpected expression pattern was found after Toll signaling knock-down. The ventral domain of *sog* expression shifts to a more anterior position after *dll-RNAi* (Figure 3.14). To further investigate the anterior-shifted phenotype after Toll signaling knockdown, other markers were used including the anterior markers *msh*, *otd* and the pan-neuroectodermal marker *SoxN* (Figure 3.21).

During blastoderm stages, the fine stripe of *msh* expression along the DV axis is shifted to the most anterior region covering the anterior pole after *Toll-1* and *dll* knockdown (Figure 3.21B, C). In *Oncopeltus* blastoderm embryos, *SoxN* is expressed more intensively on the dorsal side than the ventral side of the embryos. After *Toll-1* and *dll* RNAi, the stripes of *SoxN* expression show no differences along the DV axis and the first stripe moves to the anterior pole (Figure 3.21E, F).

In the beginning of gastrulation, *SoxN* is expressed in the lateral region marking every segment from head to thorax. However, the expression of *SoxN* remains in the anterior pole of the embryo and in the extended germband after *Toll-1* knockdown (Figure 3.21H). Another anterior marker, *otd* also remains in the anterior pole of the embryo, rather than in the presumptive head region after *Toll-1* knockdown (Figure 3.21J). The anterior-shifted phenotypes of *Toll-1* and *dll* RNAi are further categorized in Table 3.7.

The expression of *sog* in *Toll-1* and *dll* knockdown embryos is shown in Figure 3.14. Anterior-shifted phenotypes of *sog* expression were observed only in *dll-RNAi* embryos. The expression of *sog* in *Toll-1* knockdown embryos is eliminated or reduced, but not shifted anteriorly. The anterior-shifted phenotypes of *Toll-1* and *dll* knockdown suggest that Toll signaling might have a dual role for DV and AP patterning.

Table 3.7. Statistics of anterior-shifted phenotypes with marker gene expression in *Toll-1* and *dll* knockdown embryos

Marker gene	<i>Toll-1</i> knockdown		<i>dll</i> knockdown	
	Percentage	Embryos	Percentage	Embryos
<i>msh</i>	52 %	n=25	78 %	n=9
<i>SoxN</i>	100 %	n=17	20 %	n=15
<i>otd</i>	71 %	n=7	-	-
<i>sog</i>	ND		47 %	n=32

After Toll signaling knockdown, the expression of *msh* and *SoxN* is shifted to the most anterior region during blastoderm stages. In addition, the expression of *SoxN* and *otd* remains in the anterior pole of the extended germband.

ND: *sog* expression in *Toll-1* knockdown embryos is not shifted anteriorly. There are not enough *dll* knockdown embryos with the expression of *otd* at this stage to be analyzed.

3.14 Interaction between Toll and BMP signaling

In *Drosophila*, the expression of *dpp* is regulated by Dorsal, which acts downstream of Toll signaling (Huang et al., 1993). The expression of *sog* and *twist* is also dependent on Toll signaling. The interplay between Toll and BMP signaling contributes to the DV patterning system and specifies distinct domains along the DV axis in *Drosophila* (Wharton et al., 1993). To understand the interaction between Toll and BMP signaling in *Oncopeltus*, the double knockdown situation was established to study which pathway is more dominant for DV patterning and the influence on patterning genes.

3.14.1 Double Knockdown of *Toll-1* and *dpp*

In the milkweed bug, Toll signaling is necessary for the robust expression of *sog* and *twist*. The expression of *sog* and *twist* is eliminated after *Toll-1* knockdown (Figure 3.14). On the contrary, BMP signaling is used to pattern the entire DV axis in *Oncopeltus* (Sachs, 2014). After *dpp-RNAi*, the expression of *sog* and *twist* is expanded throughout the embryonic circumferences (Figure 3.22 B, E), which is the opposite of the *Toll-1* knockdown phenotype. To understand the expression of *sog* and *twist* in the embryos simultaneously lacking Toll and BMP signaling, double knockdown of *Toll-1* and *dpp* was achieved via coinjection of dsRNAs. Eggs laid by the injected mother were analyzed according to the expression pattern of the ventral marker genes *sog* and *twist*. After double knockdown, expression of *sog* and *twist* expands throughout the entire embryonic circumferences, which is similar to the expression in the *dpp* knockdown (Figure 3.22). The resembling phenotypes of the *dpp* and double knockdown suggest that *dpp* is epistatic to *Toll-1* for the ventral expression. Expression of *sog* and *twist* can be activated in the absence of Toll signaling under the double knockdown condition.

3.14.2 Validation of double knockdown efficiency

In the double knockdown embryos, the expansion of *sog* and *twist* expression is similar to the single *dpp* RNAi. To confirm the double knockdown, the expression level of transcripts was estimated by the semi-quantitative PCR to validate the RNAi efficiency (Figure 3.23). The absence of *Toll-1* and *dpp* transcripts on the gel is an evidence that the double knockdown is efficient.

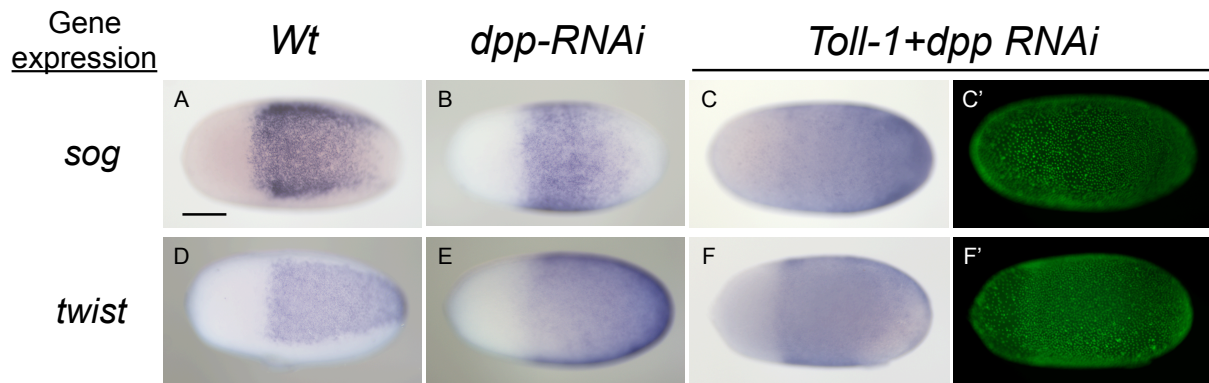


Figure 3.22. Expression of *sog* and *twist* in *dpp* knockdown and double knockdown embryos

The expression of ventral markers *sog* and *twist* expands throughout the entire embryonic circumferences in the *dpp* knockdown (B and E) and double knockdown embryos (C and F). However, the distribution of nuclei is affected after double knockdown, which is not detectable in the *dpp-RNAi* or *Toll1-RNAi* embryos (C' and F'). Embryos are all at the blastoderm stage. Embryos in C' and F' are identical to C and F with the SytoxGreen staining. Ventral view of the embryo is shown in A and D, while in the others the DV polarity can not be determined. The scale bar size in all figures corresponds to 250 μm .

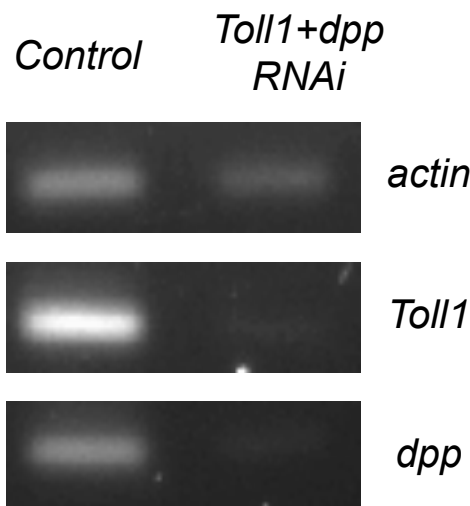


Figure 3.23. Validation of *Toll-1* and *dpp* knockdown efficiency by the semi-quantitative PCR

The expression of *Toll-1* and *dpp* is highly down-regulated after pRNAi. cDNA was synthesized from the RNA of blastoderm embryos (26-32 AEL) and served as the template for the semi-quantitative PCR. Expression of the gene *actin* served as the internal control.

3.14.3 The contrary roles of Toll and BMP signaling

To investigate the interaction between Toll and BMP signaling and their influence on DV patterning genes, the expression level of *sog* and *twist* was estimated by qPCR after *Toll-1* and *dpp* knockdown (Figure 3.24). The expression level of *sog* and *twist* is down-regulated after *Toll-1* knockdown, but up-regulated after *dpp* knockdown during blastoderm stages. This indicates that *dpp* inhibits the expression of *sog* and *twist*, while *Toll-1* activates their expression. Toll and BMP signaling play contrary roles in regulating DV patterning genes. However, the expression of *sog* and *twist* can be activated in the absence of Toll signaling under the double knockdown condition. Therefore, it seems like the effect of inhibition from BMP signaling is stronger than the effect of activation from Toll signaling.

3.15 Twist has a conserved function in mesoderm formation

The previous results demonstrate that Toll signaling is important for the transcriptional expression of *twist* (Figure 3.14, 3.24). Furthermore, it has been studied that the basic helix-loop-helix (bHLH) transcription factor Twist plays a conserved role in mesoderm formation (Thisse et al., 1988; Sommer, R. J. and Tautz, D., 1994; Handel et al., 2005). Taken together, it seems that Toll signaling controls the mesoderm formation through the activation of *twist* in the milkweed bug. Thus, knockdown embryos after *twist-RNAi* were studied and compared with the Toll knockdown phenotypes.

In *twi-RNAi* embryos, the invaginated germband is slimmer and the size of leg buds is reduced (Figure 3.25). These embryos stop to develop at a later stage and never hatch as nymphs (100%, N=45). Moreover, *twi-RNAi* embryos exhibit distinct phenotypes from Toll signaling knockdown embryos. Based on *sim* expression, a ventrally shifted mesodermal position can be observed in *twist* knockdown embryos (Figure 3.26). The *twist* expression in *twi-RNAi* embryo served as the negative control to validate the knockdown efficiency (Figure 3.26 D). The knockdown phenotypes indicate the absence of mesodermal tissues. In contrast to the *twi-RNAi* embryos, the neuroectoderm and the mesoderm are both absent when knocking down *Toll-1* (Figure 3.14). During the invagination stage, the dorsalized embryos produced by *Toll1-RNAi* lack the entire ventral midline (Figure

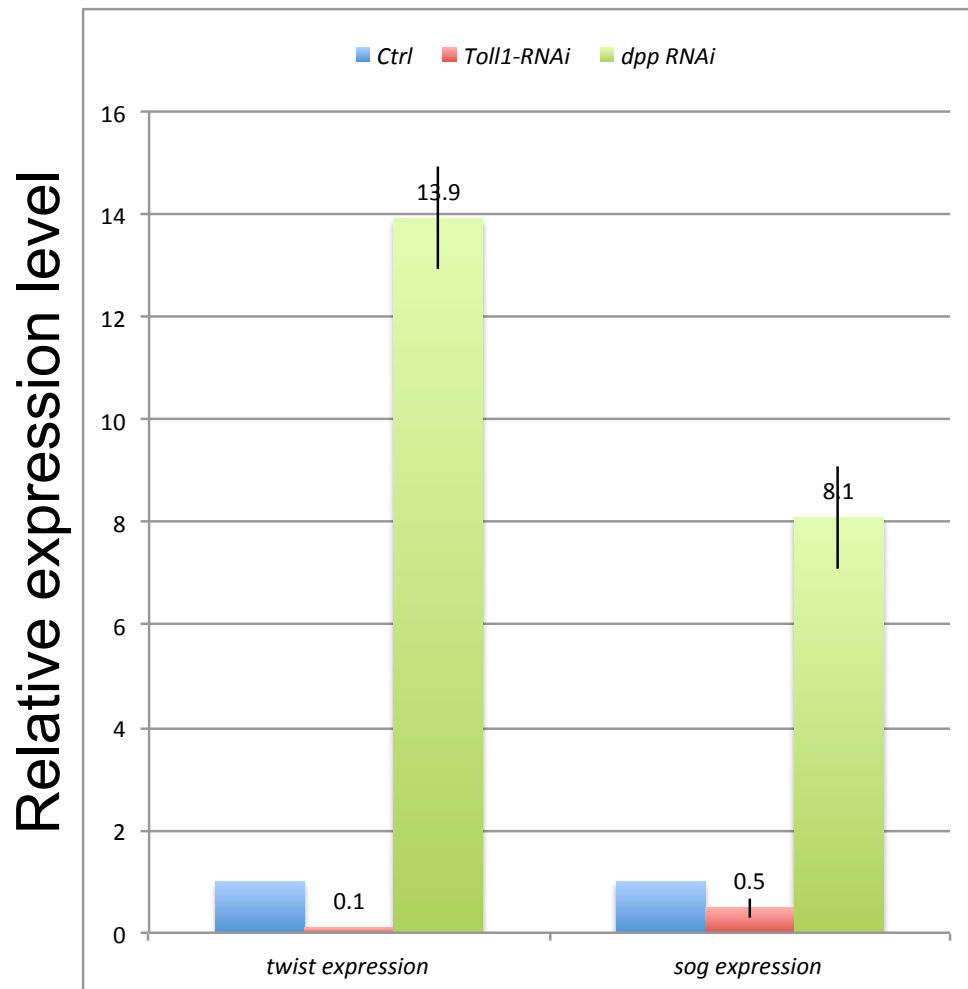


Figure 3.24. The expression levels of *sog* and *twist* after *Toll-1* and *dpp* knockdown

The expression level of *sog* and *twist* was measured after *Toll-1* and *dpp* knockdown during blastoderm stages (26-29 hours after egg lay). The quantification was normalized using 18S ribosomal RNA gene as reference. The expression level of the control group is set to 1.0 while the expression level of knockdown groups is indicated above the bar. Bars = means \pm standard deviation (n=3)

The expression level of *sog* and *twist* are down-regulated after *Toll-1* knockdown, but up-regulated after *dpp* knockdown during blastoderm stages.

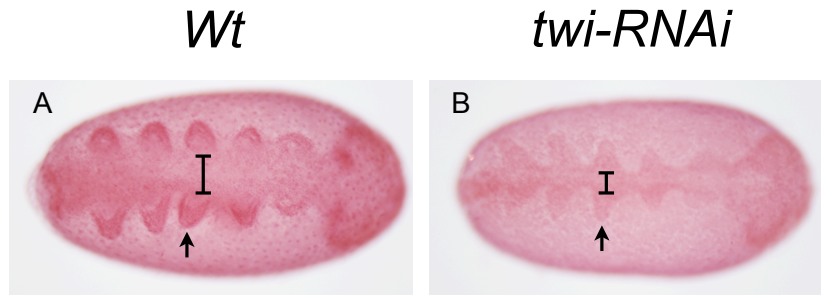


Figure 3.25. Fuchsin staining of *twist* knockdown during germband stages

Anterior pole of the egg is to the left, embryo anterior is to the right. Embryos are at the germband stage. The arrows mark the limb bud and the width of T1 segment is also indicated (A and B).

3.15).

3.16 The distribution of Dorsal1 proteins

Since knockdown of *dorsal1* leads to a DV defect, it is possible that the *Oncopeltus* Dorsal1 protein acts as a morphogen forming the nuclear gradient along the DV axis as in *Drosophila* (Roth et al., 1989).

3.16.1 Dorsal1 is constantly expressed during development

A purified Dorsal1 (OfDorsal1) antibody was produced, specifically recognizing the RHD domain to detect the temporal and spacial expression of Dorsal1 proteins. The temporal expression of endogenous Dorsal1 proteins was detected from early blastoderm stage to late germband extension stage in a western blot (Figure 3.27).

3.16.2 Dorsal1 is ubiquitously expressed

Since the Dorsal1 protein is expressed constantly (Figure 3.27), the spatial expression was studied by whole-mount immunostaining. However, there is no nuclear gradient of Dorsal1. Even when the purified antibody was preabsorbed with wildtype blastoderm embryos, the background was too high to detect the nuclear gradient.

After several trials of immunostaining, empirical staining results were described here. First, there is a cytoplasmic staining with DV differences, but no staining in the nuclei

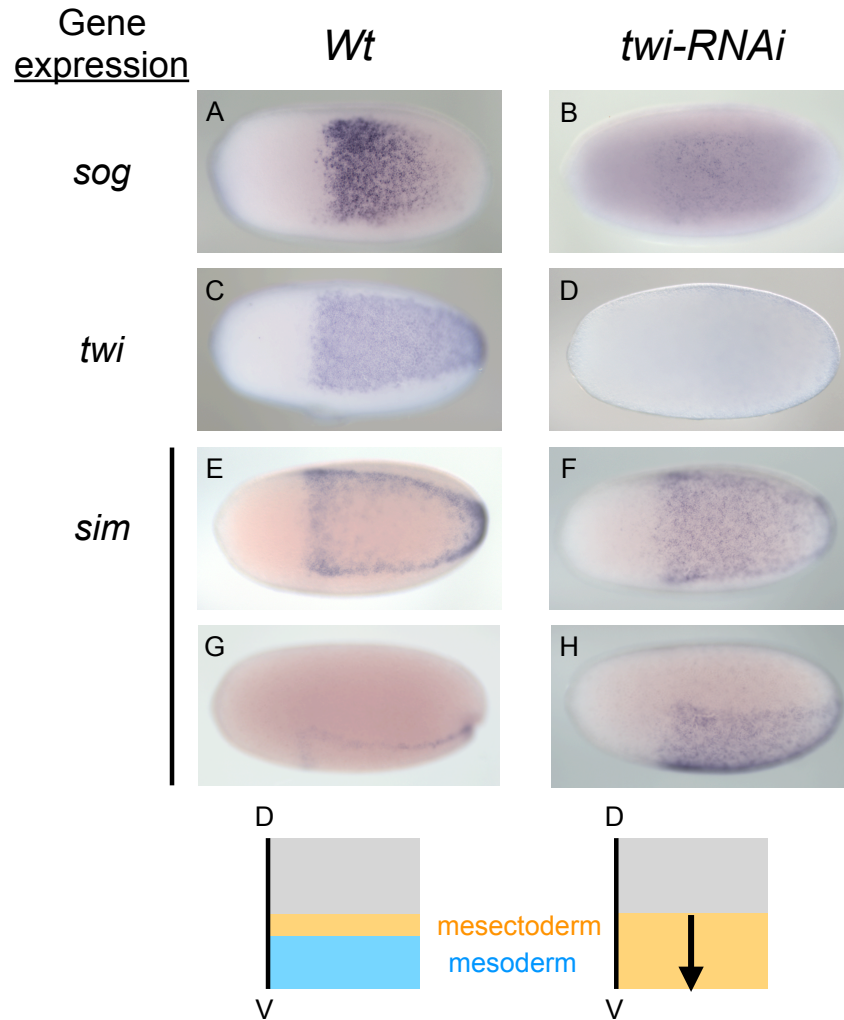


Figure 3.26. ISH staining of *twist* knockdown embryos during blastoderm stage

ISH staining of *sog* expression (A and B) in wildtype and *twist* knockdown embryos. ISH staining of *twist* expression (C and D) served as the negative control to validate the knockdown efficiency. ISH staining of *sim* expression in wildtype (E and G) and *twist* knockdown embryos (F and H). Ventral view of embryos is shown in A-C, E and F; lateral view of embryos is shown in G and H. In *twist* knockdown embryos, the mesectoderm shifted ventrally to replace the mesoderm (F and H), which is also illustrated below.

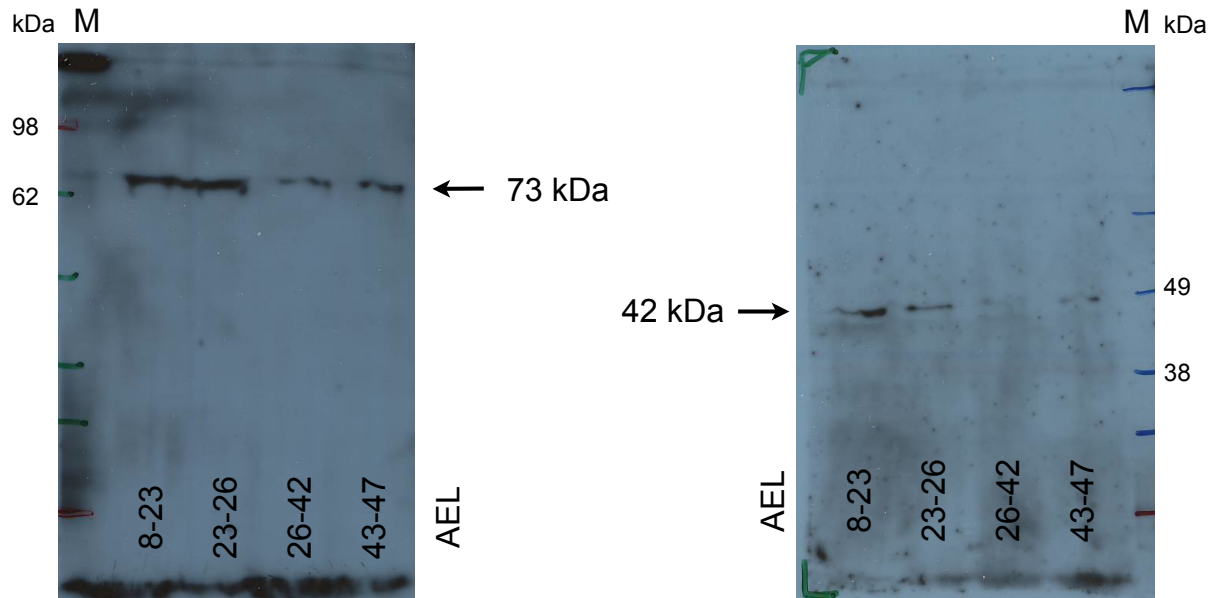


Figure 3.27. OfDorsal1 antibody specifically detects endogenous proteins

The OfDorsal1 antibody specifically recognizes the endogenous Dorsal1 proteins at 73 KDa across different embryonic stages. The beta-actin antibody was used as a loading control recognizing a band at 42 KDa shown on the right film. The temporal expression of proteins is indicated as hours after egg lay (AEL) ranging from early blastoderm stages to late germband extension stages.

(Figure 3.28 A-C). Secondly, there is an ubiquitous nuclear staining without DV differences (Figure 3.28 D-F). Thirdly, there is an ubiquitous nuclear and cytoplasmic staining (Figure 3.28 G-I). These staining results indicate that there might be an extremely dynamic translocation of Dorsal1 into the nucleus or it is due to the unspecific signals. More specified stages of blastoderm embryos are needed to detect if there is any transiently expressed nuclear Dorsal1 gradient. A cross-section of blastoderm embryos might be another solution to investigate whether there is a weak nuclear gradient, which can not be detected by whole-mount immunostaining.

3.16.3 Bioinformatic prediction of Dorsal binding sites

Due to ubiquitous Dorsal protein distribution, it is possible that low levels of nuclear Dorsal are sufficient to activate *sog* expression on the ventral side. Therefore, there could be some high-affinity Dorsal binding sites regulating the expression of *sog*.

First, all of the Dorsal binding motifs from *Drosophila* (Papatsenko and Levine, 2005) were used to predict the location of binding clusters in the cis-regulatory region of *sog*

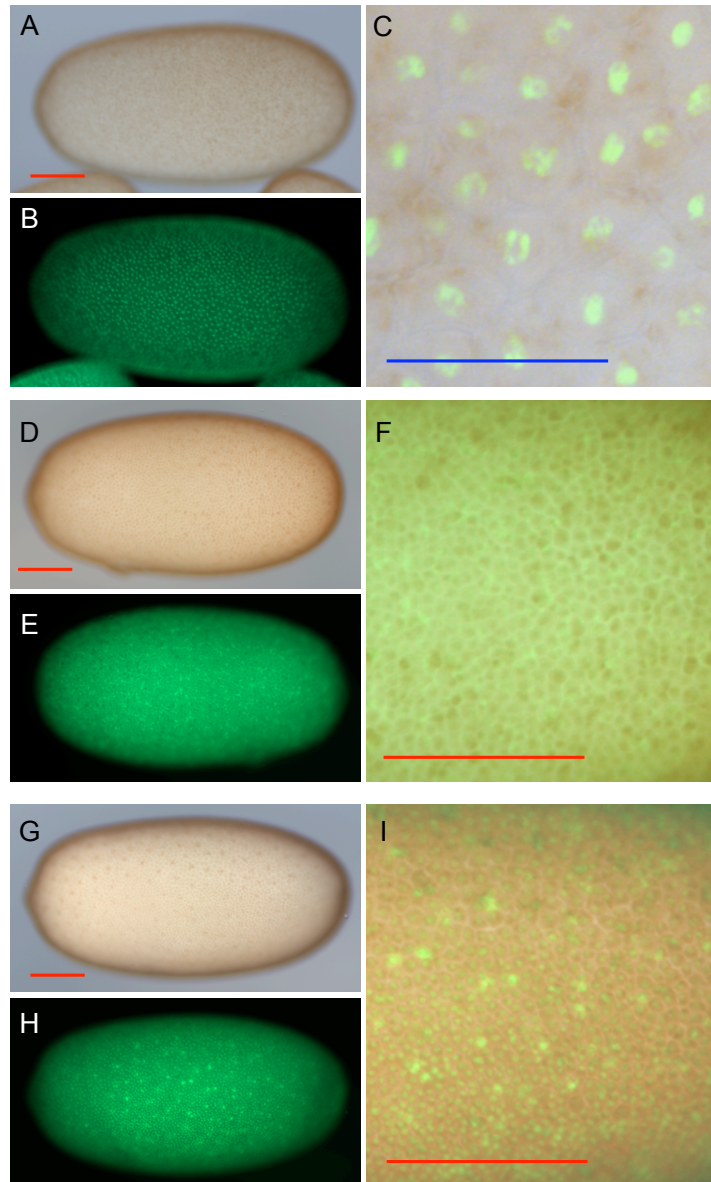
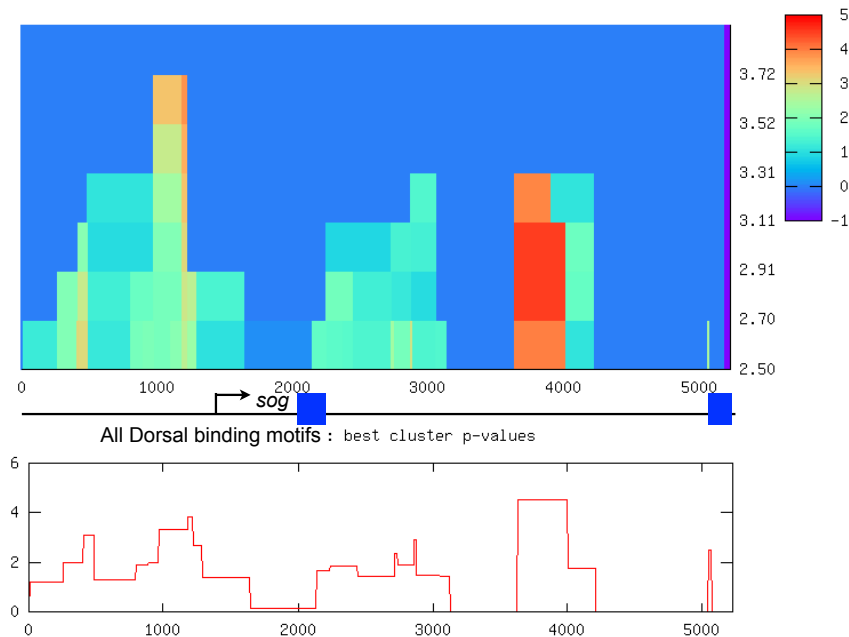


Figure 3.28. Whole-mount immunostaining of Dorsal1 in blastoderm embryos

All embryos are in the blastoderm stages after cellularization. The embryo in B is identical to A with SytoxGreen staining to show the nuclei. The magnification (C) of merged channels (A+B) shows the cytoplasmic staining with DV difference, but no specific staining in the nucleus. The embryo in E is identical to D with fluorescent Wheat Germ Agglutinin (WGA) staining to show the cell membrane. The magnification (F) of merged channels (D+E) shows the ubiquitous nuclear staining by DAB. The embryo in H is identical to G with SytoxGreen staining to show the nuclei. The magnification (I) of merged channels (G+H) shows the ubiquitous nuclear and cytoplasmic staining without DV differences. Scale bar size corresponds to 50 μm in C; Scale bar size corresponds to 200 μm in the others.



(a) Location of all Dorsal binding sites

Cluster #1, score = 4.54, match cutoff = 2.50

```
>sog:5Kupstream 3634-3999 4.54 2.50
GGGAAACCCCTCTATCATCATAGTTACATTGTAATATTTACACCTTCAATTGATAAAAAATAATTAATTC
AATATCAAATTAATAATCAATAATAAATTACTGAGGATACTCTTGAATTAAGGCTAACACTAGTAGAATA
CTTTGATTATTAATATTAAGAGAGAACTGGATTGGACTTCCATTGTCATAGGATGAGACAGAGAGAGA
GTTTATGGGAAGAAAAATTCATATTGAGGATGTGACTTAGTAACTGGGTGCATCCCCACAGTTCTATCT
TGATCTGCCATTTCTATTATTTGCTTTCCGATTGGTAAAAATTAATAATTTATTTATATTTTGATCATA
CTTTAGTTATACTTGGAAATCTGC
```

Matches:

Position	Name	Orient.	Sequence	Score	-log(P)
1	d1	R	GGGGTTTCCC	11.4	6.17
175	d1	D	TGGACTTCCA	3.7	2.91
259	d1	D	GTGCATCCCC	4.55	3.15
303	d1	D	TTGCTTTCCG	3.52	2.87
366	d1	R	GCAGATTTC	4.29	3.07

(b) Sequence of predicted Dorsal binding motifs

Figure 3.29. Prediction of all Dorsal binding sites in *Oncopeltus sog*

The bioinformatic prediction of all Dorsal binding sites was conducted by ClusterDraw web server (Papatsenko, 2007). The cluster significance cutoff value was set to 3. The background model setting to *T. castaneum* or *D. melanogaster* does not change the cluster peaks. About 5Kb nucleotide sequence of *Oncopeltus sog* was provided to conduct the bioinformatic prediction. The first and second exon of *sog* are indicated in (a). The Dorsal binding clusters are located upstream of the transcription start site and in the intronic region of *Of-sog*.

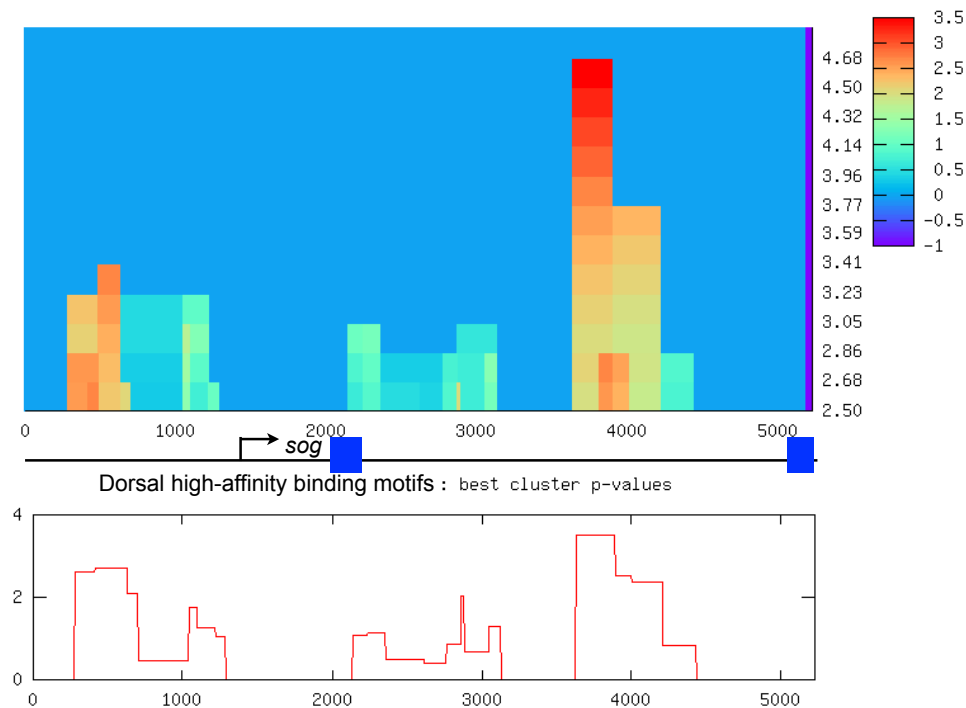
in *Oncopeltus*. The potential Dorsal binding peaks and the sequence of binding motifs are shown in Figure 3.29. The Dorsal binding clusters are located upstream of the transcription start site and in the intronic region of *sog*. Secondly, two consensus sequences of high-affinity Dorsal binding sites from *Drosophila* (Markstein et al., 2002)¹ were used to conduct a bioinformatic prediction in *Oncopeltus* to confirm if the potential Dorsal binding peaks are high-affinity binding sites.

From the bioinformatic prediction, there are three significant peaks of predicted Dorsal binding sites (Figure 3.29 and 3.30). One is located upstream of the transcription start site and the others are in the intronic region. Predicted peaks of the binding clusters colocalize for all Dorsal and high-affinity Dorsal binding sites. This indicates that these binding clusters are high-affinity Dorsal binding sites. The location of Dorsal binding sites on *sog* in *Oncopeltus* coincides with the conservation of enhancer positions discovered in *Drosophila* and *Tribolium* (Cande et al., 2009), which is upstream of the transcription start site or in the intronic region. However, the precise binding sites of Dorsal protein in *Oncopeltus* need to be validated by Chromatin immunoprecipitation (ChIP).

3.17 Signaling components downstream of the Toll receptors

The Myd88 and Tube adaptors, and the Pelle kinase are known to be downstream components of Toll signaling in *Drosophila*. Myd88 is an adaptor protein containing a TIR domain to interact with the Toll receptor (Xu et al., 2000), and a death domain (DD) to recruit the IRAK (interleukin-1 receptor-associated kinase) proteins such as Pelle (Galindo et al., 1995). The BLAST against the *Oncopeltus* transcriptome identifies only one *myd88* (Table 3.1). However, there are two candidates for IRAK-related homologs in the *Oncopeltus* transcriptome. The BLAST against the NCBI database shows that both of the candidates are homologous to *pelle* or unidentified protein kinases in other insect species (Table 3.1). To identity whether they are homologous to *Drosophila pelle* or *Drosophila tube*, the comparison of conserved domains is needed.

¹Dm-high affinity binding sites 1 (Dm-high1) GGGWWWWCCM
Dm-high affinity binding sites 2 (Dm-high2) GGGWDWWWCCM
(where W = A or T, M = C or A; and D = A, T, or G)



(a) Location of high-affinity Dorsal binding sites

Cluster #1, score = 3.50, match cutoff = 4.14

>sog:5Kupstream 3634-3890 3.50 4.14

```
GGGAAACCCCTCTATCATCATAGTTACATTGTAATATTTACCTTCAATTGATAAAAAATAATTAATTC
AATATCAAAATTAATAATCAATAATAAATTACTGAGGATACTCTTGAATTAAGGCTAACACTAGTAGAATA
CTTTGATTATTAATATTTAAAGAGAGAACTGGATTGGACTTCCATTGTCATAGGATGAGACAGAGAGAGA
GTTTATGGGAAGAAAAATTCATATTGAGGATGTGACTTAGTAAACTGGGTGCATCCC
```

Matches:

Position	Name	Orient.	Sequence	Score	$-\log(P)$
1	Dm-high1	D	GGGAAACCC	6.91	4.67
175	Dm-high1	D	TGGACTTCCA	4.5	2.85
257	Dm-high2	D	GGGTGCATCCC	7.31	4.91

(b) Sequence of predicted high-affinity Dorsal binding motifs

Figure 3.30. Prediction of high-affinity Dorsal binding sites on *Oncopeltus sog*

The bioinformatic prediction of high-affinity Dorsal binding sites was conducted by ClusterDraw web server (Papatsenko, 2007). The cluster significance cutoff value was set to 3. The background model setting to *T. castaneum* or *D. melanogaster* does not change the cluster peaks. About 5Kb nucleotide sequence of *Oncopeltus sog* is provided to conduct the bioinformatic prediction. The first and second exon of *sog* are indicated in (a). The high-affinity Dorsal binding clusters are located upstream of the transcription start site and in the intronic region of *Of-sog*.

3.17.1 Pelle or Tube? That is the question.

It is reported that IRAK proteins share similarity with *Drosophila* Pelle, which is a protein kinase essential for the activation of Dorsal (Cao et al., 1996). The ortholog of vertebrate IRAK-4 in *Drosophila* is Tube (Towb et al., 2009), which lacks a catalytic domain of the Serine/Threonine kinases. In contrast to *Drosophila*, two candidates for *Oncopeltus* IRAK-related homologs (isotig15858 and isotig05547) both contain a DD and a catalytic domain. The comparison of DD and protein kinase domain (PK) with *Drosophila* Pelle and Tube is listed in Table 3.8.

Table 3.8. Similarity of conserved domains compared with *Drosophila* Pelle and Tube

	<i>Drosophila</i> Pelle	
	death domain (DD)	+ protein kinase domain (PK)
isotig15858	35.42 %	49.62 %
isotig05547	19.59 %	36.60 %
	<i>Drosophila</i> Tube	
	death domain (DD)	
isotig15858	18.56 %	
isotig05547	34.71 %	

A Percent Identity Matrix was created by Clustal2.1 (<http://www.ebi.ac.uk/Tools/msa/clustalw2/>) based on the similarity of conserved domains compared to *Drosophila* Pelle and Tube. The conserved DD and PK encoded by isotig15858 are more similar to *Drosophila* Pelle. The conserved DD encoded by isotig05547 is more similar to *Drosophila* Tube.

Based on the comparison of conserved domains, the DD and PK encoded by isotig15858 are more similar to *Drosophila* Pelle (with 35% and 50% similarity). Henceforth, the transcript isotig15858 is suggested to be *pelle*. The conserved DD encoded by isotig05547 is more similar to *Drosophila* Tube (with 35% similarity) rather than Pelle (only with 20% similarity). Additionally, the transcript isotig05547 also encodes a kinase domain on the C-terminus. Hence, it is suggested to be *tube-like kinase*.

3.17.2 Phylogenetic analysis of Pelle, Tube, and Myd88

Since Pelle, Tube, and Myd88 share the conserved death domain (DD), a phylogenetic analysis was conducted to prove that the similarity of the shared domain is competent to distinguish Pelle from Tube proteins (Figure 3.31). The phylogenetic analysis indicates that Pelle, Tube, and Myd88 are clustered as distinct families. Within the Pelle family,

Oncopeltus Pelle is clustered with *Tribolium* Pelle as a sister group to *Drosophila* Pelle. Within the Tube family, the Tube-like kinase of *Oncopeltus* is clustered with *Tribolium* as a sister group to *Drosophila* Tube. Within the Myd88 family, the Myd88 of *Oncopeltus* is clustered with *Drosophila* as a sister group to *Tribolium* Myd88. Members of Myd88 proteins served as an outgroup of Pelle and Tube proteins.

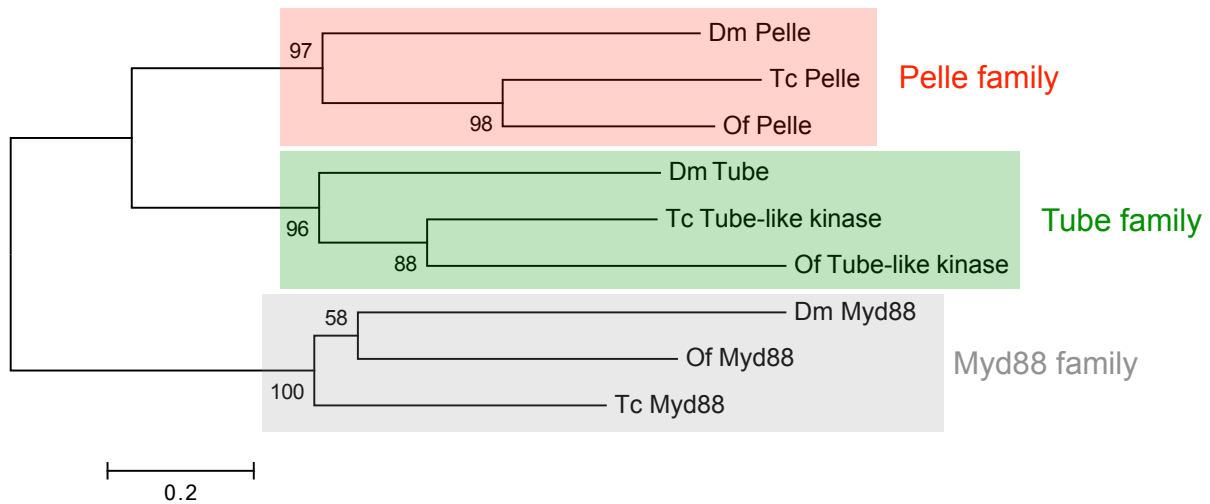


Figure 3.31. Phylogenetic analysis of Pelle, Tube, and Myd88

Proteins sequences of Pelle, Tube, and Myd88 are compared between *Oncopeltus*, *Drosophila*, and *Tribolium*. Only the death domain (DD) was aligned to construct the phylogenetic analysis in MEGA6 (Tamura et al., 2013). Proteins sequences of Pelle, Tube, and Myd88 are clustered as distinct families. The evolutionary history was inferred using the Neighbor-Joining method. The percentage of replicate trees in which the associated taxa clustered together in the bootstrap test (1000 replicates) are shown next to the branches. The tree is drawn to scale, with branch lengths in the same units as the evolutionary distances. The evolutionary distances were computed using the Poisson correction method and are in the units of the number of amino acid substitutions per site. The analysis involved 9 amino acid sequences.

3.17.3 Tube or Tube-like kinase? case study in other insects

The catalytic domain is absent in *Drosophila* Tube, but the catalytic domain of Tube orthologs can be found in other species (Towb et al., 2009). To understand if the absence of the catalytic domain in *Drosophila* Tube was an independent event during the evolution of insects, orthologs of *pelle* and *tube* were compared in different insect lineages. Protein sequences from the silkworm, flies, mosquitoes, beetles, pea aphid, body louse, and several hymenopteran species were compared. The comparison of Tube or Tube-like kinase between different insects is shown in Figure 3.32.

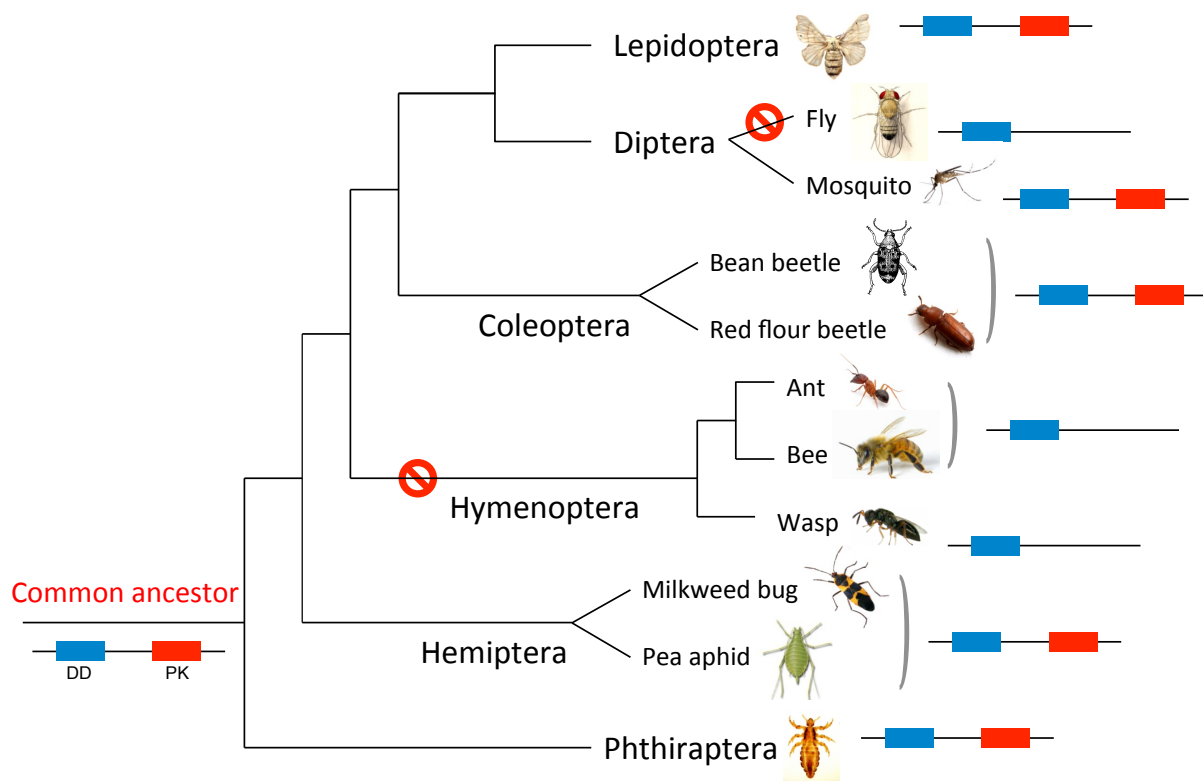


Figure 3.32. Comparison of Tube or Tube-like kinase in different insect species

The orthologs of Tube were compared in different insect lineages. The blue rectangle indicates the death domain (DD) and the red rectangle indicates the protein kinase domain (PK). The PK domain is lost independently in the flies and in the branch of Hymenoptera. This indicates that the common ancestor of insects might have two kinase proteins (Pelle and Tube-like kinase) with catalytic domains. Protein sequences from different insect species with abbreviations were listed here: the silkworm *Bombyx mori*, two flies *Drosophila melanogaster*, *Drosophila pseudoobscura pseudoobscura*, three mosquitoes *Aedes asgypti* (Aa), *Culex quinquefasciatus* (Cq), *Anopheles gambiae* (Ag), the red flour beetle *Tribolium castaneum* (Tc), the ants *Camponotus floridanus* (Cf), *Harpegnathos saltator* (Hs), the honey bee *Apis mellifera* (Am), the buff-tailed bumblebee *Bombus terrestris* (Bt), the pea aphid *Acyrtosiphon pisum*, and the body louse *Pediculus humanus humanus*. Sequences from the jewel wasp *Nasonia vitripennis* (Nv) were kindly provided by T. Buchta. The transcriptome of the bean beetle *Callosobruchus maculatus* was kindly provided by J. Lynch.

The catalytic domain of Tube homologs is lost in the ants (*Cf* and *Hs*), bees (*Am* and *Bt*), and the wasp *Nasonia*. This indicates that the PK domain is lost in the common ancestor of Hymenopterans. Within the order Diptera, orthologs of *pelle* and *tube* were predicted in a cyclorrhaphous hover fly *Episyrphus balteatus* based on the 454 reads from the NCBI Short Read Archive (SRA). The catalytic domain of the Tube homolog in the hover fly seems to be absent as well as in *Drosophilidae*. However, the Tube homologs of mosquitoes (*Aa*, *Cq*, *Ag*) all contain the catalytic domain. This indicates that the loss of the PK domain might have occurred in the common ancestor of cyclorrhaphous flies, but not in the common ancestor of Diptera. Taken together, the PK domain was lost independently only in the flies and in the branch of Hymenoptera. The comparison indicates that the common ancestor of insects might have had two kinase proteins (Pelle and Tube-like kinase) with catalytic domains.

3.17.4 Knockdown of the adaptor and kinase proteins

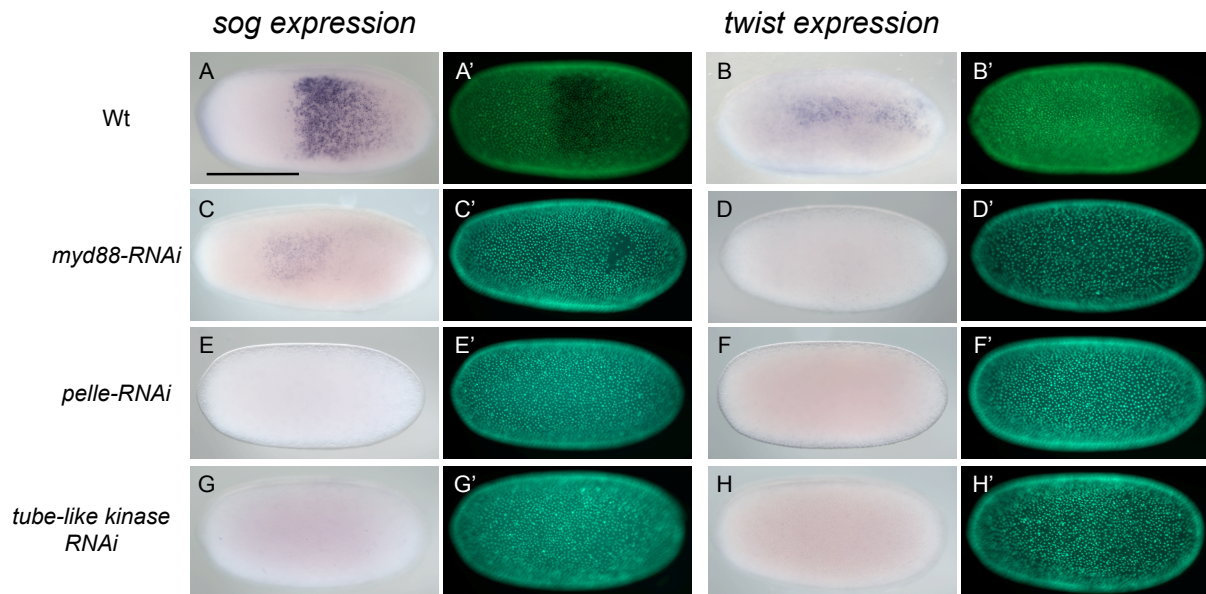


Figure 3.33. Knockdown phenotypes of *myd88*, *pelle* and *tube-like kinase*

The *myd88*, *pelle* and *tube-like kinase* Knockdown embryos exhibit eliminated *sog* and *twist* expression as *Toll1-RNAi* embryos. All embryos are at the early blastoderm stages. Embryos shown in A'-H' are identical to A-H with SytoxGreen staining. Anterior is always to the left. Ventral view of embryos is shown in A-C. The orientation of DV axis can not be determined in other Knockdown embryos. Scale bar size corresponds to 500 μm .

Morphological analysis of *myd88* knockdown embryos shows that the phenotype is similar to the mild defect after *dll-RNAi* (Figure 3.12G). Furthermore, the *pelle* knockdown embryos resemble the *Toll1-RNAi* phenotype (Figure 3.12H). ISH staining of *myd88*, *pelle* and *tube-like kinase* Knockdown embryos exhibits eliminated *sog* and *twist* expression as in *Toll1-RNAi* embryos (Figure 3.33). This indicates that these components are involved in Toll signaling and are required for proper DV patterning.

Table 3.9. Statistics of *Myd88*, *Pelle* and *Tube-like kinase* Knockdown phenotypes

Group	<i>sog</i> expression		Embryos
	remnant (%)	absent (%)	
<i>myd88-RNAi</i>	65	35	n=17
<i>pelle-RNAi</i>	8	92	n=12
<i>tube-like kinase RNAi</i>	33	67	n=18

There is a high percentage of *myd88* knockdown embryos with remnant *sog* expression (65%). The statistic data derives from three independent dsRNA-injections. Knockdown embryos were collected for ISH during early blastoderm stages.

In *myd88*, *pelle* and *tube-like kinase* knockdown embryos, the *twist* expression is totally abolished and the ventral *sog* expression is down-regulated during blastoderm stages (Figure 3.33). However, there is a high percentage of *myd88* knockdown embryos with remnant *sog* expression (65%, in the Table 3.9). The DV asymmetry remains in *myd88* knockdown embryos (Figure 3.33), probably because of insufficient knockdown.

3.18 Inhibitors of the NF κ B transcription factor (I κ B)

In *Drosophila*, loss-function of *cactus* produces ventralized embryos since Cactus is an inhibitor of Dorsal protein (Roth et al., 1989; Nüsslein-Volhard, 1991; Geisler et al., 1992). The sequence of *cactus* encodes several ankyrin repeats and shares high homology to I κ B proteins (Kidd, 1992; Geisler et al., 1992). In vertebrates, the NF κ B transcription factor is inhibited by I κ B proteins, which is analogous to the interaction between Dorsal and Cactus.

3.18.1 The putative *cactus* genes in *Oncopeltus*

There are four putative *cactus* (*cact*) genes in *Oncopeltus* (Table 3.10). The BLAST results show that they are all homologous to *Drosophila cactus* or homologous to I κ B proteins from other arthropods. All of the genes encode several ankyrin repeats (ANK). There are 45-31% identity shared with the ANK of *Drosophila Cactus* (Table 3.10). The genes are called *cactus 1-4* in the order of decreasing similarity to *Drosophila Cactus*. The multiple alignments of ANKs are shown in Figure 3.34.

Table 3.10. List of putative *cactus* genes in *Oncopeltus*

Name	Transcripts	Blasting results ★			ANK Identity (%)
		Against <i>Dm</i>	E-value	Best Hit	
<i>cact-1</i>	cap3_12011	<i>cactus</i>	$2e^{-30}$	Phc-I κ B	45.30
<i>cact-2</i>	isotig01670	<i>cactus</i>	$6e^{-26}$	Phc-I κ B	35.76
<i>cact-3</i>	isotig06987†	<i>cactus</i>	$8e^{-17}$	Cr-I κ B	31.07
<i>cact-4</i>	isotig09451	<i>cactus</i>	$1e^{-16}$	Phc-I κ B	32.19

All transcripts were found in the *Oncopeltus* transcriptome.

†: with RACE-PCR extension

★: The BLAST results are aligned constantly to *Drosophila cactus*. The E-value of tBlastX is listed. Transcripts were translated to amino acid sequences by EMBOSS Sixpack. The best hits were annotated by NCBI BLAST using the blastP algorithm. Abbreviation of species: *Dm*= *Drosophila melanogaster*, *Phc*= *Pediculus humanus corporis*, *Cr*= *Carcinoscorpius rotundicauda* (horseshoe crab).

A Percent Identity Matrix was created by Clustal2.1 based on the similarity of the conserved ankyrin repeats domain (ANK) compared to *Drosophila Cactus*.

3.18.2 Expression pattern of putative *cactus* genes

During the blastoderm stages, transcripts of *cact-1*, *cact-2*, and *cact-4* are expressed ubiquitously without significant asymmetry along the DV axis (Figure 3.35). In later stages before gastrulation, *cact-1* and *cact-2* are expressed in the anterior pole, while *cact-4* is not. Transcripts of *cact-1* and *cact-2* are also expressed in the lateral stripes, especially in the presumptive head region. After gastrulation, *cact-1*, *2*, *4* are expressed ubiquitously in the extended germband.

The expression of *cact-1*, *2*, *4* is not as significant as in *Tribolium* and *Nasonia* embryos where it is expressed in a ventral stripe (Nunes da Fonseca et al., 2008; Buchta et al., 2013). However, the expression of *cact-3* is more specifically localized in blastoderm

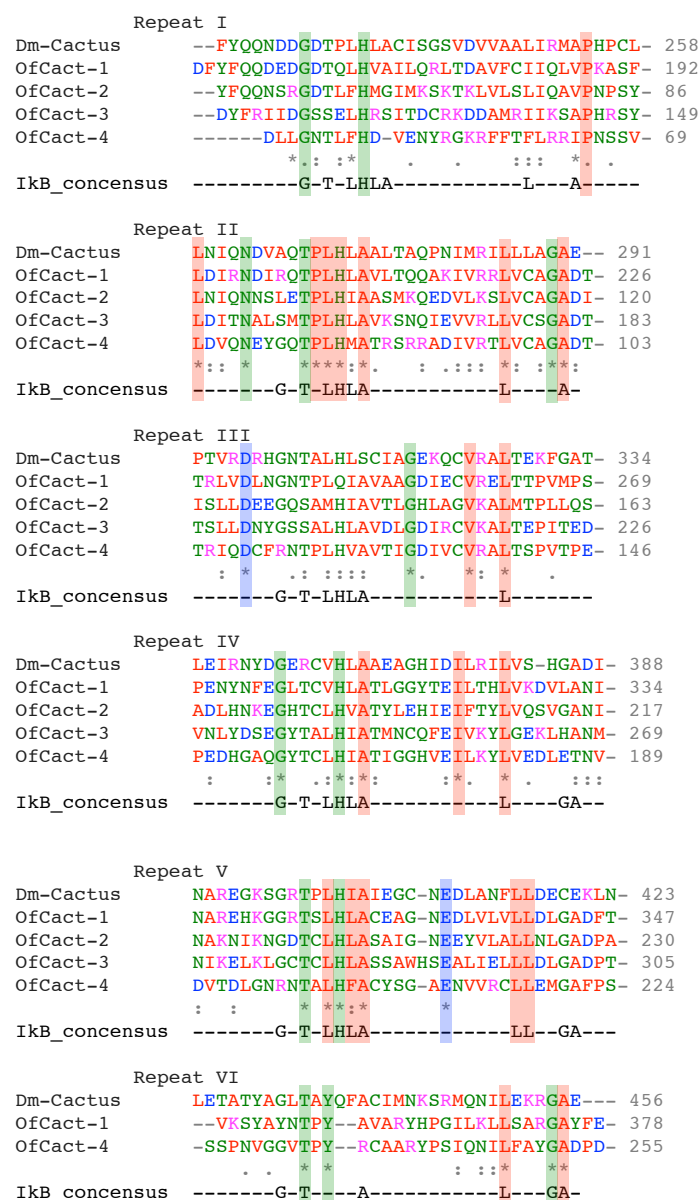


Figure 3.34. Alignments of ankyrin repeats (Ank) between *Drosophila* Cactus and putative Cactus in *Oncopeltus*

There are six ankyrin repeats (Ank) in *Drosophila* Cactus (Kidd, 1992). The amino acid sequences of putative *Oncopeltus cactus* genes were aligned to these six Ank. All of the *Oncopeltus* Cactus contain five conserved ankyrin repeats. The repeats VI is only detected in *Oncopeltus* Cactus-1 and Cactus-4. The sites with 100% identity were marked in shaded color. The IκB consensus shared by *Drosophila* Cactus and vertebrate IκB was shown at the bottom of the repeats.

Genes

age

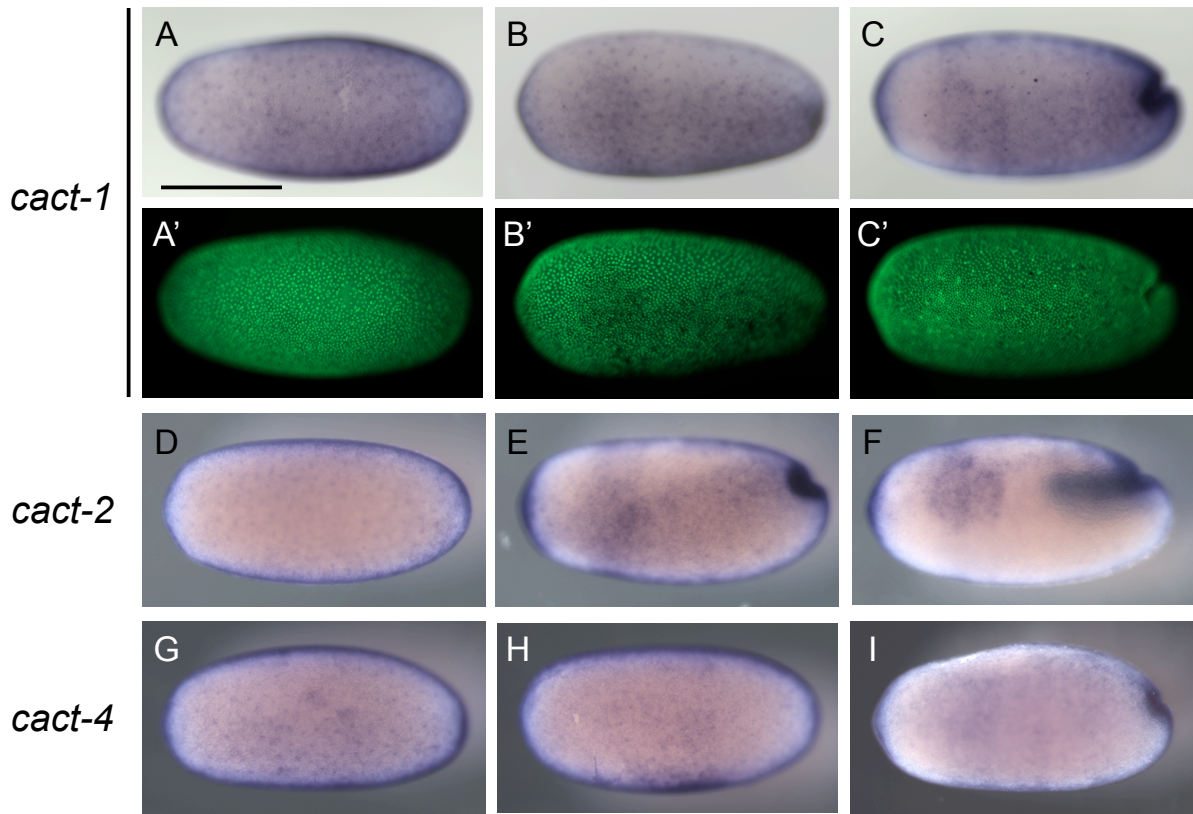


Figure 3.35. Expression pattern of *cactus-1, 2, 4* in *Oncopeltus* embryos

The expression pattern of *cact-1, 2, 4* transcripts in blastoderm embryos and during gastrulation. Embryos are arranged from left to right, according to the developmental stages (A-C, D-F, G-I). During the blastoderm stages, *cact-1, 2, 4* are expressed ubiquitously (A, B, D, G, H). In later stages before gastrulation, *cact-1* and *cact-2* are expressed in the anterior pole (C, E), while *cact-4* is not. Transcripts of *cact-1* and *cact-2* are also expressed in the lateral stripes, especially in the presumptive head region (C, F). Scale bar size corresponds to 500 μm . Embryos of A'-C' are identical to embryos of A-C with SytoxGreen staining. Lateral view of embryos is shown in B, C, E, F and I.

embryos. During blastoderm stages, *cact-3* is expressed intensively on one side of the embryo and colocalizes with the *sog* expression domain, marking the ventral side of the embryo. Expression of the *cact-3* domain becomes slightly broader in later blastoderm stages (Figure 3.36 D). The ventral expression pattern indicates that *cact-3* might be required for proper formation of the DV axis.

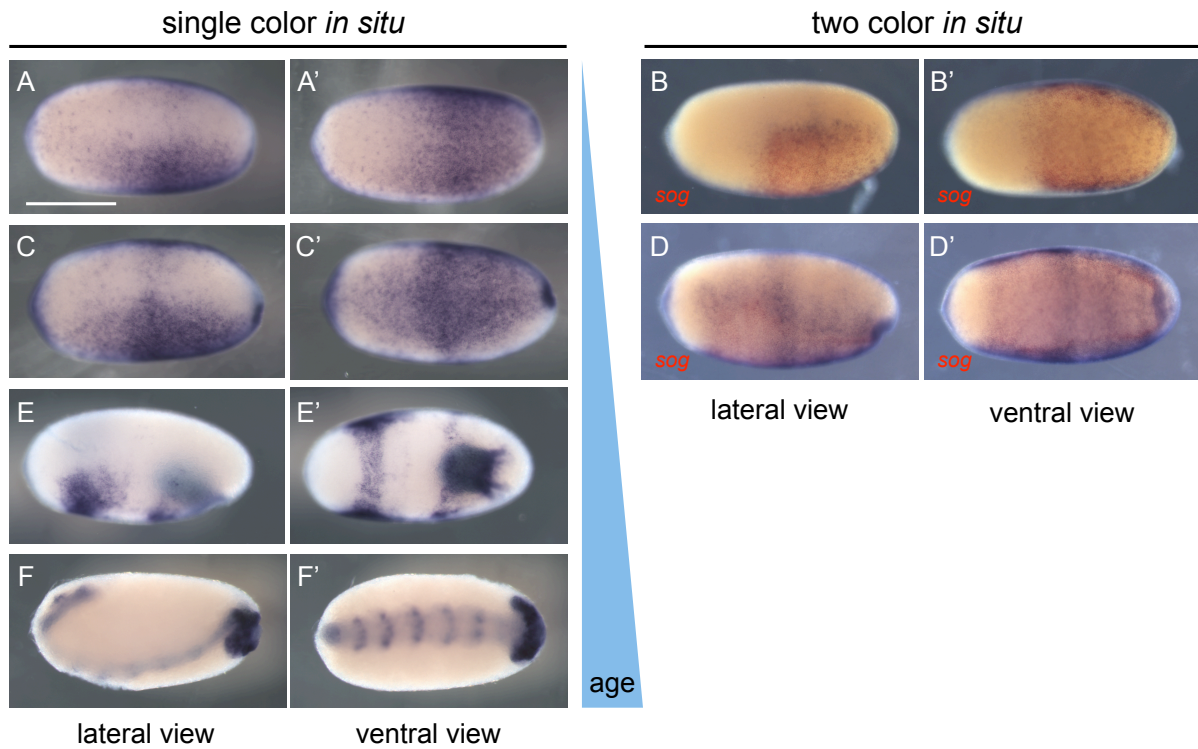


Figure 3.36. Expression pattern of *cactus-3*

Expression pattern of *cact-3* is shown in A, C, E, F using single or two color *in situ* (B, D). The red staining shows the expression of ventral marker *sog*. Transcripts of *cact-3* colocalize with *sog* expression on the ventral side (B, D). Embryos of A-F are identical to A'-F' showing different views. Lateral view of embryos is shown in A-F; Ventral view of embryos is shown in A'-F'. Embryos are at the blastoderm stage (A-D), gastrulation (E), or germband stage (F). During the germband stages, *cact-3* is expressed in the head and each segmental stripes. Scale bar size corresponds to 500 μm .

3.18.3 Functional analysis of *cactus* (*cact*) genes

Functional analysis of the *cactus* genes was preformed by pRNAi. However, after knock-down of the *cactus-1* (*cap3_12011*) in *Oncopeltus*, there were not enough embryos to determine whether there is any significant phenotype based on the embryonic morphol-

ogy. Some eggs stop to develop and are enriched with yolk after *cactus-1* knockdown. Furthermore, the expression of *cact-1* is ubiquitous during blastoderm stages (Figure 3.35). Taken together, *cact-1* was excluded as a putative candidate to play a role in DV patterning.

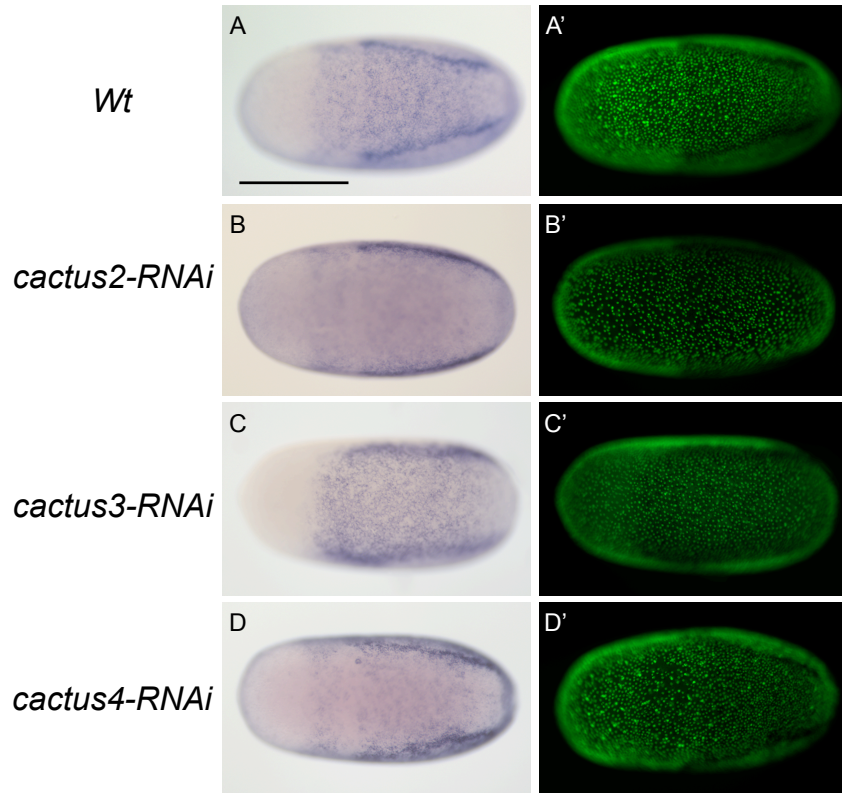


Figure 3.37. Expression pattern of *sog* in *cactus* knockdown embryos

The ventral *sog* domain is expanded in *cactus-2* and *cactus-3* knockdown embryos, but not in *cactus4-RNAi* embryos. In wildtype, the *sog* domain is expressed about 40% ventrally with distinct lateral stripes during late blastoderm stages. However, the ventral *sog* domain is expanded to 50% and 45% in the *cactus-2* and *cactus-3* knockdown embryos. Anterior pole of the egg is to the left. All embryos are at the blastoderm stage. The ventral view of embryos is shown here. Embryos of A-D are identical to A'-D', which are stained with SytoxGreen to show the nuclei. disrupted in *cactus-2* knockdown embryos. The scale bar size corresponds to 500 μm .

To study the function of other putative *cactus* genes, knockdown analysis of *cactus-2*, *cactus-3*, and *cactus-4* was performed via pRNAi and the *sog* expression was examined in blastoderm embryos. More than 50% of *cact-2* knockdown embryos (n=371) show the unequal nuclear distribution phenotype, which is different from *dll2* knockdown. The unequal nuclear distribution disrupts the *sog* expression pattern during blastoderm stages

and disrupts the gastrulation during germband stages. Only 6% (n=371) of *cactus-2* knockdown embryos are morphologically wildtype-like with nuclei distributed equally. However, the ventral *sog* domain is expanded to 50% of the embryonic circumferences in the *cactus-2* knockdown and the strongly expressed *sog* domain is shifted to the lateral side (Figure 3.37B). In contrast, the *sog* domain in wildtype embryos is ventrally expressed in about 40% of the embryonic circumferences with distinct lateral stripes during late blastoderm stages (Figure 3.37A). A similar expansion of the ventral *sog* domain is also observed in *cactus-3* knockdown embryos. The ventral *sog* domain is expanded to 45% of the *cact-3* knockdown embryo and the strongly expressed *sog* lateral domain becomes more straight along the AP axis (Figure 3.37C). Probably, this indicates that the posterior part of the ventral *sog* domain expands more than the anterior part. In *cact-4* knockdown embryos, the *sog* expression is identical to wildtype (Figure 3.37D) and no expansion of the ventral *sog* domain is visible. The expansion of the ventral *sog* domain in *cactus-2* and *cactus-3* knockdown indicates that the embryos are slightly ventralized.

3.19 Maternal cues for axial determination in ovaries

Studies from *Drosophila* indicate that there is maternally deposited information in the ovaries upstream of Toll signaling to establish the body axes (Nüsslein-Volhard, 1991; Stein and Stevens, 2014). For example, EGF (epidermal growth factor) signaling is conserved to establish embryonic axial polarity during oogenesis (Lynch et al., 2010). Genes required for DV patterning upstream of Toll signaling were found in the *Oncopeltus* transcriptome and listed in Table 3.11. The phylogenetic relationship of putative serine proteases is analyzed in section 3.19.4. The functional analysis of *pipe* and *nudel* is described in section 3.19.3 and 3.19.6.

3.19.1 Location of the oocyte nuclei

Studies in the other insects show that the migration of the oocyte nucleus to the cortex represents a symmetry-breaking event for DV patterning (Lynch et al., 2010). However, it has never been studied in the milkweed bug. Although there are histochemical studies of the ovary in *Oncopeltus* (Bonhag and Wick, 1953; Bonhag, 1955), it is not clear whether the oocyte nucleus migrates to the cortex. To visualize the location of oocyte nuclei in

Table 3.11. Genes required for DV patterning acting upstream of Toll signaling

	Genes	Gene annotation in		Best Hit of BlastX
		<i>Drosophila</i>	<i>Oncopeltus</i>	
EGFR ligand	<i>TGFα</i>	CG17610	†	<i>Rp EGF-like</i>
Sulfotransferase	<i>pipe</i>	CG9614	contig13359*	<i>Zn pipe</i>
Serine/threonine protease	<i>nudel</i>	CG10129	isotig08204+ GEQE5QV01B8NB6	<i>Ap nudel</i> <i>Mr nudel-like</i>
	<i>gd</i>	CG1505	isotig06561	<i>Nl gd-like</i>
	<i>snake</i>	CG7996	isotig16254	<i>Nl trypsin-17</i>
	<i>easter</i>	CG4920	ND	
Toll ligand	<i>spätzle</i>	CG6134	isotig13391* contig03840	<i>Phc PHUM596260</i> <i>XP__002432638.1</i>

ND: not detected (found) in the *Oncopeltus* transcriptome.

Abbreviation of genes: *gastrulation defective* (*gd*), *epidermal growth factor receptor* (*EGFR*), *transforming growth factor* (*TGF α*). Abbreviation of insect species: *Rp* = *Riptortus pedestris* (Bean bug), *Zn* = *Zootermopsis nevadensis* (Termite), *Ap* = *Acyrtosiphon pisum* (pea aphid), *Mr* = *Megachile rotundata* (Bee), *Nilaparvata lugens* (brown planthopper) *nudel* is composed of two separate transcripts (isotig08204 and GEQE5QV01B8NB6) from the transcriptome.

† The sequence was kindly provided by J. Lynch

* with RACE-PCR extension

gradually developing oocytes, the ovarioles of *Oncopeltus* were stained with vital dyes. The location of the oocyte nuclei can be visualized under the DIC II (differential interference contrast) channel of the microscope. By taking Z-stack images, the cross-section of single oocyte shows the position of the oocyte nuclei during oogenesis (Figure 3.38).

Observation of more than 50 ovarioles supports that the oocyte nucleus migrates to the cortex in *Oncopeltus* like in other examined insect species (Lynch et al., 2010). Starting from the third maturing oocyte, the oocyte nucleus migrates to an asymmetric position. Then, the oocyte nucleus becomes invisible in later developing stages after the chorion and the vitelline membrane are formed (Figure 3.38).

3.19.2 The ligand of the EGF receptor in *Oncopeltus*

EGF signaling is conserved among insects for the encapsulation and embryonic patterning during oogenesis (Lynch et al., 2010). The transforming growth factor α (TGF α) is a ligand of the EGF receptor (EGFR). Single genes encoding the TGF α -like ligands were found in the wasp *Nasonia*, the beetle *Tribolium*, and the cricket *Gryllus* (Lynch

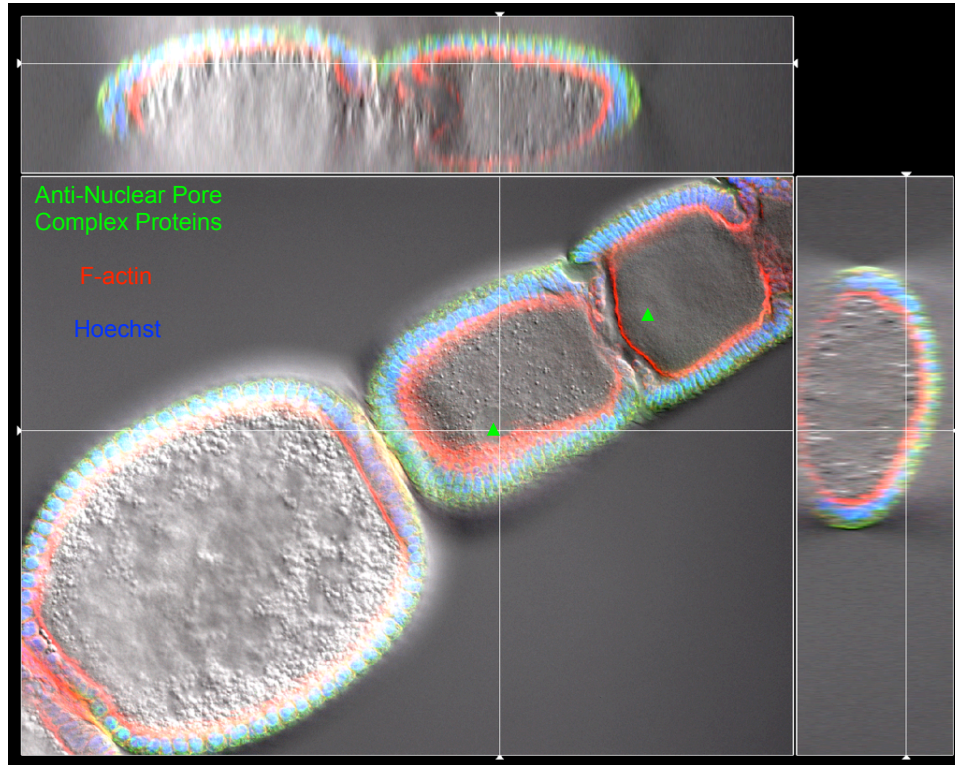


Figure 3.38. Location of the oocyte nucleus

The tropharium of this ovariole is located to the upper right. Three maturing oocytes are shown here. Green arrowheads indicate the position of oocyte nuclei. The nucleus of the first oocyte is located in the posterior pole. The nucleus of the second oocyte is located close to the cortex. The cross-section view consists of 30 different focal planes of Z-stacked images using 4 channels. The nuclear pore antibody is stained by the green color. The red color stains the F-actin marking the cell boundaries. The blue channel stands for Hoechst33258 as a nuclear dye.

et al., 2010). The sequence of *Oncopeltus* *TGF α* was kindly provided by J. Lynch. A RACE-PCR was performed to extend the 5' end sequence. As in *Nasonia* and *Tri-bolium*, there is only one gene encoding a *TGF α* ligand in *Oncopeltus*. The expression pattern of *TGF α* in the *Oncopeltus* ovariole is shown in Figure 3.41. Although there is no asymmetric localization of *TGF α* transcripts, the EGF signaling could be activated asymmetrically. The activation of EGF signaling in ovaries can be observed by the MAP kinase (diphosphorylated ERK-1&2) antibody (Lynch et al., 2010). However, the staining has never been achieved in *Oncopeltus* due to the non-specific background signals. The pRNAi against *TGF α* was tested in *Oncopeltus*. The knockdown of *TGF α* interferes with the egg production, which is due to the failure of encapsulation as reported in *Nasonia*,

Tribolium, and *Gryllus* (Lynch et al., 2010).

3.19.3 The function of *pipe* in DV patterning

In *Drosophila*, the ventral expression of *pipe* in the egg chamber, which is restricted by EGF signaling, is required for the the formation of embryonic DV axis (Sen et al., 1998). However, knockdown of *pipe* shows no phenotype via pRNAi and there is no detectable asymmetry of *pipe* expression in *Tribolium*, *Nasonia* and *Gryllus* (Lynch and Roth, 2011). It seems that *pipe* does not contribute to the establishment of the DV axis in other insects.

Although there is no asymmetric expression pattern of *pipe* along the DV axis of oocytes, knockdown of *pipe* via pRNAi shows phenotypes in *Oncopeltus*.

After *pipe* knockdown, the lateral stripes and the anterior ventral domain of *sim* expression is eliminated (Figure 3.39 B). Moreover, ventral expression of *twist* is lost in *pipe-RNAi* embryos (Figure 3.39 D). However, the expression of *sim* and *twist* is still intensively detectable at the posterior invagination site. Knockdown of *pipe* produces the tube-like shape germband embryo with segmental *msh* expression, which is similar to the phenotype after *Toll1-RNAi*. Although the DV polarity is absent in *pipe* knockdown embryos, the segmentation and germband elongation is not affected. Taken together, knockdown phenotypes of *pipe* show that it is functional in *Oncopeltus* and it is necessary for DV patterning.

3.19.4 From the serine protease cascade to DV patterning

The protease cascade acting upstream of Toll signaling leads to the cleavage of Spätzle ligands, which is the onset of DV patterning in *Drosophila* (LeMosy et al., 2001). There were five different transcripts found in the *Oncopeltus* transcriptome, encoding serine proteases (Table 3.11). However, no transcripts was found to be homologous to *Drosophila easter*. The putative *nudel* is composed of two separate transcripts (isotig08204 and GEQE5QV01B8NB6) from the transcriptome. In addition, the transcript isotig06561 is homologous to *gastrulation defective (gd)*-like genes in other insects. Furthermore, the transcript isotig16254 is homologous to *trypsin*-like genes. Since the serine proteases share a conserved Trypsin-like serine peptidase (SP) domain, protein sequences containing SP domains were aligned to conduct a phylogenetic analysis by MEGA6 (Figure 3.40).

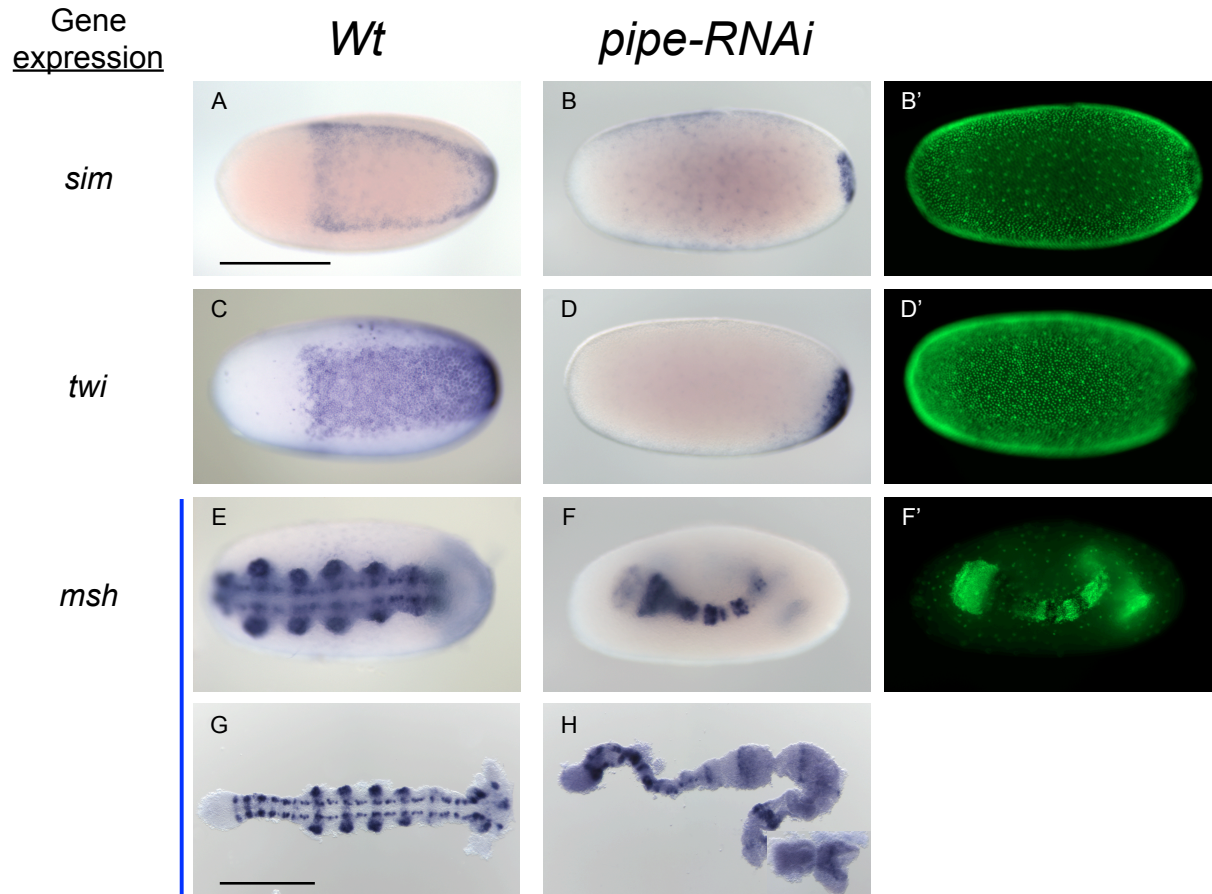


Figure 3.39. Knockdown phenotypes of *pipe* in *Oncopeltus*

Knockdown embryos of *pipe* were stained for *sim*, *twist* and *msh* expression by ISH. Blastoderm embryos are shown in A-D. After *pipe* knockdown, the lateral stripes and the anterior ventral domain of *sim* expression is eliminated (B). The ventral expression of *twist* is lost in *pipe* knockdown embryos (D). The expression of *sim* and *twist* is still intensively detectable at the invagination site. Germband embryos after gastrulation are shown in E-H. The germband embryo after *pipe* knockdown forms a tube-like shape with segmental *msh* expression. The head structure is reduced in *pipe-RNAi* embryos. Ventral view of the embryo is shown in A, C, E. In *pipe* knockdown embryos (B, D, F), the orientation can not be determined due to the absence of DV polarity. Embryos of B', D', F' are identical to B, D, F with nuclear staining by SytoxGreen. Anterior pole of the egg is to the left. Embryo anterior is to the right. The embryos shown in G and H are dissected out of the egg. Scale bar size corresponds to 500 μm in A-F, while the scale bar size corresponds to 1 mm in G and H.

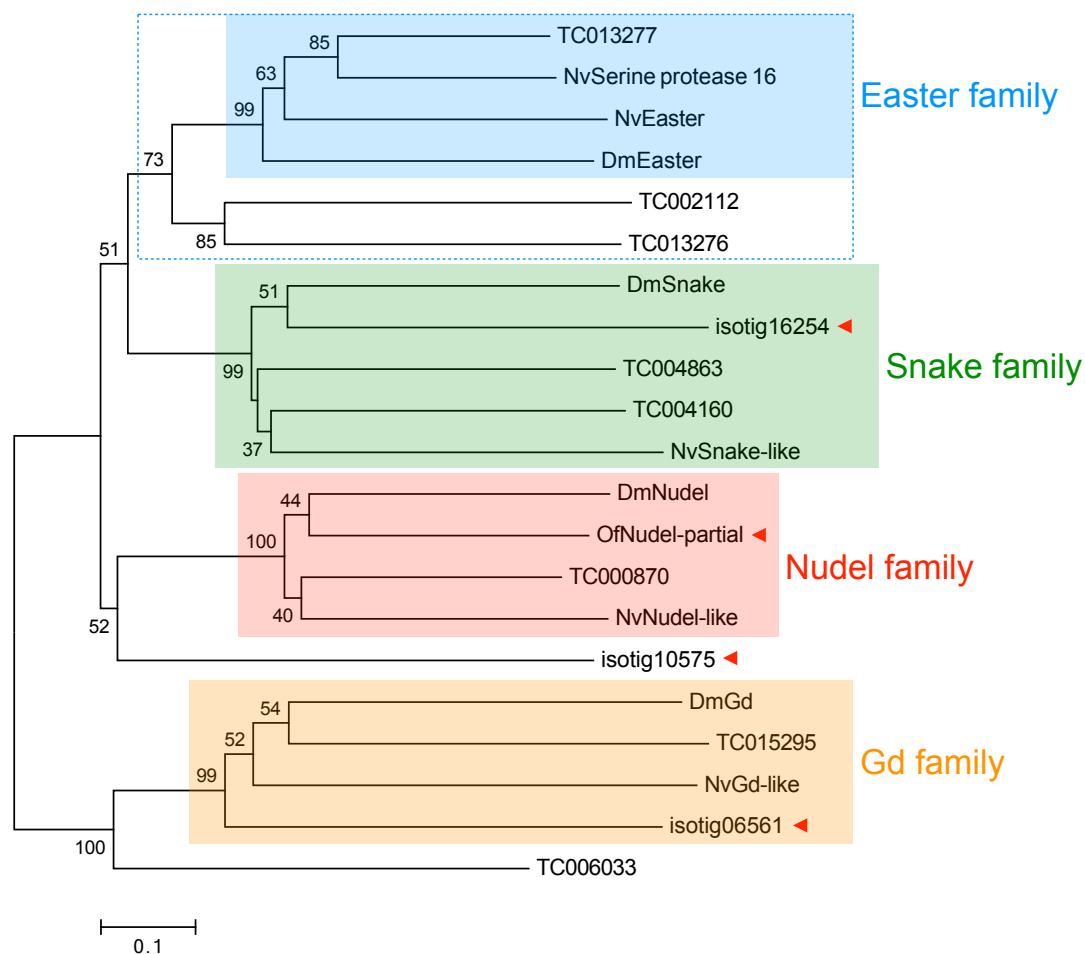


Figure 3.40. Phylogenetic analysis of serine protease families

Only the SP domains of the serine proteases were aligned to conduct a phylogenetic analysis by MEGA6. There are four distinct clusters of serine protease families: Easter, Snake, Nudel, and Gd (Gastrulation defective). The protein sequence of isotig16254 is belonging to the Snake family, closely related to *Drosophila* Snake. The putative *Oncopeltus* Nudel is belonging to the Nudel family, closely related to *Drosophila* Nudel. The protein sequence of isotig06561 is belonging to the Gd family, clustered as a sister branch to the other insect Gd proteins. The dotted square indicates that the Easter family could consist of more candidates. The evolutionary history was inferred using the Neighbor-Joining method. The percentage of the bootstrap test (1000 replicates) are shown next to the branches. The tree is drawn to scale, with branch lengths as evolutionary distances. The evolutionary distances were computed using the Poisson correction method. The analysis involved 21 amino acid sequences. Protein sequences of serine proteases in *Tribolium* is kindly provided by V.A. Dao. Protein sequences of serine proteases in *Nasonia* is kindly provided by T. Buchta.

There are four distinct clusters of serine protease families: Easter, Snake, Nudel, and Gd (Gastrulation defective). The protein sequence of isotig16254 is belonging to the Snake family, closely related to *Drosophila* Snake. In addition, the putative *Oncopeltus* Nudel is belonging to the Nudel family, closely related to *Drosophila* Nudel. Furthermore, the protein sequence of isotig06561 is belonging to the Gd family, clustered as a sister branch to the other insect Gd proteins. The branching in the Gd family reflects the phylogenetic relationships of *Drosophila*, *Tribolium*, *Nasonia*, and *Oncopeltus*. The functional analysis of serine proteases in *Tribolium* showed that the knockdown of Tc002112 produces DV phenotypes via pRNAi (Dao, 2014). Therefore, it is considered to be the *Tribolium* Easter, which indicates that the Easter family shown here could consist of more candidates. The protein sequence of isotig10575 is clustered as a sister branch to the Nudel family.

3.19.5 Expression of *TGF α* , *pipe* and *nudel*, *gd*, *snake* transcripts in ovarioles

The expression of *TGF α* , *pipe* and *nudel*, *gd*, *snake* is shown in Figure 3.41. Expression of *TGF α* and *gd* transcripts is present in oocytes. In addition, *gd* is expressed extensively at the poles and *nudel* is expressed in the follicular epithelium surrounding the maturing oocytes ubiquitously. Furthermore, *pipe* is expressed in the follicular epithelium, with more intensive expression on the posterior side. However, there is no asymmetric expression pattern of any transcripts along the DV axis of oocytes.

3.19.6 Knockdown phenotypes of *nudel*

The function of *nudel* was studied by pRNAi. The predominant phenotype after *nudel* knockdown is an eggshell defect. Knockdown embryos tend to dissipate the moisture and they shrink to yolk-enriched eggs (Figure 3.42). However, the observed eggshell defect can be recovered by water supply in a humid condition. This makes the *nudel* knockdown phenotypes analyzable by ISH. The eggshell defect has been reported in *Drosophila nudel* mutants where Nudel protease is required for eggshell biogenesis in addition to embryonic patterning (LeMosy and Hashimoto, 2000).

Expression patterns of *sim*, *twist* and *msh* are shown in *nudel-RNAi* embryos (Figure 3.42). The lateral stripes and the anterior ventral domain of *sim* expression is eliminated in

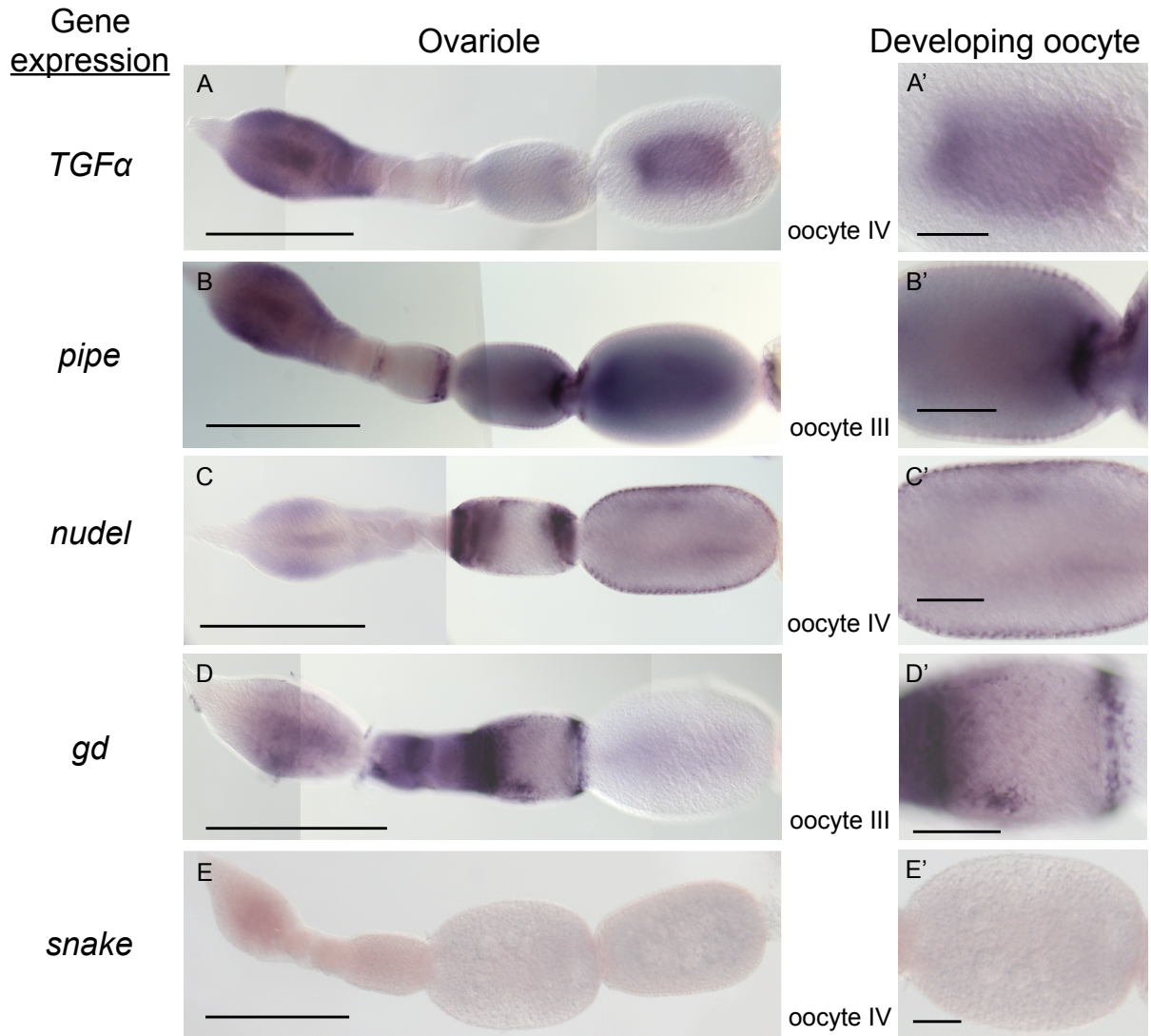


Figure 3.41. Expression of *TGFα*, *pipe* and *nudel*, *gd*, *snake* transcripts in ovarioles

Expression patterns of *TGFα*, *pipe*, *nudel*, *gastrulation defective (gd)* and *snake* in *Oncopeltus* ovarioles (A-E). The magnification of specific maturing oocyte from A-E is shown on the right (A'-E').

Expression of *TGFα* and *gd* transcripts is present in oocytes. There is no specific localization of *TGFα* transcripts (A'), and *gd* is expressed extensively at the poles (D'). *pipe* is expressed in the follicular epithelium and oocytes, with more intensive expression on the posterior side (B'). *nudel* is expressed in the follicular epithelium surrounding the maturing oocytes ubiquitously (C'). The scale bar size in figure A-E corresponds to 1 mm; while the scale bar size in figure A'-E' corresponds to 250 μ m.

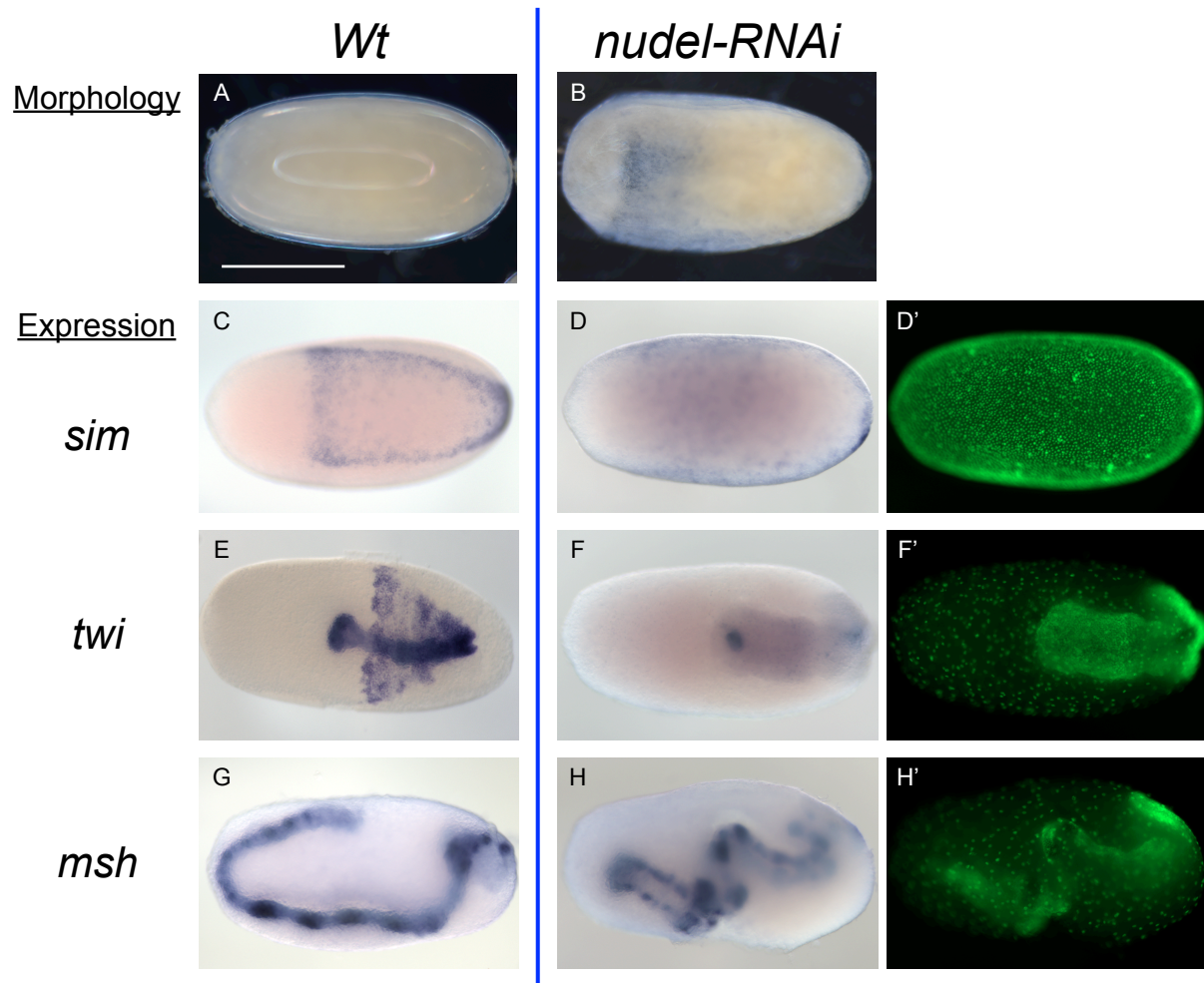


Figure 3.42. Knockdown phenotypes of *nudel* in *Oncopeltus*

The predominant phenotype after *nudel* knockdown is an eggshell defect. Knockdown embryos tend to dissipate the moisture and they shrink to yolk-enriched eggs (B) within 24 hours after egg lay (AEL). Expression patterns of *sim*, *twist* and *msh* are shown in *nudel-RNAi* embryos. Blastoderm embryos are shown in A-D. Embryos during gastrulation are shown in E and F. Germband embryos after gastrulation are shown in G and H. The lateral stripes and the anterior ventral domain of *sim* expression is eliminated in *nudel* knockdown embryos (D). The mesodermal fate marked by *twist* expression is lost in *nudel-RNAi* embryos (F). The germband embryo after *nudel* knockdown forms a twisted shape with *msh* expression on the lateral margin (H). Ventral view of the embryo is shown in C-F; lateral view of the embryo is shown in G. Embryos of D', F', H' are identical to D, F, H with nuclear staining by SytoxGreen. Anterior pole of the egg is to the left. Embryo anterior is to the right. Scale bar size corresponds to 500 μm .

nudel knockdown embryos. In addition, the mesodermal fate marked by *twist* expression is lost in *nudel-RNAi* embryos. During early germband stages, expression of *twist* is only detectable in the proctodeum. The *nudel-RNAi* embryos are invaginated into the egg with disrupted DV polarity. They form a twisted shape with *msh* expression on the lateral margin. The eliminated *sim* expression is similar in *pipe* and *nudel* knockdown embryos (Figure 3.39 and 3.42). This suggests that *nudel* is functional and necessary for DV patterning in *Oncopeltus*.

3.20 The ligands of Toll receptor: Spätzle

Binding of the *Drosophila* Spätzle ligands to the Toll receptor establishes the signaling, which is important for immunity and DV patterning (Weber et al., 2003).

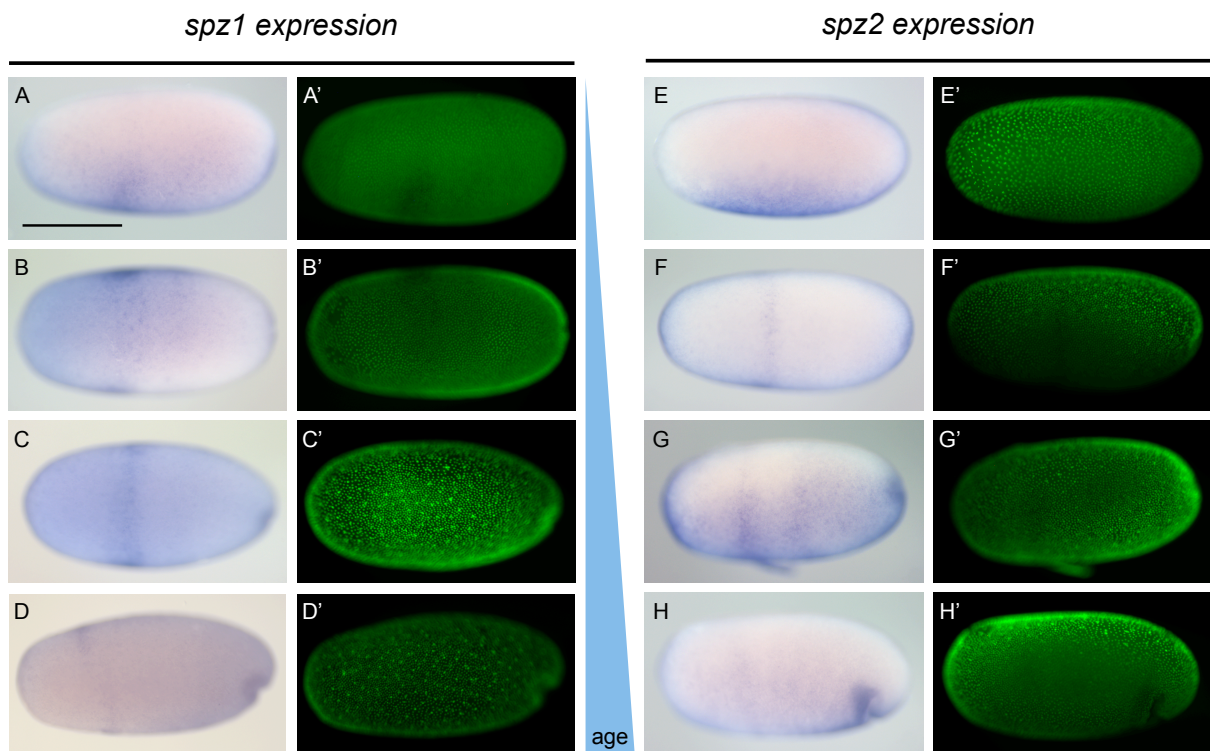


Figure 3.43. Expression pattern of the two *spätzle* transcripts

Transcripts of the two *spätzle* are first expressed asymmetrically along the DV axis. The developing embryos during blastoderm stages were arranged from top to bottom with increasing ages. Expression of *spz1* is localized in a lateral stripe (C) perpendicular to the AP axis, and *spz2* is expressed in two lateral stripes (G), with asymmetrical expression pattern along the DV axis. When the embryo starts to invaginate, *spz2* is expressed at the invagination site posteriorly (G and H). Embryos of A'-H' are identical to embryos of A-H, with SytoxGreen staining. Scale bar size corresponds to 500 μm .

There are two transcripts homologous to *spätzle* in the *Oncopeltus* transcriptome (Table 3.11). Both of them encode a signal peptide domain and the cystine knot domain. The protein sequence of contig03840 is more similar to *Drosophila* Spätzle (with 35% identity). Thus, the transcript contig03840 is called *spätzle1* (*spz1*) and the other transcript isotig13391 is called *spätzle2* (*spz2*) in the following paragraphs. Expression of the *spätzle* transcripts is shown in Figure 3.43.

In the early blastoderm stage, transcripts of the two *spätzle* are expressed asymmetrically along the DV axis (Figure 3.43 A and E). In the late blastoderm stage, *spz1* is gradually expressed in a lateral stripe perpendicular to the AP axis, and *spz2* is expressed in two lateral stripes with asymmetrical expression along the DV axis (Figure 3.43 C and G). When the embryo starts to invaginate, *spz2* is expressed at the invagination site posteriorly (G and H).

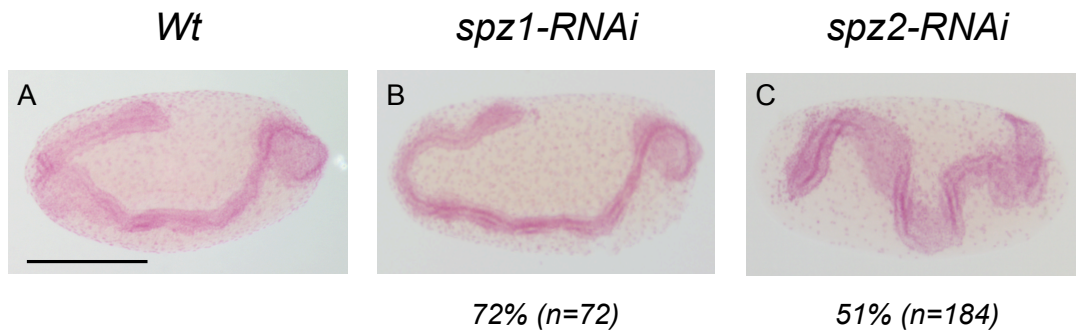


Figure 3.44. Fuchsin staining of *spz1* and *spz2* knockdown embryos during germband stages

Anterior pole of the egg is to the left, embryo anterior is to the right. Embryos are at the germband stage. There is no significant phenotypes detectable after knockdown of *spz1*. About 72% of knockdown embryos are wildtype-like after *spz1-RNAi* (B). After *spz2* knockdown, there is a phenotype during germband stages. About 51% of the *spz2-RNAi* germband embryos are extended with disrupted guidance (C). Scale bar size corresponds to 500 μm .

Since there is an asymmetric expression pattern of the *spätzle* transcripts (Figure 3.43 A and E), they might play a role in DV patterning. However, there is no significant phenotype after knockdown of *spz1* based on the fuchsin staining (Figure 3.44) and about 72% of knockdown embryos ($n=72$) are wildtype-like after *spz1-RNAi*. After *spz2* knockdown, there is a phenotype detected during germband stages based on the fuchsin staining (Figure 3.44). About 51% of the *spz2-RNAi* germband embryos ($n=184$) are extended in S-shape with disrupted guidance. This might indicate that the *spz2* knockdown disturbs

the DV polarity. However, investigations with ISH markers is necessary to address the question whether knockdown of *spätzle* cause DV patterning defects.

Chapter 4

Discussion

4.1 Function of the Toll receptors

In the fly *Drosophila*, *Toll* was found to have the ability to rescue dorsalized mutant phenotypes (Anderson et al., 1985a) and overexpression of *Toll* causes a ventralized embryo. In contrast, the depletion of *Toll* causes a dorsalized embryo (Anderson et al., 1985b), which indicates that *Toll* is important for the establishment of DV polarity in the embryo. Few years later, it was found that *Toll* can activate an immune response in a *Drosophila* cell line (Rosetto et al., 1995) and that Toll signaling controls the anti-fungal immunity in adult flies (Lemaitre et al., 1996).

As there are more and more Toll or Toll-like receptors (TLRs) identified in insects (Christophides et al., 2002; Zou et al., 2007; Gerardo et al., 2010; Bao et al., 2013; Li et al., 2013), what is the function of Toll receptors? Are there any *Toll*-related genes involved in DV patterning in other insects? In this thesis, the categorization of Toll-related families among insects is clarified by phylogenetic analyses, which shows that there are five distinct subfamilies clustered as Toll-1, Toll-6/8 (Tollo), Toll-7/2 (18w), Toll-9/13, and Toll-10 (Figure 3.7). Based on the comparison of functional studies in other insects, only genes from the first Toll-1 subfamily are involved in DV patterning (Nunes da Fonseca et al., 2008; Wilson et al., 2014; Ozüak et al., 2014). Here, the function of *Toll-1* is studied in the milkweed bug *Oncopeltus* demonstrating that *Toll-1* and the downstream components of the signaling are involved in DV patterning. Without *Toll-1*, embryos are dorsalized (or lateralized) losing the DV polarity (Figure 3.14 and 3.15).

Although the function of other TLRs has not yet been investigated in *Oncopeltus*, members of the other Toll families were characterized as pattern recognition receptors (PRRs) to have a main function in recognizing different pathogens and establishing the innate immunity in insects and mammals (Christophides et al., 2002; Zou et al., 2007; Gerardo et al., 2010; Bao et al., 2013; Akira et al., 2001; Janssens and Beyaert, 2003). The TLR homologs identified in *Oncopeltus* might have a similar function in pathogen recognition or other functions in the developing processes. Tissue and stage-specific expression patterns of Toll-related genes have been demonstrated in the fly *Drosophila* and the mosquito *Anopheles gambiae* (Kambris et al., 2002; Luna et al., 2002) indicating their potential functions in embryonic development, neurogenesis, and immune-responsive tissues. Moreover, Yagi et al. (2010) showed that overexpression of Toll-related genes caused lethality and various phenotypes, indicating that some of them might have redundant functions in regulating developmental processes. A recent paper further proved that *Toll-2*, *Toll-6* and *Toll-8* cooperate together for the planar polarity and direct polarized cell rearrangement during convergent extension (Paré et al., 2014). The members of the Toll-9/13 subfamily encoding the leucine-rich repeats (LRRs) might have an extracellular role in pathogen recognition or in neural axon guidance, target selection, and synapse formation (Dolan et al., 2007; de Wit et al., 2011). To sum up, there are more puzzles about the function of Toll receptors that need to be solved.

4.2 Knockdown of the Toll signaling pathway

In the absence of Toll signaling components, knockdown embryos usually form a twisted, tube-like shape and the development of embryos is disrupted (Figure 3.12, 3.15, 3.18). Toll signaling knockdown embryos are completely or partially dorsalized, losing the expression of marker genes *twist*, *sim* and *sog* (Figure 3.14 and 3.33). The consistent phenotypes imply that these components are acting in the same signaling pathway as predicted. Although the dosage of dsRNA injection is lower than in previous studies (Angelini and Kaufman, 2004; Liu and Kaufman, 2004, 2005a; Liu and Patel, 2010; Ben-David and Chipman, 2010; Ewen-Campen et al., 2013), the knockdown of Toll signaling is efficient producing similar phenotypes and the knockdown efficiency is further supported by the semi-quantitative PCR and qPCR (Figure 3.13, 3.16, 3.24). Based on the knockdown validations in the *Toll*-

1 and *dorsal-1* (*dll*) RNAi embryos, the transcripts are eliminated robustly via pRNAi.

4.2.1 Knockdown of *myd88* and the putative TIR-domain-containing adaptors

In *Drosophila*, the Toll signaling transduction is mediated by the adaptor protein Myd88 (Charatsi et al., 2003). Knockdown of the *myd88* homolog in *Oncopeltus* phenocopies the *Toll-1* and *dll* RNAi with eliminated expression of *sog* and *twist* (Figure 3.14 and 3.33). However, there is a high percentage of *myd88* knockdown embryos (65%) with residual DV asymmetry (Table 3.9). This might be due to the insufficient knockdown or there might be more TIR-domain containing adaptors, which have not been identified in *Oncopeltus*. There are five members of TIR-domain-containing adaptors discovered in vertebrates (O'Neill et al., 2003; O'Neill and Bowie, 2007). Furthermore, the study of the Interleukin-1 receptor (IL1R) signaling revealed that the signaling is capable to function through a Myd88-independent pathway (Kenny and O'Neill, 2008). Therefore, the other unidentified TIR-domain-containing adaptors might have the ability to mediate individual TLR signaling pathways with or without the involvement of Myd88.

4.2.2 The functions of Spätzle ligands

When the active form of Spätzle ligands bind to the Toll receptor, the Toll signaling is activated, which is important for immunity and DV patterning in *Drosophila* (Weber et al., 2003). In this thesis, two *spätzle* homologs are identified in the milkweed bug (Table 3.11). Both of them are expressed asymmetrically along the DV axis in the blastoderm embryos, but only one might disrupt DV polarity during the germband stages (Figure 3.43 and 3.44). Additionally, the phenotype is weaker than the knockdowns of other Toll signaling components. This might be due to the redundant functions between the two *spätzle* homologs or there could be more unidentified *spätzle* homologs. In the genome, there are four Spätzle-like ligands predicted (personal communication from M. van der Zee). Two of the Spätzle-like ligands are located on the same scaffold adjacent to each other. According to the Spätzle related families found in *Drosophila* (Parker et al., 2001), one is related to *Drosophila* Spätzle-4, and two of them are related to the *Drosophila* Neurotrophin family. In *Drosophila*, Neurotrophins have a common mechanism for nervous system formation

(Zhu et al., 2008). The other Spätzle homologs might have functions in innate immunity and development interacting with TLRs (Parker et al., 2001). However, functions of the four Spätzle-like ligands have to be tested in *Oncopeltus* to answer the question whether they play any role in DV patterning.

4.2.3 Functions of Toll signaling upstream components

The EGF signaling is conserved among insects to establish the embryonic axial polarity during oogenesis (Lynch et al., 2010). In *Drosophila*, the ventral expression of *pipe* in the egg chamber is restricted by EGF signaling and acts as the link between egg chamber and the embryonic DV polarity (reviewed in Stein and Stevens, 2014). The function of *pipe* has never been studied outside of *Drosophila* because the knockdown via pRNAi shows no phenotype in *Tribolium*, *Nasonia* and *Gryllus* (Lynch et al., 2010; Lynch and Roth, 2011). Although *Oncopeltus pipe* is not expressed asymmetrically along the DV axis in the follicular epithelium, it is considered to play a role in DV patterning based on the dorsalized (or lateralized) phenotype in *pipe* knockdown embryos (Figure 3.41 and 3.39). Furthermore, the tube-like phenotype and the head defects in *pipe-RNAi* germband embryos resemble the *Toll1-RNAi* phenotype.

The phenotypes of *nudel* knockdown in *Oncopeltus* indicate the conserved function in egg shell formation and in DV patterning as one of the serine protease in the perivitelline space. As in *Drosophila nudel* mutants, the perivitelline environment might be affected to influence the activity of a downstream protease cascade and the initiation of embryonic DV axis formation (Hong and Hashimoto, 1996; LeMosy et al., 1998). Based on the *sim* and *twist* expression in *Oncopeltus nudel* knockdown embryos, there might be a dorsalized (or lateralized) phenotype indicating that the embryonic DV polarity is disrupted (Figure 3.42). Therefore, the data show a conserved function of *pipe* and *nudel* in a hemipteran insect.

The functions of other serine proteases (SPs) such as Gd, Snake, and Easter need to be investigated in *Oncopeltus* via pRNAi. However, it is possible that the proteolytic cascades upstream of Toll signaling and the processing of Spätzle ligands might be regulated differently from *Drosophila* (Lynch and Roth, 2011). One supporting evidence is that the *easter* homolog could not be found in the *Oncopeltus* transcriptome (Table 3.11). Furthermore, there might be more unidentified SPs or Spätzle-ligand-processing enzymes acting

upstream of Toll signaling in *Oncopeltus*. Members of the SP family were assumed to be involved in innate immunity or embryonic development of insects (Zou et al., 2006, 2007; Altincicek et al., 2013). For example, the CLIP domain-containing protease Snake is predicted to have a conserved function in prophenoloxidase (proPO) activation and Spätzle processing (Zou et al., 2007; Cerenius et al., 2008). Nevertheless, there is no expression of *snake* in the *Oncopeltus* ovaries (Figure 3.41). This might indicate that Snake is not part of the signaling components to be involved in the axial determination of *Oncopeltus* embryos. In addition, it supports the idea that the components of a proteolytic cascade acting upstream of Toll signaling might have diverged in other insects. To sum up, the links between the axial patterning through the proteolytic cascades and the activation of Toll signaling have to be investigated further in other insects outside of *Drosophila*.

4.2.4 Short-germ development and the function of growth zone

The development of the milkweed bug represents the more ancestral type of short germ development (Liu and Kaufman, 2005b) where the head and thorax are specified during blastoderm stages and the abdominal segments are generated from the posterior growth zone (gz) during germband stages. In *Toll-1* and *dll* knockdown, the germband embryos still invaginate and elongate with periodic expression of *msh* and *en* in the segments. This means that even if the embryos lack DV polarity, they still possess an active gz. When the new segments arise from the posterior gz, they retain undisturbed segment polarity along the AP axis. This phenotype is similar to the *Toll* knockdown in *Tribolium* (Nunes da Fonseca et al., 2008).

4.2.5 Mesoderm formation and the possible function of *snail*

The knockdown phenotypes of *Toll-1* and *twist* suggest that Toll signaling has the ability to activate the expression of *twist*, which is important for mesoderm formation. However, the *twist-RNAi* phenotype in *Oncopeltus* is more similar to the *Drosophila snail* mutant rather than the *twist* mutant (Leptin, 1991; Rao et al., 1991). In *Oncopeltus twist* knockdown embryos, the ventrally-shifted domain of *sim* expression indicates the mesectoderm taking over the presumptive mesoderm domain (Figure 3.26). Since *twist* and *snail* are both required for mesoderm formation in *Drosophila* (Alberga et al., 1991; Leptin, 1991),

is it possible that *twist* replaces the role of *snail* in *Oncopeltus*? *Oncopeltus snail* was found by A. Drechsler and the sequence was extended by RACE-PCR. In the late blastoderm stage before gastrulation, there is an asymmetric expression of *snail* along the DV axis (Figure 5.12). During germband stages, *snail* is expressed in clusters of neuroectodermal cells flanking the ventral midline (Figure 5.12). The asymmetric expression of *snail* in the late blastoderm stage is similar to the pattern in *Tribolium* (Sommer, R. J. and Tautz, D., 1994), suggesting an early role in mesoderm specification. Furthermore, the *snail* expression during germband stages is similar to the expression of *klumpfuss*, suggesting a late role in neuroblast development and neurogenesis, which might act in concert with other Zinc-finger (C_2H_2) proteins such as Klumpfuss (Berger et al., 2012; Xiao et al., 2012). However, there is not enough data to fully understand the function of *twist* and *snail* in *Oncopeltus*.

4.2.6 Phenotypes related to the function of NF κ B proteins

In this thesis, two NF κ B proteins (Dorsal1 and Dorsal2) have been identified and studied. Knockdown of *dl1* phenocopies the *Toll1-RNAi* with eliminated expression of the marker genes *sog*, *sim* and *twist*. Similarly, the expression is also eliminated in *dl2-RNAi* germband embryos (Figure 3.19). These knockdown phenotypes suggest that Dorsal proteins are needed for proper DV patterning upon the activation of Toll signaling in *Oncopeltus*. To act as transcription factors, NF κ B proteins might cooperate together as homo-dimers or hetero-dimers regulating downstream target genes (Tanji et al., 2010), which could explain the weak DV phenotypes in *dl1* and *dl2* knockdown embryos.

Besides the DV defect after *dl2* knockdown, there is another phenotype of unequal nuclear distribution during early blastoderm stages (Figure 3.20). While the NF κ B transcription factors have multiple roles for the immune and cellular response, it is possible that active NF κ B turns on the expression of genes that keep the cell proliferating and protect from cell death via apoptosis (Viatour et al., 2005; Dutta et al., 2006). Thus, disruption of the the NF κ B related Dorsal2 in *Oncopeltus* might inhibit cell proliferation and lead to nuclear degradation.

A similar phenotype of unequal nuclear distribution was detected in the *cactus-2* (*cact-2*) knockdown embryos. Cactus is closely related to vertebrate B-cell lymphoma 3-encoded protein (Bcl-3) and I κ B proteins containing several ankyrin repeats (Kidd, 1992; Geisler

et al., 1992). Bcl-3 and I κ B proteins can act as specific inhibitors of NF κ B proteins (Hatada et al., 1992). Thus, an opposite phenotype of apoptosis would be expected in *I κ B* or *cactus* knockdown embryos because the NF κ B proteins should be activated. However, the apoptotic pathway is complicated and NF κ B can act as a promoter or antagonist of apoptosis depending on the stimulus (Kaltschmidt et al., 2000). Additionally, another NF κ B transcription factor Relish was found to trigger cell death in *Drosophila* photoreceptors (Chinchore et al., 2012). It is likely that Cact-2 is the inhibitor of Relish in *Oncopeltus* and that cell death is taking place in the *cact-2* knockdown embryos (Figure 5.16). To clarify the protein–protein interactions between Cactus and Dorsal/Relish, it is necessary to perform Co-Immunoprecipitation (Co-IP).

4.3 The Dorsal protein and the nuclear gradient

DV patterning in *Drosophila* embryos relies on the broad nuclear Dorsal gradient, with the highest level of Dorsal proteins at the ventral side while the protein remains in the cytoplasm at the dorsal side (Roth et al., 1989). The nuclear gradient of Dorsal is also formed in *Tribolium* blastoderm embryos, but the Dorsal gradient is gradually refined, restricted to the ventral midline in a dynamic manner, and the gradient disappears completely before gastrulation (Chen et al., 2000). Further investigations found that the Dorsal gradient in *Tribolium* is regulated by feedback loops from *Toll* and *cactus* (Nunes da Fonseca et al., 2008), which is different from *Drosophila*. The morphogen Dorsal gradient has never been studied in other insects. Antibodies against *Oncopeltus* Dorsal proteins were produced and the whole-mount immunostaining was performed to investigate whether there is a nuclear Dorsal gradient in the blastoderm embryo of *Oncopeltus*.

4.3.1 The *Oncopeltus* Dorsal1 and the relationship to *sog* expression

From the empirical immunostaining results, it is not clear whether there is a nuclear Dorsal gradient in the blastoderm embryo of *Oncopeltus*. If there is a nuclear gradient of *Oncopeltus* Dorsal1, it might be extremely dynamic, which could be similar to the gradient in *Tribolium* or even more transiently regulated. A tiny difference on the nuclear Dorsal

level might be sufficient to break the DV symmetry while *sog* expression is asymmetrically enhanced on one side to polarize the blastoderm embryo. Once the embryo is polarized, the DV polarity is established. Thus, a weak or shallow gradient might be sufficient to activate target gene expression and to tell the embryonic differences from dorsal to ventral. In *Oncopeltus*, a residual expression of *sog* is detected in *dll-RNAi* embryos (Table 3.4). This might be due to the insufficient knockdown or the redundant function from Dorsal2 to activate *sog* expression on the ventral half of the embryo. However, the activation of *sog* expression is regulated by Dorsal proteins.

Dorsal binding sites upstream of the *sog* gene

There are clusters of predicted Dorsal binding sites in the cis-regulatory region of the *Oncopeltus sog* gene (Figure 3.29). The similarity of binding peaks indicates that the predicted Dorsal binding sites are indeed high-affinity Dorsal binding motifs (Figure 3.30). Furthermore, these sites are located within the *sog* locus at similar position as in other insects (Cande et al., 2009). These high-affinity Dorsal binding sites of *sog* support that *sog* could be regulated by Dorsal and enhancers of the *Oncopeltus sog* might have the ability of reacting to low level of Dorsal proteins. Consequently, a high level of nuclear Dorsal could be dispensable even in the most ventral domain of *Oncopeltus* embryos and the gradient of nuclear Dorsal might be very shallow if present.

4.3.2 The interaction between Dorsal and its inhibitor Cactus

Studies in *Drosophila* show that Cactus inhibits Dorsal by retaining it in the cytoplasm (Roth et al., 1989; Bergmann et al., 1996) and the degradation of Cactus leads to the nuclear translocation of Dorsal (Roth et al., 1991). In *Oncopeltus*, there is no significant ventralization in knockdown embryos of all *cactus* genes. The weak phenotypes of *cactus* knockdowns indicate that the *cactus* genes might have redundant functions. Another possibility is that the absence of Cactus has little or no effect on the nuclear translocation of Dorsal in the milkweed bug. In the *Drosophila cactus* null mutant, embryos are still polarized with a shallow gradient of nuclear Dorsal distribution (Bergmann et al., 1996). This corresponds to the putative situation in *Oncopeltus* that Dorsal1 could be ubiquitously expressed in the blastoderm embryo without an obvious nuclear gradient. In this

situation, Cactus protein might act as the inhibitor of Dorsal, but the signal-dependent degradation of Cactus is not leading to the nuclear translocation of Dorsal. The nuclear import of Dorsal might be regulated by a signal-dependent phosphorylation, which is also important for the stability of Dorsal protein (Drier et al., 2000). From the comparisons among insects, the critical phosphorylation site of Dorsal (Serine317 in *Drosophila*) is conserved within the RHD of all Dorsal proteins (Figure 5.15). Thus, the minimal amount of nuclear Dorsal without interaction with the inhibitor might be sufficient to activate target gene expression.

To sum up, Dorsal might act as an polarizer to enhance the ventral fate through *sog* activation in *Oncopeltus*, but not act as a morphogen to form a nuclear gradient along the DV axis as detected in *Drosophila*. Unequivocally, if there is no nuclear Dorsal gradient, the ventral signal might rely on other maternal determinants to break the DV symmetry, which is still unknown in *Oncopeltus*.

4.4 The DV patterning in *Oncopeltus* also contributes to AP patterning

In the milkweed bug, the disruption of DV patterning result in an anterior-shifted pattern of gene expression along the AP axis (Figure 3.21). These results indicate that the DV patterning in *Oncopeltus* also contributes to AP patterning. This seems to be surprisingly different from *Drosophila*, where there is no interaction between the DV and AP patterning system (Roth, 1993). Although the classical genetic studies in *Drosophila* argue that the DV and AP patterning are controlled by separate maternal systems (St Johnston and Nüsslein-Volhard, 1992), the expression pattern of a segmentation gene along the AP axis is affected in DV polarity mutants (Carroll et al., 1987). Furthermore, it was found from the ChIP-chip analysis that the AP patterning genes were regulated by the Dorsal, Twist, and Snail binding motifs (Zeitlinger et al., 2007). It is conceivable that the expression of AP target genes is modulated by the DV patterning network. In the honeybee *Apis mellifera*, it was observed that knockdown of *Toll* or *dpp* both lead to DV and AP patterning defects in blastoderm embryos (Wilson et al., 2014). In the beetle *Tribolium*, the head gap gene *orthodenticle* (*otd*) has an apparent role in AP blastoderm

patterning, but is also essential for DV patterning (Kotkamp et al., 2010). Thus, the interaction between AP and DV patterning could be bidirectional. From the anterior-shifted phenotypes in *Oncopeltus*, the crosstalk between AP and DV patterning could be explained from several aspects described in the following text.

4.4.1 Fate map shift

Based on the studies in the basal flies, red flour beetle, and honeybee, the most anterior fate of the insect blastoderm embryo is the presumptive serosa anlage (Goltsev et al., 2007; Lemke and Schmidt-Ott, 2009; Nunes da Fonseca et al., 2008; Wilson et al., 2014). The direct evidence is the anterior dorsal expression of *zerknüllt* (*zen*), which is required to sustain the serosa fate in *Tribolium* (van der Zee et al., 2005). Although the anterior pole and the dorsal surface of *Oncopeltus* embryos were presumed as the extraembryonic territory (Johannsen and Butt, 1941; Butt, 1949), *zen* can not be used to mark the serosa fate because *zen* is not involved in the specification of extraembryonic tissues in the milkweed bug (Panfilio et al., 2006). Therefore, based on the anterior-shifted phenotypes produced by *Toll-1* and *dll* RNAi, the serosa-germ rudiment boundary might be affected and the serosa fate could be reduced to a certain amount.

4.4.2 Dorsal might interact with the terminal system

The transcription factor Dorsal might act as a repressor to prevent target genes from being expressed in the most anterior region of *Oncopeltus* blastoderm embryos. For example, Dorsal acts as a transcriptional repressor modulating the Torso signaling pathway at the poles in *Drosophila* (Rusch and Levine, 1994). Without functional Dorsal or Toll signaling in *Oncopeltus*, repressed genes could start to be expressed at the poles, which would account for the anterior-shifted phenotype and the remnant gene expression in the most posterior proctodeum. Although the gene *dorsal* has not been shown to be involved in the terminal patterning of *Oncopeltus* (Weisbrod et al., 2013), it is possible that Dorsal is interacting with the terminal system.

4.4.3 AP patterning genes are also Dorsal target genes

The *Drosophila* ChIP data demonstrate that there are Dorsal binding sites in the *orthodenticle* (*otd*) enhancer (Zeitlinger et al., 2007). It is possible that in *Oncopeltus* Dorsal proteins also regulate AP patterning genes such as *otd* through the cis-regulating elements to modify the AP patterning system.

4.5 Establishment of the DV axis in the milkweed bug

The Z-stacked dissection images of *Oncopeltus* ovarioles show that the oocyte nucleus migrates to the cortex, which might represent a symmetry-breaking event for DV patterning (Figure 3.38). This phenomenon is similar to the findings in other examined insect species (Lynch et al., 2010), which might indicate that the maternal cues for axial determination are provided in ovaries, probably through conserved EGF signaling. Although the positional information is deposited in the oocytes, no significant DV difference can be observed in early embryos of *Oncopeltus*. The ubiquitous *sog* expression in the early blastoderm stage indicates that the DV patterning could be initiated from different positions along the entire embryonic circumferences. Moreover, the initial distribution of *sog* expression is not dependent on Toll signaling because weak and uniform expression of *sog* is still observed in *Toll-1* or *dll* knockdown embryos. The Toll signaling might be only needed to enhance the *sog* expression on one side as a symmetry-breaking polarizer. Once the DV polarity is established, the BMP signaling could be self-enhanced by the transport of BMP ligands (Dpp) to the dorsal side.

4.5.1 Interaction between BMP and Toll signaling

The opposite roles of Toll and BMP signaling are demonstrated here by ISH staining and qPCR in *Oncopeltus* (Figure doubleRT). While Toll signaling activates *sog* and *twist* expression on the ventral side, their expression is suppressed by BMP signaling to the ventral side. The double knockdown of *Toll-1* and *dpp* in *Oncopeltus* phenocopies the *dpp-RNAi* phenotype. This indicates that the expression of ventral markers can be activated in the absence of Toll signaling under the double knockdown condition. However, there

could be a connection between Toll and BMP signal transduction, though it might be indirect. The crosstalk between Toll and BMP pathways might be linked through the evolutionarily conserved signaling intermediate in Toll pathways (Ecsit) (Kopp et al., 1999; Moustakas and Heldin, 2003; Xiao et al., 2003; Ding et al., 2014) because Ecsit was known to associate with the Toll signaling components and embryos of *Ecsit* knockout mouse phenocopies loss of BMP signal. Nevertheless, the role of Ecsit in Toll and BMP signal transduction has not been further studied in insects.

4.5.2 Evolutionary changes of the DV patterning system among insects

BMP signaling is a conserved pathway for DV axis formation in bilaterians (De Robertis and Sasai, 1996). Within the insect, the DV patterning network has been studied in the mosquito (Goltsev et al., 2007). In *Anopheles gambiae*, a broader domain of Dpp signaling was discovered and combined with the expansion of the dorsal ectoderm territory compared to *Drosophila* embryos. In the beetle *Tribolium*, *dpp-RNAi* embryos are ventralized with an expansion of neuroectoderm, but the ventral mesoderm is not expanded (van der Zee et al., 2006). Additionally, BMP signaling was co-opted for head formation independently in *Tribolium*. A recent study in the wasp *Nasonia* reported that the DV polarity of the *Nasonia* embryo relies mainly on the BMP gradient with very limited input from Toll signaling (Ozüak et al., 2014). In contrast to BMP signaling, the diminished function of Toll signaling in *Oncopeltus* (compared to holometabolous insects) is likely to represent an ancestral aspect of DV axis formation in insects.

4.5.3 The emergence of Toll's role in DV axis formation

The immune function of Toll signal transduction is evolutionarily conserved in metazoans (Wiens et al., 2007; Hoffmann and Reichhart, 2002). However, Toll signaling is not used for axis formation in any metazoan studied so far, except for insects. In *Drosophila*, Toll signaling not only mediates DV polarity in the embryo, but also activates an immune response (Anderson et al., 1985b; Rosetto et al., 1995; Lemaitre et al., 1996). There are more and more studies showing that the insect eggs are immune competent. They can response to microbial infections (Gorman et al., 2004; Esfahani and Engström, 2011) or

to control their own bacterial endosymbionts (Login et al., 2011). Furthermore, the extraembryonic tissue has the potential to induce several immune-related genes to protect *Tribolium* embryos against pathogens (Jacobs and van der Zee, 2013), which is mediated through the transcription factor Dorsal (Yokoi et al., 2012) while high amounts of Dorsal are expressed in the serosa (Chen et al., 2000). Thus, the immune function of the Toll/Dorsal pathway might be conserved in all insects to protect embryos from invading pathogens. Toll signaling might be recruited from an ancestral immune function to a novel function in DV patterning during the evolution of insect lineages (Lynch and Roth, 2011). Since *Oncopeltus dl1* is expressed uniformly in early blastoderm embryos and *Oncopeltus dl2* is expressed in the anterior part of late blastoderm embryos (Figure 3.11), they could be deposited for the immune defense and upon the activation of Toll signaling they were also recruited for the patterning, which sheds a light on the emergence of Toll's role in DV axis formation.

4.5.4 The regulation of *Toll* in insects

In *Drosophila* and the moth fly *Clogmia* embryos, the *Toll* transcripts are provided maternally in an uniform distribution and then transcribed zygotically (Gerttula et al., 1988; Maxton-Küchenmeister et al., 1999). On the contrary, maternal *Toll* transcripts are barely detectable in *Tribolium* and there is a zygotic gradient of *Toll* expression in early blastoderm embryos with higher concentration at the ventral side (Maxton-Küchenmeister et al., 1999). In this thesis, asymmetric localization of *Toll* transcripts along the DV axis was also observed in *Oncopeltus* blastoderm embryos. The localized pattern indicates that the *Toll* expression could be regulated by a positive feedback mechanism. Once the Toll protein is translated, it could be self-enhanced. The similar *Toll* localization patterns in *Tribolium* and *Oncopeltus* also imply that the expression of *Toll* might be modulated similarly by a dynamic feedback loop.

4.6 Summary of Toll's role in DV patterning of *Oncopeltus*

In this thesis, the function of the entire Toll signaling pathway has been studied in a basally branching insect, the milkweed bug *Oncopeltus* (section 4.1). Upstream and downstream signaling components of the Toll pathway are involved in establishing the DV polarity (section 4.2.3). In the loss-of-function experiments produced by pRNAi, the development of embryos is disrupted. Knockdown embryos form the classical tube-like shape during germband stages, which is representatively produced by the *Toll1-RNAi* (section 4.2). During blastoderm stages, knockdown embryos are lateralized or dorsalized, which is shown by the expression patterns of marker genes. With the validation of RNAi efficiency, weak DV defects might indicate the redundant compensation from other paralogs such as the knockdown of *dorsal*, *spätzle* and *cactus* genes. Although there might be no nuclear Dorsal gradient in blastoderm embryos, Toll signaling mediated through the transcription factors is still needed for the activation of downstream target genes (section 4.3). Furthermore, the anterior-shifted phenotypes after Toll signaling knockdown indicate the crosstalk between AP and DV patterning in the milkweed bug (section 4.4). In *Oncopeltus*, BMP signaling has a large impact on DV patterning (Sachs, 2014) and Toll signaling provides the polarity cues, which might be close to the ancestral mode of DV patterning during the evolution of insects (section 4.5).

4.7 Future perspectives

4.7.1 Post-genomic era and the mechanism of DV patterning in the hemipterans

As there are more and more genomes of hemipteran insects being sequenced (Figure 4.1), it is possible to study mechanisms of DV patterning in more species of basally-branching insects. Genes involved in the DV-patterning system could be identified from the genomic data and the functions of DV-patterning genes could be investigated via parental RNAi, which has been established in many hemipterans (Figure 4.1). It is necessary to have a broad sampling to investigate if the recruitment of Toll signaling for DV patterning is

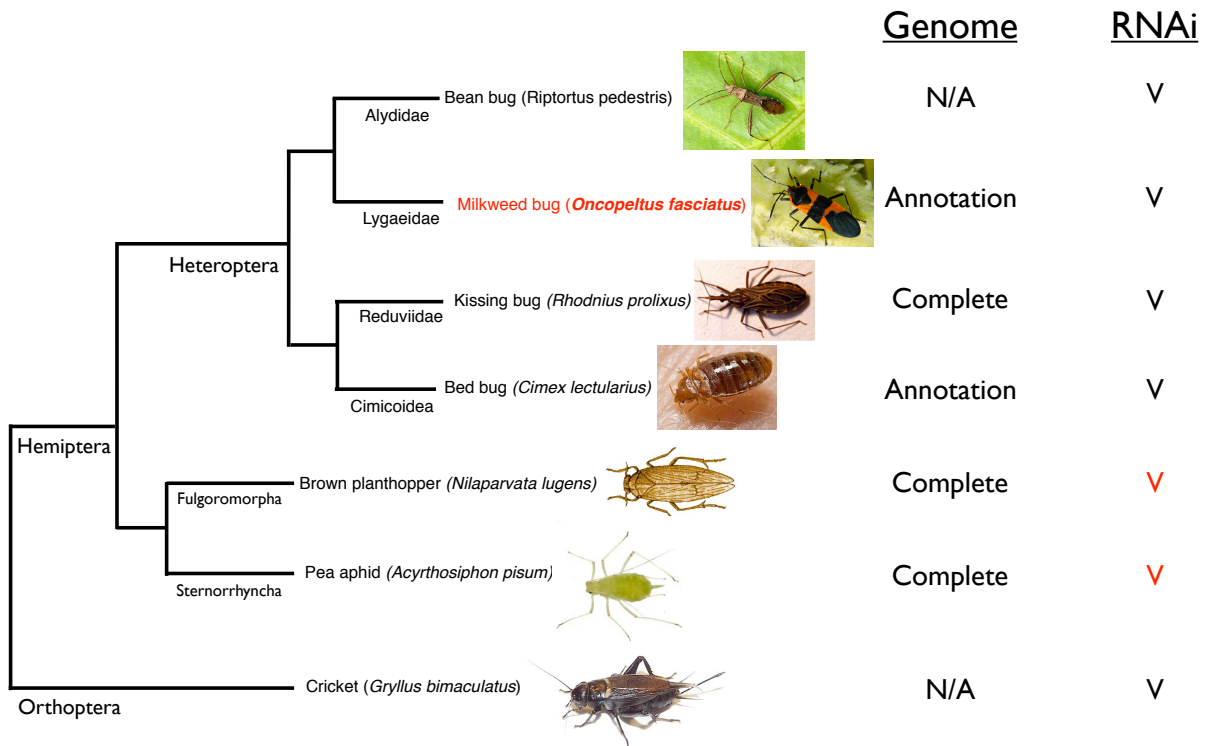


Figure 4.1. Phylogeny of recently sequenced hemiptera insects

The genome of the pea aphid *Acyrtosiphon pisum* was the first published sequence in hemimetabolous insects (Consortium, 2010). The genome of the brown planthopper *Nilaparvata lugens* was announced together with the transcriptome (Bao et al., 2013). Genomic annotation of the milkweed bug *Oncopeltus fasciatus* and the bed bug *Cimex lectularius* is still ongoing. Although the genome of the bean bug *Riptortus pedestris* has not been sequenced, there is a transcriptome available (personal communication with Dr. Y. Kikuchi and Y. Matsuura). The genome of several kissing bugs including the species *Rhodnius prolixus* is finished and waiting to be published. The cricket belonging to the Orthoptera served as an outgroup to the other hemiptera insects.

conserved in other insect lineages.

With the advantage of genomic annotation in the milkweed bug, there are many tools accessible for genome editing, including the zinc finger nucleases (ZFNs), transcription activator-like effector nucleases (TALENs), and the clustered regularly interspaced short palindromic repeats/caspase (CRISPR/Cas) system. These techniques will help to study the gene function and to create a complete loss-of-function of candidate genes in *Oncopeltus*, which is not feasible via parental RNAi.

4.7.2 The novel imaging and transgenic techniques

The new technique of light-sheet microscopy (Tomer et al., 2012), which is also called selective-plane illumination microscope (SPIM) (Krzic et al., 2012), allows to visualize an embryo with multiple views simultaneously in a cellular resolution. The embryonic development of zebrafish (Keller et al., 2008), fly (Tomer et al., 2012), and mouse (Udan et al., 2014) has been studied using the technique. With this technique, the cell movement of the entire embryos could be observed in real-time by tracking of the nuclei and cell shape. This could be utilized to understand the consequence of disrupted embryonic development in the absence of Toll signaling (or other signaling) because insect embryos are enriched with yolk and are often not transparent. If the embryonic cell fate could be marked, the fate map change could be visualized in time-lapse, which is still not feasible in *Oncopeltus*. Thus, it is necessary to generate a transgenic line of non-model insects with fluorescent markers. For example, a nuclear GFP line in the cricket *Gryllus bimaculatus* has been established (Shinmyo et al., 2004) and a Dorsal-GFP transgenic line of *Drosophila* was utilized to visualize the dynamic shuttling of the Dorsal proteins between the nucleus and the cytoplasm (DeLotto et al., 2007). Furthermore, several transgenic insects are generated by the piggyBac transposon-mediated transformation such as the silkworm *Bombyx mori* (Masumoto et al., 2012), the ladybird beetle *Harmonia axyridis* (Kuwayama et al., 2014), and the red flour beetle *Tribolium castaneum* (Koelzer et al., 2014). Recently, it has been tested to establish a transgenic line of *Oncopeltus*. However, there are still difficulties for the transformation and for the efficient expression in a non-model animal like *Oncopeltus* (personal communication with Dr. Y. Matsuura).

4.7.3 The immune functions of Toll signaling in *Oncopeltus*

The Toll signaling pathway was found to have dual functions in DV patterning and innate immunity in *Drosophila* (Anderson et al., 1985b; Rosetto et al., 1995; Lemaitre et al., 1996). In this thesis, the role of Toll signaling in DV patterning has been studied in the milkweed bug. Additionally, the immune function of Toll signaling could be implied by the life span reduction of injected females. There is a tendency that the adult females injected with *Toll-1*, *dll2*, *rel* dsRNAs seem to live shorter than the mock-treated groups (Table 5.3). Thus, they might be more vulnerable to pathogens. To further investigate

the immune function of Toll signaling in *Oncopeltus*, the whole set of immune-related genes should be identified including the genes from the Immune deficiency (IMD) signaling pathway. Because Toll and Imd pathways are the major regulators of the immune response in *Drosophila* (De Gregorio et al., 2002; Tanji et al., 2007). Although the IMD pathway genes are missing in the aphid genome (Gerardo et al., 2010), genes involved in the IMD pathway such as the *imd*, *relish* and the *lysozyme* have been found in the *Oncopeltus* transcriptome (unpublished data). It is also important to identify members of the antimicrobial peptides (AMPs) (Bulet et al., 1999; Bulet and Stöcklin, 2005) because the AMPs have the ability to fight against specific pathogens directly. In addition, the up-regulation of AMP genes could be an indicator to estimate the activation of the immune system. The induction of AMP genes was proven to be activated by the NF κ B transcription factors upon an immune response in *Tribolium* (Yokoi et al., 2012) and it seems to be conserved in mammalian and insect innate immunity (Silverman and Maniatis, 2001). Nowadays, it is possible to investigate how the immune-related genes are regulated via transcriptomic analysis based on the Next Generation Sequencing (NGS) technique (Altincicek et al., 2013; Bao et al., 2013; Sackton et al., 2013). The whole-transcriptomic comparison between wildtype and Toll signaling-deficient embryos could help to understand the dual functions of the Toll pathway in *Oncopeltus*.

References

- Akira, S.; Takeda, K.; and Kaisho, T. 2001: Toll-like receptors: critical proteins linking innate and acquired immunity. *Nat Immunol* 2(8):675–680.
- Akiyama-Oda, Y. and Oda, H. 2006: Axis specification in the spider embryo: *dpp* is required for radial-to-axial symmetry transformation and *sog* for ventral patterning. *Development* 133(12):2347–2357.
- Alberga, A.; Boulay, J. L.; Kempe, E.; Dennefeld, C.; and Haenlin, M. 1991: The *snail* gene required for mesoderm formation in *Drosophila* is expressed dynamically in derivatives of all three germ layers. *Development* 111(4):983–992.
- Altincicek, B.; Elashry, A.; Guz, N.; Grundler, F. M. W.; Vilcinskas, A.; and Dehne, H.-W. 2013: Next generation sequencing based transcriptome analysis of septic-injury responsive genes in the beetle *Tribolium castaneum*. *PLoS One* 8(1):e52004.
- Anderson, K. V.; Bokla, L.; and Nüsslein-Volhard, C. 1985a: Establishment of dorsal-ventral polarity in the *Drosophila* embryo: the induction of polarity by the Toll gene product. *Cell* 42(3):791–798.
- Anderson, K. V.; Jürgens, G.; and Nüsslein-Volhard, C. 1985b: Establishment of dorsal-ventral polarity in the *Drosophila* embryo: genetic studies on the role of the Toll gene product. *Cell* 42(3):779–789.
- Angelini, D. R. and Kaufman, T. C. 2004: Functional analyses in the hemipteran *Oncopeltus fasciatus* reveal conserved and derived aspects of appendage patterning in insects. *Developmental Biology* 271(2):306 – 321.

- Bao, Y.-Y.; Qu, L.-Y.; Zhao, D.; Chen, L.-B.; Jin, H.-Y.; Xu, L.-M.; Cheng, J.-A.; and Zhang, C.-X. 2013: The genome- and transcriptome-wide analysis of innate immunity in the brown planthopper, *Nilaparvata lugens*. *BMC Genomics* 14(1):160.
- Barbara Wigand, M. K., Gregor Bucher. 1998: A simple whole mount technique for look *Tribolium* embryos. Technical Note in *Tribolium* Information Bulletin.
- Belvin, M. P.; Jin, Y.; and Anderson, K. V. 1995: Cactus protein degradation mediates *Drosophila* dorsal-ventral signaling. *Genes Dev* 9(7):783–793.
- Ben-David, J. and Chipman, A. D. 2010: Mutual regulatory interactions of the trunk gap genes during blastoderm patterning in the hemipteran *Oncopeltus fasciatus*. *Developmental Biology* 346(1):140 – 149.
- Berger, C.; Harzer, H.; Burkard, T. R.; Steinmann, J.; van der Horst, S.; Laurenson, A.-S.; Novatchkova, M.; Reichert, H.; and Knoblich, J. A. 2012: FACS purification and transcriptome analysis of drosophila neural stem cells reveals a role for Klumpfuss in self-renewal. *Cell Rep* 2(2):407–418.
- Bergmann, A.; Stein, D.; Geisler, R.; Hagenmaier, S.; Schmid, B.; Fernandez, N.; Schnell, B.; and Nüsslein-Volhard, C. 1996: A gradient of cytoplasmic Cactus degradation establishes the nuclear localization gradient of the *dorsal* morphogen in *Drosophila*. *Mech Dev* 60(1):109–123.
- Birkan, M.; Schaeper, N. D.; and Chipman, A. D. 2011: Early patterning and blastodermal fate map of the head in the milkweed bug *Oncopeltus fasciatus*. *Evolution & Development* 13(5):436–47.
- Bland, J. M. and Altman, D. G. 2004: The logrank test. *BMJ* 328(7447):1073.
- Blom, N.; Gammeltoft, S.; and Brunak, S. 1999: Sequence and structure-based prediction of eukaryotic protein phosphorylation sites. *J Mol Biol* 294(5):1351–1362.
- Bonhag, P. F. 1955: Histochemical studies of the ovarian nurse tissues and oocytes of the milkweed bug, *Oncopeltus fasciatus* (Dallas). II. Sudanophilia, phospholipids, and cholesterol. *Journal of Morphology* 97(2):283–311.

- Bonhag, P. F. and Wick, J. R. 1953: The functional anatomy of the male and female reproductive systems of the milkweed bug, *Oncopeltus fasciatus* (Dallas) (Heteroptera: Lygaeidae). *Journal of Morphology* 93(2):177–283.
- Brown, S. J.; Patel, N. H.; and Denell, R. E. 1994: Embryonic expression of the single *Tribolium engrailed* homolog. *Dev Genet* 15(1):7–18.
- Buchta, T.; Özüak, O.; Stappert, D.; Roth, S.; and Lynch, J. A. 2013: Patterning the dorsal-ventral axis of the wasp *Nasonia vitripennis*. *Developmental Biology* 381(1):189 – 202.
- Buescher, M.; Hing, F. S.; and Chia, W. 2002: Formation of neuroblasts in the embryonic central nervous system of *Drosophila melanogaster* is controlled by *SoxNeuro*. *Development* 129(18):4193–4203.
- Bulet, P.; Hetru, C.; Dimarcq, J. L.; and Hoffmann, D. 1999: Antimicrobial peptides in insects; structure and function. *Dev Comp Immunol* 23(4-5):329–344.
- Bulet, P. and Stöcklin, R. 2005: Insect antimicrobial peptides: structures, properties and gene regulation. *Protein Pept Lett* 12(1):3–11.
- Butt, F. 1949: Embryology of the milkweed bug: *Oncopeltus fasciatus* (Hemiptera). Memoir (Cornell University. Agricultural Experiment Station). Cornell University Agricultural Experiment Station.
- Campbell, G. L. and Caveney, S. 1989: Engrailed gene expression in the abdominal segment of *Oncopeltus*: gradients and cell states in the insect segment. *Development* 106(4):727–737.
- Cande, J.; Goltsev, Y.; and Levine, M. S. 2009: Conservation of enhancer location in divergent insects. *Proc Natl Acad Sci U S A* 106(34):14414–14419.
- Cao, Z.; Henzel, W. J.; and Gao, X. 1996: IRAK: a kinase associated with the interleukin-1 receptor. *Science* 271(5252):1128–1131.
- Capco, D. G. and Jeffery, W. R. 1977: Differential distribution of poly(A)-containing RNA in the embryonic cells of *Oncopeltus fasciatus*: Analysis by in situ hybridization with a [³H]poly(U) probe. *Developmental Biology* 67(1):137–151.

- Carroll, S. B.; Winslow, G. M.; Twombly, V. J.; and Scott, M. P. 1987: Genes that control dorsoventral polarity affect gene expression along the anteroposterior axis of the *Drosophila* embryo. *Development* 99(3):327–332.
- Cerenius, L.; Lee, B. L.; and Söderhäll, K. 2008: The proPO-system: pros and cons for its role in invertebrate immunity. *Trends Immunol* 29(6):263–271.
- Chapman, R.; Simpson, S.; and Douglas, A. 2013: *The Insects: Structure and Function*. Cambridge University Press.
- Charatsi, I.; Luschnig, S.; Bartoszewski, S.; Nüsslein-Volhard, C.; and Moussian, B. 2003: Krapfen/dMyd88 is required for the establishment of dorsoventral pattern in the *Drosophila* embryo. *Mech Dev* 120(2):219–226.
- Chen, G.; Handel, K.; and Roth, S. 2000: The maternal NF-kappaB/dorsal gradient of *Tribolium castaneum*: dynamics of early dorsoventral patterning in a short-germ beetle. *Development* 127(23):5145–5156.
- Chinchore, Y.; Gerber, G. F.; and Dolph, P. J. 2012: Alternative pathway of cell death in *Drosophila* mediated by NF- κ B transcription factor Relish. *Proc Natl Acad Sci U S A* 109(10):E605–E612.
- Cho, Y. S.; Stevens, L. M.; Sieverman, K. J.; Nguyen, J.; and Stein, D. 2012: A ventrally localized protease in the *Drosophila* egg controls embryo dorsoventral polarity. *Curr Biol* 22(11):1013–1018.
- Christophides, G. K.; Zdobnov, E.; Barillas-Mury, C.; Birney, E.; Blandin, S.; Blass, C.; Brey, P. T.; Collins, F. H.; Danielli, A.; Dimopoulos, G.; Hetru, C.; Hoa, N. T.; Hoffmann, J. A.; Kanzok, S. M.; Letunic, I.; Levashina, E. A.; Loukeris, T. G.; Lycett, G.; Meister, S.; Michel, K.; Moita, L. F.; Müller, H.-M.; Osta, M. A.; Paskewitz, S. M.; Reichhart, J.-M.; Rzhetsky, A.; Troxler, L.; Vernick, K. D.; Vlachou, D.; Volz, J.; von Mering, C.; Xu, J.; Zheng, L.; Bork, P.; and Kafatos, F. C. 2002: Immunity-related genes and gene families in *Anopheles gambiae*. *Science* 298(5591):159–165.
- Coleman, K. G.; Poole, S. J.; Weir, M. P.; Soeller, W. C.; and Kornberg, T. 1987: The invected gene of *Drosophila*: sequence analysis and expression studies reveal a close kinship to the engrailed gene. *Genes Dev* 1(1):19–28.

- Consortium, I. A. G. 2010: Genome sequence of the pea aphid *Acyrthosiphon pisum*. PLoS Biol 8(2):e1000313.
- Crémazy, F.; Berta, P.; and Girard, F. 2000: Sox Neuro, a new *Drosophila* Sox gene expressed in the developing central nervous system. Mechanisms of Development 93(1-2):215–219.
- Daigneault, J.; Klemetsaune, L.; and Wasserman, S. A. 2013: The IRAK homolog Pelle is the functional counterpart of I κ B kinase in the *Drosophila* Toll pathway. PLoS One 8(9):e75150.
- Dao, V. A. 2014: Genome-wide RNAi screening and the analysis of candidate genes for dorsoventral patterning in *Tribolium castaneum*. Ph.D. thesis, Universität zu Köln.
- De Gregorio, E.; Spellman, P. T.; Tzou, P.; Rubin, G. M.; and Lemaitre, B. 2002: The Toll and Imd pathways are the major regulators of the immune response in *Drosophila*. EMBO J 21(11):2568–2579.
- De Robertis, E. M. and Sasai, Y. 1996: A common plan for dorsoventral patterning in Bilateria. Nature 380(6569):37–40.
- de Wit, J.; Hong, W.; Luo, L.; and Ghosh, A. 2011: Role of leucine-rich repeat proteins in the development and function of neural circuits. Annu Rev Cell Dev Biol 27:697–729.
- DeLotto, R.; DeLotto, Y.; Steward, R.; and Lippincott-Schwartz, J. 2007: Nucleocytoplasmic shuttling mediates the dynamic maintenance of nuclear Dorsal levels during *Drosophila* embryogenesis. Development 134(23):4233–4241.
- DeLotto, Y. and DeLotto, R. 1998: Proteolytic processing of the *Drosophila* Spätzle protein by easter generates a dimeric NGF-like molecule with ventralising activity. Mech Dev 72(1-2):141–148.
- Ding, D.; Chen, X.-W.; Kang, L.-H.; Jiang, H.-S.; and Kang, C.-J. 2014: Role of evolutionarily conserved signaling intermediate in Toll pathways (ECSIT) in the antibacterial immunity of *Marsupenaeus japonicus*. Dev Comp Immunol 46(2):246–254.

- Dissing, M.; Giordano, H.; and DeLotto, R. 2001: Autoproteolysis and feedback in a protease cascade directing *Drosophila* dorsal–ventral cell fate. *The EMBO Journal* 20(10):2387–2393.
- Dolan, J.; Walshe, K.; Alsbury, S.; Hokamp, K.; O’Keeffe, S.; Okafuji, T.; Miller, S. F. C.; Tear, G.; and Mitchell, K. J. 2007: The extracellular leucine-rich repeat superfamily; a comparative survey and analysis of evolutionary relationships and expression patterns. *BMC Genomics* 8:320.
- Dorn, A. 1976: Ultrastructure of Embryonic Envelopes and Integument of *Oncopeltus fasciatus* Dallas (Insecta, Heteroptera) I. Chorion, Amnion, Serosa, Integument. *Zoomorphologie* 85:111–131.
- Drier, E. A.; Govind, S.; and Steward, R. 2000: Cactus-independent regulation of Dorsal nuclear import by the ventral signal. *Curr Biol* 10(1):23–26.
- Drier, E. A.; Huang, L. H.; and Steward, R. 1999: Nuclear import of the *Drosophila* Rel protein Dorsal is regulated by phosphorylation. *Genes Dev* 13(5):556–568.
- Dutta, J.; Fan, Y.; Gupta, N.; Fan, G.; and G  linas, C. 2006: Current insights into the regulation of programmed cell death by NF-kappaB. *Oncogene* 25(51):6800–6816.
- Edwards, D. N.; Towb, P.; and Wasserman, S. A. 1997: An activity-dependent network of interactions links the Rel protein Dorsal with its cytoplasmic regulators. *Development* 124(19):3855–3864.
- Esfahani, S. S. and Engstr  m, Y. 2011: Activation of an innate immune response in large numbers of permeabilized *Drosophila* embryos. *Dev Comp Immunol* 35(3):263–266.
- Evans, J. D.; Aronstein, K.; Chen, Y. P.; Hetru, C.; Imler, J.-L.; Jiang, H.; Kanost, M.; Thompson, G. J.; Zou, Z.; and Hultmark, D. 2006: Immune pathways and defence mechanisms in honey bees *Apis mellifera*. *Insect Mol Biol* 15(5):645–656.
- Ewen-Campen, B.; Jones, T. E. M.; and Extavour, C. G. 2013: Evidence against a germ plasm in the milkweed bug *Oncopeltus fasciatus*, a hemimetabolous insect. *Biology Open* 2(6):556–568.

- Ewen-Campen, B.; Shaner, N.; Panfilio, K.; Suzuki, Y.; Roth, S.; and Extavour, C. 2011: The maternal and early embryonic transcriptome of the milkweed bug *Oncopeltus fasciatus*. *BMC Genomics* 12(1):61.
- Feir, D. 1974: *Oncopeltus fasciatus*: a research animal. *Annu. Rev. Entomol.* 19:81–96.
- Frank, L. and Rushlow, C. 1996: A group of genes required for maintenance of the amnioserosa tissue in *Drosophila*. *Development* 122(5):1343–1352.
- Futahashi, R.; Tanaka, K.; Tanahashi, M.; Nikoh, N.; Kikuchi, Y.; Lee, B. L.; and Fukatsu, T. 2013: Gene expression in gut symbiotic organ of stinkbug affected by extracellular bacterial symbiont. *PLoS One* 8(5):e64557.
- Galindo, R.; Edwards, D.; Gillespie, S.; and Wasserman, S. 1995: Interaction of the pelle kinase with the membrane-associated protein tube is required for transduction of the dorsoventral signal in *Drosophila* embryos. *Development* 121(7):2209–2218.
- Gangloff, M.; Murali, A.; Xiong, J.; Arnot, C. J.; Weber, A. N.; Sandercock, A. M.; Robinson, C. V.; Sarisky, R.; Holzenburg, A.; Kao, C.; and Gay, N. J. 2008: Structural insight into the mechanism of activation of the Toll receptor by the dimeric ligand Spätzle. *J Biol Chem* 283(21):14629–14635.
- Geisler, R.; Bergmann, A.; Hiromi, Y.; and Nüsslein-Volhard, C. 1992: cactus, a gene involved in dorsoventral pattern formation of *Drosophila*, is related to the ICE/B gene family of vertebrates. *Cell* 71(4):613 – 621.
- Gerardo, N. M.; Altincicek, B.; Anselme, C.; Atamian, H.; Barribeau, S. M.; de Vos, M.; Duncan, E. J.; Evans, J. D.; Gabaldón, T.; Ghanim, M.; Heddi, A.; Kaloshian, I.; Latorre, A.; Moya, A.; Nakabachi, A.; Parker, B. J.; Pérez-Brocal, V.; Pignatelli, M.; Rahbé, Y.; Ramsey, J. S.; Spragg, C. J.; Tamames, J.; Tamarit, D.; Tamborindeguy, C.; Vincent-Monegat, C.; and Vilcinskis, A. 2010: Immunity and other defenses in pea aphids, *Acyrtosiphon pisum*. *Genome Biol* 11(2):R21.
- Gerttula, S.; Jin, Y. S.; and Anderson, K. V. 1988: Zygotic expression and activity of the *Drosophila* Toll gene, a gene required maternally for embryonic dorsal-ventral pattern formation. *Genetics* 119(1):123–133.

- Goltsev, Y.; Fuse, N.; Frasch, M.; Zinzen, R. P.; Lanzaro, G.; and Levine, M. 2007: Evolution of the dorsal-ventral patterning network in the mosquito, *Anopheles gambiae*. *Development* 134(13):2415–2424.
- Gönczy, P. and Rose, L. S. 2005: Asymmetric cell division and axis formation in the embryo. eBook.
- Gorman, M. J.; Kankanala, P.; and Kanost, M. R. 2004: Bacterial challenge stimulates innate immune responses in extra-embryonic tissues of tobacco hornworm eggs. *Insect Mol Biol* 13(1):19–24.
- Grimaldi, D. and Engel, M. 2005: *Evolution of the Insects*. Cambridge Evolution Series. Cambridge University Press.
- Handel, K.; Basal, A.; Fan, X.; and Roth, S. 2005: *Tribolium castaneum* twist: gastrulation and mesoderm formation in a short-germ beetle. *Development Genes and Evolution* 215(1):13–31.
- Hartenstein, G., V. Technau and Campos-Ortega, J. A. 1985: Fate-mapping in wild-type *Drosophila melanogaster* III. A fate map of the blastoderm. *Roux's Arch. Dev. Biol.* 194:213–216.
- Hatada, E. N.; Nieters, A.; Wulczyn, F. G.; Naumann, M.; Meyer, R.; Nucifora, G.; McKeithan, T. W.; and Scheidereit, C. 1992: The ankyrin repeat domains of the NF-kappa B precursor p105 and the protooncogene bcl-3 act as specific inhibitors of NF-kappa B DNA binding. *Proc Natl Acad Sci USA* 89(6):2489–2493.
- Hawley, S. H.; Wünnenberg-Stapleton, K.; Hashimoto, C.; Laurent, M. N.; Watabe, T.; Blumberg, B. W.; and Cho, K. W. 1995: Disruption of BMP signals in embryonic *Xenopus* ectoderm leads to direct neural induction. *Genes Dev* 9(23):2923–2935.
- Hoffmann, J. A. and Reichhart, J.-M. 2002: *Drosophila* innate immunity: an evolutionary perspective. *Nat Immunol* 3(2):121–126.
- Holley, S. A.; Jackson, P. D.; Sasai, Y.; Lu, B.; De Robertis, E. M.; Hoffmann, F. M.; and Ferguson, E. L. 1995: A conserved system for dorsal-ventral patterning in insects and vertebrates involving *sog* and *chordin*. *Nature* 376(6537):249–253.

- Hong, C. C. and Hashimoto, C. 1996: The maternal nudel protein of *Drosophila* has two distinct roles important for embryogenesis. *Genetics* 143(4):1653–1661.
- Hong, J.-W.; Hendrix, D. A.; Papatsenko, D.; and Levine, M. S. 2008: How the Dorsal gradient works: insights from postgenome technologies. *Proc Natl Acad Sci U S A* 105(51):20072–20076.
- Horng, T. and Medzhitov, R. 2001: *Drosophila* MyD88 is an adapter in the Toll signaling pathway. *Proc Natl Acad Sci U S A* 98(22):12654–12658.
- Huang, J. D.; Schwyster, D. H.; Shirokawa, J. M.; and Courey, A. J. 1993: The interplay between multiple enhancer and silencer elements defines the pattern of decapentaplegic expression. *Genes Dev* 7(4):694–704.
- Hughes, C. and Kaufman, T. 2000: RNAi analysis of Deformed, proboscipedia and Sex combs reduced in the milkweed bug *Oncopeltus fasciatus*: novel roles for Hox genes in the hemipteran head. *Development* 127(17):3683–3694.
- Irish, V. F. and Gelbart, W. M. 1987: The decapentaplegic gene is required for dorsal-ventral patterning of the *Drosophila* embryo. *Genes Dev* 1(8):868–879.
- Jacobs, C. G. C. and van der Zee, M. 2013: Immune competence in insect eggs depends on the extraembryonic serosa. *Dev Comp Immunol* 41(2):263–269.
- Janssens, S. and Beyaert, R. 2003: Role of Toll-Like Receptors in Pathogen Recognition. *Clinical Microbiology Reviews* 16(4):637–646.
- Johannsen, O. A. and Butt, F. H. 1941: Embryology of insects and myriapods; the developmental history of insects, centipedes, and millepedes from egg desposition to hatching. New York, McGraw-Hill Book Company, inc.,. [Http://www.biodiversitylibrary.org/bibliography/6583](http://www.biodiversitylibrary.org/bibliography/6583).
- Kaltschmidt, B.; Kaltschmidt, C.; Hofmann, T. G.; Hehner, S. P.; Dröge, W.; and Schmitz, M. L. 2000: The pro- or anti-apoptotic function of NF- κ B is determined by the nature of the apoptotic stimulus. *European Journal of Biochemistry* 267(12):3828–3835.

- Kambris, Z.; Hoffmann, J. A.; Imler, J.-L.; and Capovilla, M. 2002: Tissue and stage-specific expression of the Tolls in *Drosophila* embryos. *Gene Expr Patterns* 2(3-4):311–317.
- Keller, P. J.; Schmidt, A. D.; Wittbrodt, J.; and Stelzer, E. H. K. 2008: Reconstruction of zebrafish early embryonic development by scanned light sheet microscopy. *Science* 322(5904):1065–1069.
- Kenny, E. F. and O’Neill, L. A. J. 2008: Signalling adaptors used by Toll-like receptors: an update. *Cytokine* 43(3):342–349.
- Kidd, S. 1992: Characterization of the *Drosophila* cactus locus and analysis of interactions between cactus and dorsal proteins. *Cell* 71(4):623–635.
- Koelzer, S.; Kölsch, Y.; and Panfilio, K. A. 2014: Visualizing late insect embryogenesis: extraembryonic and mesodermal enhancer trap expression in the beetle *Tribolium castaneum*. *PLoS One* 9(7):e103967.
- Kopp, E.; Medzhitov, R.; Carothers, J.; Xiao, C.; Douglas, I.; Janeway, C. A.; and Ghosh, S. 1999: ECSIT is an evolutionarily conserved intermediate in the Toll/IL-1 signal transduction pathway. *Genes Dev* 13(16):2059–2071.
- Kotkamp, K.; Klingler, M.; and Schoppmeier, M. 2010: Apparent role of *Tribolium* orthodenticle in anteroposterior blastoderm patterning largely reflects novel functions in dorsoventral axis formation and cell survival. *Development* 137(11):1853–1862.
- Krzic, U.; Gunther, S.; Saunders, T. E.; Streichan, S. J.; and Hufnagel, L. 2012: Multiview light-sheet microscope for rapid in toto imaging. *Nat Methods* 9(7):730–733.
- Kuwayama, H.; Gotoh, H.; Konishi, Y.; Nishikawa, H.; Yaginuma, T.; and Niimi, T. 2014: Establishment of transgenic lines for jumpstarter method using a composite transposon vector in the ladybird beetle, *Harmonia axyridis*. *PLoS One* 9(6):e100804.
- Lemaitre, B.; Nicolas, E.; Michaut, L.; Reichhart, J. M.; and Hoffmann, J. A. 1996: The dorsoventral regulatory gene cassette *spätzle*/Toll/cactus controls the potent antifungal response in *Drosophila* adults. *Cell* 86(6):973–983.

- Lemke, S. and Schmidt-Ott, U. 2009: Evidence for a composite anterior determinant in the hover fly *Episyrphus balteatus* (Syrphidae), a cyclorrhaphan fly with an anterodorsal serosa anlage. *Development* 136(1):117–127.
- LeMosy, E. K. and Hashimoto, C. 2000: The Nudel Protease of *Drosophila* Is Required for Eggshell Biogenesis in Addition to Embryonic Patterning. *Developmental Biology* 217(2):352 – 361.
- LeMosy, E. K.; Kemler, D.; and Hashimoto, C. 1998: Role of Nudel protease activation in triggering dorsoventral polarization of the *Drosophila* embryo. *Development* 125(20):4045–4053.
- LeMosy, E. K.; Tan, Y. Q.; and Hashimoto, C. 2001: Activation of a protease cascade involved in patterning the *Drosophila* embryo. *Proc Natl Acad Sci USA* 98(9):5055–5060.
- Leptin, M. 1991: twist and snail as positive and negative regulators during *Drosophila* mesoderm development. *Genes Dev* 5(9):1568–1576.
- Leptin, M. and Grunewald, B. 1990: Cell shape changes during gastrulation in *Drosophila*. *Development* 110(1):73–84.
- Levine, M. and Davidson, E. H. 2005: Gene regulatory networks for development. *Proc Natl Acad Sci U S A* 102(14):4936–4942.
- Li, R.; Zhang, L.; Fang, Y.; Han, B.; Lu, X.; Zhou, T.; Feng, M.; and Li, J. 2013: Proteome and phosphoproteome analysis of honeybee (*Apis mellifera*) venom collected from electrical stimulation and manual extraction of the venom gland. *BMC Genomics* 14:766.
- Liu, P. and Kaufman, T. C. 2004: hunchback is required for suppression of abdominal identity, and for proper germband growth and segmentation in the intermediate germband insect *Oncopeltus fasciatus*. *Development* 131(7):1515–1527.
- Liu, P. Z. and Kaufman, T. C. 2005a: even-skipped is not a pair-rule gene but has segmental and gap-like functions in *Oncopeltus fasciatus*, an intermediate germband insect. *Development* 132(9):2081–2092.

- . 2005b: Short and long germ segmentation: unanswered questions in the evolution of a developmental mode. *Evolution & Development* 7(6):629–646.
- Liu, P. Z. and Patel, N. H. 2010: giant is a bona fide gap gene in the intermediate germband insect, *Oncopeltus fasciatus*. *Development* 137(5):835–844.
- Liu, Paul and Kaufman, Thomas C. 2009: Morphology and husbandry of the large milkweed bug, *Oncopeltus fasciatus*. *Cold Spring Harb Protoc* 2009(8):pdb.emo127.
- Login, F. H.; Balmand, S.; Vallier, A.; Vincent-Monégat, C.; Vigneron, A.; Weiss-Gayet, M.; Rochat, D.; and Heddi, A. 2011: Antimicrobial peptides keep insect endosymbionts under control. *Science* 334(6054):362–365.
- Luna, C.; Wang, X.; Huang, Y.; Zhang, J.; and Zheng, L. 2002: Characterization of four Toll related genes during development and immune responses in *Anopheles gambiae*. *Insect Biochem Mol Biol* 32(9):1171–1179.
- Lynch, J. A.; Peel, A. D.; Drechsler, A.; Averof, M.; and Roth, S. 2010: *EGF* Signaling and the Origin of Axial Polarity among the Insects. *Current Biology* 20(11):1042 – 1047.
- Lynch, J. A. and Roth, S. 2011: The evolution of dorsal-ventral patterning mechanisms in insects. *Genes Dev* 25(2):107–118.
- Majerowicz, D.; Alves-Bezerra, M.; Logullo, R.; Fonseca-de Souza, A. L.; Meyer-Fernandes, J. R.; Braz, G. R. C.; and Gondim, K. C. 2011: Looking for reference genes for real-time quantitative PCR experiments in *Rhodnius prolixus* (Hemiptera: Reduviidae). *Insect Mol Biol* 20(6):713–722.
- Markstein, M.; Markstein, P.; Markstein, V.; and Levine, M. S. 2002: Genome-wide analysis of clustered Dorsal binding sites identifies putative target genes in the *Drosophila* embryo. *Proc Natl Acad Sci U S A* 99(2):763–768.
- Marone, M.; Mozzetti, S.; De Ritis, D.; Pierelli, L.; and Scambia, G. 2001: Semiquantitative RT-PCR analysis to assess the expression levels of multiple transcripts from the same sample. *Biol Proced Online* 3:19–25.

- Masumoto, M.; Ohde, T.; Shiomi, K.; Yaginuma, T.; and Niimi, T. 2012: A Baculovirus immediate-early gene, ie1, promoter drives efficient expression of a transgene in both *Drosophila melanogaster* and *Bombyx mori*. PLoS One 7(11):e49323.
- Maxton-Küchenmeister, J.; Handel, K.; Schmidt-Ott, U.; Roth, S.; and Jäckle, H. 1999: Toll homolog expression in the beetle *Tribolium* suggests a different mode of dorsoventral patterning than in *Drosophila* embryos. Mechanisms of Development 83(1):107 – 114.
- Micklem, D. R.; Dasgupta, R.; Elliott, H.; Gergely, F.; Davidson, C.; Brand, A.; González-Reyes, A.; and St Johnston, D. 1997: The mago nashi gene is required for the polarisation of the oocyte and the formation of perpendicular axes in *Drosophila*. Current Biology 7(7):468–478.
- Miller, D. J.; Hemmrich, G.; Ball, E. E.; Hayward, D. C.; Khalturin, K.; Funayama, N.; Agata, K.; and Bosch, T. C. G. 2007: The innate immune repertoire in cnidaria—ancestral complexity and stochastic gene loss. Genome Biol 8(4):R59.
- Moussian, B. and Roth, S. 2005: Dorsoventral Axis Formation in the *Drosophila* Embryo—Shaping and Transducing a Morphogen Gradient. Current Biology 15(21):R887 – R899.
- Moustakas, A. and Heldin, C.-H. 2003: Ecsit-ement on the crossroads of Toll and BMP signal transduction. Genes Dev 17(23):2855–2859.
- Mullis, K.; Erlich, H.; Arnheim, N.; Horn, G.; Saiki, R.; and Scharf, S. 1987: One of the first Polymerase Chain Reaction (PCR) patents. US patent 4,683,195.
- Naito, Y.; Yamada, T.; Matsumiya, T.; Ui-Tei, K.; Saigo, K.; and Morishita, S. 2005: dsCheck: highly sensitive off-target search software for double-stranded RNA-mediated RNA interference. Nucleic Acids Res 33(Web Server issue):W589–W591.
- Nambu, J. R.; Lewis, J. O.; Wharton, K., Jr; and Crews, S. T. 1991: The *Drosophila* single-minded gene encodes a helix-loop-helix protein that acts as a master regulator of CNS midline development. Cell 67(6):1157–1167.
- Neuman-Silberberg, F. S. and Schüpbach, T. 1993: The *Drosophila* dorsoventral patterning gene *gurken* produces a dorsally localized RNA and encodes a TGF alpha-like protein. Cell 75(1):165–174.

- Nunes da Fonseca, R.; von Levetzow, C.; Kalscheuer, P.; Basal, A.; van der Zee, M.; and Roth, S. 2008: Self-regulatory circuits in dorsoventral axis formation of the short-germ beetle *Tribolium castaneum*. *Dev Cell* 14(4):605–615.
- Nüsslein-Volhard, C. 1991: Determination of the embryonic axes of *Drosophila*. *Dev Suppl* 1:1–10.
- O’Neill, L. A.; Fitzgerald, K. A.; and Bowie, A. G. 2003: The Toll-IL-1 receptor adaptor family grows to five members. *Trends in Immunology* 24(6):286 – 289.
- O’Neill, L. A. J. and Bowie, A. G. 2007: The family of five: TIR-domain-containing adaptors in Toll-like receptor signalling. *Nat Rev Immunol* 7(5):353–364.
- Ozüak, O.; Buchta, T.; Roth, S.; and Lynch, J. A. 2014: Dorsoventral Polarity of the *Nasonia* Embryo Primarily Relies on a BMP Gradient Formed without Input from Toll. *Curr Biol* .
- Panfilio, K. A.; Liu, P. Z.; Akam, M.; and Kaufman, T. C. 2006: *Oncopeltus fasciatus zen* is essential for serosal tissue function in *katatrepsis*. *Developmental Biology* 292(1):226 – 243.
- Papatsenko, D. 2007: ClusterDraw web server: a tool to identify and visualize clusters of binding motifs for transcription factors. *Bioinformatics* 23(8):1032–1034.
- Papatsenko, D. and Levine, M. 2005: Quantitative analysis of binding motifs mediating diverse spatial readouts of the Dorsal gradient in the *Drosophila* embryo. *Proc Natl Acad Sci U S A* 102(14):4966–4971.
- Paré, A. C.; Vichas, A.; Fincher, C. T.; Mirman, Z.; Farrell, D. L.; Mainieri, A.; and Zallen, J. A. 2014: A positional Toll receptor code directs convergent extension in *Drosophila*. *Nature* .
- Parker, J. S.; Mizuguchi, K.; and Gay, N. J. 2001: A family of proteins related to Spätzle, the toll receptor ligand, are encoded in the *Drosophila* genome. *Proteins: Structure, Function, and Bioinformatics* 45(1):71–80.

- Patel, N. H.; Martin-Blanco, E.; Coleman, K. G.; Poole, S. J.; Ellis, M. C.; Kornberg, T. B.; and Goodman, C. S. 1989: Expression of engrailed proteins in arthropods, annelids, and chordates. *Cell* 58(5):955–68.
- Petersen, C. P. and Reddien, P. W. 2009: Wnt Signaling and the Polarity of the Primary Body Axis. *Cell* 139(6):1056 – 1068.
- Prothmann, C.; Armstrong, N. J.; and Rupp, R. A. 2000: The Toll/IL-1 receptor binding protein MyD88 is required for *Xenopus* axis formation. *Mech Dev* 97(1-2):85–92.
- Pujol, N.; Link, E. M.; Liu, L. X.; Kurz, C. L.; Alloing, G.; Tan, M. W.; Ray, K. P.; Solari, R.; Johnson, C. D.; and Ewbank, J. J. 2001: A reverse genetic analysis of components of the Toll signaling pathway in *Caenorhabditis elegans*. *Curr Biol* 11(11):809–821.
- Queenan, A. M.; Barcelo, G.; Buskirk, C. V.; and Schüpbach, T. 1999: The transmembrane region of Gurken is not required for biological activity, but is necessary for transport to the oocyte membrane in *Drosophila*. *Mechanisms of Development* 89(1-2):35 – 42.
- Queenan, A. M.; Ghabrial, A.; and Schüpbach, T. 1997: Ectopic activation of torpedo/Egfr, a *Drosophila* receptor tyrosine kinase, dorsalizes both the eggshell and the embryo. *Development* 124(19):3871–3880.
- Rao, A.; Luo, C.; and Hogan, P. G. 1997: Transcription factors of the NFAT family: regulation and function. *Annu Rev Immunol* 15:707–747.
- Rao, Y.; Vaessin, H.; Jan, L. Y.; and Jan, Y. N. 1991: Neuroectoderm in *Drosophila* embryos is dependent on the mesoderm for positioning but not for formation. *Genes Dev* 5(9):1577–1588.
- Ray, R. P.; Arora, K.; Nüsslein-Volhard, C.; and Gelbart, W. M. 1991: The control of cell fate along the dorsal-ventral axis of the *Drosophila* embryo. *Development* 113(1):35–54.
- Reeves, G. T. and Stathopoulos, A. 2009: Graded dorsal and differential gene regulation in the *Drosophila* embryo. *Cold Spring Harb Perspect Biol* 1(4):a000836.
- Rosetto, M.; Engstrom, Y.; Baldari, C.; Telford, J.; and Hultmark, D. 1995: Signals from the IL-1 Receptor Homolog, Toll, Can Activate an Immune Response in a *Drosophila*

- Hemocyte Cell Line. *Biochemical and Biophysical Research Communications* 209(1):111 – 116.
- Roth, S. 1993: Mechanisms of dorsal-ventral axis determination in *Drosophila* embryos revealed by cytoplasmic transplantations. *Development* 117(4):1385–1396.
- Roth, S.; Hiromi, Y.; Godt, D.; and Nüsslein-Volhard, C. 1991: *cactus*, a maternal gene required for proper formation of the dorsoventral morphogen gradient in *Drosophila* embryos. *Development* 112(2):371–388.
- Roth, S. and Lynch, J. A. 2009: Symmetry breaking during *Drosophila* oogenesis. *Cold Spring Harb Perspect Biol* 1(2):a001891.
- Roth, S. and Schüpbach, T. 1994: The relationship between ovarian and embryonic dorsoventral patterning in *Drosophila*. *Development* 120(8):2245–2257.
- Roth, S.; Stein, D.; and Nüsslein-Volhard, C. 1989: A gradient of nuclear localization of the dorsal protein determines dorsoventral pattern in the *Drosophila* embryo. *Cell* 59(6):1189–1202.
- Rusch, J. and Levine, M. 1994: Regulation of the dorsal morphogen by the Toll and torso signaling pathways: a receptor tyrosine kinase selectively masks transcriptional repression. *Genes Dev* 8(11):1247–1257.
- Sachs, L. M. 2014: BMP signaling in the dorsal-ventral patterning system of the milkweed bug *Oncopeltus fasciatus*. Ph.D. thesis, University of Cologne.
- Sackton, T. B.; Werren, J. H.; and Clark, A. G. 2013: Characterizing the infection-induced transcriptome of *Nasonia vitripennis* reveals a preponderance of taxonomically-restricted immune genes. *PLoS One* 8(12):e83984.
- Sasai, Y.; Lu, B.; Steinbeisser, H.; and De Robertis, E. M. 1995: Regulation of neural induction by the *Chd* and *Bmp-4* antagonistic patterning signals in *Xenopus*. *Nature* 376(6538):333–336.
- Sasai, Y.; Lu, B.; Steinbeisser, H.; Geissert, D.; Gont, L. K.; and De Robertis, E. M. 1994: *Xenopus chordin*: a novel dorsalizing factor activated by organizer-specific homeobox genes. *Cell* 79(5):779–790.

- Sen, J.; Goltz, J. S.; Stevens, L.; and Stein, D. 1998: Spatially restricted expression of pipe in the *Drosophila* egg chamber defines embryonic dorsal-ventral polarity. *Cell* 95(4):471–481.
- Shen, B. and Manley, J. L. 2002: Pelle kinase is activated by autophosphorylation during Toll signaling in *Drosophila*. *Development* 129(8):1925–1933.
- Shinmyo, Y.; Mito, T.; Matsushita, T.; Sarashina, I.; Miyawaki, K.; Ohuchi, H.; and Noji, S. 2004: piggyBac-mediated somatic transformation of the two-spotted cricket, *Gryllus bimaculatus*. *Dev Growth Differ* 46(4):343–349.
- Silverman, N. and Maniatis, T. 2001: NF-kappaB signaling pathways in mammalian and insect innate immunity. *Genes Dev* 15(18):2321–2342.
- Skeath, J. B. 1999: At the nexus between pattern formation and cell-type specification: the generation of individual neuroblast fates in the *Drosophila* embryonic central nervous system. *Bioessays* 21(11):922–931.
- Sommer, R. J. and Tautz, D. 1993: Involvement of an orthologue of the *Drosophila* pair-rule gene hairy in segment formation of the short germ-band embryo of *Tribolium* (Coleoptera). *Nature* 361(6411):448–450.
- Sommer, R. J. and Tautz, D. 1994: Expression patterns of twist and snail in *Tribolium* (Coleoptera) suggest a homologous formation of mesoderm in long and short germ band insects. *Dev Genet* 15(1):32–37.
- St Johnston, D. and Nüsslein-Volhard, C. 1992: The origin of pattern and polarity in the *Drosophila* embryo. *Cell* 68(2):201–219.
- Stathopoulos, A. and Levine, M. 2002: Dorsal gradient networks in the *Drosophila* embryo. *Dev Biol* 246(1):57–67.
- Stathopoulos, A. and Levine, M. 2004: Whole-genome analysis of *Drosophila* gastrulation. *Curr Opin Genet Dev* 14(5):477–484.
- Stein, D.; Roth, S.; Vogelsang, E.; and Nüsslein-Volhard, C. 1991: The polarity of the dorsoventral axis in the *Drosophila* embryo is defined by an extracellular signal. *Cell* 65(5):725–735.

- Stein, D. S. and Stevens, L. M. 2014: Maternal control of the *Drosophila* dorsal-ventral body axis. *Wiley Interdiscip Rev Dev Biol* 3(5):301–330.
- Sulston, J.; Schierenberg, E.; White, J.; and Thomson, J. 1983: The embryonic cell lineage of the nematode *Caenorhabditis elegans*. *Developmental Biology* 100(1):64 – 119.
- Takeda, K. and Akira, S. 2005: Toll-like receptors in innate immunity. *International Immunology* 17(1):1–14.
- Tamura, K.; Peterson, D.; Peterson, N.; Stecher, G.; Nei, M.; and Kumar, S. 2011: MEGA5: molecular evolutionary genetics analysis using maximum likelihood, evolutionary distance, and maximum parsimony methods. *Molecular biology and evolution* 28(10):2731–2739.
- Tamura, K.; Stecher, G.; Peterson, D.; Filipski, A.; and Kumar, S. 2013: MEGA6: Molecular Evolutionary Genetics Analysis version 6.0. *Mol Biol Evol* 30(12):2725–2729.
- Tanji, T.; Hu, X.; Weber, A. N. R.; and Ip, Y. T. 2007: Toll and IMD pathways synergistically activate an innate immune response in *Drosophila melanogaster*. *Mol Cell Biol* 27(12):4578–4588.
- Tanji, T.; Yun, E.-Y.; and Ip, Y. T. 2010: Heterodimers of NF-kappaB transcription factors DIF and Relish regulate antimicrobial peptide genes in *Drosophila*. *Proc Natl Acad Sci U S A* 107(33):14715–14720.
- Theurkauf, W. E.; Smiley, S.; Wong, M. L.; and Alberts, B. M. 1992: Reorganization of the cytoskeleton during *Drosophila* oogenesis: implications for axis specification and intercellular transport. *Development* 115(4):923–936.
- Thisse, B.; Stoetzel, C.; Gorostiza-Thisse, C.; and Perrin-Schmitt, F. 1988: Sequence of the twist gene and nuclear localization of its protein in endomesodermal cells of early *Drosophila* embryos. *EMBO J* 7(7):2175–2183.
- Tomer, R.; Khairy, K.; Amat, F.; and Keller, P. J. 2012: Quantitative high-speed imaging of entire developing embryos with simultaneous multiview light-sheet microscopy. *Nat Methods* 9(7):755–763.

- Toutges, M. J.; Hartzer, K.; Lord, J.; and Oppert, B. 2010: Evaluation of reference genes for quantitative polymerase chain reaction across life cycle stages and tissue types of *Tribolium castaneum*. *J Agric Food Chem* 58(16):8948–8951.
- Towb, P.; Sun, H.; and Wasserman, S. A. 2009: Tube Is an IRAK-4 homolog in a Toll pathway adapted for development and immunity. *J Innate Immun* 1(4):309–321.
- Turcotte, C. L. and Hashimoto, C. 2002: Evidence for a glycosaminoglycan on the nudel protein important for dorsoventral patterning of the drosophila embryo. *Developmental Dynamics* 224(1):51–57.
- Udan, R. S.; Piazza, V. G.; Hsu, C.-W.; Hadjantonakis, A.-K.; and Dickinson, M. E. 2014: Quantitative imaging of cell dynamics in mouse embryos using light-sheet microscopy. *Development* 141(22):4406–4414.
- Ursic-Bedoya, R.; Buchhop, J.; and Lowenberger, C. 2009: Cloning and characterization of Dorsal homologues in the hemipteran *Rhodnius prolixus*. *Insect Mol Biol* 18(5):681–689.
- Valanne, S.; Wang, J.-H.; and Rämet, M. 2011: The *Drosophila* Toll signaling pathway. *J Immunol* 186(2):649–656.
- van der Zee, M.; Berns, N.; and Roth, S. 2005: Distinct functions of the *Tribolium* *zerknüllt* genes in serosa specification and dorsal closure. *Curr Biol* 15(7):624–636.
- van der Zee, M.; Stockhammer, O.; von Levetzow, C.; Nunes da Fonseca, R.; and Roth, S. 2006: Sog/Chordin is required for ventral-to-dorsal Dpp/BMP transport and head formation in a short germ insect. *Proc Natl Acad Sci U S A* 103(44):16307–16312.
- Viatour, P.; Merville, M.-P.; Bours, V.; and Chariot, A. 2005: Phosphorylation of NF- κ B and I κ B proteins: implications in cancer and inflammation. *Trends in Biochemical Sciences* 30(1):43 – 52.
- Von Ohlen, T. L. and Moses, C. 2009: Identification of Ind transcription activation and repression domains required for dorsoventral patterning of the CNS. *Mech Dev* 126(7):552–562.

- Weber, A. N. R.; Tauszig-Delamasure, S.; Hoffmann, J. A.; Lelièvre, E.; Gascan, H.; Ray, K. P.; Morse, M. A.; Imler, J.-L.; and Gay, N. J. 2003: Binding of the *Drosophila* cytokine Spätzle to Toll is direct and establishes signaling. *Nat Immunol* 4(8):794–800.
- Weisbrod, A.; Cohen, M.; and Chipman, A. D. 2013: Evolution of the insect terminal patterning system- insights from the milkweed bug, *Oncopeltus fasciatus*. *Developmental Biology* 380(1):125 – 131.
- Whalen, A. M. and Steward, R. 1993: Dissociation of the dorsal-cactus complex and phosphorylation of the dorsal protein correlate with the nuclear localization of dorsal. *J Cell Biol* 123(3):523–534.
- Wharton, K. A.; Ray, R. P.; and Gelbart, W. M. 1993: An activity gradient of decapentaplegic is necessary for the specification of dorsal pattern elements in the *Drosophila* embryo. *Development* 117(2):807–822.
- Wheeler, S. R.; Carrico, M. L.; Wilson, B. A.; and Skeath, J. B. 2005: The *Tribolium* columnar genes reveal conservation and plasticity in neural precursor patterning along the embryonic dorsal-ventral axis. *Dev Biol* 279(2):491–500.
- Wiens, M.; Korzhev, M.; Perović-Ottstadt, S.; Luthringer, B.; Brandt, D.; Klein, S.; and Müller, W. E. G. 2007: Toll-like receptors are part of the innate immune defense system of sponges (demospongiae: Porifera). *Mol Biol Evol* 24(3):792–804.
- Wilson, M. J.; Kenny, N. J.; and Dearden, P. K. 2014: Components of the dorsal-ventral pathway also contribute to anterior-posterior patterning in honeybee embryos (*Apis mellifera*). *Evodevo* 5(1):11.
- Xiao, C.; Shim, J.-h.; Klüppel, M.; Zhang, S. S.-M.; Dong, C.; Flavell, R. A.; Fu, X.-Y.; Wrana, J. L.; Hogan, B. L. M.; and Ghosh, S. 2003: Ecsit is required for Bmp signaling and mesoderm formation during mouse embryogenesis. *Genes Dev* 17(23):2933–2949.
- Xiao, Q.; Komori, H.; and Lee, C.-Y. 2012: *klumpfuss* distinguishes stem cells from progenitor cells during asymmetric neuroblast division. *Development* 139(15):2670–2680.

- Xiao, T.; Towb, P.; Wasserman, S. A.; and Sprang, S. R. 1999: Three-dimensional structure of a complex between the death domains of Pelle and Tube. *Cell* 99(5):545–555.
- Xu, Y.; Tao, X.; Shen, B.; Horng, T.; Medzhitov, R.; Manley, J. L.; and Tong, L. 2000: Structural basis for signal transduction by the Toll/interleukin-1 receptor domains. *Nature* 408(6808):111–115.
- Yagi, Y.; Nishida, Y.; and Ip, Y. T. 2010: Functional analysis of Toll-related genes in *Drosophila*. *Dev Growth Differ* 52(9):771–783.
- Yokoi, K.; Koyama, H.; Ito, W.; Minakuchi, C.; Tanaka, T.; and Miura, K. 2012: Involvement of NF- κ B transcription factors in antimicrobial peptide gene induction in the red flour beetle, *Tribolium castaneum*. *Dev Comp Immunol* 38(2):342–351.
- Yu, J.; Satou, Y.; Holland, N.; Tadasu, S.; Kohara, Y.; Satoh, N.; Marianne, B.; and Holland, L. 2007: Axial patterning in cephalochordates and the evolution of the organizer. *Nature* 445(7128):613–617.
- Yu, J. K. S. and Holland, L. Z. 2009: Amphioxus whole-mount in situ hybridization. *Cold Spring Harb Protoc* 2009(9):pdb.prot5286.
- Zeitlinger, J.; Zinzen, R. P.; Stark, A.; Kellis, M.; Zhang, H.; Young, R. A.; and Levine, M. 2007: Whole-genome ChIP-chip analysis of Dorsal, Twist, and Snail suggests integration of diverse patterning processes in the *Drosophila* embryo. *Genes Dev* 21(4):385–390.
- Zhang, Z.; Stevens, L. M.; and Stein, D. 2009: Sulfation of Eggshell Components by Pipe Defines Dorsal-Ventral Polarity in the *Drosophila* Embryo. *Current Biology* 19(14):1200 – 1205.
- Zhao, T.; Graham, O. S.; Raposo, A.; and St Johnston, D. 2012: Growing Microtubules Push the Oocyte Nucleus to Polarize the *Drosophila* Dorsal-Ventral Axis. *Science* 336(6084):999–1003.
- Zhu, B.; Pennack, J. A.; McQuilton, P.; Forero, M. G.; Mizuguchi, K.; Sutcliffe, B.; Gu, C.-J.; Fenton, J. C.; and Hidalgo, A. 2008: *Drosophila* neurotrophins reveal a common mechanism for nervous system formation. *PLoS Biol* 6(11):e284.

Zou, Z.; Evans, J.; Lu, Z.; Zhao, P.; Williams, M.; Sumathipala, N.; Hetru, C.; Hultmark, D.; and Jiang, H. 2007: Comparative genomic analysis of the *Tribolium* immune system. *Genome Biology* 8(8):R177.

Zou, Z.; Lopez, D. L.; Kanost, M. R.; Evans, J. D.; and Jiang, H. 2006: Comparative analysis of serine protease-related genes in the honey bee genome: possible involvement in embryonic development and innate immunity. *Insect Mol Biol* 15(5):603–614.

Chapter 5

Supplementary data

5.1 Embryonic development in *Oncopeltus*

The embryology of the milkweed bug *Oncopeltus fasciatus* was well-described by Butt (1949). From the morphology of *Oncopeltus* embryos, it is easy to distinguish the anterior from the posterior side. The anterior pole of the egg is surrounded by a circle of micropyles (Dorn, 1976; Chapman et al., 2013). After dechorion, the blastoderm embryo shows a protruding end at the anterior side. During the gastrulation stages, the embryo invaginates from the posterior side. Interestingly, there is a difference on nuclear density along the dorsoventral (DV) axis during mid-late blastoderm stages, which happens exclusively after the blastodermal cellularization and before the nuclear aggregation on the lateral disc (before the invagination of the germband embryo). The cellularization and the developmental stages of *Oncopeltus* embryos can be visualized by the cytoplasmic and nuclear staining using fluorescent dyes (Figure 5.1).

5.1.1 The difference of nuclear density along the dorsoventral (DV) axis

After the nuclear staining, blastoderm embryos were analyzed under the SteREO Lumar V12 microscope (Zeiss). The images were processed by the Photoshop software (Adobe) and the nuclear density were calculated by the ImageJ software. Based on the analysis of nuclear density along the DV axis, the nuclei are distributed with a lower density on the

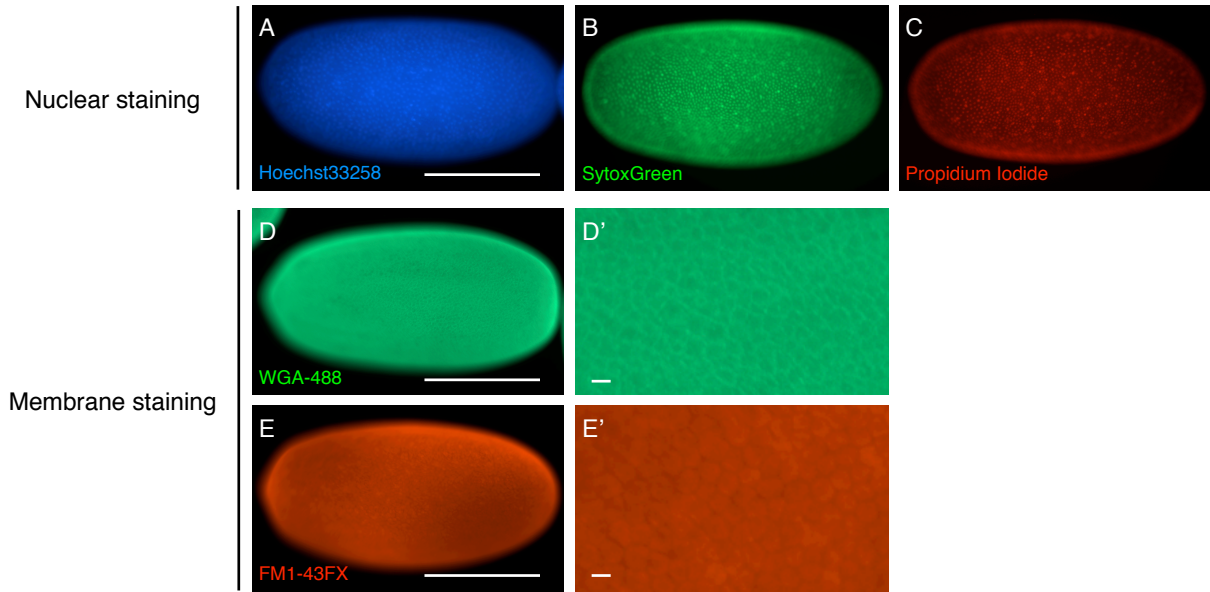


Figure 5.1. Fluorescent staining of nuclei and membranes in *Oncopeltus* blastoderm embryos

The nuclei and cell membranes of *Oncopeltus* embryos can be stained by fluorescent dyes. The nuclei are stained by Hoechst33258 (A), SytoxGreen (B), and Propidium Iodide (C), respectively. The SytoxGreen staining (B) is the best choice with strongest signals. The cell membranes are stained by Wheat Germ Agglutinin (WGA) conjugated with Alexa Fluor®488 (D, D') and FM1-43FX (E, E'), respectively. The WGA staining marks the cell boundaries and the FM1-43FX staining marks the surface of cells. Embryos shown here are at the blastoderm stages. Scale bar size corresponds to 500 μm .

ventral side where *sog*, *twist* and *sim* are expressed (Figure 5.2). In contrast, the nuclei are distributed with a higher density on the dorsal side where early expression of *msh* and *SoxN* are localized (Figure 5.2). These differences on nuclear density offer a tool to distinguish the DV orientation during mid-late blastoderm stages. Similar findings were shown by the nuclear phospho-Mad (pMad) staining on the dorsal side where the nuclei are distributed with a higher density (Sachs, 2014).

5.2 Detailed expression pattern of DV marker genes

The detailed expression patterns of marker genes during *Oncopeltus* embryogenesis are shown here.

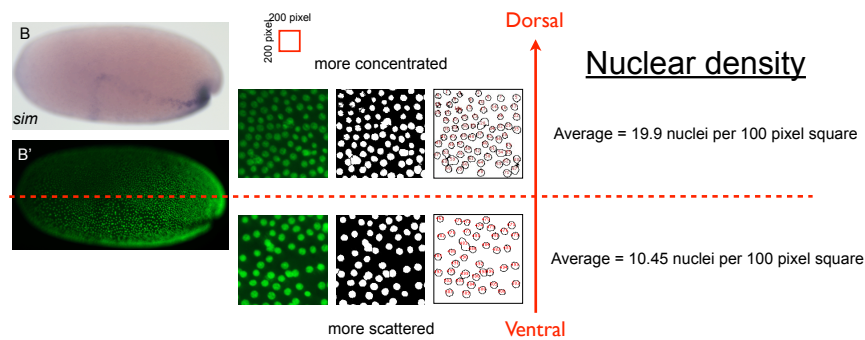
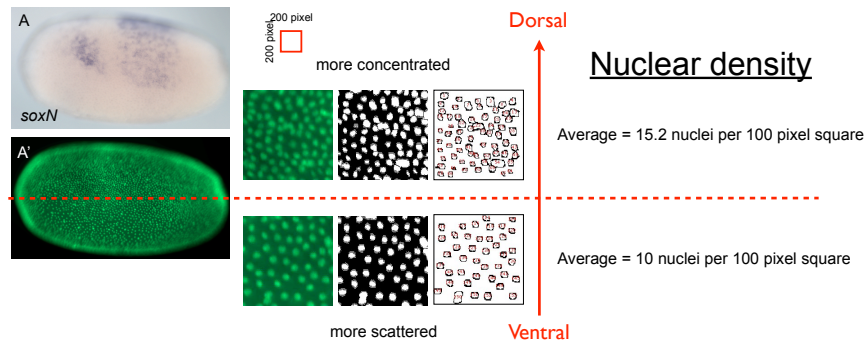


Figure 5.2. The difference of nuclear density between dorsal and the ventral sides

During mid-late blastoderm stages, there is a difference on nuclear density along the dorsoventral (DV) axis. The nuclei are distributed more concentrated on the dorsal side where early expression of *msh* and *SoxN* are localized. The early *SoxN* expression with higher nuclear density is shown in A. In contrast, the nuclei are distributed more scattered on the ventral side where *sog*, *twist* and *sim* are expressed. The *sim* expression with lower nuclear density is shown in B. The average of nuclear density was calculated from five different sampling region in the blastoderm embryo. Similar results were identified in the other embryos. The embryos in A and B were shown as the representatives.

5.2.1 Expression of columnar genes

The *Drosophila* columnar genes including *muscle segment homeobox (msh)*, *intermediate nerve cord defective (ind)* and *ventral nerve cord defective (vnd)* genes, which are key regulators for neural precursor formation (Skeath, 1999). The sequences of these genes in *Oncopeltus* were obtained from the degenerate PCR and extended by RACE-PCR. They were not included in the *Oncopeltus* transcriptome (Ewen-Campen et al., 2011). The *vnd* and *ind* were not selected as marker genes because there is no specific pattern along the DV axis during early blastoderm stages.

Expression pattern of *msh*

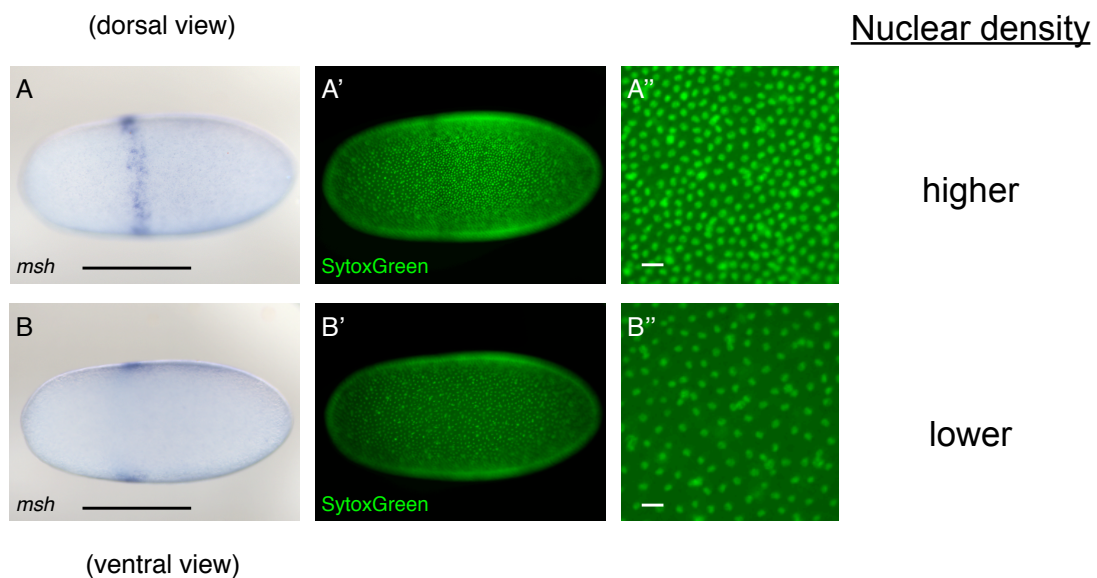


Figure 5.3. The early expression of the *msh* stripe is on the dorsal side with a higher nuclear density

The expression of *msh* is not in the longitudinal column as described in *Drosophila*, but in a fine stripe along the DV axis. The early expression of the *msh* stripe is exclusive on the side with a higher nuclear density, which is the dorsal side. The embryo in A and B are identical with the dorsal view shown in A and the ventral view shown in B. The nuclei is stained by SytoxGreen, shown in A' and B' and the magnification is shown in A'' and B''. Scale bar size in A and B corresponds to 500 μm . Scale bar size in A'' and B'' corresponds to 50 μm . Lateral view of embryos is shown in A-D; ventral view of the embryo is shown in E.

Expression pattern of *msh* were shown in Figure 3.1. During blastoderm stages, The expression of *msh* is not in the longitudinal column as described in *Drosophila* (Skeath, 1999). The early expression of the *msh* stripe is exclusive on the side with a higher nuclear

density, which is the dorsal side (Figure 5.3). As the development proceeds, the stripe extends toward the ventral side (Figure 3.1 C).

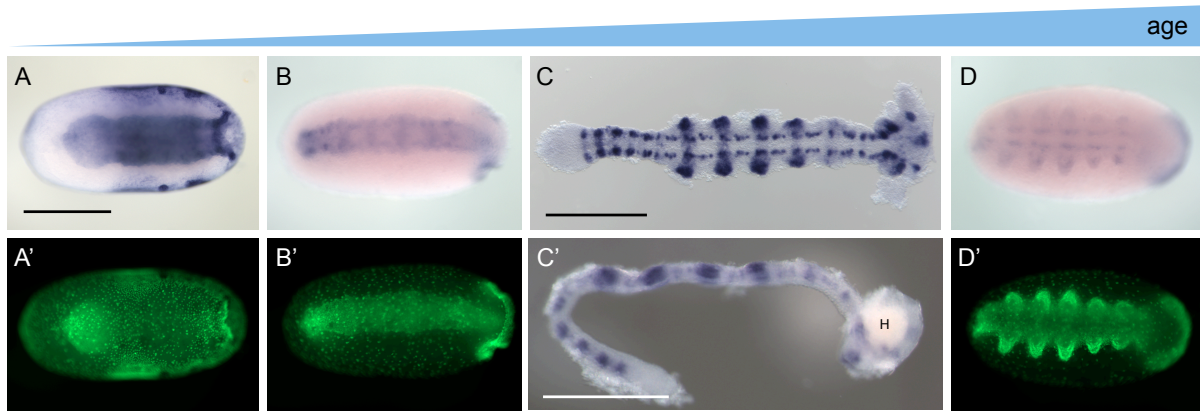


Figure 5.4. Expression pattern of *msh* in *Oncopeltus* germband embryos

After the onset of gastrulation, *msh* is expressed in the lateral column (A). Scale bar size in A corresponds to 500 μm (as same for B and D). *msh* expression is maintained throughout germband elongation in a cluster of dorsal ectoderm cells (B, C) and in the cluster of neural precursor cells as the lateral column (C, D). Embryos in A', B' and D' are identical to A, B and D with nuclear staining by SytoxGreen. Abbreviation: H=head. The embryo in C and C' are identical with the dorsal view shown in C and the lateral view shown in C'. The expression of *msh* is in clusters of ectoderm cells close to the dorsal side (C'). Scale bar size in C and C' corresponds to 500 μm .

After the onset of gastrulation, *msh* is expressed in the lateral column (Figure 5.4 A). The *msh* expression is maintained during germband elongation in a cluster of dorsal ectoderm cells (Figure 5.4 B, C) and in the cluster of neural precursor cells as the lateral column (Figure 5.4 C, D).

Expression pattern of *ind*

The expression of *msh* and *ind* in *Oncopeltus* embryos are similar to the patterns in *Tribolium* (Wheeler et al., 2005) that they are not expressed in the lateral column until the onset of gastrulation (Figure 3.1 and 5.5). During germband stages, *ind* is expressed in the intermedial column of neural precursors (Figure 5.5 E, F).

The conserved domains of *ind* The transcriptional activation and repression domains have been identified in *Drosophila*. These domains are important for the function of *ind* to pattern the CNS along the DV axis (Von Ohlen and Moses, 2009). Protein sequences of *ind* in *Anopheles*, *Drosophila*, *Tribolium* and *Oncopeltus* were aligned here

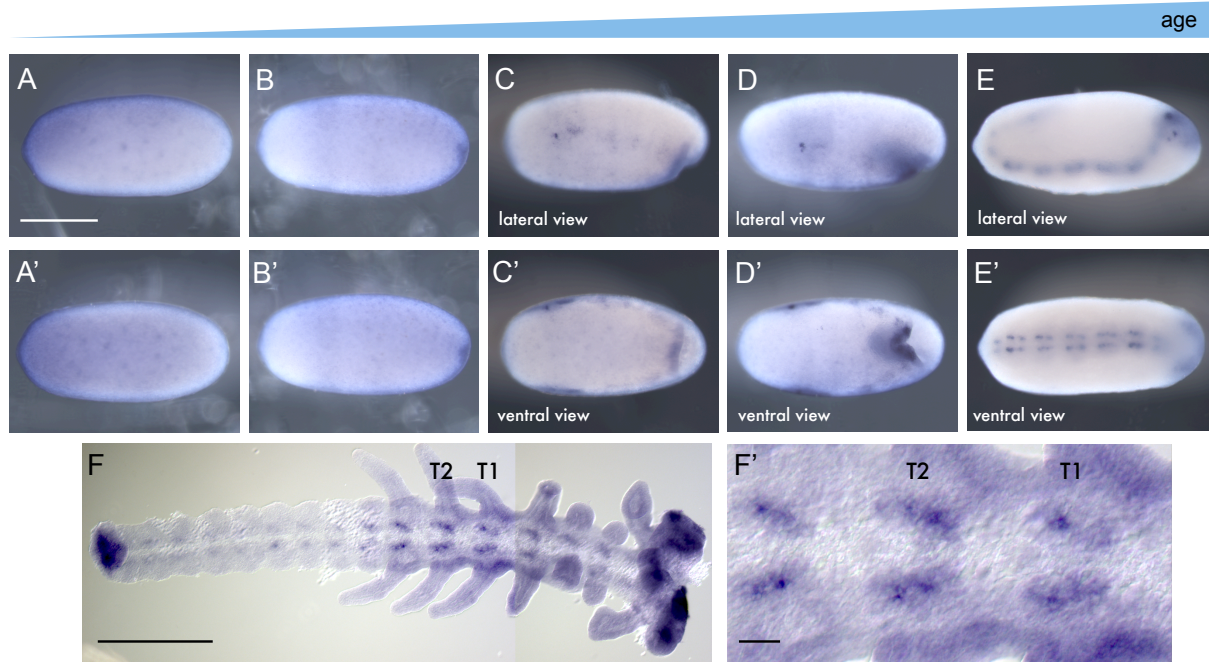


Figure 5.5. Expression pattern of *ind* in *Oncopeltus* embryos

The expression of *ind* is non-specific during blastoderm stages (A-B). After the onset of gastrulation, *ind* is expressed in the longitudinal column on the lateral side of (C-D). Embryos in A-E are identical to A'-E' with different views indicated. During germband stages, *ind* is expressed in the intermedial column of neural precursors (E, F). F' is the magnification of F in the thorax region (T1 and T2 are indicated). Scale bar size in A and F corresponds to 500 μm , while the scale bar size in F' corresponds to 50 μm .

(Figure 5.6). However, the authentic function of *Oncopeltus ind* needs to be studied by pRNAi.

Expression pattern of *vnd*

The expression of *vnd* in *Oncopeltus* blastoderm embryos is not in the longitudinal column as described in *Drosophila* (Skeath, 1999), but rather on the ventral side and specifically in an anteroventral domain. The anteroventral domain of *vnd* expression is adjacent to the *msh* stripe (Figure 5.7 A, B, C). After the onset of gastrulation, *vnd* is expressed in the invagination site and later in the longitudinal column on the lateral side (Figure 5.7 C, D). In the extended germband embryos, *vnd* is expressed in the medial column of the neuroectoderm, flanking the ventral midline (Figure 5.7 E, F).

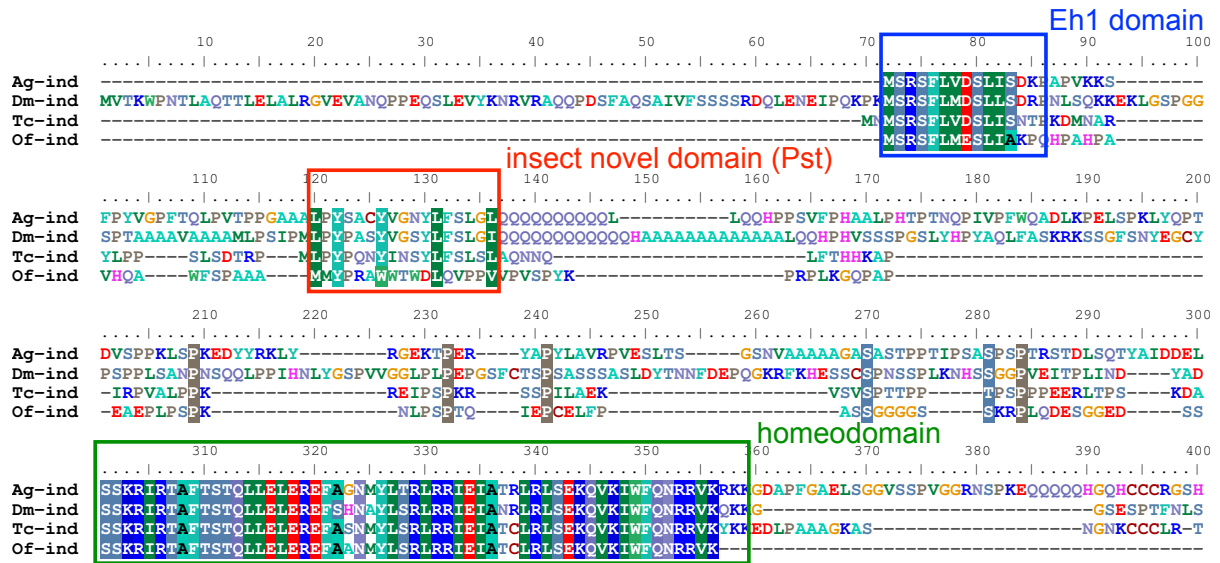


Figure 5.6. Alignment of *ind* protein sequences

Alignment of *ind* protein sequences in four insect species. There are three evolutionarily conserved domains (Von Ohlen and Moses, 2009). The engrailed homology domain 1 (Eh1) is indicated in blue square, which is predicted to interact with Groucho (Gro). The Pst domain is marked in red square, which is identified to be conserved between insects. The homeodomain is highlighted in green square. The sites with high identity were marked in shaded color. Abbreviation of insect species: the mosquitoes *Anopheles gambiae* (Ag), the fly *Drosophila melanogaster* (Dm), the red flour beetle *Tribolium castaneum* (Tc), and the milkweed bug *Oncopeltus fasciatus* (Of).

5.2.2 The ISH difficulties in the milkweed bug

The two-color double ISH in *Oncopeltus* embryos were first introduced in Liu and Kaufman (2004). In this thesis, the double ISH of *vnd* and *msh* expression are shown in Figure 5.7 and the double ISH of *sog* and *cact-3* expression are shown in Figure 3.36. However, the staining is more clear in germband embryos than in blastoderm embryos. If there is any co-localized expression, the signal could not be distinguished by the red and purple color. To visualize the overlapped expression pattern, it is necessary to perform the double ISH by fluorescent signals.

The fluorescent ISH (FISH) is feasible to detect *Toll-1* and *sog* expression respectively, using the DiG-labeled probe together with the help of amplification kits (Figure 3.8 and 5.8). However, it is not possible to achieve the two-color fluorescent ISH in *Oncopeltus* because of the higher fluorescent background, which might be produced by the corresponding antibodies (anti-Fluorescein-POD, anti-Biotin-POD).

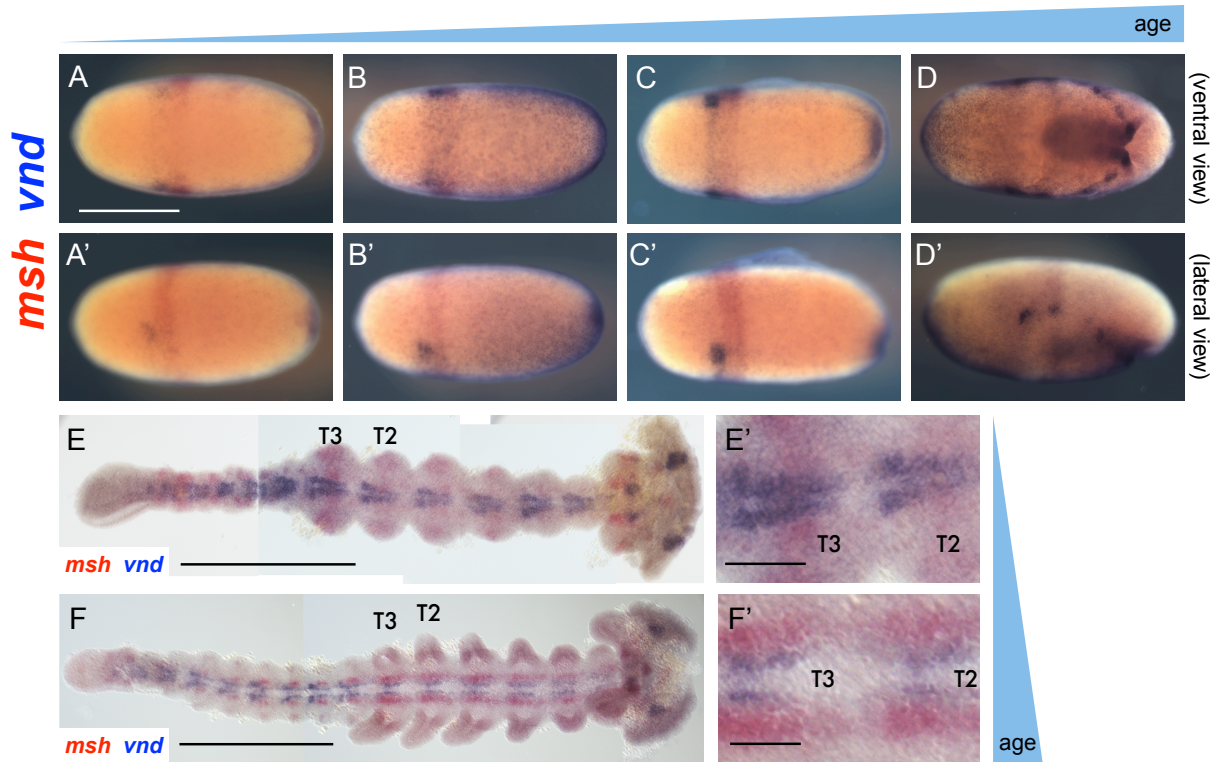


Figure 5.7. Double ISH of *vnd* and *msh* expression in *Oncopeltus* embryos

The expression of *vnd* and *msh* was shown by a double ISH. The red staining labeled the *msh* transcripts and the purple staining labeled the *vnd* transcripts. The expression of *vnd* is in an anteroventral domain adjacent to the *msh* stripe (A, B, C). Embryos in A-D are identical to A'-D' with the ventral view shown in A-D and the lateral view shown in A'-D'. After the onset of gastrulation, *vnd* is expressed in the invagination site and later in the longitudinal column on the lateral side (C, D). In the extended germband embryos, *vnd* is expressed in the medial column of the neuroectoderm, flanking the ventral midline (E, F). E' and F' is the magnification of E and F in the thorax region (T2-T3 are indicated). Scale bar size in A, E and F corresponds to 500 μm , while the scale bar size in E' and F' corresponds to 100 μm .

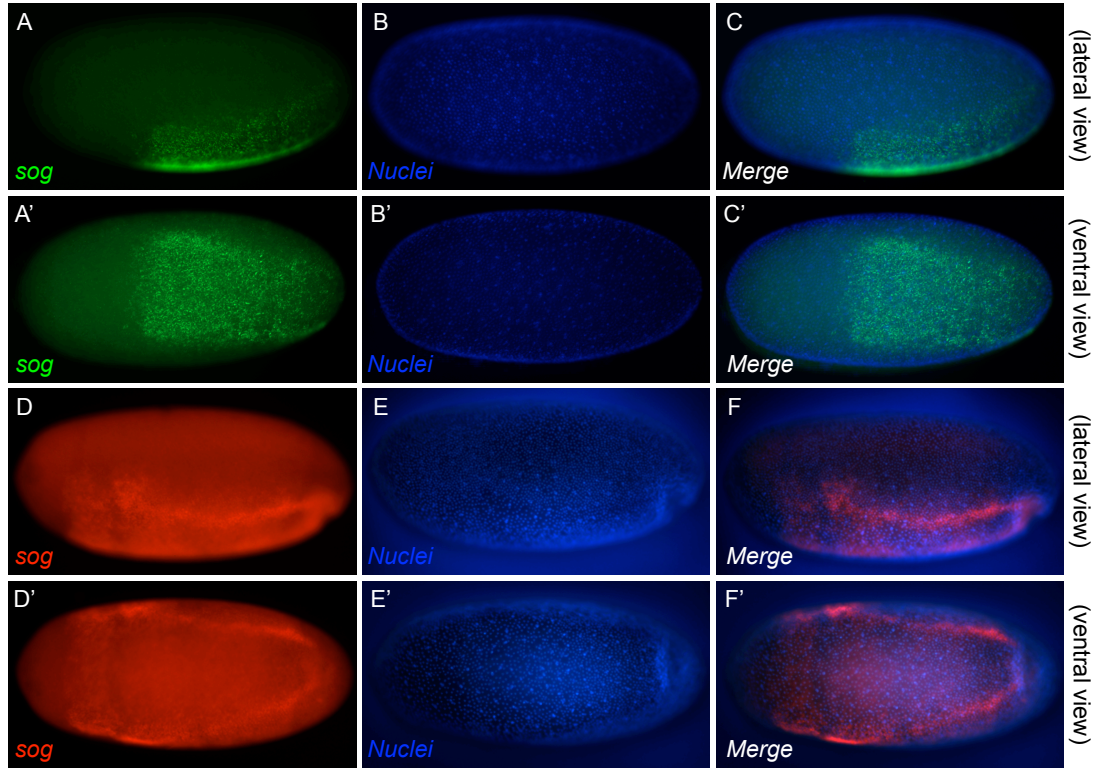


Figure 5.8. The fluorescent signals of *sog* expression in *Oncopeltus* embryos

The fluorescent ISH (FISH) is feasible to detect *sog* transcripts in *Oncopeltus* embryos using the DiG-labeled probe together with the amplification kits. Embryos in A-C are identical to A'-C' while the lateral view is shown in A-C and the ventral view is shown in A'-C'. The staining in A and B consist of ten Z-stacked images and C is the merged image from A and B. The expression of *sog* is stained by TSA-488 and the nuclei is stained by Propidium Iodide. Embryos in D-F are identical to D'-F' while the lateral view is shown in D-F and the ventral view is shown in D'-F'. The expression of *sog* is stained by HNPP and the nuclei is stained by Hoechst33258. F is the merged image from D and E.

5.2.3 Late expression pattern of ventral markers

Expression pattern of *sog*

In this thesis, *sog* is used as the ventral marker of blastoderm embryos. During the blastoderm stages, *sog* is expressed on the ventral side of the embryo (Figure 5.8 C). In later stages before gastrulation, *sog* is expressed more strongly in lateral stripes of the ventral domain (Figure 5.8 F). In the extended germband embryos, *sog* is expressed in the ventral column and split into two stripes in the most posterior segment (Figure 5.9 A-C). As the development proceeds, *sog* is weakly expressed in the medial column of the neuroectoderm flanking the ventral midline and in the margin of the limb buds (Figure 5.9 D).

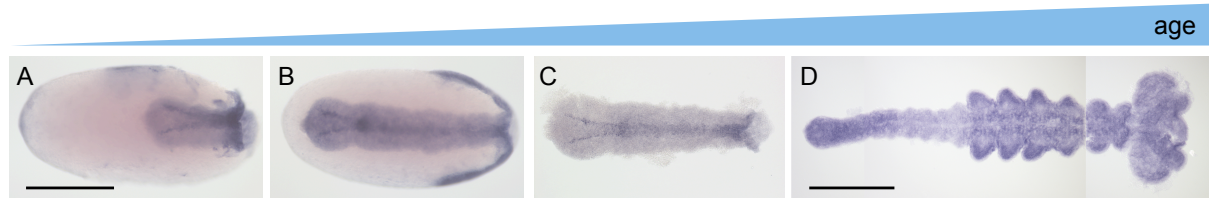


Figure 5.9. Expression pattern of *sog* in *Oncopeltus* germband embryos

In the extended germband embryos, *sog* is expressed in the ventral column and split into two stripes in the most posterior segment (A-C). As the development proceeds, *sog* is weakly expressed in the medial column of the neuroectoderm flanking the ventral midline and in the margin of the limb buds (D). Scale bar size corresponds to 500 μm . Ventral view of embryos is shown in A-D.

Expression pattern of *twist*

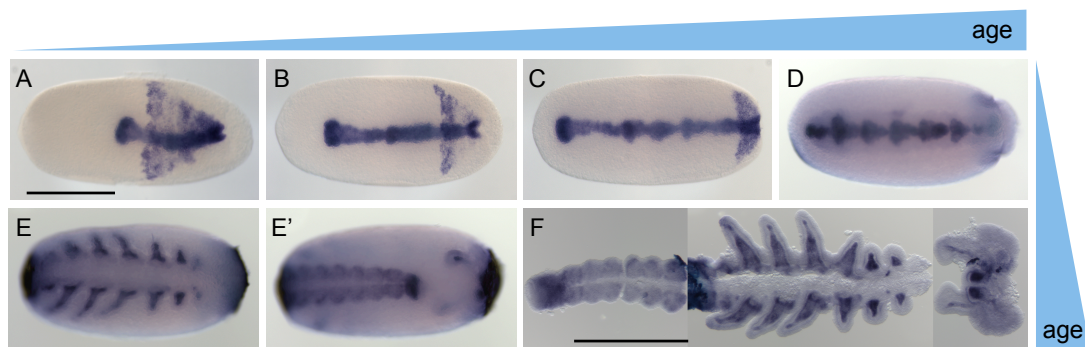


Figure 5.10. Expression pattern of *twist* in *Oncopeltus* germband embryos

In the extended germband embryos, *twist* is expressed in the ventral domain marking the mesodermal fate (A-C). The *twist* expression is getting more and more obvious in each segments (B-D). Embryos in A-E are shown in the ventral view and the embryo in E' is shown in the dorsal view. In the late germband embryos, the expression of *twist* is absent from the trunk and is expressed in the limbs (E and F). F is the identical embryo dissected from E. Scale bar size in A and F corresponds to 500 μm .

In this thesis, *twist* is used as the ventral and mesodermal marker of blastoderm embryos. In the extended germband embryos, *twist* is expressed in the ventral domain marking the mesodermal fate (Figure 5.10 A-C). The *twist* expression is getting more and more obvious in each segments (Figure 5.10 B-D). In the late germband embryos, the expression of *twist* is absent from the trunk and is expressed in the limbs (Figure 5.10 E, F).

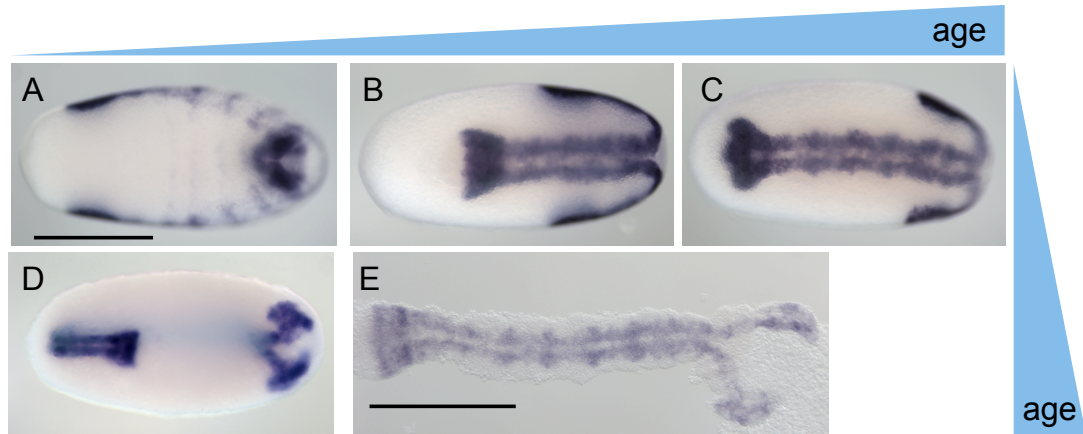


Figure 5.11. Expression pattern of *SoxN* in *Oncopeltus* germband embryos

After the onset of gastrulation, *SoxN* is expressed in the segmental stripes on the lateral side of the embryo (A). In the extended germband embryos, *SoxN* is expressed in the cephalic and ventral neurogenic regions (B-E) similar to the pattern described in *Drosophila* embryos (Crémazy et al., 2000). Embryos in A-C are shown in the ventral view and the embryo in D is shown in the dorsal view. Scale bar size in A and E corresponds to 500 μm .

5.2.4 Expression pattern of the dorsal marker *SoxN*

In this thesis, *SoxN* is used as the dorsal marker of early blastoderm embryos. The early expression of *SoxN* is stronger on the side with a higher nuclear density, which is supposed to be the dorsal side of blastoderm embryos (Figure 5.2 A). After the onset of gastrulation, *SoxN* is expressed in the segmental stripes on the lateral side of the embryo (Figure 5.11 A). In the extended germband embryos, *SoxN* is expressed in the cephalic and ventral neurogenic regions, which is described in *Drosophila* embryos (Crémazy et al., 2000).

5.2.5 Mesoderm formation and the expression of *snail*

It is known in *Drosophila* that *twist* and *snail* are both required for mesoderm formation (Alberga et al., 1991; Leptin, 1991). The *Oncopeltus snail* was found by A. Drechsler and the sequence was extended by RACE-PCR. From the results of degenerate PCR, another gene *klumpfuss* encoding a Zinc-finger transcription factor was also identified. The expression patterns of *snail* and *klumpfuss* are shown in Figure 5.12. In the late blastoderm stage before gastrulation, there is an asymmetric expression of *snail* along the DV axis (Figure 5.12). During germband stages, *snail* is expressed in clusters of neuroectodermal cells flanking the ventral midline (Figure 5.12). The asymmetric expression of *snail* in the

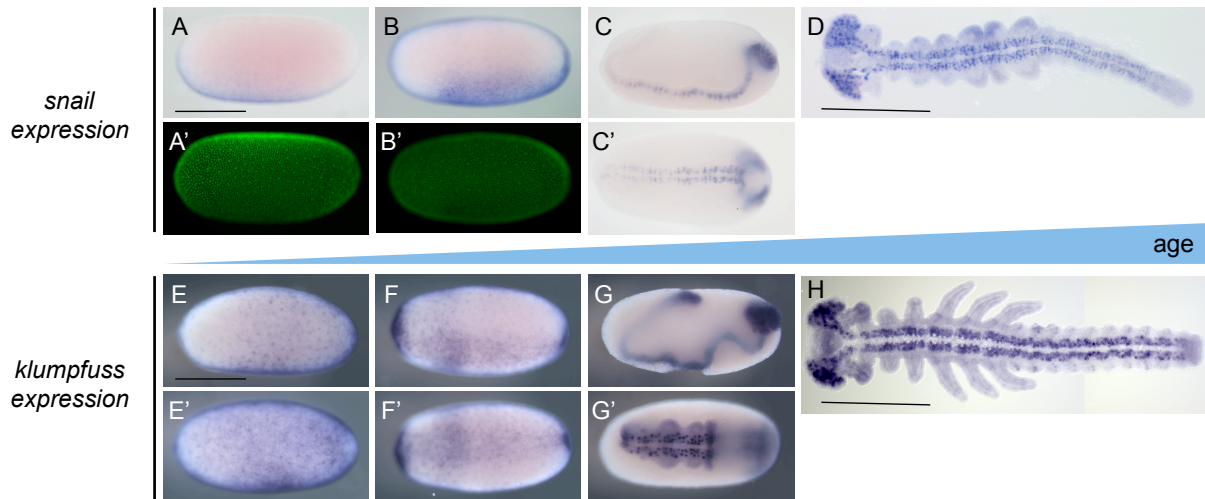


Figure 5.12. Expression pattern of *snail* and *klumpfuss* in *Oncopeltus* embryos

Expression of *snail* transcripts in blastoderm embryos are shown in A and B. Embryos in A' and B' are identical to A and B with nuclear staining by SytoxGreen. There is an asymmetric expression of *snail* along the DV axis (B) in the late blastoderm stage before gastrulation. The asymmetric expression pattern of *snail* is similar to the *twist* expression pattern (Figure 3.3) and the patterns in *Tribolium* (Sommer, R. J. and Tautz, D., 1994), suggesting an early role in mesoderm specification. The blastoderm embryos are shown in A, B, E, F and the germband embryos are shown in C, D, G, H. Germband embryos shown in D and H were dissected out. The *snail* expression in late germband embryos is similar to the *klumpfuss* expression, suggesting a late role in neuroblast development and neurogenesis. Lateral view of embryos is shown in Figure B, C, F, G; ventral view of embryos is shown in Figure C', F', G'. The anterior side of embryos is always to the left. Scale bar size corresponds to 500 μm .

late blastoderm stage is similar to the pattern in *Tribolium* (Sommer, R. J. and Tautz, D., 1994), suggesting an early role in mesoderm specification. Furthermore, the *snail* expression during germband stages is similar to the expression of *klumpfuss*, suggesting a late role in neuroblast development and neurogenesis, which might act in concert with other Zinc-finger (C_2H_2) proteins such as Klumpfuss (Berger et al., 2012; Xiao et al., 2012). However, the function of *snail* and *klumpfuss* in *Oncopeltus* needs to be studied by pRNAi.

5.3 Gene annotation in the *Oncopeltus* transcriptome

The *Oncopeltus* transcriptome consists of over 500 million bases of cDNA from the ovaries and embryos (Ewen-Campen et al., 2011). Nevertheless, some genes known to be required

for the early development such as *msh*, *vnd*, *ind*, *sim*, *twist*, *snail* etc. are absent in the transcriptome. These genes were obtained by degenerate PCR and extended by RACE-PCR. Moreover, several genes were identified in the transcriptome, but the sequences are incomplete. Probably, this is due to the assembly error. The genes were predicted into different small contigs and the sequences inbetween are missing. When compared to the orthologs in the other insects, small contigs can be connected together. A simple PCR using specific primers is feasible to connect two or three contigs together. Furthermore, some predicted genes in the transcriptome paper (Ewen-Campen et al., 2011) are repeated with different contigs coding for the same gene such as the *Toll-related* genes. The genes with more than one contigs are listed in Table 5.1 and the assembled product size is also indicated.

Table 5.1. Genes with more than one contigs in the *Oncopeltus* transcriptome

Genes	contigs	(bp)	product size (bp)	Ref. genes
<i>sog</i>	contig14795	254	2328	<i>sog</i> [<i>Acyrtosiphon pisum</i>]
	contig18465	615		
	contig20850	254		
	GAP9EXG07H2FSD	519		
<i>Toll-6</i>	GEQE5QV02GW91E	355	1716	<i>Toll-6</i> [<i>Nilaparvata lugens</i>]
	Contig24056	413		
<i>Toll-7</i>	FQTBZRY01BD13M	242	821	<i>Toll-7</i> [<i>Nilaparvata lugens</i>]
	isotig11499	375		
<i>Toll-8</i>	GEQE5QV01D10V5	434	2856	<i>Toll-8</i> [<i>Nilaparvata lugens</i>]
	isotig20558	947		
<i>Toll-10</i>	GESJTKM01BPGV1	281	2940	<i>Toll-10</i> [<i>Nilaparvata lugens</i>] <i>slit homolog2</i> [<i>Acyrtosiphon pisum</i>]
	FQTBZRY02I7PQ6	215		
	isotig09603	531		
<i>nudel</i>	GEQE5QV01B8NB6	322	2425	<i>serine protease nudel</i> [<i>Apis mellifera</i>]
	isotig08204	1054		
<i>SoxN</i> †	isotig18590	251	708	<i>Tribolium SoxNeuro</i> *
	Contig23323	295		

There are more than one contigs coding for the same gene, but they are separated in the *Oncopeltus* transcriptome. † Sequence information was further extended by RACE-PCR.

* The sequence of *Tribolium SoxNeuro* was kindly provided by V. Dao.

5.3.1 Identification of Toll or Toll-like receptors (TLRs)

There are 11 hits of *Toll* genes identified in the *Oncopeltus* transcriptome (Ewen-Campen et al., 2011). However, some contigs are coding for the same gene. The total number of TLRs in *Oncopeltus* might be 7 instead of 11. According to the phylogenetic analysis, the TLRs in *Oncopeltus* are clustered as Toll-1, Toll-6/8 (Tollo), Toll-7/2 (18w), Toll-9/13, and Toll-10 subfamilies.

The Toll-9/13 subfamily

In a phylogenetic analysis of TLRs between *Drosophila*, *Tribolium* and *Oncopeltus*, OFAS006184 is clustered within the Toll-9/13 subfamily, not with the other subfamilies (Figure 5.13). In a phylogenetic analysis of identified Toll-9 and Toll-13 in insects, GAP9EXG07H56OG is clustered within the *Drosophila* Toll-9 and OFAS008757 is closely related to the Toll-13 identified in the brown planthopper *Nilaparvata lugens* (Nl) (Bao et al., 2013) (Figure 5.14). Within the Toll-13 family, the Toll-13 of *Nilaparvata* and OFAS008757 are clustered with the Toll-13 like protein identified in the honeybee Toll-13 (Li et al., 2013) (Figure 5.14).

5.4 Phosphorylation sites of Dorsal proteins

The signal-dependent phosphorylation site (serine317), which is prove to be critical for nuclear import (Drier et al., 1999), is conserved in all insect Dorsal proteins (Figure 5.15).

5.5 Phenotypes of the *cactus-2* knockdown

From the embryonic morphology staining by fuchsin and SytoxGreen, more than 50%(n=371) of *cactus-2* knockdown embryos show the unequal nuclear distribution phenotype (Figure 5.16). There are empty patches without nuclei in the blastoderm embryos of *cactus-2* knockdown, especially located in the posterior half of the egg (Figure 5.16) B, C, H). After gastrulation, the germband extension is disrupted in *cactus-2* knockdown embryos (Figure 5.16 E, F, J).

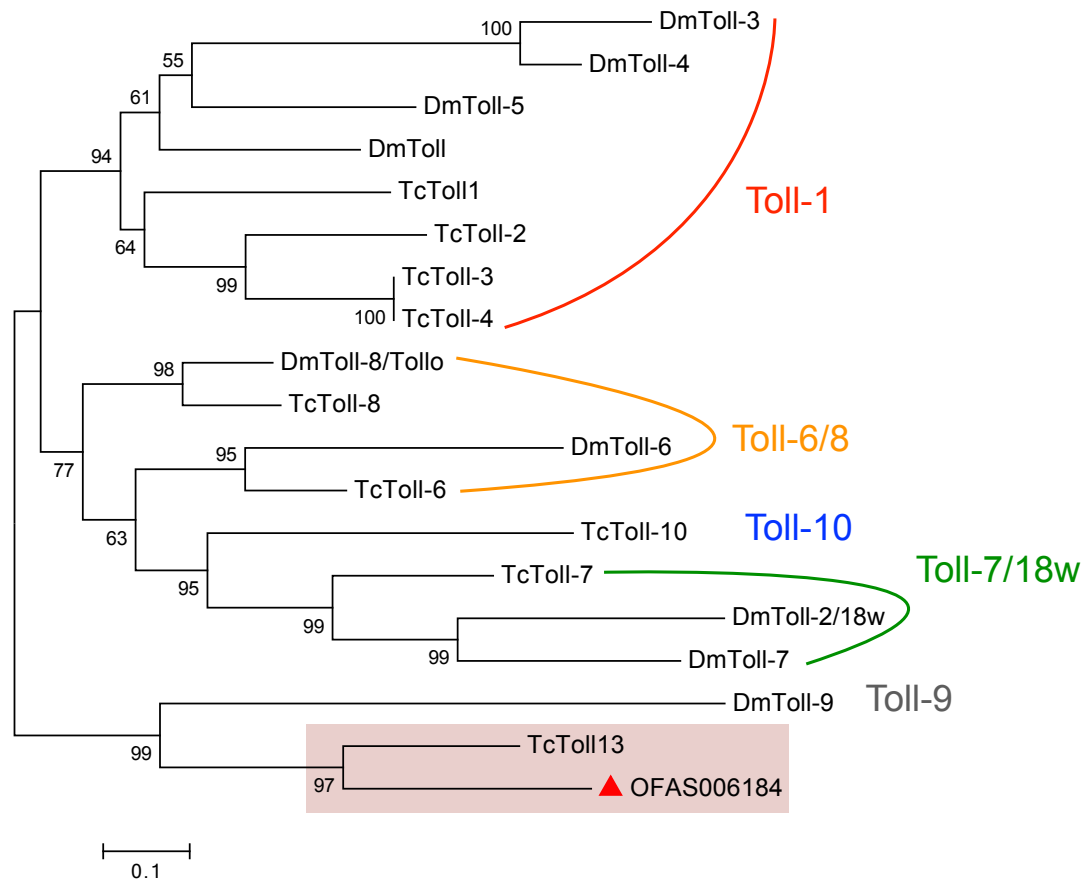


Figure 5.13. Phylogenetic analysis of the Toll family

In a phylogenetic analysis of TLRs between *Drosophila*, *Tribolium* and *Oncopeltus*, OFAS006184 is clustered within the Toll-9/13 subfamily, not with the other subfamilies. The TLRs are aligned exclusively using the conserved TIR domain. The evolutionary history was inferred using the Neighbor-Joining method. The associated taxa clustered together were replicated in the bootstrap test (1000 replicates) shown next to the branches. The tree is drawn to scale, with branch lengths representing the evolutionary distances. The evolutionary distances were computed using the Poisson correction method. The analysis involved 19 amino acid sequences. The phylogenetic analysis was conducted in MEGA6.

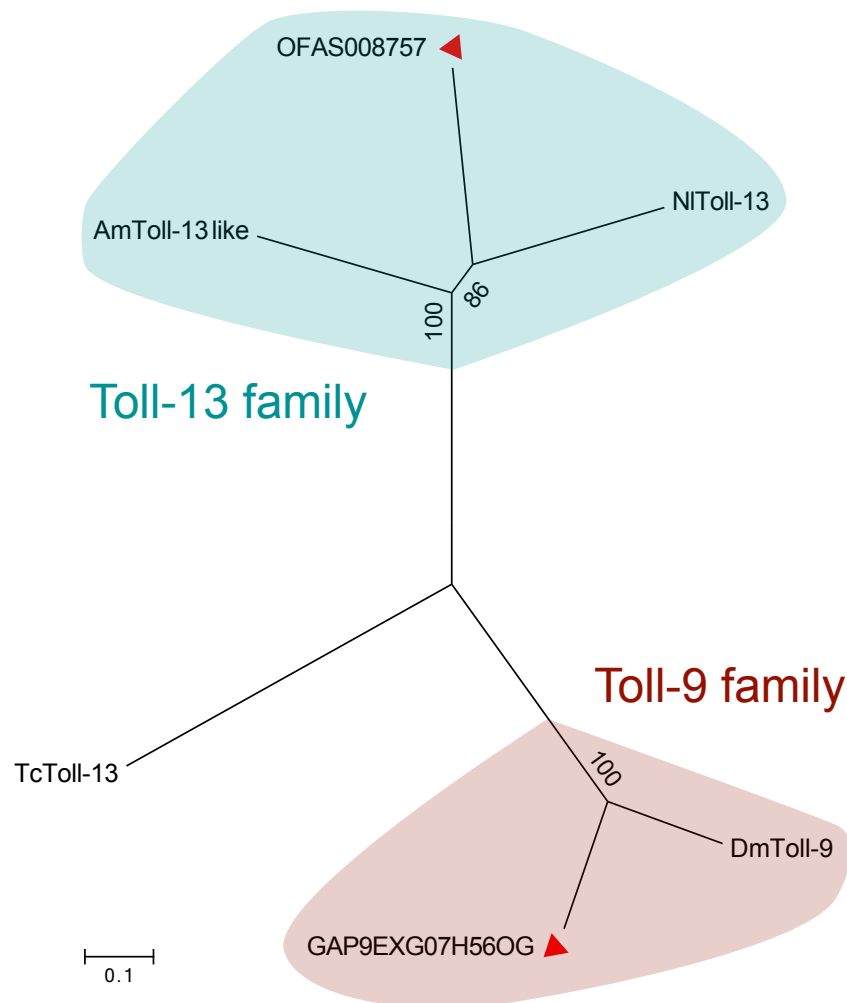
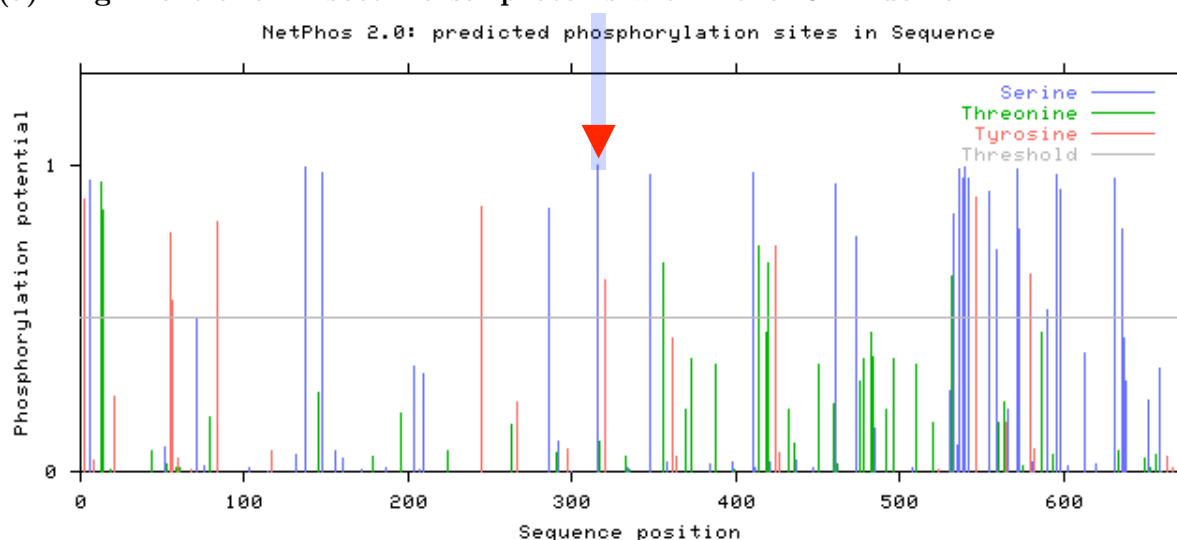


Figure 5.14. Phylogenetic analysis of the Toll family

In a phylogenetic analysis of identified Toll-9 and Toll-13 in insects, GAP9EXG07H56OG is clustered within the *Drosophila* Toll-9 and OFAS008757 is closely related to the Toll-13 identified in the brown planthopper *Nilaparvata lugens* (*Nl*). Within the Toll-13 family, the Toll-13 of *Nilaparvata* and OFAS008757 are clustered with the Toll-13 like protein identified in the honeybee Toll-13. The TLRs are aligned exclusively using the conserved LRR domain. The evolutionary history was inferred using the Neighbor-Joining method. The associated taxa clustered together were replicated in the bootstrap test (1000 replicates) shown next to the branches. The tree is drawn to scale, with branch lengths representing the evolutionary distances. The evolutionary distances were computed using the Poisson correction method. The analysis involved 6 amino acid sequences. The phylogenetic analysis was conducted in MEGA6.



(a) Alignment of all insect Dorsal proteins within the RHD domain



(b) Predicted phosphorylation sites of *Oncopeltus* Dorsal1

Figure 5.15. The critical phosphorylation site for nuclear import is conserved in all insect Dorsal proteins

The conserved phosphorylation site on serine is indicated with red arrowheads. The prediction of phosphorylation sites was conducted by NetPhos 2.0 Server (Blom et al., 1999). (<http://www.cbs.dtu.dk/services/NetPhos/>).

The abbreviation of insect species: the fruit fly *Drosophila melanogaster* (*Dm*), the milkweed bug *Oncopeltus fasciatus* (*Of*), the beetle, the jewel wasp *Nasonia vitripennis* (*Nv*), the assassin bug *Rhodnius prolixus*, the human lice *Pediculus humanus corporis* (*Phc*), the pea aphid *Acyrtosiphon pisum* (*Ap*), the honeybee *Apis mellifera* (*Am*). Both of the *Oncopeltus* Dorsal proteins (Dl1 and Dl2) are included in the alignments.

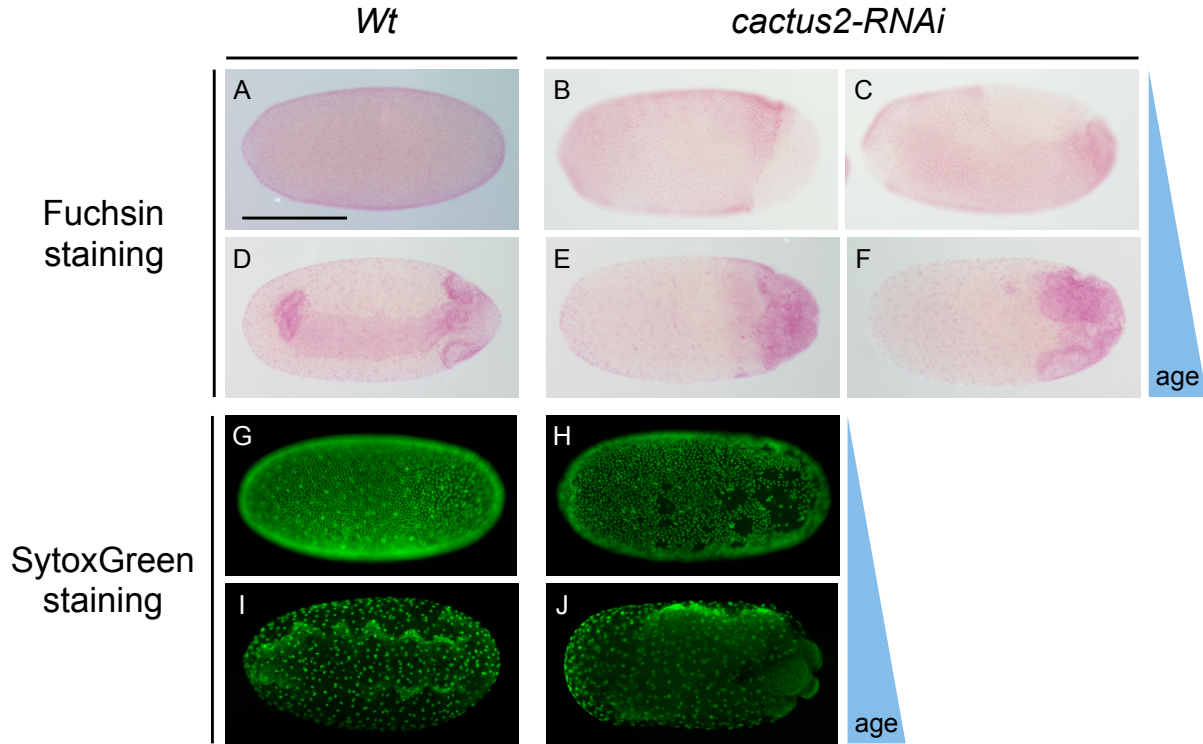


Figure 5.16. Morphological phenotype of *cactus2-RNAi* embryos

Fuchsin and nuclear staining of *cactus-2* knockdown embryos. Anterior pole of the egg is to the left, embryo anterior is to the right. Embryos of A-C, G and H are at the blastoderm stage; Embryos of D-F are at the germband extension stage few hours after gastrulation; Embryos of I and J are at the germband stage. The dorsal view of the embryo is shown in D; The ventral view of the embryo is shown in I. The DV polarity can not be determined in E, F and J because the germband extension is disrupted in *cactus-2* knockdown embryos. The scale bar size (A) correspond to 500 μm .

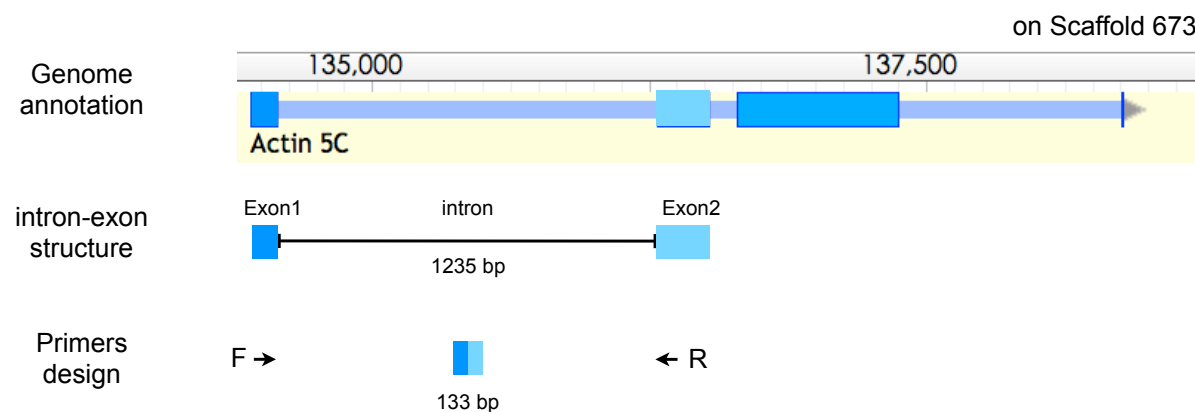
The phenotype of unequal nuclear distribution in *cactus2-RNAi* embryos is not detected in the other *cactus* knockdowns. This phenotype could indicate that the nuclei are degrading in *cact-2* knockdown embryos, which results in patches of empty spaces in the blastoderm embryo (Figure 5.16). However, it is different from the *dl2-RNAi* phenotype because the empty patches are located in the posterior half of the embryo.

5.6 Experimental controls and the reference gene

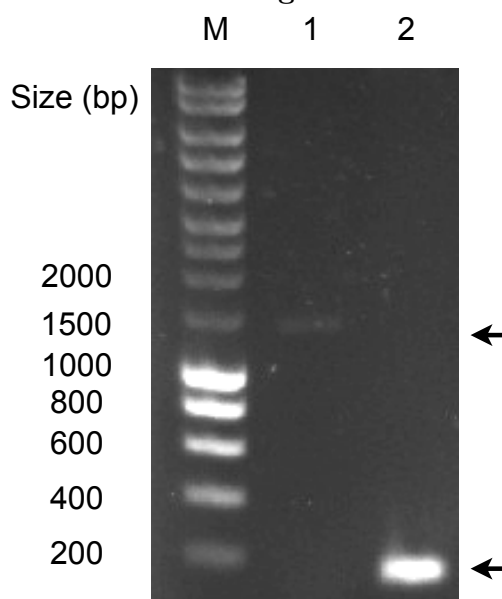
5.6.1 The control for semi-quantitative PCR

In the the semi-quantitative PCR, the expression of *Oncopeltus actin* served as the internal control. The primers of *actin* were designed across an intron-exon boundary to ensure

that there is no genomic DNA contamination in cDNA samples. If the genomic DNA exists in the cDNA sample, the product size increases to 1235 bp rather than 133 bp (Figure 5.17b).



(a) Intron/Exon structure of *actin* on the genomic scaffold



(b) Different product size of *actin* amplicons

Figure 5.17. The gene *actin* served as a perfect control for RT-PCR

Intron/Exon structure of *actin* was confirmed by the *Oncopeltus* genome annotation. Product size of intron is confirmed by molecular cloning and DNA sequencing. Wells of the agarose gel are loaded sequentially from left to right with DNA ladder (M), genomic DNA (1) and cDNA (2) from the *Oncopeltus* embryos. PCR products in the well (1) and (2) are indicated with black arrows.

5.6.2 The reference genes for qPCR normalization

To estimate the relative expression level of genes, a good reference gene with constant expression is important during the normalization of qPCR data. Although *actin* served as an excellent internal control for the semi-quantitative PCR, the expression level of *actin* is not constant across different developmental stages during the first round of qPCR test. Thus, it might not be an optimal reference gene for qPCR. Instead of the *actin*, the *18S ribosomal* gene was selected as the reference gene for qPCR assay in this thesis. In the beetle *Tribolium*, the ribosomal genes were the most stable normalizers across different developmental stages and they are were recommended for the gene expression analysis (Toutges et al., 2010). In the assassin bug *Rhodnius prolixus*, the *18S* and *elongation factor 1 (EF1)* were the most reliable genes for normalization in qPCR (Majerowicz et al., 2011). The expression of *18S ribosomal* is constant and abundant in *Oncopeltus* across blastoderm stages. However, the expression level of *18S ribosomal* gene is much higher than the other genes with low C_T values. This results a problem during the normalization of qPCR data that the down-regulated genes or genes expressed in low levels might be over- or under-estimated. Thus, it is important to find the optimal reference gene for different experimental purpose to avoid the incorrect interpretation of qPCR data.

5.6.3 The dsRNA targeting sites of *Toll-1*

According to the sequence information of the *Toll-1* gene in *Oncopeltus*, two dsRNA targeting on different region of *Toll-1* coding sequence were designed. The primer sequence and product size are listed in Materials and Methods. The predicted dsRNA targeting sites of *Toll-1* are shown in the Figure 5.18. The targeting site of dsRNA-a is designed locating in the TIR domain, while the other dsRNA-b is not.

Identical amount of dsRNA-a and dsRNA-b (four μg per female) were used for pRNAi. There is no difference on the morphology of knockdown phenotypes analyzed in late stages. However, the percentage of knockdown phenotype is variable using different dsRNAs. The knockdown phenotypes shown in the results were produced by the dsRNA-a. Percentage of knockdown phenotype produced by dsRNA-a is higher than dsRNA-b (Table 5.2).

The efficiency of knockdown might be variable using different dsRNAs. Percentage of knockdown phenotype produced by dsRNA-a is higher than dsRNA-b (Table 5.2),

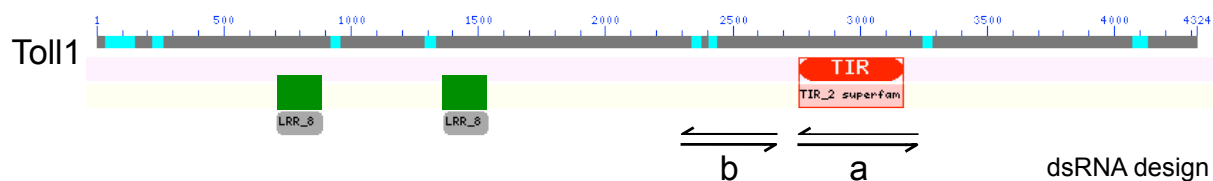


Figure 5.18. The dsRNA targeting sites of *Toll-1*

Structure of the *Toll-1* gene was predicted by NCBI conserved domain search. N-terminus of Toll-1 is to the left side with two LRRs predicted. The targeting site of *Toll-1* dsRNA-a is located in the TIR domain.

Table 5.2. Percentage of knockdown phenotype produced by dsRNA-a and dsRNA-b

Group	knockdown phenotype	wildtype-like	empty eggs	Sample size
dsRNA-a	93%	0	7%	30
dsRNA-b	62%	5%	33%	130

Identical amount of *Toll-1* dsRNA-a and b (four μ g per female) were used for pRNAi. In each group, three individual females were injected with identical dsRNA, with same amount. Percentage of knockdown phenotypes were calculated from prolonged developing embryos after RNAi.

which might indicate a higher penetrance of dsRNA-a. When the dsRNA-b was used to knockdown *Toll-1*, more empty eggs enriched with yolk were produced and the percentage of knockdown phenotype declines. It is possible that there are some off-target effects when the dsRNA-b was used to knockdown *Toll-1*. To avoid off-target effects in RNAi, it is suggested to design the dsRNA with minimum off-target effect by a web-based estimation (Naito et al., 2005).

5.7 Toll signaling together with Imd pathway are important for innate immunity among insects

Among insects, the Toll signaling is important for DV patterning, but also involved in innate immunity to defense the pathogens. In the fly *Drosophila*, the Toll and Imd pathways are the major regulators of the immune response (De Gregorio et al., 2002; Tanji et al., 2007). Here, the components of the the IMD pathway *immune deficiency (imd)* and *relish* are identified in *Oncopeltus*. The transcription factor Relish acts downstream of Imd pathway to regulate target gene expression (Tanji et al., 2010). After the knockdown

of *relish* via pRNAi, the offsprings laid by the injected females showed no DV defect phenotypes. Majority of the offsprings can hatch as normal nymphs. This indicates that *relish* is not involved in DV patterning in *Oncopeltus* and Relish might not act downstream of the Toll signaling pathway as same as in *Drosophila*.

5.7.1 Life span reduction of injected females after pRNAi

The immune function could be implied by the life span reduction of injected females. There is a tendency that the adult females injected with dsRNA seem to live shorter than the mock-treated groups (Table 5.3).

Table 5.3. Life span reduction after pRNAi

Group	dsRNA (μ g)	Surviving days				Sample size ♀n=
		min	max	Average	Standard deviation	
Mock-treated control	-	5	37	20.4	7.38	28
<i>Toll-1</i> RNAi	4	5	34	13.9	8.43	10
<i>Toll-1</i> RNAi	2	4	28	14.1	6.22	17
<i>dorsal-1</i> RNAi	4	3	33	17.1	8.21	21
<i>dorsal-2</i> RNAi	0.1	4	34	14.5	8.25	16
<i>relish</i> RNAi	0.1	4	12	5.7	2.87	6

Identical *Toll-1* dsRNA with different amount was used for pRNAi. In each group, more than six females were injected individually The surviving days after injection were recorded here showing the life span reduction after pRNAi.

The injection procedure is similar to the sterile injury. Although it is not the septic injury, the injected females might be more vulnerable to pathogens. The life span of *relish* dsRNA injected females is reduced to 5.7 days in average. Compared to mock-treated controls who can survive about 20.4 days, this indicates that *relish* might be critical for the immune defense acting downstream of Imd pathway. The knockdown of *Toll-1* also reduces the average life span of injected females. However, there is no significant difference between the RNAi groups and mock-treated control through the logrank test (Bland and Altman, 2004). Although it could not be excluded that Toll signaling is also important for immunity in *Oncopeltus*, the relationship between the immunity and the Imd pathway seems to be more direct. To further investigate the immune function in *Oncopeltus*, the regulation of immune-related genes including components of the Toll and Imd pathway should be studied using the whole transcriptomic analysis after pathogenic challenging or

gene knockdowns via pRNAi.

Acknowledgement

There are so many thanks to say. First of all, thank my parents and grandparents who support me heartily and financially. Special thanks to my wife Fang-Chun, who takes care of the family when I focused on the thesis. Thank my daughter, who came to the world at the same time when I started to write. Oh my little cutie, you have brought us so much fun. Thank my parents in law, who flew thousand miles to Germany, helped us taking care the baby, and gave us the financial support. Thank my supervisor Prof. Dr. Siegfried Roth, who accepted me to work in the lab at the first beginning, and offered ideas, opened a deep discussion and supported my study after the graduate program. Thank the International Graduate School in Development Health and Disease (IGSDHD) of the University of Cologne, which offered fellowships for three years. Thank the coordinator of the program Dr. Isabell Witt, who encouraged the students a lot and organized a variety of soft-skill courses. In addition, thank the secretaries of the program Kathy, Eva, Rita, and Dr. Johanna Majczak. Especially thank Kathy, who helped me to deal with all the difficulties and complicated affairs. To make a living is always not easy in a foreign country. Thank Dr. Rodrigo Nunes da Fonseca, who highly recommended the AG Roth group and offered suggestions for the experiments. Thank Dr. Jeremy Lynch and Dr. Kristen Panfilio, who supervised me when I was a rotation student. Furthermore, Jeremy kindly provided a lot of knowledge and inspired me to investigate more. Thank my former colleagues Orhan and Thomas, who did a great work in the wasp *Nasonia*. They always encourage me to move on when I encountered difficulties. A special thank to Orhan, who saved my life once from the severe allergy. Thank my colleague Lena, who cooperated with me, doing an excellent work on BMP signaling in *Oncopeltus*. Thank my colleague Waldemar, who has read my writings over and over again. Thank my colleague Van Anh, who has read my writings and kindly provided the *Tribolium* sequences. Thank Prof. Dr. Günter Plickert from the Institute of Zoology and Prof. Dr. Mirka Uhlirova from the CECAD to read my whole thesis. Thanks for your suggestions and comments. Thank my colleague Dominik for always caring about us. Thank the other lab members Meike, Stefan, Oliver, Nadine, Kai, Danka, Jan, Jan, Anne, and Dr. Matthias Pechmann, Dr. Thorsten Horn, Dr. Maarten Hilbrant and, and Dr. Matt Benton... etc. Thank Dr. Yu Matsuura from the AIST for the cooperation and his contribution on the transgenic and symbiosis projects. He offered me many ideas and broadened my mind. Thank Dr.

Maurijn van der Zee for the cooperation on the immune project and genome annotation. Thank Dr. Jen-Chih Chi from the Institute of Biochemistry for the personal instructions on protein induction, purification, and storage. Thank the Taiwanese students and friends, who had lived in Europe, USA or Taiwan. Without your encouragement, I can not stay here for more than five years. Thank the thieves, who stole my MacBook Pro, stole my wife's bag, and broke into our apartment twice. Although it was very frustrated back then, the spirit of never give up is that what we stand up for. Finally, thank you all. This thesis will not be finished without you. Thank you very much.

Erklärung

Ich versichere, dass ich die von mir vorgelegte Dissertation selbständig angefertigt, die benutzten Quellen und Hilfsmittel vollständig angegeben und die Stellen der Arbeit - einschließlich Tabellen, Karten und Abbildungen -, die anderen Werken im Wortlaut oder dem Sinn nach entnommen sind, in jedem Einzelfall als Entlehnung kenntlich gemacht habe; dass diese Dissertation noch keiner anderen Fakultät oder Universität zur Prüfung vorgelegen hat; dass sie - abgesehen von unten angegebenen Teilpublikationen - noch nicht veröffentlicht worden ist sowie, dass ich eine solche Veröffentlichung vor Abschluss des Promotionsverfahrens nicht vornehmen werde. Die Bestimmungen der Promotionsordnung sind mir bekannt. Die von mir vorgelegte Dissertation ist von Prof. Dr. Siegfried Roth betreut worden.

Köln, 28.11.2014

.....
(Ort, Datum)

.....
(Yen-Ta Chen)

Lebenslauf

Persönliche Daten

Name	Yen-Ta Chen
Anschrift	Bonn-Beuel
Geburtsdatum und -ort	31.12.1981 in Pingtung, Taiwan

Schulische Ausbildung

1988-1994	Taipei städtische JianTan Schule
1994-1997	Taipei städtische Bailing Schule (Junior High School)
1997-2000	Taipei städtische ChengGong Schule (Senior High School)

Studium

2000-2004	National Taiwan Normal University (NTNU) Bachelor am Department of Geowissenschaften und Biologie der NTNU
2004-2006	National Taiwan University (NTU), College of Life Science Masterarbeit bei Prof. Dr. Tsai, Huai-Jen am Institute of Molecular and Cellular Biology (IMCB) und Prof. Dr. Lee, Ying-Chou am Institute of Fisheries Science (IFS) Titel: Gene transfer of brine shrimp (<i>Artemia sinica</i>) by electroporation
Seit 2010	Doktorarbeit bei Prof Dr. Siegfried Roth am Institut für Entwicklungsbiologie der Universität zu Köln Titel: The role of Toll signaling in dorsoventral axis formation in the milkweed bug <i>Oncopeltus fasciatus</i>
